Para-Functionalized NCN-Pincer Palladium and Platinum Complexes as Building Blocks in Organometallic Chemistry

Para-Gefunctionaliseerde NCN-Pincer Palladium- en Platinacomplexen als Bouwstenen in de Organometaalchemie

(met een samenvatting in het Nederlands)

Proefschrift ter verkrijging van de graad van doctor
aan de Universiteit Utrecht
op gezag van de Rector Magnificus, Prof. Dr. W.H. Gispen
ingevolge het besluit van het College voor Promoties
in het openbaar te verdedigen
op 6 november 2002 des middags te 12.45 uur

door

Martijn Quico Slagt

geboren op 8 maart 1973 te Zevenaar

Promotor: Prof. Dr. G. van Koten
verbonden aan het Debye Instituut van de Universiteit Utrecht
Co-promotor: Dr. R.J.M. Klein Gebbink
verbonden aan het Debye Instituut van de Universiteit Utrecht

CIP-GEGEVENS KONINKLIJKE BIBLIOTHEEK, DEN HAAG

Slagt, Martijn Quico
Para-Functionalized NCN-Pincer Palladium and Platinum Complexes as Building Blocks in Organometallic Chemistry /
Martijn Quico Slagt
Utrecht, Universiteit Utrecht, Faculteit Scheikunde.
Thesis Universiteit Utrecht. – With ref. – With summary in Dutch
ISBN 90-393-3166-9

The work described in this thesis was carried out at the Debye Institute, Department of Metal-Mediated Synthesis, Utrecht University, the Netherlands.
This research was financed by the Dutch Technology Foundation (STW) with financial aid from the Council for Chemical Science of the Netherlands Organization for Scientific Research (NWO/CW).

Voor Randi

Table of Contents

Chapter 1	Building Blocks in Organometallic and Coordination Chemistry	1
Chapter 2	Synthesis of *para*-Substituted NCN-Pincer Complexes: Versatile Building Blocks in Organometallic Chemistry	31
Chapter 3	Self-assembly of *para*-nitro NCN-pincer palladium complexes into dimers through electron donor-acceptor interactions	61
Chapter 4	NCN-Pincer Palladium(II) - Pyrenoxy based Molecular Tweezers: Synthesis, Properties in Solution and Catalysis	71
Chapter 5	NCN-Pincer Palladium Complexes with Multiple Anchoring Points for Functional Groups	95
Chapter 6	Encapsulation of Hydrophilic NCN-Pincer Platinum Complexes in Amphiphilic Hyperbranched Polyglycerol Nanocapsules	109
Chapter 7	Synthesis and Visualization of Immobilized of NCN-Pincer Platinum(II) Complexes on Hyperbranched Polyglycerol supports	119
Chapter 8	Chiral Hyperbranched Polyglycerol as Scaffolds for the Covalent and Non-Covalent Immobilization of *para*-COOH and *para*-SO_3H NCN-pincer Platinum(II) Complexes	133

Graphical Abstract	149
Summary	151
Samenvatting	157
Dankwoord	163
Curriculum Vitae	167
List of Publications	169

Chapter One

Building Blocks in Organometallic and Coordination Chemistry

Abstract

Suitably functionalized organometallic and coordination transition metal complexes can be applied as molecular building blocks for the (supramolecular) construction of new materials which can be applicable as catalysts or sensor materials. This chapter illustrates their use in (supramolecular) catalysis, self-assembly, crystal engineering, and bio-organometallic chemistry by presenting selected examples from the respective fields.

1.1 Introduction

A rapidly evolving field in inorganic chemistry is the application of organometallic and coordination complexes as building blocks or active components in the construction of new materials exhibiting specific catalytic, redox, optical or sensor activities.[1] Coordinatively unsaturated transition metal complexes can self-assemble in the presence of suitable ligands to form superstructures. The wide range of bonding geometries available in transition metal chemistry allows the targeted construction of linear, square, cubic, spherical, or other geometrical assemblies. These structures can be functional as catalysts, sensors and molecular devices, or are prepared for purely aesthetic reasons.[2] Besides this, functionalization of catalytically active transition metal complexes allows regulation of their solubility behavior or immobilization on supports. This offers the opportunity to separate homogeneous catalysts from the reaction products for recycling of the expensive transition metal or ligand system, generating cleaner product streams. An exciting development in the field of ligand functionalization is the design and construction of supramolecular catalysts.[3] Catalytically active transition metal building blocks can be combined with strategically placed receptor/host moieties, metal ions, functional groups or steric bulk, to mimic the substrate and product selectivities encountered in biological enzymatic systems.

The availability and synthetic accessibility of suitably functionalized organometallic building blocks forms a crucial factor in the expanding field of organometallic materials science. Since the metal-to-ligand bonds are often the most reactive part of transition metal complexes, ligands are generally metallated in the final stage of the synthesis. Coordination complexes based on ligands such as phosphanes, pyridines, and oxazolines, are prepared by facile treatment of the ligand with a suitable metal salt. In contrast, the formation of a metal-to-carbon bond often requires more stringent conditions, which should be compatible with the functional groups already present in the ligand. Consequently, the use of coordination complexes as molecular synthons is further developed compared to organometallic complexes, with heterocyclic nitrogen ligands dominating the field. This chapter highlights the use of organometallic and coordination complexes as building blocks with illustrative examples concerning (catalyst) assembly, crystal engineering, catalyst immobilization, supramolecular catalysis, and bio-organometallic chemistry. Furthermore, ligand functionalization offers the opportunity to tune the electronic properties of its metal complex. The final paragraph describes the aim and scope of this thesis.

1.2 Assembly in Solution and in the Solid State

The assembly of organic building blocks in solution or in the solid state (crystal engineering) relies on weak intermolecular interactions such as hydrogen bonding, π-π stacking, dipole-

dipole interactions, and coulombic interactions. Strong hydrogen bond donor and acceptor groups, *e.g.* COOH, OH, $CONH_2$, and CONHR groups, form essentially the same type of hydrogen bonding interactions whether part of an organic molecule or of a metal-coordinating ligand.[4] In contrast, (transition) metal complexes offer additional bonding features, namely coordinate and covalent bonds. As a result, materials containing covalent or metal-based coordination networks are generally more robust than those relying on weak interactions between organic building blocks alone.[2b] In addition, the presence of metal atoms in the molecular building block generates new types of interactions, which are characteristic of inorganic and organometallic systems, including M···M interactions[5] and M–X···H hydrogen bonds.[6] The ample availability of metal-binding ligands, and the varying coordination geometries and numbers of different metal ions allows the formation of any imaginable structure.[7] The strategic use of kinetically labile or inert metal ions, and conversions between them during or after the assembly process, allows efficient scanning of the potential energy surface for the thermodynamically most stable product and subsequent kinetic immobilization of the obtained structure.[8]

1.2.1 Self-Assembly in Solution

Porphyrin systems, in particular zinc(II) tetraphenylporphyrin (ZnTPP), offer readily accessible building blocks for the construction of supramolecular assemblies, utilizing the complexation of nitrogen based (pyridyl) ligands to the zinc(II) ion. Additionally, numerous functionalizations on porphyrin systems have made them highly versatile building blocks in supramolecular transition metal chemistry.[9] Pyridyl functionalized Zn(II) porphyrins were found to self-assemble in solution and in the solid state. Combinations of free-base porphyrins and various degrees of pyridyl functionalisation on the porphyrins allows self-assembly in controllable supramolecular architectures (Figure 1).[10]

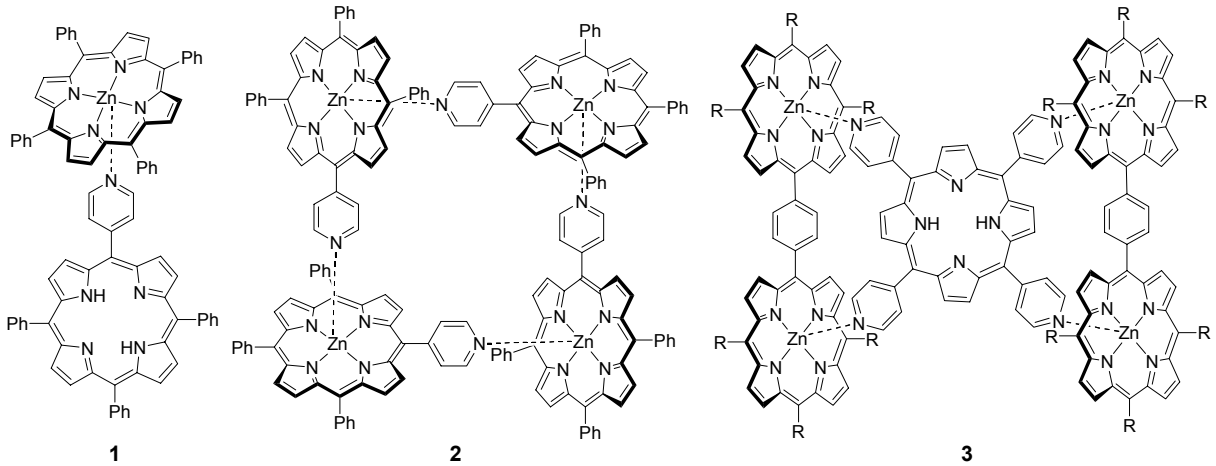

Figure 1. Self-assembly of pyridyl porphyrins in dimers (**1**)[10a], tetramers (**2**)[10b], and other architectures (**3**)[10c].

The group of Hupp applied the complexing abilities of ZnTTP towards pyridyl groups for the introduction of steric bulk around a chiral manganese(III) salen based catalyst (**4**, Figure 2). The presence of the ZnTPP moieties in the vicinity of the catalyst improved its activity and lifetime, but hardly altered its enantioselectivity.[11]

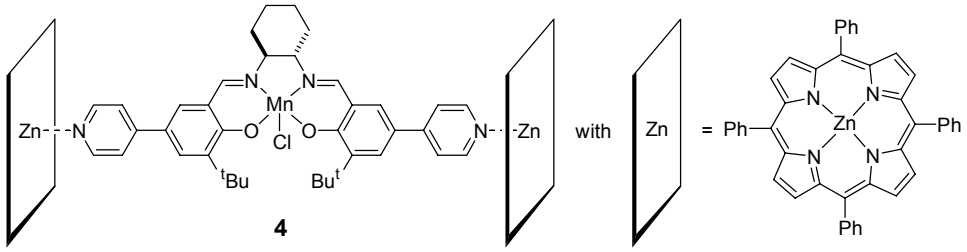

Figure 2. Chiral manganese(III) salen catalyst with ZnTPP.[11]

A more complex system published by this group uses large supramolecular assemblies of pyridyl functionalized zinc(II) and manganese(III) porphyrins, held together by coordination to rhenium atoms (**5**, Figure 3). The authors state that this assembly resembles the catalytic core of cytochrome P450, both structurally and functionally. Although the catalyst is embedded in steric bulk, an apical ligand is missing on the central manganese porphirin. This ligand is of crucial importance in the structure and catalytic activity of cytochrome P450, but not included in its mimic **5**. In epoxidation experiments with several functionalized *cis*-stilbenes, shape selectivity was observed. The least bulky substrates were epoxidized preferentially over the bulky substrates.[12]

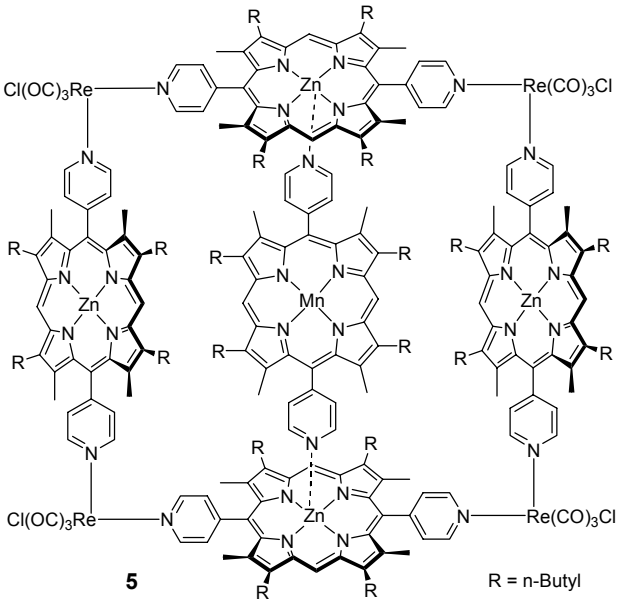

Figure 3. Self-assembled Mn(III) based epoxidation catalyst.[12]

The group of van Leeuwen prepared hemispherical assemblies with the metal center completely encapsulated in steric bulk by combining pyridylphosphanes, ZnTPP and transition metal salts. Ligand **6** can complex to three porphyrin moieties forming an extremely bulky phosphane (Figure 4).[13]

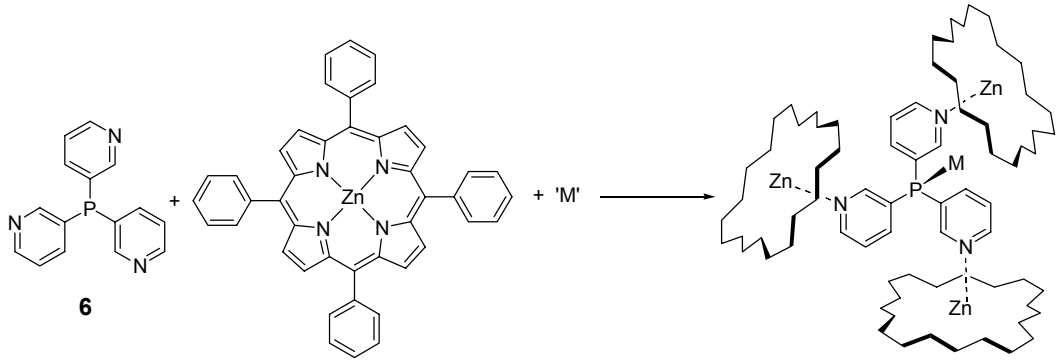

Figure 4. Supramolecular assembly of encapsulated transition metal catalysts with altered activities and selectivities.[13]

The palladium(II) complex of ligand **6** has hardly any activity in the Heck reaction of styrene and iodobenzene, in the absence of zinc(II)porphyrins. However, the addition of ZnTPP to the complex leads to the assembly of a highly active Heck catalyst when compared to its triphenylphosphane analogue. A similar effect is observed for ligand **6** in the rhodium(I) catalysed hydroformylation of 1-octene, showing a significant drop in the linear to branched ratio and higher activities in the presence of the porphyrin. The enhanced activity and altered selectivity of the catalyst is attributed to the preferred formation of monophosphane complexes as a result of the steric bulk of the assembled ligands.

The versatility of pyridyl-type ligands in the construction of supramolecular assemblies is represented by the work of Fujita *et al.* The combination of designed ligands, appropriate metal salts, and templates allows the supramolecular assembly of various rings, cages, and two- or three-dimensional synthetic receptors.[14] One illustrative example involves the spontaneous assembly of pyridyl-based ligands and metal salts into two interlocked coordination cages (**7**, Figure 5).[15] This assembly uses ten components, which have to be organized in a specific way. While at first a statistically distributed mixture is formed, a gradual increase in the thermodynamic product (**7**) is observed after prolonged heating.

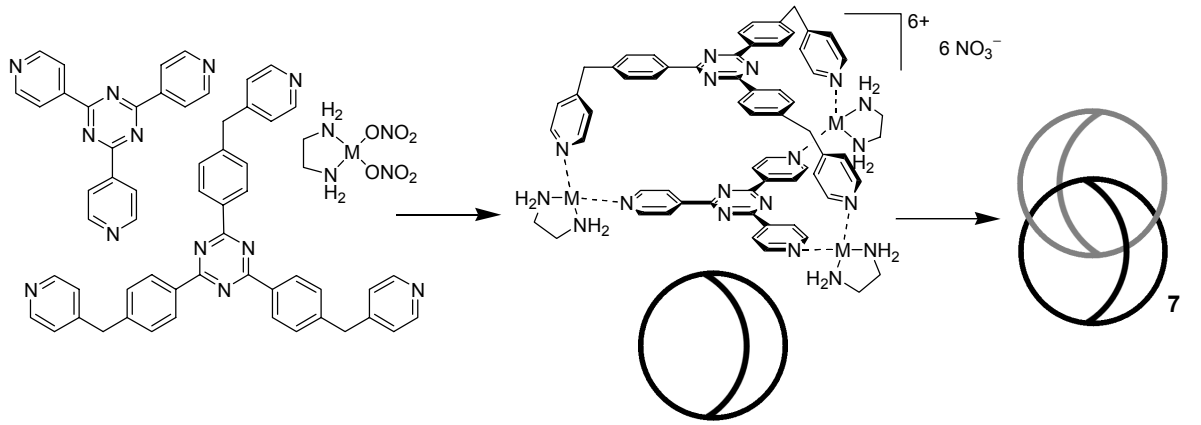

Figure 5. Assembly of ten components into two interlocked coordination cages.[15]

Functionalized transition metal terpyridine units have been studied in detail as building blocks for the construction of coordination dendrimers.[16,17] Main emphasis in these studies has been put on the ruthenium terpyridines, since these can exhibit interesting electrochemical, photophysical and photochemical properties.[18] An interesting assembly is prepared by the selective reaction of a polyol functionalized coordination dendrimer with $[(tpy)Ru(tpyCl)]^{2+}$ moieties, affording a fully functionalized coordination dendrimer (**8**, Figure 6).[19] Functionalisation of the polyol dendrimer is quantitative and selective, and is a rare example of ligand functionalization on metallated amine ligands.

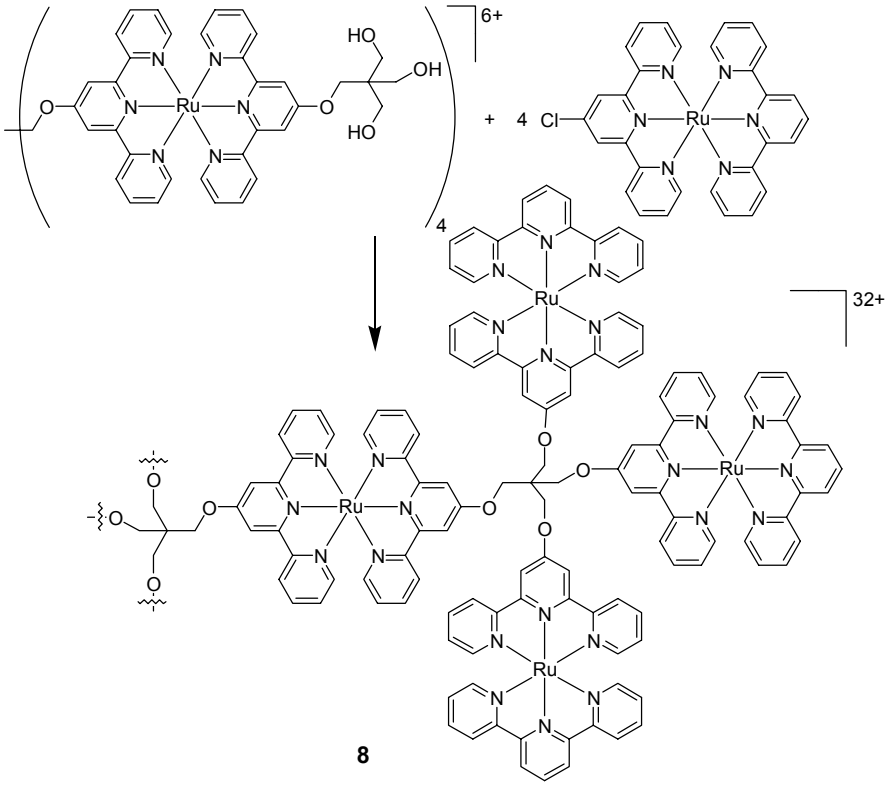

Figure 6. Ru(II) terpyridine based coordination dendrimer.

The concept of preparing dendritic macromolecules based on metal complexation was used by the group of Reinhoudt for the construction of organometallic coordination dendrimers from cyclopalladated SCS-pincer (SCS-pincer = 2,6-bis((thiophenolato)methyl)phenyl anion) complexes. The building blocks are activated upon dehalogenation to afford Lewis acidic palladium complexes, forming coordinative bonds with cyano-ligands (Figure 7). Dendrimers of generation one (**9**) to five were obtained *via* a step-wise growth strategy.[20]

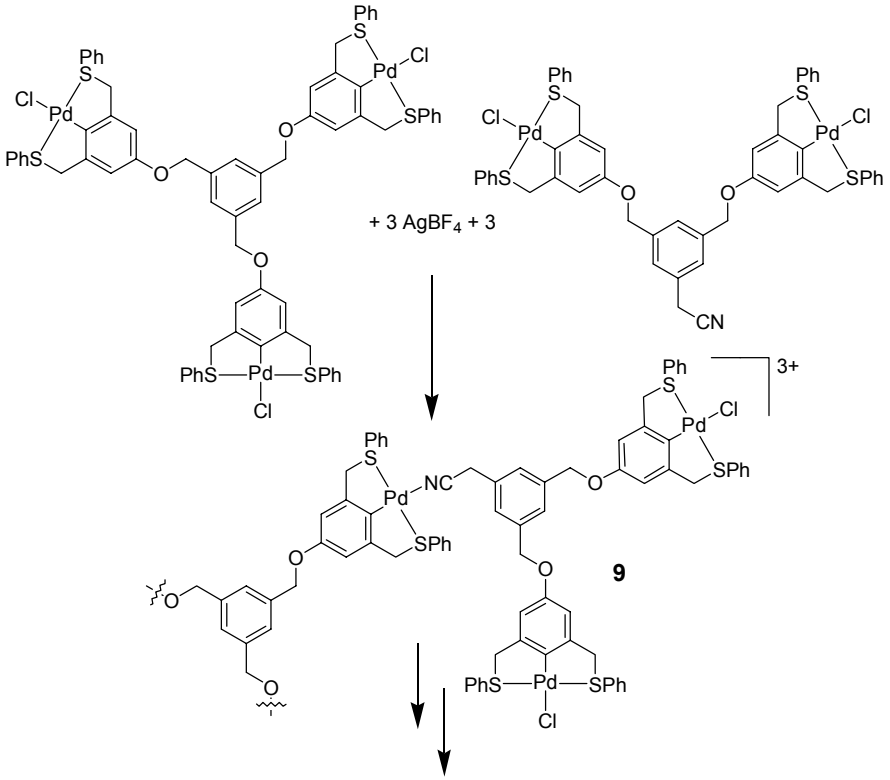

Figure 7. Step-wise assembly of coordination dendrimers.[20]

Highly elegant examples using transition metal complexes as building blocks and active units have been reported by Sauvage *et al*.[21] Linear 'molecular machines' resembling shuttles and muscles, were prepared making use of the ability of copper(I) to assemble two phenanthroline ligands in a stable tetrahedral environment, combined with the affinity of copper(II) species for higher coordination numbers. A molecular rod functionalized with phenanthroline and terpyridine building blocks was combined with a phenanthroline based rotaxane copper(I) complex (**10**, Figure 8). In the 1+ oxidation state the copper ion is accommodated between both phenanthroline units. Oxidation of the copper ion to its 2+ oxidation state increases the affinity of the phenanthroline rotaxane copper complex towards the terpyridine unit, resulting in shuttling of the macrocycle over the molecular rod. This process is fully reversible and could also be induced photochemically by irradiating the MLCT transition of the bis-

phenanthroline copper(I) complex.[21] These studies were extended to mimic muscle action by designing a molecular assembly in which two filaments can glide along one another.[18a]

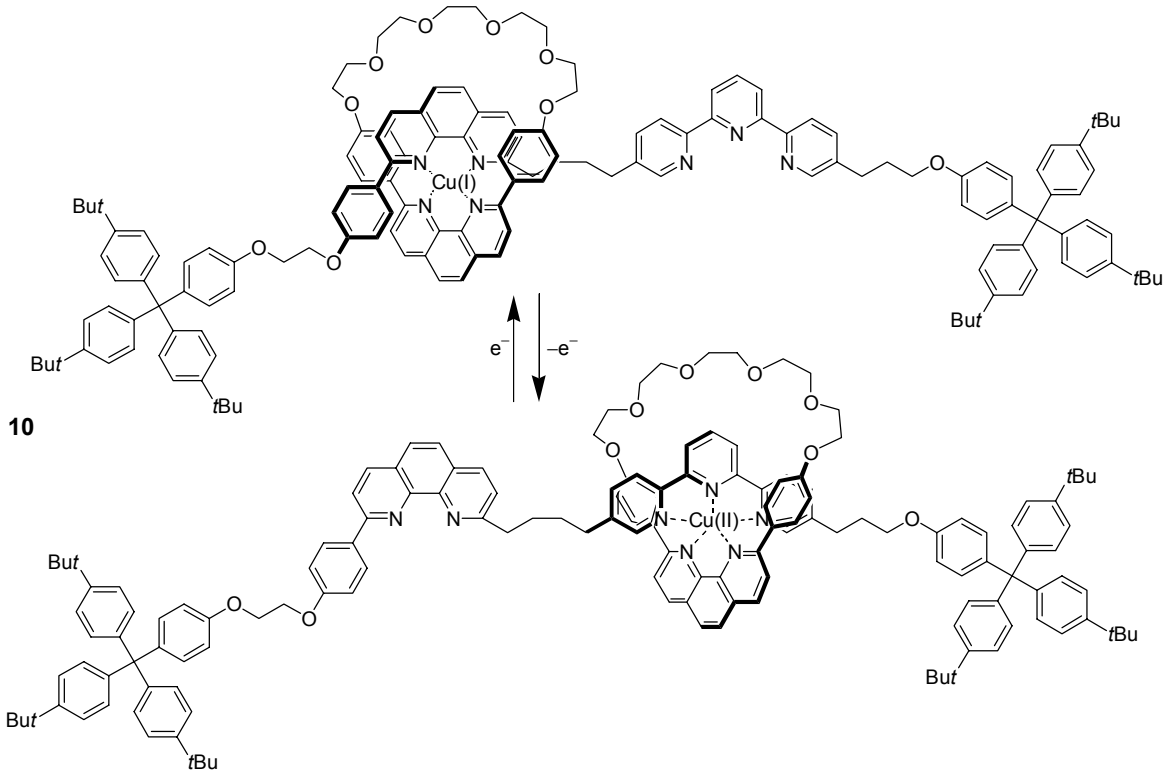

Figure 8. Shuttling of copper(I) phenanthroline rotaxanes over a molecular rod.

1.2.2. Crystal Engineering

The design, modeling and synthesis of ordered solids, *i.e.* crystal engineering, by predefined aggregation of molecules and ions is of interest for applications in fields within material science, such as (opto)electronics and the construction of nanoporous or biomimetic materials.[2a] A prerequisite for success is the understanding of the intermolecular forces involved in the assembly of the individual parts. The fast majority of molecular architectures in the field of inorganic crystal engineering are covered by coordination networks. The coordination bonding capacity of transition metals is utilized to build-up three-dimensional supramolecular arrangements with crystalline periodicity.[2b] These networks generally utilize bipyridyl-type ligands with the N-donor atoms situated in a predefined geometrical arrangement to act as a bridge or joint between (late transition) metal atoms.[22] The suitability of the obtained materials for solid-state reactivity, catalysis, or in sensor applications appears to be dependent on the availability of large accessible spaces. It is often difficult to obtain this nanoporosity, since self-entanglement or interpenetration of the networks, can lead to densely packed structures.[2b] Crystallization in the presence of removable guest molecules has given some success in this respect, creating channels and cavities in the crystal lattice.[23] A special

case in the adsorption and desorption of guest molecules in the crystalline state is based on the SO_2 adsorbing properties of platinum(II) NCN-pincer complexes (NCN = 2,6-bis[(dimethylamino)methyl]phenyl anion).[24] The *para*-hydroxy functionalized cycloplatinated NCN-pincer complex (**11**) forms α-type linear hydrogen bonded networks in the crystalline state, an example of M–X···H bonding. Adsorption and desorption of SO_2 on the platinum center of **11** is fully reversible in the crystalline state (Figure 9) and occurs *via* crystal-to-crystal transformations accompanied by a color change, and expansion and shrinkage of the crystal. Interestingly, the crystalline gas sensor material does not contain a channeled structure, indicating that large voids in the structure are no prerequisite for nanoporosity.

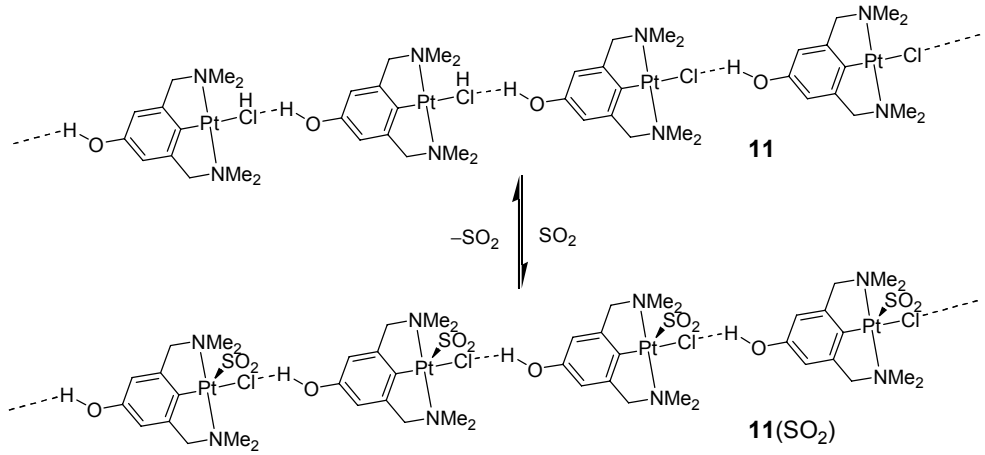

Figure 9. Reversible SO_2 adsorption and desorption op NCN-pincer platinum complexes in the crystalline state.

Apart from ligand coordination, hydrogen bonds are widely employed to obtain predefined crystalline architectures.[25] Hydrogen bonds are considered to be essentially electrostatic in nature, are relatively strong and posses a highly directional character. Their strength can be improved by employing ionic charges, *i.e.* cationic donors and anionic acceptors, combining the hydrogen bond directionality and the strength of coulombic forces. Additionally, the use of metal ions permits a larger choice of components, which may possess different topologies, as well as different bonding and electronic characteristics.[2] An illustrative example in this respect is the study of metallocene dicarboxylic acid structures.[26] The solid-state structure of various hydrogen bonded, nearly isostructural, organometallic building blocks depends on their charges. While neutral ferrocene dicarboxylic acid (**12**) forms dimers in the solid state, its positively charged cobalt(III) analogue (**13**) forms chains, as well as the anionic singly deprotonated ferrocene dicarboxylic acid (**14**) (Figure 10). These studies were also performed with carboxylic acid functionalized chromium bis-arene complexes, showing similar trends.[27]

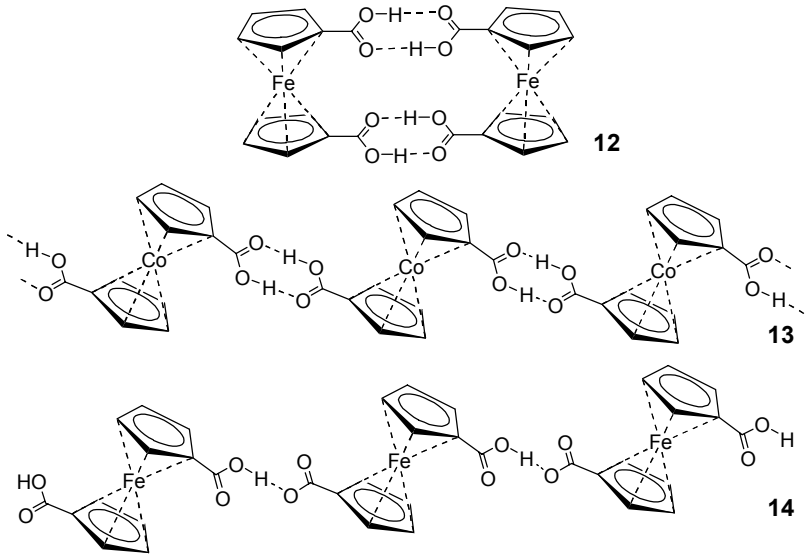

Figure 10. Hydrogen bonding motives in (charged) metallocene dicarboxylic acids.[26]

In addition to the carboxylic acid functionalized complexes, Braga *et al.* introduced alcohols and amines on the cyclopentadienyl ring to extend their library of ferrocene based organometallic building blocks for crystal engineering.[28] The group of Brammer prepared hydrogen bonded zigzag ribbons based on the π-bonded $Cr(CO)_3$ benzene tricarboxylic acid building block. While two carboxylic acid moieties are involved in the formation of the ribbon, the third is hydrogen bonded to an ether molecule. No honeycomb structure, as is known for benzene tricarboxylic acid, is observed.[29] Recently, a catalytically active indium(III) three-dimensional solid-state framework was obtained by assembly of 1,4-benzene dicarboxylic acid and an indium(III) salt in the presence of water and base.[30] The crystals are constructed from $[In_2(OH)_3]_\infty^{3+}$ sheets which are interconnected by 1,4-benzene dicarboxylate units acting as pillars, with each carboxylate connected to two indium ions. This material is active in the reduction of nitroaromatics and the oxidation of sulfides. Kinetic data suggest that the catalyzed reactions only take place at the surface of the material, due to the small size of the pores in this structure.

Although ligand coordination and hydrogen bonding can be considered as most useful for crystal engineering purposes, other interactions also possess a sufficient degree of directionality. The π-π stacking of arene ligands, especially porphyrins, forms a reoccurring motive in crystalline systems.[31] Hosseini *et al* applied weak van der Waals interaction in the construction of linear one-dimensional networks based on unsymmetrical bis-calixarene molecules (coilands) and appropriate connectors.[32] The linear rods are hold together by a lock-and-key fit of the connector in the coiland, with van der Waals interactions acting as single attractive force.

1.3 Catalyst Immobilization

Immobilization of homogeneous transition metal catalyst on (solid) supports allows facile separation of catalyst and reaction products. This makes recycling of expensive transition metals and ligand systems feasible. The efficient removal of the catalysts leads to cleaner product streams in fine-chemical synthesis. In general, the ligand is grafted on the support system prior to introduction of the transition metal. Ligands are, for this purpose, functionalized at positions distal from the metal binding site, with suitable anchoring groups. Alternatively, metallated ligands can be immobilized directly on the support in either a covalent or non-covalent fashion. While immobilization on regular polymers,[33] and solid supports,[34] has attracted considerable attention, much research has been directed to the use of dendrimers as support systems for catalyst immobilization.[35] These tree-like macromolecules possess well-defined structures and can be functionalized selectively at their core, shell or periphery, depending on their composition. This makes them ideal systems to study various properties of immobilized transition metal complexes in great detail.

An illustrative example in this field was published by Togni *et al.* and involves the use of dendrimers functionalized at their periphery with chiral *(R)-(S)*-Josiphos ligands.[36] The dendrimer is constructed form cores based on a cyclophosphazene core (**15a**)[36a] or polycarboxylic acids (**15b-c**),[36b] functionalized with aryl based branching points, containing the phosphane ligand attached by amide linkages (Figure 11). Conversion into their corresponding rhodium(I) complexes was achieved by treatment with [Rh(cod)](BF_4) affording chiral catalysts for the asymmetric hydrogenation of dimethyl itaconate in methanol. High enantioselectivities (>98%), only slightly lower than those of the parent *(R)-(S)*-Josiphos complex, were obtained with these dendritic systems.

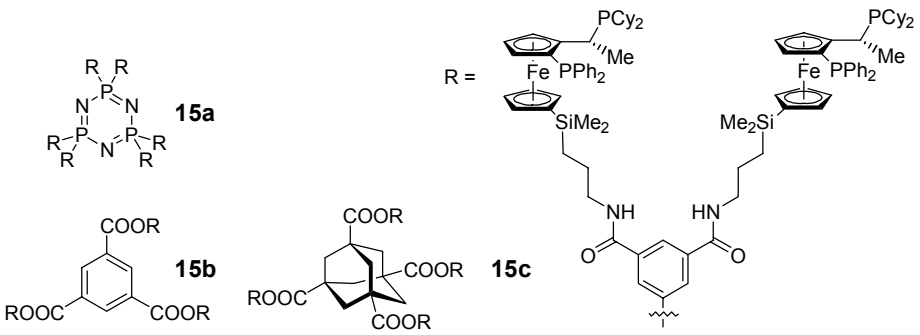

Figure 11. Chiral dendritic phosphane ligands for asymmetric rhodium(I) catalysis.[36]

The ferrocenyl based phosphane functionalized dendritic wedge forms the essential organometallic building block in the preparation of this system, since the catalytically active rhodium(I) complex is prepared *in situ* as final step of the total synthesis. This exemplifies the

stability of selected organometallic fragments such as ferrocene, which can be treated as inert functional groups in organic synthesis.

The encapsulation of a catalytically active transition metal complex within dendrimer wedges allows shielding of the catalytic system and tuning of its microenvironment. Starting from a chiral TALDOL building block, Seebach *et al* prepared titanium(IV) TALDOLates functionalised with Fréchet-type wedges up to the fourth generation (**16**, Figure 12).[37] The chiral catalyst shows very high enantioselectivities (98:2) in the addition of diethyl zinc to benzaldehydes. Additional functionalisation of the dendritic wedges with styrene moieties allowed cross-linking of the system in a polystyrene support, making successful catalyst recycling facile.

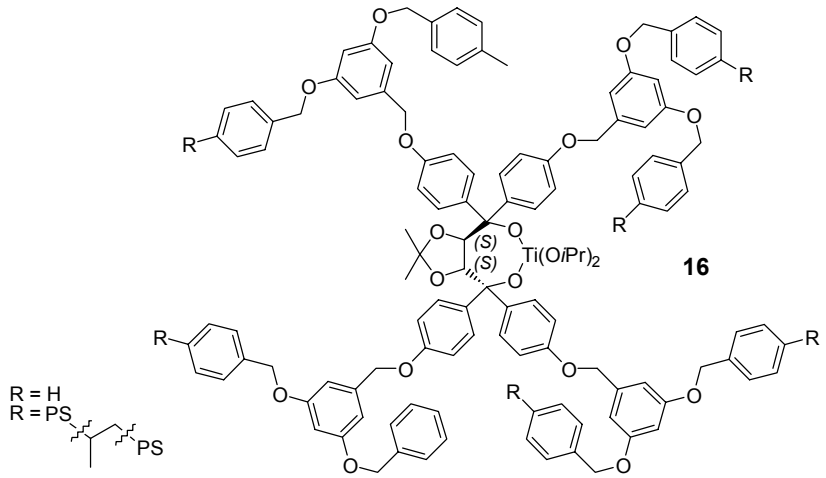

Figure 12. Dendrimer/polystyrene encapsulated Ti(IV) TALDOLates for the enantioselective addition of $ZnEt_2$ to benzaldehyde.[37]

A recent alternative approach for catalyst immobilization is the non-covalent anchoring of transition metal complexes onto dendritic support systems. Loading of the dendrimer by non-covalent interactions allows separate construction of support and catalyst, followed by facile immobilization under mild conditions. Additional advantages involve refunctionalization of the support in the case of catalyst deactivation, and eventually immobilization of mixtures of catalytically active components. While the use of dendrimers for the supramolecular immobilization of organic guest molecules has been well established,[38] there are only few examples involving the non-covalent immobilization of homogeneous catalysts.[39,40] Reek and Meijer reported the non-covalent immobilization of phosphane ligands on urea adamantyl functionalized poly(propylene imine) dendrimers (**16**, Figure 13).[39] Multiple hydrogen bonding interactions, in addition to a strong coulombic attraction, between the urea-functionalized phosphane ligand and the dendrimer allow selective binding of 32 ligands on

the periphery of the dendrimer. Subsequent treatment of the material with [(cod)PdMeCl] afforded a supramolecularly assembled system with catalytic activity in allylic amination reactions. The coordination complexes formed with a phosphane-to-palladium ratio of 2 showed high retentions in a continuous flow membrane reactor. Lower phosphane:palladium ratios led to considerable leaching of the catalyst.

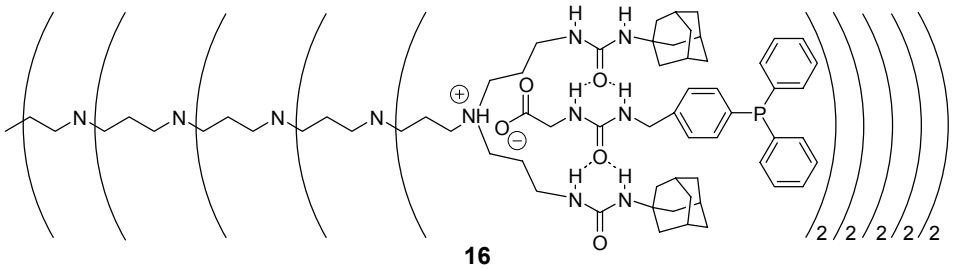

16

Figure 13. Immobilized phosphane ligand on the periphery of urea adamantyl functionalized poly(propylene imine) dendrimer.

In our group, coulombic interactions were applied for the immobilization of organometallic NCN-pincer complexes.[40] Polycationic dendrimers, based on a polybenzylammonium core and Fréchet-type dendritic wedges, were loaded with sulfate functionalized NCN-pincer palladium complexes using anion exchange (**17**, Figure 14). Activation of the complex by halide abstraction afforded an assembly with catalytic activity in Lewis-acid catalyzed aldol reactions. Alternatively, the NCN-pincer palladium complex could be activated prior to assembly onto the dendrimer. The efficiency and retention of **17** in continuous flow membrane reactors was not investigated.

Systems **16** and **17** differ with respect to the assembling method. In the preparation of the palladium complex of **16** the metal center is introduced in the final stage of the synthesis by forming coordinative bonds to already immobilized phosphane ligands. These polyphosphane ligands can be used for the complexation of various metals with different catalytic properties. However, leaching of the metal by decomplexation of the ligand can occur even when the ligand is retained in the dendrimer host. In contrast, **17** is prepared by the assembly of the organometallic building block and dendritic host in one step. The covalent M–C bond ensures that the metal is retained in the coordination sphere of the ligand, and leaching of the transition metal can only occur in case of complete removal of the complex from the dendritic host.

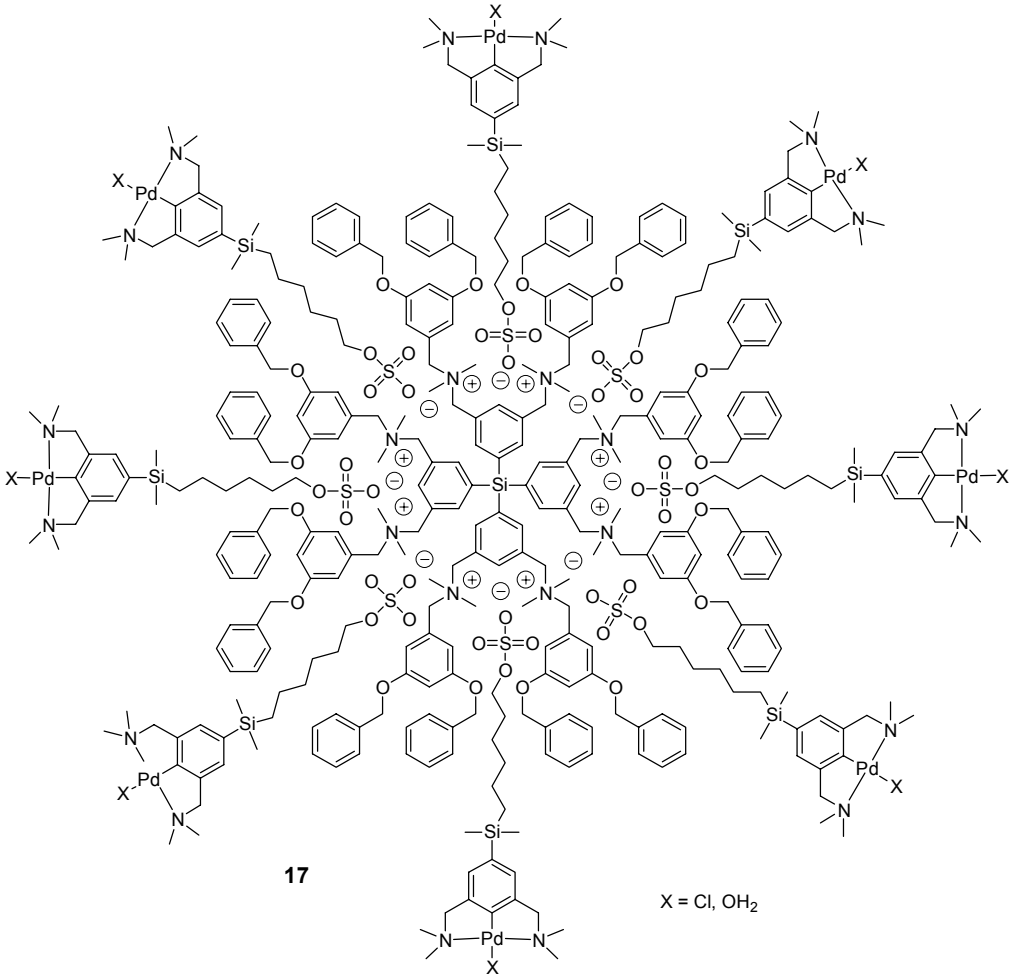

Figure 14. Catalytically active assembly of NCN-pincer palladium complexes onto a polycationic dendrimer.

1.4 Supramolecular Catalysis

An exciting application of transition metal building blocks is the design, construction, and evaluation of supramolecular catalysts.[3] A key source of inspiration in the development of supramolecular catalysts is found in enzymatic catalysis. Enzymatic catalysts have evolved over millions of years through mutation and selection, and represent the highest expression of chemical catalysis. They achieve astonishing selectivities by deploying intermolecular forces to guide the substrate precisely along a predestinated reaction pathway. Catalysis takes place within a supramolecular aggregate, resulting in high effective concentrations of substrate near the catalytic site, leading to high catalytic activities.[3] Another feature of (enzymatic) catalysts involves selective stabilization of the highest energy transition state, thereby reducing the activation enthalpy of the reaction.[41] Transition metal based supramolecular catalysts are generally constructed by combining known homogeneous catalysts with known host molecules, such as crown ethers, cyclodextrins, cyclophanes, and calixarenes. Modification of the ligand, allowing strategic placement of receptor sites with respect to the catalyst, forms an

essential step in the preparation of supramolecular catalysts. Examples are ordered with respect to the type of catalyzed reactions, and thus the type of catalytic building block.

1.4.1 Ester Hydrolysis

The fast majority of supramolecular catalysts is active in ester cleavage reactions, based on either fully organic groups for general acid-base catalysis, or on the use of zinc(II), cobalt(III), barium(II) or copper(II) coordination complexes. The combination of multiple metal sites on a linker is often a successful approach to obtain highly active catalysts with synergic action of the metal sites in catalysis.

The cation complexing abilities of crown ethers have been applied in the construction of a dinuclear barium(II) complex (**18**) for ester and amide cleavage (Figure 15).[42] Complex **18** has two identical Ba^{2+} sites, which perform different functions. One of the metal ions binds and activates the ethoxide nucleophile, while the other side anchors the amide or ester by the distal carboxylate moiety on the substrate. Hence, the amide or ester moiety is in close vicinity of the activated ethoxide, resulting in cleavage.

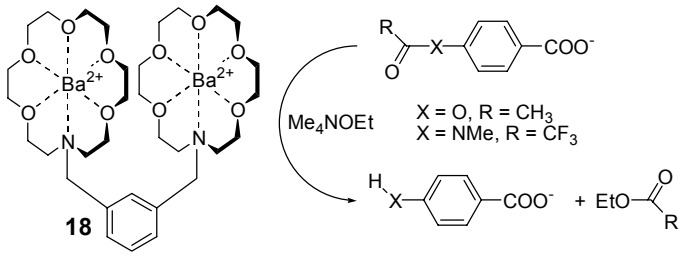

Figure 15. Dinuclear barium(II) complex for supramolecular ester and amide cleavage.[42]

Extended studies were performed towards the hydrolytic activity of di- (and tri-)nuclear metal ion complexes based on calix[4]arenes and N-donor ligands as molecular scaffolds by Reinhoudt *et al*. The metal ions in complexes **19** and **20** are placed at the upper rim of the calix[4]arene, at diametrical positions (Figure 16). The substituents on the lower ring (ethoxyethyl) prevent inversion of the aromatic units through the cavity of the macrocycle.[43]

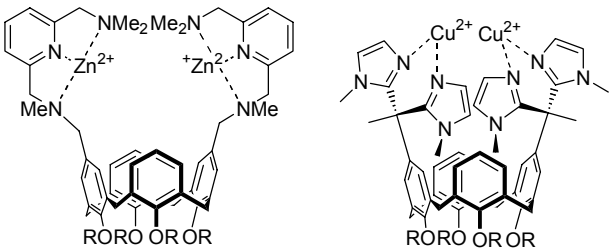

Figure 16. Calix[4]arene based dinuclear complexes as metallo-phosphodiesterase model.[43]

In the studies, various phosphate esters and RNA 3',5'-dinucleotides (NpN) were used to screen the catalysts for their phophodiesterase activity. The activity of the dinuclear complexes **19** and **20** was increased considerably when compared to the mononuclear complex (50-fold), or the mononuclear complex lacking the calix[4]arene scaffold (300-fold). The bimetallic complexes show saturation kinetics, with binding constants with the substrate in the order of 10^4 M^{-1}. Both the flexibility and the preorganizing ability of the calix[4]arene, are important factors in their efficiency. A decrease in flexibility by connecting the oxygens on the lower rim with a rigid spacer, resulted in reduced activity. The pH-rate profiles of both catalysts are bell-shaped with optimums located at pH 7.4 and 6.4 for **19** and **20**, respectively. Introduction of a third metal binding site at the upper rim leads to a threefold increase in turnover rate, while the binding affinity of the substrate is reduced considerably. The application of a statistical 1:2 mixture of copper(II) and zinc(II) leads to species with higher activity than their homonuclear analogues.[43]

Another successful example in the supramolecular cleavage of esters is published by the group of Breslow.[44] Two β-cyclodextrins are attached to a bipyridine moiety, according to a design based on computer models (**21**, Figure 17). Complexation of a metal(II) ion (Cu(II), Ni(II), Zn(II)) to the bipyridine fragment places the metal in an ideal place to coordinate to the carbonyl oxygen, and to deliver a hydroxide anion to the substrate. Since the sum of the binding energy of the products is less compared to the binding energy of the substrate alone, product inhibition is not observed. Rate enhancements up to 225,000 for designed substrates (**22**) are observed. In the absence of the copper(II) ion this rate enhancement is only 80-fold. Copper(II) is the most active metal, albeit that in the presence of a nucleophilic bound oxime ligand zinc(II) ions give rate accelerations up to 1,700,000 in the hydrolysis of **22**.

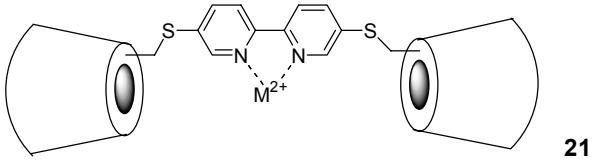

21

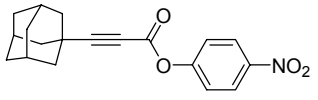

22

Figure 17. Catalytic cyclodextrin dimer with a metallobipyridyl group.[44]

Porphyrin complexes are, apart from their application as (ep)oxidation and hydroxylation catalysts, useful building blocks in the construction of host molecules. Sanders *et al.* synthesized a cyclic zinc(II) porphyrin trimer (**23**) which is capable of acyl transfer by holding the substrates in close proximity (Figure 18).[45]

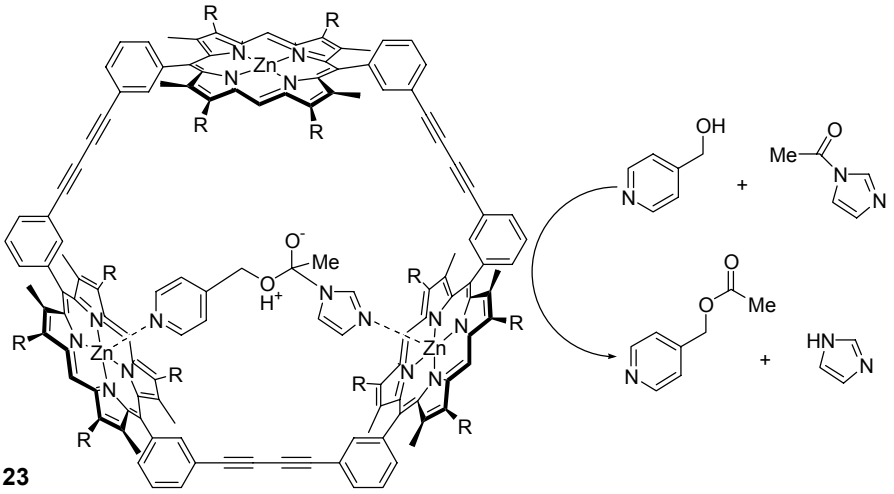

Figure 18. Cyclic zinc(II) porphyrin trimer for acyl transfer reactions.[45]

The substrates are functionalized with pyridyl and imidazole groups which can coordinate to the zinc(II) ions, positioning the substrates in an optimal way to react. The reaction rate was enhanced 16 fold compared to a monomeric zinc(II) porphyrin. The reaction is inhibited by 1,3-bis(4-pyridyl)propane, and the average turnover number per trimer after 160 hours is around 25, without detectable decomposition or loss in activity.[45]

1.4.2 Oxidation Reactions

Selective (mild) oxidations, epoxidations and hydroxylations form an important class of reactions in organic synthesis. Most homogeneous catalysts in these fields are based on their biological counterparts, for their astonishing substrate and product selectivities. Metalloporphyrins constitute an important class of epoxidation and hydroxylation catalysts in attempts to mimic the behavior of the enzyme cytochrome P450, which converts alkanes into alcohols. The naked manganese porphyrins degrade fairly rapidly under catalytic reaction conditions, like the iron heme mimics. The primary mode of deactivation under these conditions is the formation of an inactive μ-oxo bridged dimer (Mn–O–Mn).[46] In analogy with the protein superstructure, with the metalloporphyrin encapsulated in a regulated nanospace formed by the folded amino acid chain, synthetic metalloporphyrins have been functionalized with bulky substituents and other functional units. The steric bulk not only prevents the primary deactivation mode, but also introduces regioselectivity in, for example, alkane hydroxylations.[47]

Apart from creating steric bulk around the metalloporphyrin to induce shape selectivity, iron(III) porphyrins 'capped' with chiral bridging groups have been applied in asymmetric catalysis (**24** and **25**, Figure 19). Iron(III) porphyrin **24** is an elegant example of asymmetric

induction in the hydroxylation of ethylbenzenes. The chiral binaphtyl cavity imposes a preferential orientation of the substrate to the catalyst, leading to a stereoselective outcome of the reaction.[48] In the iron(III) binaphtyl 'capped' porphyrin **25** two chiral binaphtyl groups are placed above each face of the metalloporphyrin. The ether linkages force the binaphtyl groups into close proximity to the metal center, imposing a rigid chiral environment. Asymmetric epoxidations of various aromatic alkenes with iodosylbenzene as oxygen donor gave high ee's (up to 63%) for monosubstituted alkenes. The more sterically demanding disubstituted alkenes gave only moderate ee's (20-30%).[49]

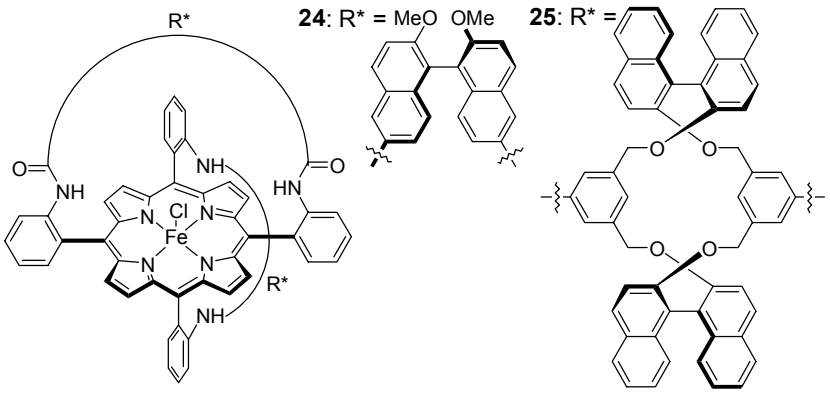

Figure 19. Chiral 'capped' iron(III) porphyrins for asymmetric hydroxylation (**24**) and epoxidation (**25**).[48,49]

Substrate binding in the vicinity of the metalloporphyrin was accomplished by Breslow and co-workers, giving access to the regioselective hydroxylation of steroids. A manganese(III) TPP with β-cyclodextrins connected to the phenyl rings, hydroxylated an andostanediol derivative selectively at the 6α-position (**26**, Figure 20). The substituents attached to andostanediol are chosen to optimize complexation of the substrate in two opposite cyclodextrins, placing the 6α-carbon atom on top of the oxygenated manganese atom for hydroxylation. The stability of the catalyst against oxidative degradation is increased to a great extent by fluorination of the four phenyl rings, improving the turnover number from 3-5 to 95.[50]

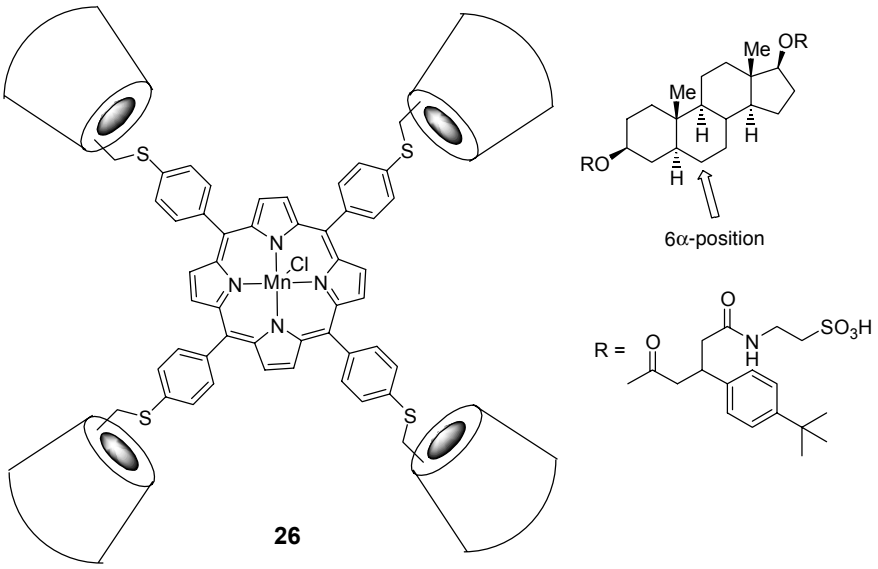

Figure 20. Supramolecular manganese-porphyrin hydroxylation catalyst.[50]

A similar system was synthesized by Woggon *et al.* for the central (15,15') cleavage of β,β-carotene (Figure 21), mimicking carotene dioxygenases. Two cyclodextrin moieties are attached with their primary rim on the two opposite sites of a tetraphenylporphyrin using ether linkages instead of the thioether links used in **26**. This spatial orientation makes it an ideal host to complex both distal aliphatic groups of the β,β-carotene in the cyclodextrin cavities with binding constants in the order of 10^6 M^{-1}, enforcing the central C=C bond above the metal coordination site of the porphyrin. Its ruthenium complex is capable of central cleavage of β,β-carotene, however competitive cleavage of the C11'–C12' and the C9'–C10' double bonds form serious site reactions due to lateral movement of the carotene in the cyclodextrin cavities. Modification of the substrate into Phe-β-carotene, suppresses the lateral movement, giving exclusive central cleavage at C15–C15'. Exocentric cleavage at C7'–C8' is in both cases not observed.[51]

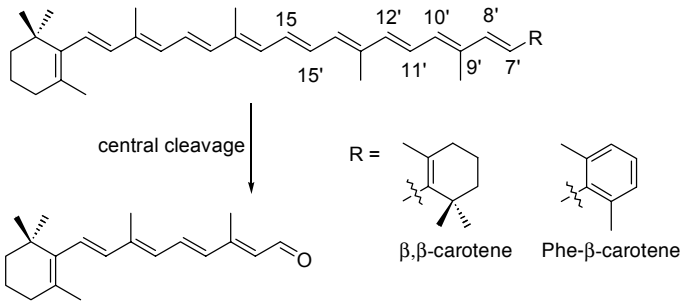

Figure 21. Central cleavage of β,β-carotene or Phe-β-carotene by cyclodextrin functionalized ruthenium porphyrins.

Supramolecular catalysis with systems based on cyclophane hosts has been extensively studied by the group of Diederich. Cyclophanes provide excellent hosts for the encapsulation of aromatic guest molecules in aqueous and other protic solvents.[52] A porphyrin bridge was introduced on a tetramine cyclophane and tested for its catalytic activity in the oxidation of acenaphtylene, a substrate which binds strongly in the macrocyclic cyclophane ring (**27**, Figure 22). Acenaphten-1-one is the major isolable product in the oxidation with iodosylbenzene as oxygen-transfer reagent. Support for supramolecular catalysis is provided in a competition experiment with the unreactive phenanthrene, reducing the yield of naphten-1-one considerably.[53]

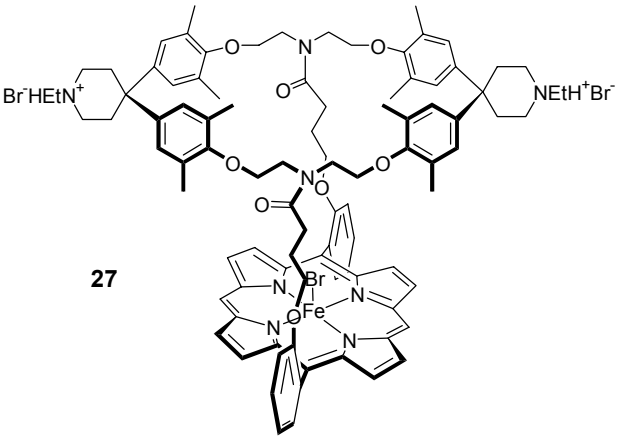

Figure 22. Porphyrin-bridged cyclophane host for supramolecular oxidation of acenaphtylene.[53]

1.4.3 Carbon-Carbon bond formation and activation

In contrast to supramolecular ester hydrolysis and oxidation reactions, less is known concerning supramolecular catalysis of C–C bond forming reactions. While homogeneous transition metal catalysts play a crucial role in important organic transformations involving the C–C bond, they were hardly studied in the context of supramolecular catalysis. A cyclophane-type host molecule, functionalized with a bisoxazoline ligand incorporated in the macrocyclic ring, was applied in the supramolecular Cu(I) catalysed cyclopropanation of styrene with diazoacetate (**28**, Figure 23).[54] The cyclophane ligand forms a C_2-symmetric complex with copper(I) inducing a certain degree of helicity to the bridge. The cyclopropane ring is formed in the catalytic cycle by nucleophilic attack of the copper-bound carbene to the prochiral alkene. The helicity of the macrocyclic ring can be seen as an extension of the symmetry around the metal center, and can transfer its chiral information over to the substrate bound inside the cavity. The effectiveness of this concept is evident from the high ee's and even more from the high diastereoselectivities observed in the test reactions, compared to those of the parent complex without macrocycle.[54]

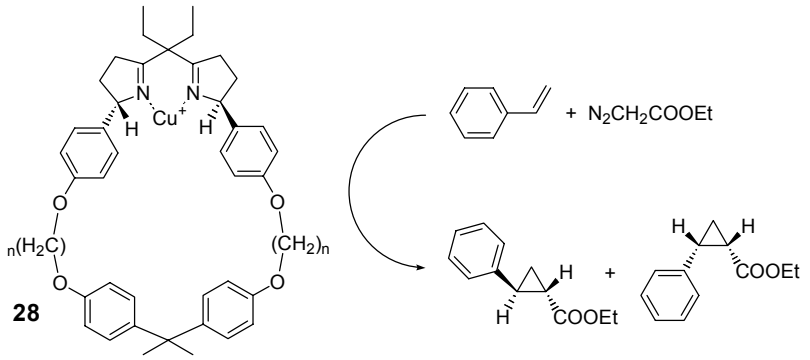

Figure 23. Cyclophane-based copper(I) catalyst for stereoselective cyclopropanation.[54]

Diphenylglycoluryl molecular clips, intensively studied by the group of Nolte, were applied as hosts for supramolecular transition metal catalysed hydroformylation and hydrogenation reactions. Although various architectures failed to show activity or increased selectivity, a molecular clip functionalized with aza-crown ether bis-phosphite building blocks shows substrate selectivity in hydrogenation reactions of functionalized allylarenes (**29**, Figure 24).[55] The exchange of the phosphite ligands for phosphane ligands (**30**) afforded metallohosts capable of shape selective hydroformylations.[56]

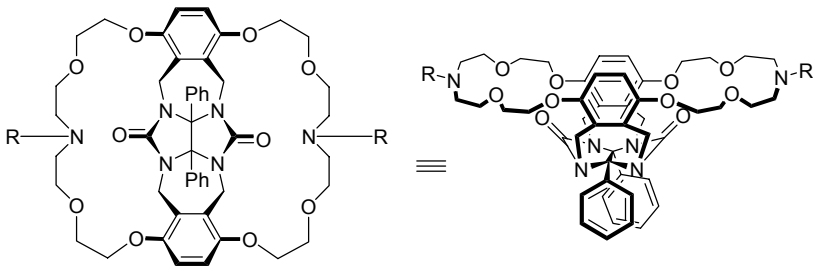

29 R = $CH_2PhOP(OPh)_2$
30 R = CH_2PhPPh_2

Figure 24. Basket-shaped metallohosts for substrate selective hydrogenation (**29**) [55] and hydroformylation (**30**).[56]

Substrates with the ability to bind in the cleft by a combination of hydrogen bonding to the carbonyl groups and π-π stacking with the aromatic walls, such as allylresorcinol and allylcatechol, are converted preferentially over substrates incapable of hydrogen bonding interactions. Surprisingly, the metallohost hardly influences the linear to branched ratio in the hydroformylation reactions with **30**.

1.5 Bio-Organometallic Chemistry

The modification of biologically active molecules, such as proteins or sugars, with transition metal complexes can give useful insights in structure and function of biomolecules and has given rise to various medicinal applications.[57] Werner-type complexes with hard N, O, or S

donor ligands have been applied mostly in this respect. Of recent interest is the application of robust organometallic complexes in biochemistry.[58] Characteristic chemical and spectroscopic properties of organometallic complexes can be applied for site-selective reaction with biomolecules, or as markers for the direct detection of the bio-organometallic material.[57]

The use of transition metal carbonyl complexes is attractive, since the carbonyl stretching frequency forms a valuable probe for (drug) detection purposes. Characteristic bands are formed for adducts of the carbonyl complexes with peptides or steroid hormones, allowing a simultaneous qualitative and quantitative essay of multiple components with very small detection limits without the need for radioactive markers.[59] Grotjahn *et al* applied donor substituted cyclopentadienyl ruthenium complexes (**31**) for selective labeling of amino acids in a peptide chain. Treatment of a model polypeptide with **31** resulted in the selective formation of η^6-bonded ruthenium complexes on the arene rings of the phenylalanine residues of the polypeptide (Figure 25).[60] This method was effective for the selective labeling of the 27 amino acid polypeptide secretin.

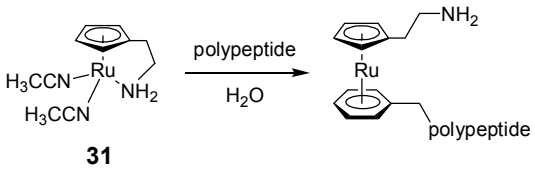

31

Figure 25. Labeling of a polypeptides with ruthenium complexes.[60]

NCN-pincer platinum complexes are used in our group as peptide labels with potential applications as diagnostic biomarkers and biosensors. NCN-pincer platinum complexes exhibit characteristic ^{195}Pt-NMR signals, which is a valuable tool for probing the steric and electronic environment of the metal. Additionally they form bright orange complexes in the presence of SO_2 making facile detection of the complex feasible. The high robustness of the NCN-pincer platinum complexes allows their application in the aqueous and aerobic conditions encountered in biological systems. As a consequence of this stability, pincer platinum species could be covalently bonded to the N-terminus of L-valine, or on the side-chain of L-lysine.[61] Interestingly, transformations on the ligand were possible after metallation of the ligand, generating more flexibility in the synthesis of the bio-organometallic species. Indeed, NCN-pincer palladium complexes could be functionalized at the N- and C- terminus of L-valine, and on the N-terminus of the dipeptide L-Phe-L-Val-OMe (**32**, Figure 26).[62]

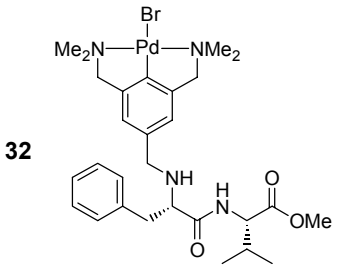

Figure 26. NCN-pincer palladium functionalized dipeptide L-Phe-L-Val-OMe.[62]

1.6. Tuning of Transition Metal Complexes

Apart from ligand-functionalization employed for anchoring opportunities, *i.e.* the building block approach, it can be used to tune the metal center of the resulting complexes electronically. This methodology can be especially useful in cases where the influence of the substituent can be rationalized. The empirical Hammett equation has been used widely for treating the effect of substituents on rates and equilibria of organic reactions. Furthermore, correlation analysis is applied with success with several other properties, such as ^{13}C- and ^{19}F-NMR chemical shifts.[63] The use of the Hammett correlation to quantify the influence of substituted (aromatic) ligands on transition metal complexes, and consequently on their catalytic and/or optical properties has been used with varying success. However, if successful it allows theoretical prediction of properties from the resulting complexes.

In studies directed toward the prediction of the oxidative reactivity of vanadium peroxo complexes, Di Furia *et al*. found Hammett-type correlations between the ^{51}V-NMR chemical shift and the σ values of the substituents on *meta*- and *para*-substituted pyridine and aniline ligands (**33**, Figure 27).[64] Upon increasing the electron density on the vanadium nucleus by placement of electron donating substituents, the chemical shift of the complexes decreases. By calculation of the ^{51}V gyromagnetic ratios from the chemical shift data of various N∩O or O∩O ligated peroxo vanadium complexes (not shown), the authors found linear correlations between the gyromagnetic ratios and λ_{max} values of the lowest energy electronic (n→d) transition. These correlations allow the prediction of reactivity for the peroxo vanadium complexes and tuning of the band gap of the frontier orbitals, based on ^{51}V-NMR chemical shift data.

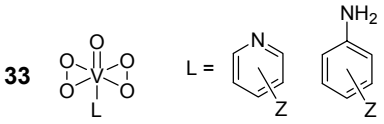

Figure 27. Peroxo vanadium complexes with substituted pyridine and aniline ligands.[64]

Reinhoudt *et al*. studied the coordination chemistry of cationic SCS-pincer palladium complexes with substituted pyridines (**34**, Figure 28).[65] Linear Hammett correlations were found between σ^+ substituent constants and the stability of the resulting pyridine-palladium complex, reflected in their association constants.

34

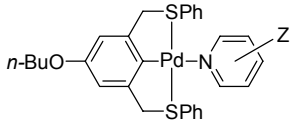

Figure 28. SCS-pincer palladium complexes with substituted pyridines.[65]

An example from our group involves the electronic tuning of NCN-pincer nickel complexes by *para*-substitution (**35**, Figure 29).[66] Investigation of the complexes by ^{13}C-NMR and electrochemistry revealed Hammett-type correlations for ^{13}C chemical shift differences (δC_{ipso}-δC_{ortho}), as well as for the oxidation potentials ($E_{p.a}$) of the nickel complexes with the σ_p substituent constants. Especially the quantification of the substituent effect on the Ni(II)/Ni(III) oxidation potential by correlation analysis is a powerful tool for tuning the reactivity of the catalytically active NCN-pincer nickel complexes. Their catalytic activity in the Kharasch addition of polyhalogenated alkanes to alkenes, involving one-electron transfer of the nickel(II) atom to the substrate, is directly affected by *para*-functionalization. Electron donating substituents decrease the oxidation potential of the Ni(II)/Ni(III) couple, resulting in more active one-electron transfer catalysts.

35

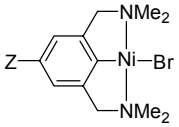

Figure 29. *Para*-substituted NCN-pincer nickel complexes.[66]

1.7 Conclusions and Outlook

Organometallic and coordination chemistry is originally mainly focused on the metal center itself, tuning its direct coordination environment, and consequently its properties by subtle variations in the ligand system. By choosing the appropriate combination of metal and ligand systems, transition metal complexes can exhibit characteristic properties, allowing applications as catalyst or as sensor materials. A more recent challenge in inorganic chemistry forms the application of organometallic and coordination complexes as building blocks in the construction of new (transition) metal based materials, as is evident from the ample examples available in literature. The selected examples shown in this chapter illustrate the broad field of potential applications, but should not be considered as comprehensive. Key sources of

inspiration are found in biological systems, but also in organic chemistry, which is more developed with respect to supramolecular chemistry and crystal engineering.

Apart from few selected examples, ligands are functionalized or immobilized prior to the introduction of the metal, making the suitably functionalized ligand the actual building block in the syntheses. The transition metal complex is recognizable as building block in the final product, but is often not introduced as such. This is especially true for coordination complexes, which are prepared under mild conditions by treatment of the ligand with a metal salt. The formation of organometallic complexes in the final stage of the synthesis is often more problematic, as formation of M–C bonds requires more demanding reaction conditions. Metallation in earlier stages of the synthesis forms an attractive alternative, generating true organometallic building blocks. Obviously, this approach is only applicable for relatively stable organometallic complexes. The increasing availability of easily accessible transition metal building blocks, and the stability of part of them, generates a transition metal complex 'meccano kit' for the preparation of materials ranging from engineering solids to supramolecular catalysts and bio-organometallic materials.

Apart from the use of functionalized transition metal complexes as (supramolecular) building blocks, ligand substitution offers a powerful tool to tune the metal center of the resulting complexes electronically. In cases where correlation analysis can be applied to rationalize the influence of the substituent, theoretical prediction of their properties becomes feasible.

1.8 Aim and Scope of this Thesis

The work described in this thesis was part of the CW/STW project 'Molecular Recognition in Dendritic Catalysts'.[67] The aim of this project was the use of supramolecular interactions for either substrate binding in catalytic dendrimers or catalyst immobilization in dendrimers. Both concepts combine the advantage found in homogeneous (supramolecular) catalysis, *i.e.* well-defined catalytic sites with high substrate and product selectivities, with the ease of separation and recycling found in heterogeneous catalysis. Essential for the development of these systems is the availability of suitably functionalized organometallic building blocks. The NCN-pincer ligand forms an attractive ligand to use in this respect, since it has shown its versatility in various catalytic and sensor applications.[68,69] The central theme in this thesis is the preparation and application of organometallic NCN-pincer complexes as building blocks in the construction of new (macromolecular) organometallic materials. *Chapter Two* describes the development of synthetic routes towards new *para*-functionalized NCN-pincer complexes, and the influence of the substituent on the properties of the complex. Surprisingly, various substitution reactions, involving rather vigorous reaction conditions, can be performed after

metalation of the ligand, exemplifying the high stability of these complexes. The NCN-pincer palladium and platinum complexes presented in *Chapter Two* form the essential building blocks for the preparation of the organometallic materials described later in this thesis. One aspect of the functional groups introduced on the pincer ligand system can give rise to new interactions and assembly features, in solution as well as in the solid state. *Chapter Three* describes the formation of *para*-nitro functionalized NCN-pincer palladium dimers in the solid state by electron donor-acceptor interactions between the metal center and the nitro substituent.

The availability of an additional anchoring point on the NCN-pincer ligand in the form of a *para*-substituent makes the introduction of additional functional moieties feasible. The synthesis, properties and catalytic application of a tweezer shaped complex based on an NCN-pincer palladium complex and a polycyclic aromatic pyrenoxy unit is presented in *Chapter Four*. The flexibility of the tweezer is studied in detail using various analytical tools, among which the pyrenoxy unit is used as fluorescent probe. *Chapter Five* describes the synthesis of NCN-pincer palladium complexes for immobilization purposes containing an additional binding site for functional groups.

The final chapters of this thesis are directed to the use of hyperbranched polymers (polyether polyols), as alternative for dendrimers as macromolecular support systems. These polymers are randomly branched, but still possess a low polydispersity, and offer the advantage of being synthesized in a one-step polymerization step. In *Chapter Six*, nanocapsules based on hyperbranched polyglycerol are applied in the non-covalent encapsulation of sulfonated NCN-pincer platinum complexes. *Chapter Seven* describes the covalent immobilization of metalated NCN-pincer platinum complexes on hyperbranched polyglycerols. The size and shape of the resulting materials is investigated by TEM, making imaging of these relatively small-sized molecules feasible without staining procedures. The research presented in *Chapter Eight* makes use of chiral hyperbranched polyglycerols for immobilization of NCN-pincer platinum complexes in either a non-covalent or covalent manner, using the methodologies described in *Chapter Six* and *Seven*.

1.7 References

1. (a) Leininger, S.; Olenyuk, B.; Stang, P. J. *Chem. Rev.* **2000**, *100*, 853-908; (b) Stang, P. J.; Olenyuk, B. *Acc. Chem. Res.* **1997**, *30*, 502-518.
2. (a) Braga, D.; Grepioni, F. *Acc. Chem. Res.* **2000**, *33*, 601-608 and references cited. (b) Braga, D. *J. Chem. Soc., Dalton Trans.* **2000**, 3705-3713. Schwab, P. F. H.; Levin, M. D.; Michl, J. *Chem. Rev.* **1999**, *99*, 1863-1934; de Cola, L.; Belser, P. *Coord. Chem. Rev.* **1998**, *177*, 301; Balzani, V.; Juris, A.; Venturi, M.; Campagna, S.; Serroni, S. *Chem. Rev*. **1996**, *96*, 759-834.
3. (a) Beer, P. D.; Gale, P. A. *Angew. Chem. Int. Ed.* **2001**, *40*, 486-516; (b) Sanders, J. K. M. *Chem. Eur. J.* **1998**, *4*, 1378-1383; (c) Hisaeda, Y; Hayashida, O. *Chem. Rev*. **1996**, *96*, 721-758; Kirby, A. J. *Angew. Chem. Int. Ed.* **1996**, *35*, 707-724; (d) Feiters, M. C. in *Compr. Supramol. Chem., Vol. 10* (Ed. Reinhoudt, D. N.), Elsevier, Oxford **1996**, 267-360; (e) Lehn, J. M. *Supramolecular Chemistry*, VCH Weinheim **1995**; (f) Breslow, R. *Acc. Chem. Res.* **1995**, *28*, 146-153;
4. (a) Desijaru, G. R. *Acc. Chem. Res.* **2002**, *35*, 565-573 (b) Desijaru, G. R. *J. Chem. Soc., Dalton Trans.* **2000**, 3745-3751, and references cited.
5. (a) Mathieson, T.; Schier, A.; Schmidbaur, H. *J. Chem. Soc., Dalton Trans.* **2000**, 3881. (b) Pyykkö, P. *Chem. Rev.* **1997**, *97*, 597; (c) Aullon, G.; Alvarez, S.; Inorg. Chem. 1996, 35, 3137-3144.
6. Gillon, A. L.; Lewis, G. R.; Orpen, A. G.; Rotter, S.; Starbuck, J.; Wang, X.-M.; Rodriguez-Martin, Y.; Ruiz-Pérez, C. *J. Chem. Soc., Dalton Trans.* **2000**, 3897; Aullon, G.; Bellamy, D.; Brammer, L.; Bruton, E. A.; Orpen, A. G. *Chem. Commun.,* **1998**, 653-654; Mascal, M. *J. Chem. Soc., Perkin Trans. 2* **1997**, 1999-2001;
7. Carina, R. F.; Williams, A. F.; Bernardinelli, G. *J. Orgmet. Chem.* **1997**, *458*, 45-48.
8. For example: Desmartin, P. G.; Williams, A. F.; Bernardinelli, G. *New J. Chem.* **1995**, *19*, 1109.
9. Imamura, T.; Fukushima, K. *Coord. Chem. Rev.* **2000**, *198*, 133-156 and references cited.
10. (a) Schachter, A. M.; Fleischer, E. B.; Haltiwanger, R. C. *Chem. Commun.* **1988**, 960; (b) Funatsu, K.; Imamura, T.; Ichimura, A.; Sasaki, Y. *Inorg. Chem.* **1998**, *37*, 1798; (c) Chernook, A. V.; Rempel, U.; Borczyskowski, C.; von Shulga, A. M.; Zenkevich, E. I. *Chem. Phys. Lett.* **1996**, *254*, 229.
11. Morris, G. A.; Nguyen, S. T.; Hupp, J. T. *J. Mol. Cat. A* **2001**, *174*, 15-20.
12. Merlau, M. L.; del Pilar Mejia, M.; Nguyen, S. T.; Hupp, J. T. *Angew. Chem. Int. Ed* **2001**, *40*, 4239-4242.
13. Slagt, V. F.; Reek, J. N. H.; Kamer, P. C. J.; van Leeuwen P. W. N. M. *Angew. Chem. Int. Ed.* **2001**, *40*, 4272-4274.
14. See for example: (a) Fujita, M. *Acc. Chem. Res.* **1999**, *32*, 533-61; (b) Fujita, M. *Chem. Soc. Rev.* **1998**, *27*, 417-425; (c) Fujita, M.; Aoyagi, M.; Ibukuro, F.; Ogura, K.; Yamaguchi, K. *J. Am. Chem. Soc.* **1998**, *120*, 611-612. (d) Ibukuro, F.; Kusukawa, T.; Fujita, M. *J. Am. Chem. Soc.* **1998**, *120*, 8561-8562.
15. Fujita, M.; Fujita, N.; Ogura, K.; Yamaguchi, K. *Nature* **1999**, *400*, 52-55.
16. van Maanen, H.-J.; van Veggel, F. C. J. M.; Reinhoudt, D. N. *Top. Curr. Chem.* **2001**, *217*, 121-162.
17. For overviews see: (a) Newcome, G. R.; He, E.; Moorefield, C. N. *Chem. Rev.* **1999**, *99*, 1689-1746; (b) Constable, E. C. *Chem. Commun.* **1997**, 1073-1080.
18. Sauvage, J.-P.; Collin, J.-P.; Chambron, J. C.; Guillerez, S.; Coudret, C.; Balzani, V.; Barigelletti, F.; De Cola, I.; Flamigni, L. *Chem. Rev.* **1994**, *94*, 993-1019.
19. Constable, E. C.; Cargill Thompson, A. M. W.; Harverson, P.; Macko, L.; Zehnder, M. *Chem. Eur. J.* **1995**, *1*, 360-367.

20. (a) Huck, W. T. S.; van Veggel, F. C. J. M.; Sheiko, S. S.; Möller, M.; Reinhoudt, D. N. *J. Phys. Org. Chem.* **1998**, *12*, 540-545. (b) Huck, W. T. S.; van Veggel, F. C. J. M.; Reinhoudt, D. N. *Angew. Chem. Int. Ed.* **1996**, *35*, 1213-1215.
21. (a) Consuelo Jimenez-Molero, M.; Dietrich-Buchecker, C.; Sauvage, J.-P. *Chem. Eur. J.* **2002**, *8*, 1456-1466. (b) Collin, J.-P.; Dietrich-Buchecker, C.; Gaviña, P.; Consuelo Jimenez-Molero, M.; Sauvage, J.-P. *Acc. Chem. Res.* **2001**, *34,* 477-487.
22. For an overview on coordination networks see: Robson, R. *J. Chem. Soc.* **2000**, 3735
23. (a) Carlucci, L.; Ciani, G.; Prosperpio, D.M.; Rizzato, S. *J. Chem. Soc., Dalton Trans.* **2000**, 3821. (b) Braga, D.; Cojazzi, G.; Abati, A.; Maini, L.; Polito, L.; Scaccianoce, L.; Grepioni, F. *J. Chem. Soc., Dalton Trans.* **2000**, 3969.
24. (a) Albrecht, M.; Lutz, M.; Spek, A. L.; van Koten, G. *Nature* **2000**, *406*, 970-974. (b) Albrecht, M.; Lutz, M.; Scheurs, A. M. M.; Lutz, E. T. H.; Spek, A. L.; van Koten, G. *J. Chem. Soc., Dalton Trans.* **2000**, 3797-3804.
25. (a) Mareque Rivas, J. C.; Brammer, L. *Coord. Chem. Rev.* **1999**, *183*, 43; Guru Row, T. N. *Coord. Chem. Rev.* **1999**, *183*, 81.
26. (a) Braga, D.; Maini, l. ; Polito, M.; Grepioni, F. *Chem. Commun* **1999**, 1949; (b) Takusagawa, F.; Koetzle, T. F. *Acta Cryst. Sect. B.* **1979**, *35*, 2888.
27. Braga, D.; Maini, L. *Organometallics* **2001**, *20*, 1875-1881.
28. Braga, D.; Maini, L.; Paganelli, F.; Tagliavini, E.; Casolari, S.; Grepioni, F. *J. Orgmet. Chem.* **2001**, *637-639*, 609-615.
29. Atencio, R.; Brammer, L.; Fang, S.; Pigge, F. C. *New. J. Chem.* **1999**, *23*, 461-463.
30. Gomez-Lor, B.; Gutiérrez-Puebla, E.; Iglesias, M.; Monge, M. A.; Ruiz-Valero, C.; Snejko, N. *Inorg. Chem.* **2002**, *41*, 2429-2432.
31. For an overview see: Janiak, C. *J. Chem. Soc., Dalton Trans.* **2000**, 3885.
32. Martz, J.; Graf, E.; Hosseini, M. W.; De Cian, A.; Fischer, J. *J. Chem. Soc., Dalton Trans.* **2000**, 3791.
33. For a recent reviews see: (a) Clapham, B.; Reger, T. S.; Janda, K. D. *Tetrahedron*, **2001**, *57*, 4637-4662; (b) de Miguel, Y. R. *J. Chem. Soc., Perkin 1* **2000**, 4213-4221; (c) Shuttleworth, S. J.; Allin, S. M.; Sharma, P. K. *Synthesis* **1997**, 1217
34. For a review see: Clark, J. H.; Macquarrie, D. J. *Chem. Commun.* **1998**, 853-860
35. For recent reviews see: (a) Kreiter, R.; Kleij, A. W.; Klein Gebbink, R. J. M.; van Koten, G. *Top. Curr. Chem.* **2001**, *217*, 163-199; (b) Oosterom, G. E.; Reek, J. H. N.; Kamer, P. C. J.; van Leeuwen, P. W. N. M. *Angew. Chem. Int. Ed.* **2001**, *40*, 1828-1849. (c) Astruc, D.; Chardac, F. *Chem. Rev.* **2001**, *101*, 2991-3023; (d) van Koten, G.; Jastrzebski, J. T. B. H. *J. Mol. Cat. A.* **1999**, *146*, 217-323.
36. (a) Schneider, R.; Köllner, C.; Weber, I.; Togni, A. *Chem. Commun.* **1999**, 2415-2416; (b) Köllner, C.; Pugin, B.; Togni, A. *J. Am. Chem. Soc.* **1998**, *120*, 10274-10275.
37. (a) Rheiner, P. B.; Seebach, D. *Chem. Eur. J.* **1999**, *5*, 3221-3236; (b) Seebach, D.; Sellner, H. *Angew. Chem. Int. Ed.* **1999**, *38*, 1918-1920.
38. See for example: (a) Zimmerman, S. C.; Lawless, L. J. *Top. Curr. Chem.* **2001**, *217*, 95-120 (b) Baars, M. W. p. L.; Meijer, E. W. *Top. Curr. Chem.* **2000**, *210*, 131-182; (c) Smith, D. K.; Diederich, F.; *Top. Curr. Chem.* **2000**, *210*, 183-227, and references cited.
39. de Groot, D.; de Waal, B. F. M.; Reek, J. N. H.; Schenning, A. P. H. J.; Kamer, P. C. J.; Meijer, E. W.; van Leeuwen, P. W. N. M. *J. Am. Chem. Soc.* **2001**, *123*, 8453-8458.

40. van de Coevering, R.; Kuil, M.; Klein Gebbink, R. J. M.; van Koten, G. *Chem. Commun.* **2002**, 1636-1637.
41. (a) Kraut, J. *Science* **1988**, *242*, 533; (b) Pauling, L. *Nature*, **1948**, *161*, 707
42. (a) Cacciapaglia, R.; DiStefano, S.; Mandolini, L. *J. Org. Chem.* **2002**, *67*, 521-525; (b) Cacciapaglia, R.; Di Stefano, S.; Kelderman, E.; Mandolini, L. *Angew. Chem. Int. Ed.* **1999**, *38* 348-358.
43. For a review, see: Molenveld, P.; Engbersen, J. F. J.; Reinhoudt, D. N. *Chem. Soc. Rev.* **2000**, *29*, 75-86.
44. Zhang, B. L.; Breslow, R. *J. Am. Chem. Soc.* **1997**, *119*, 1676-1681.
45. Mackay, L. G.; Wylie, R. S.; Sanders, J. K. M. *J. Am. Chem. Soc.* **1994**, *116*, 3141-3142.
46. Merlau, M. L.; Grande, W. J.; Nguyen, S. T.; Hupp, J. T. *J. Mol. Cat. A* **2000**,*156*, 79-84.
47. Suslick, K.; Cook, B.; Fox, M. *Chem. Commun.* **1985**, 580-582.
48. Groves, J. T.; Viski, P. *J. Org. Chem.* **1990**, *55*, 3628.
49. Collman, J. P.; Zhang, X.; Lee, V. J.; Brauman, J. I. *Chem. Commun.* **1992**, 1647-1649.
50. Breslow, R.; Gabriele, B.; Yang, J. *Tetrahedron Lett.* **1998**, *39*, 2887-2890.
51. (a) French, R. R.; Holzer, P.; Leuenberger, M.; Nold, M. C.; Woggon, W.-D. *J. Inorg. Biochem.* **2002**, *88*, 295-304. (b) Woggon, W.-D. *Chimia* **2000**, *54*, 564-568.
52. For a review, see: Diederich, F. *Angew. Chem.* **1988**, *100*, 372.
53. Benson, D. R.; Valentekovich, R.; Diederich, F. *Angew. Chem. Int. Ed.* **1990**, *29*, 191-193.
54. Portada, T.; Roje, M.; Raza, Z.; Čaplar, V.; Žinić, M.; Šunjić, V. *Chem. Commun.* **2000**, 1993-1994.
55. Coolen, H. K. A. C. Thesis *Rhodium(I) Metallohosts*, University of Nijmegen **1994**.
56. Dol, G. Thesis *Basket-Shaped Metallohosts*, University of Nijmegen **1998**.
57. Metzler-Nolte, N. *Angew. Chem. Int. Ed.* **2001**, *40*, 1040-1043.
58. Special issue on bioorganometallic chemistry: *J. Organomet. Chem.* **1999**, *589*,
59. Jouen, G.; Vessières, A.; Butler, I. S. *Acc. Chem. Res.* **1993**, *26*, 361-369.
60. Grotjahn, D. B. *Coord. Chem. Rev.* **1999**, *192*, 1125-1141.
61. a) Albrecht, M.; Rodríguez, G.; Schoenmaker, J.; van Koten, G. *Org. Lett.* **2000**, *2*, 3461-3464; b) Suijkerbuijk, B. M. J. M.; Slagt, M. Q.; Klein Gebbink, R. J. M.; Lutz, M.; Spek, A. L.; van Koten, G. *Tetrahedron Lett.* **2002**, *43*, 6565-6568.
62. Guillena, G.; Rodríguez, G.; van Koten, G. *Tetrahedron Lett.* **2002**, *43*, 3895-3898.
63. Hansch, C.; Leo, A.; Taft, R. W. *Chem. Rev.* **1991**, *91*, 165-195 and references cited.
64. Conte, V.; Di Furia, F.; Moro, S. *J. Mol. Cat. A* **1995**, *104*, 159-169.
65. van Manen, H.-J.; Nakashima, K.; Shinkai, S.; Kooijman, H.; Spek, A. L.; van Veggel, F. C. J. M.; Reinhoudt, D. N. *Eur. J. Inorg Chem.* **2000**, 2533-2540.
66. van de Kuil, L. A.; Luitjes, H.; Grove, D. M.; Zwikker, J. W.; van der Linden, J. G. M.; Roelofsen, A. M.; Jenneskens, L. W.; Drenth, W.; van Koten, G. *Organometallics* **1994**, *13*, 468-477.
67. Council for Chemical Sciences of The Netherlands´ Organisation for Scientific Research (CW/NWO), and the Dutch Technology Foundation (STW).
68. Albrecht, M.; van Koten, G. *Angew. Chem. Int. Ed.* **2001**, *40*, 3750.
69. Rodríguez, G.; Albrecht, M.; Schoenmaker, J.; Ford, A.; Lutz, M.; Spek, A. L.; van Koten, G. *J. Am. Chem. Soc.* **2002**, *124*, 5127-5138.

Chapter Two

Synthesis of *para*-Substituted NCN-Pincer Complexes: Versatile Building Blocks in Organometallic Chemistry

Abstract

A variety of *para*-substituted NCN-pincer palladium(II) and platinum(II) complexes [MX(NCN-Z)] (M = Pd(II), Pt(II); X = Cl, Br, I; NCN-Z = $[2,6\text{-}(CH_2NMe_2)_2C_6H_2\text{-}4\text{-}Z]^-$; Z = NO_2, COOH, SO_3H, $PO(OEt)_2$, $PO(OH)(OEt)$, $PO(OH)_2$, CH_2OH, SMe, NH_2) have been synthesized *via* routes involving substitution reactions, either prior or, notably, after metallation of the ligand. The solubility of the pincer complexes is dominated by the nature of the *para*-substituent Z, rendering several complexes water-soluble. The influence of the *para*-substituent on the electronic properties of the metal center was studied by ^{195}Pt-NMR and DFT-calculations. Both the ^{195}Pt-chemical shift and the calculated Mulliken populations on platinum correlate linearly with the σ_p Hammett substituent constants, allowing the prediction of electronic properties of pre-designed pincer complexes. Complexes substituted with protic functional groups (CH_2OH, COOH) dimerize in the solid state by intermolecular hydrogen bonding interactions.

2.1. Introduction

Organometallic complexes based on the potentially terdentate, monoanionic NCN-pincer ligand[1] (NCN = 2,6-bis[(dimethylamino)methyl]phenyl anion) have been prepared containing a wide range of (transition) metals, and are therefore found in numerous applications.[2,3] The aromatic pincer ligand contains two *meta*-positioned substituents bearing N-, O-, P- or S-donor groups allowing chelation to the metal center, thereby enhancing stability due to the formation of metallacycles. The pincer ligands can be represented by the general formula (ECE-Z), with E representing neutral two-electron donor atoms, and Z representing a substituent most often placed *para* with respect to C_{ipso} (Chart 1). Among the most stable pincer complexes are the square planar complexes from the metals of the nickel triad (Ni, Pd, Pt).[4]

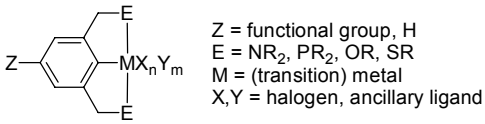

Chart 1. General representation of [M(ECE-Z)] pincer complexes.

Variations in the *para*-substituent Z of these complexes have drawn our particular interest for several reasons. The electronic properties, and consequently the catalytic, spectroscopic, and diagnostic properties of the pincer complexes can be fine-tuned by choosing the appropriate *para*-substituent. A striking example in electronic tuning of the metal center in NCN-Z nickel(II) complexes by the *para*-substituent was published earlier by our group.[5] The Hammett parameters of the *para*-substituents showed a linear relationship with the Ni(II)/Ni(III) oxidation potential and, consequently, on its catalytic activity in atom transfer radical additions.[5c] Recently, Reinhoudt *et al.* published a linear Hammett relationship for the complex stability for an array of para-substituted pyridines complexed to cationic SCS-pincer palladium complexes.[6]

Immobilization of the catalytically active pincer metal complexes on macromolecular or inorganic supports is attractive for recycling purposes. Placement of a suitable *para*-substituent, with anchoring possibilities and enough resistance towards the reaction conditions required for metallation, is crucial for the synthesis of these materials. NCN- and SCS-pincer complexes have been supported *via* the *para*-substituent Z on poly(ethylene glycol),[7] poly-(*N*-octadecyl-acrylamide),[8] polysiloxanes,[9] benzene rings,[10] hyperbranched polytriallylsilanes,[11] carbosilane[12,13] and Fréchet-type[14] dendrimers, buckminsterfullerene,[15] and silica.[16] *Para*-substitution also allows the build-up of supramolecular assemblies,[17,18] the placement of an

additional metal center,[19,20] or the introduction of functional groups such as α-amino acids or other auxiliaries,[21,22,23] leading to new materials.

The large potential of the pincer system, illustrated by the wide range of applications in the fields of catalysis, optical devices, and sensor materials, motivated us to develop synthetic routes towards new *para*-functionalized NCN-pincer complexes. Several steps in this study involve substitutions directly on metallated NCN-ligands. Except for π-aryl organometallics such as ferrocenes, reports concerning ligand substitution on σ-aryl organometallic complexes are scarce, and mainly involve complexes in which the metal is sterically shielded from the environment by bulky ligands.[24] This approach is of high interest, since it allows the creation of compact multifunctional building blocks with catalytic or sensor properties on one side, and functional substituents for (non)-covalent bonding to create nanosize structures, on the other side. The pronounced influence of the *para*-substituent on the properties of these NCN-pincer building blocks is discussed with respect to ^{195}Pt NMR, solid-state structures, and DFT-calculations.

2.2. Results

Synthesis

Two main synthetic strategies have been followed for the synthesis of para-substituted pincer metal complexes, denoted as [MX(NCN-Z)] (Chart 1).

I. Selective metallation of pre-functionalized *meta*-bis-aminoarene (NCN-pincer) ligands.

II. Selective *para*-substitution of bis-*ortho*-aminoaryl pincer complexes.

Approach I is commonly the method of choice because the metal-to-carbon bond is often the most reactive part of the complex. However, recently we observed that the metal-to-carbon bond in palladium(II) and, in particular, platinum(II) NCN-pincer complexes, has remarkable stability under a wide variety of reaction conditions. For example, the platinated complexes [PtX(NCN-Z)] are stable in refluxing acetone/HCl, as well as under the highly basic and nucleophilic conditions encountered in lithiation reactions.[21,23] This remarkable stability allows the exploration of unconventional strategies (approach II) for *para*-functionalization of pincer complexes.

Various metallation procedures for NCN-pincers are available (see Scheme 1), which form an essential part of the synthetic strategies. Firstly, both palladium and platinum can be introduced under mild reaction conditions by oxidative addition of the aryl C_{ipso}-halide bond of the NCN-halide to either $[Pd_2(dba)_3{\cdot}CHCl_3]$ or $[Pt(tol\text{-}4)_2(SEt_2)]_2$. A second method involves the selective lithiation of C_{ipso} with *n*- or *t*-BuLi in alkane solvents, followed by

transmetallation with $[PdCl_2(cod)]$ or $[PtCl_2(SEt_2)_2]$ in diethyl ether. Obviously, the latter reaction sequence is not suitable when *para*-substituents are used which are incompatible with lithium alkyls. Thirdly, direct palladation is possible by an electrophilic aromatic substitution reaction of a trimethylsilyl substituted pincer ligand with $Pd(OAc)_2$. This reaction makes use of the directing effect of the trimethylsilyl substituent in aromatic substitutions, and leads to the exclusive formation of the NCN-pincer complex with the palladium bound *ortho* with respect to both N-donor substituents.[25] Finally, halogen scrambling of the M–X bond is a process often encountered in reactions with metallated pincers. The scrambled product is easily converted to a single product by halide abstraction with a silver(I) salt, *e.g.* $AgBF_4$ or $AgPF_6$, followed by treatment of the $[M(NCN)L]^+$-cation with the ammonium, sodium or lithium salt of the desired halide.

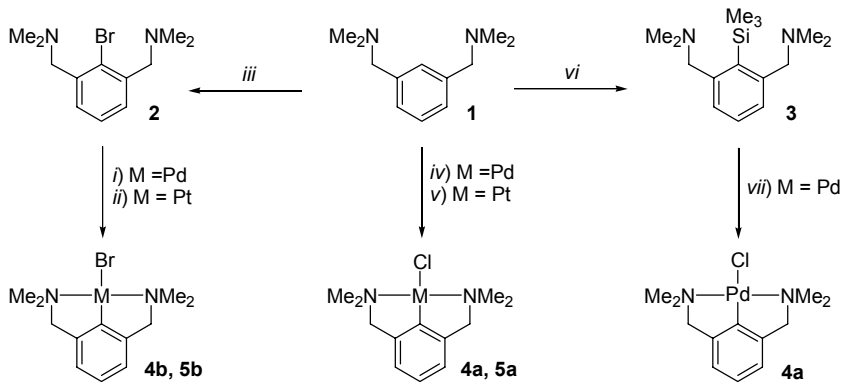

Scheme 1. Palladation and platination procedures available for the NCN-pincer ligand; *i*) $[Pd_2(dba)_3{\cdot}CHCl_3]$ *ii*) $[Pt(tol\text{-}4)_2SEt_2]_2$; *iii*) n-BuLi , Br_2; *iv*) *n*-BuLi, $[PdCl_2(cod)_2]$; *v*) *n*-BuLi, $[PtCl_2(SEt_2)_2]$; *vi*) *n*-BuLi, $SiMe_3OTf$; *vii*) $Pd(OAc)_2$, LiCl**.**

Approach I. Selective metallation of pre-functionalized NCN-pincer ligands.

The nitro, amino, and iodo *para*-substituted platinum and palladium pincers were essentially obtained from *ortho*-bromo compound **2** (Scheme 2). The nitro substituent on the *para*-position could also be introduced on *ortho*-trimethylsilyl compound **3**, albeit in a much lower yield and poorer selectivity. Metallation of *para*-nitro ligand **7** with $Pd(OAc)_2$, and subsequent treatment with LiCl afforded **10a** in 97% yield. Ligands **6**, **8** and **9** were all metallated using the mild oxidative addition procedure with $[Pd_2(dba)_3{\cdot}CHCl_3]$ and $[Pt(tol\text{-}4)_2(SEt_2)]_2$, respectively.

Nitration of **2** in H_2SO_4 with HNO_3 afforded exclusively the *para*-nitro ligand **6**.[5b] Metallation of **6** led to the clean formation of palladium(II) complex **10b** and platinum(II) complex **11** in yields of 97% and 95%, respectively. The *para*-amino substituted ligand **8** was obtained by reduction of **6** with hydrazine monohydrate in the presence of 5% Ru/C catalyst.[5] Metallation

of **8** to afford *para*-amino complexes **12** and **13** also led to the concomitant formation of Pd(0)- and Pt(0)-particles, respectively, resulting in an overall lower yield (~80%). *Para*-iodo substituted pincer ligand **9** was obtained by diazotation of **8** with $NaNO_2$, and subsequent treatment with KI. Platination of **9** with $[Pt(tol\text{-}4)_2(SEt_2)]_2$ in refluxing benzene afforded complex **15** in quantitative yield. The high selectivity of this reaction is attributed to the coordinating properties of the N-donor groups, enabling site selective platination. The synthesis of palladium analogue **14** was less straightforward. Palladation with $[Pd_2(dba)_3{\cdot}CHCl_3]$ starting at –78 °C, followed by slow warming to room temperature, ultimately afforded **14** in moderate yields.[21]

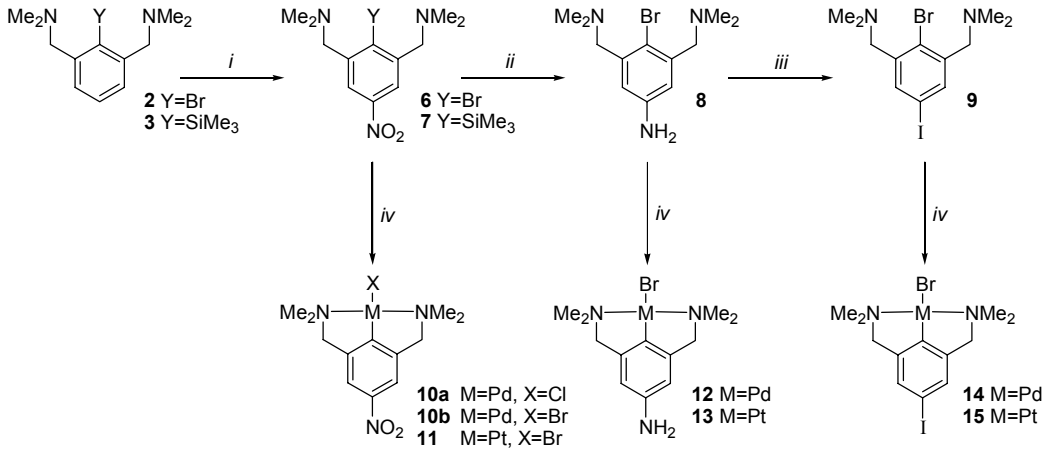

Scheme 2. Substitution of the NCN-pincer ligands prior to metallation; *i*) HNO_3 / H_2SO_4; *ii*) $N_2H_4.H_2O$ / 5 mol% Ru/C; *iii*) H_2SO_4, H_2O, $NaNO_2$, NaI; *iv*) Y=Br: $[Pd_2(dba)_3{\cdot}CHCl_3]$ (**10b**, **12**, **14**) or $[Pt_2(tol\text{-}4)_2(SEt_2)_2]_2$ (**11**, **13**, **15**); Y=$SiMe_3$: $Pd(OAc)_2$/LiCl (**10a**).

The synthesis of hydroxymethyl substituted palladium pincer compound **22** was possible *via* two different routes (Scheme 3). The first approach starts from the *para*-bromo ligand **16**. Lithiation of **16** with two equivalents of *t*-BuLi in diethylether, followed by addition of DMF afforded aldehyde **17** quantitatively. Reduction of **17** to its corresponding benzylic alcohol **18** proceeded fast in a yield of 95% using $NaBH_4$ in methanol. Protection of **18** with a *t*-butyldimethylsilyl group allowed lithiation of C_{ipso} with *n*-BuLi in hexane, followed by a quench with trimethylsilyl triflate. Deprotection with $Et_3N{\cdot}3HF$ afforded the hydroxymethyl ligand **19** in 78% yield. Subsequent treatment of **19** with $Pd(OAc)_2$ and LiCl in methanol resulted in the formation of **22a** in 87% yield. Instead of a $SiMe_3$-substituent, a bromo-substituent could be introduced in **18** by the use of Br_2 instead of $SiMe_3OTf$ in quenching the lithio-intermediate, to afford the *para*-hydroxymethyl compound **21**, which allowed both palladation and platination to obtain complexes **22b** and **23**, respectively.

An alternative route, which allowed the synthesis of both the palladium and platinum complexes, started from bifunctional bromo-iodo-pincer ligand **9**. Due to the higher reactivity of *t*-BuLi towards the aryl-iodide bond compared to the aryl-bromide bond, selective substitution reactions can be performed.[21] Lithiation of **9** at –100 °C in diethylether using two equivalents of *t*-BuLi, selectively afforded the *para*-lithio pincer *in situ*. This lithio intermediate could be reacted with electrophiles to produce novel *para*-substituted pincer ligands. For instance, quenching of the lithio intermediate with DMF afforded aldehyde **20**, which was easily reduced to benzylic alcohol **21** and subsequently metallated as described above to afford palladium and platinum complexes **22b** and **23**, respectively.[21]

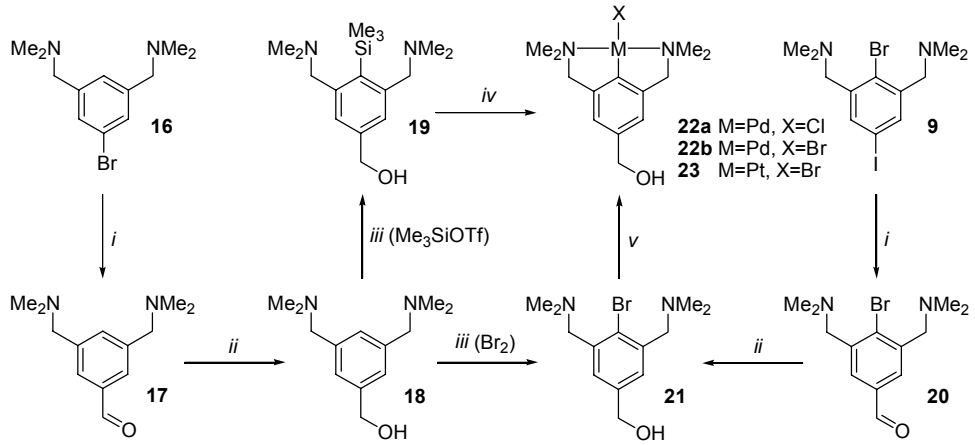

Scheme 3. Synthesis of **22** and **23** *via* two different approaches; *i*) *t*-BuLi, DMF; *ii*) $NaBH_4$; *iii*) a: TBSCl/imidazole, b: *n*-BuLi, Me_3SiOTf or Br_2, c: $Et_3N.3HF$; *iv*) $[Pd(OAc)_2]$, LiCl; *v*) M=Pd: $[Pd_2(dba)_3{\cdot}CHCl_3]$, M=Pt: $[Pt(tol\text{-}4)_2SEt_2]_2$.

Approach II. Selective para-substitution of bis-ortho-aminoaryl metal complexes

The non-substituted NCN-pincer complexes **4** (Pd) and **5** (Pt) can be obtained following the procedures depicted in Scheme 1. The choice of the preferred procedure can be made on the availability of starting materials and/or their costs, rather than on their efficiency. However, both oxidative addition and electrophilic substitution are quantitative with respect to the metal salt, while the lithiation-transmetallation route is not. Direct treatment of **4a** or **5a** with chlorosulfonic acid in dichloromethane afforded a mixture containing predominantly (~50%) the *para*-substituted sulfonated complexes **24** or **25**, together with the *meta*-isomer and several unidentified (decomposition) products (Scheme 4). Decomposition pathways starting with protonation of the amine donor arms can be envisaged. Purification of **24** was achieved by several extractions with acetonitrile followed by careful precipitation, while **25** could be purified by fractional precipitations from methanol. Complexes **24** and **25** were obtained in respective yields of 18% and 25%. As a result of the presence of the polar sulfonic acid

functional group, **24** and **25** are only soluble in highly polar (protic) solvents such as water, DMSO, acetonitrile, or THF.

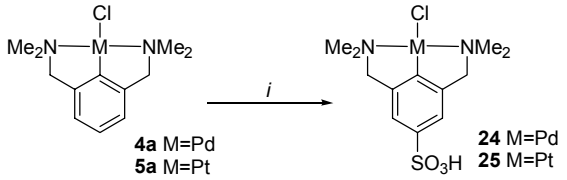

Scheme 4. Direct sulfonation of NCN-palladium and -platinum complexes; *i*) $HOSO_2Cl$.

The *para*-iodo substituted NCN-pincer complex **15** is a convenient starting material for further modifications (Scheme 5). Due to the lower stability of the *para*-iodo NCN-palladium(II) complexes compared to the corresponding NCN-platinum(II) analogues, we were unable in performing successful transformations on the *para*-iodo palladium(II) complex **14**. Remarkably, platinum(II) complex **15** allowed lithiation at the *para*-position using *t*-BuLi at −100 °C in THF to produce $[PtBr(NCN\text{-}Li)]_n$ *in situ*. The temperature control in this lithiation reaction is a crucial factor, since the lithio intermediate can polymerize to produce $[Pt(NCN)]_n$-type linear chains.[26] After lithiation, the reaction mixture was quenched at −100 °C with several electrophiles, *i.e.* CO_2, MeSSMe, $ClPO(OEt)_2$, DMF, and Me_3SiCl, to produce in high to excellent yields the *para*-substituted pincer platinum(II) complexes functionalized with a carboxylic acid (**34**, 89%), a methylthio ether (**35**, 95%), a diethylphosphonato (**36**, 95%), an aldehyde (**37**, 74%), and a trimethylsilyl (**38**, 75%) group, respectively (Scheme 5).

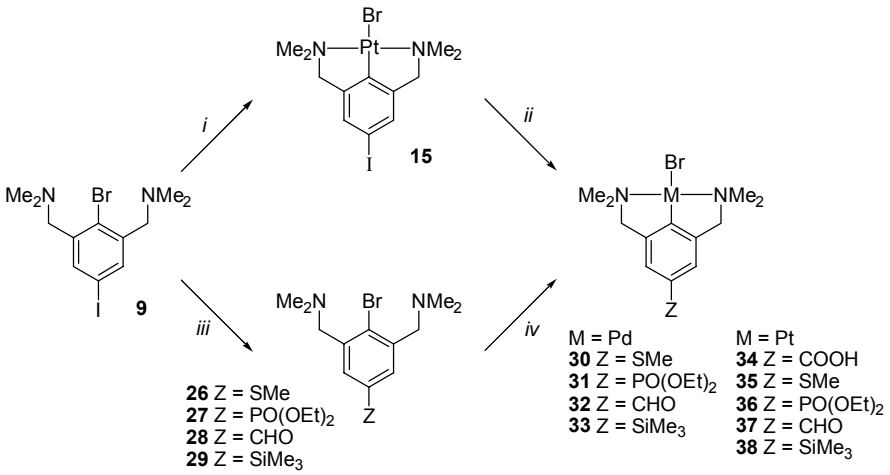

Scheme 5. Substitutions on metallated NCN-platinum complexes, and an alternative route for their palladium analogues; *i)* $[Pt(tol\text{-}4)_2SEt_2]_2$; *ii)* a: *t*-BuLi, b: CO_2 (**34**), Me_2S_2 (**35**), $ClPO(OEt)_2$ (**36**), DMF (**37**), Me_3SiCl (**38**); *iii)* a: *t*-BuLi, b: Me_2S_2 (**26**), $ClPO(OEt)_2$ (**27**) DMF (**28**), Me_3SiCl (**29**) ; iv) $[Pd_2(dba)_3{\cdot}CHCl_3]$ (**30-33**), $[Pt(tol\text{-}4)_2SEt_2]_2$ (**35-38**).

Although the analogous NCN-palladium(II) complexes **30**-**33** were not accessible *via* the selective functionalisation of *para*-iodo NCN-pincer palladium(II) complex **14**, they could be synthesized *via* the methylthio (**26**), diethylphosphonato (**27**), aldehyde (**28**), and trimethylsilyl (**29**) *para*-substituted NCN-pincer ligands. These precursors were obtained in near quantitative yields by selective lithiation at the *para*-position (iodo-substituent) of **9** with *t*-BuLi in diethyl ether and subsequent treatment with dimethyl disulfide, chlorodiethylphosphate, DMF, or trimethylsilyl chloride. Palladation of ligands **26**-**29** with $[Pd_2(dba)_3{\cdot}CHCl_3]$ afforded the metallated methylthio (**30**, 85%), diethylphosphonato (**31**, 92%), aldehyde (**32**, 74%), and trimethylsilyl (**33**, 78%) derivatives. Platinum(II) complexes **35**-**38** were also accessible via this route upon treatment of **26**-**29** with $[Pt(tol\text{-}4)_2(SEt_2)]_2$, respectively.

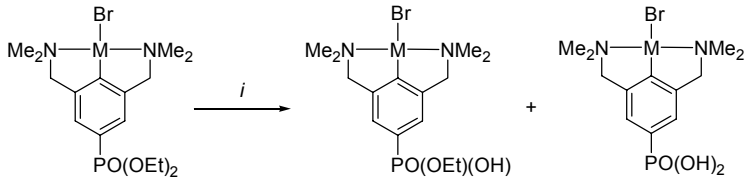

Scheme 6. (Partial) saponification of phosphonate esters on metallated ligands; *i*) a: Me_3SiBr, b: MeOH.

The diethylphosphonato substituted NCN-palladium and -platinum complexes **31** and **36** were subsequently (partially) hydrolyzed to obtain their phosphonic acid derivatives, in order to make them water-soluble. Scheme 6 illustrates this saponification into the monoethylphosphonic acid (**39** and **40**), and phosphonic acid derivatives (**41** and **42**), upon treatment with trimethylsilyl bromide and methanol. Repeated extractions of the crude product with dichloromethane afforded the monoethylphosphonic acid palladium and platinum pincer complexes **39** and **40** as pure materials in yields of 15% and 23%, respectively. However, unfavorable solubility properties of **41** and **42** hampered their complete purification.

Solubility

During the synthesis and work-up of this series of *para*-substituted pincer palladium and platinum complexes, we observed that the nature of the *para*-substituent has a crucial influence on the solubility properties of the pincer-metal complexes. A much smaller effect, as compared to the influence of the *para*-substituent, is exerted by the halogen positioned on the metal atom. Larger halides possess a more diffuse charge, and their bonds to the metal have more covalent character, resulting in slightly enhanced solubilities in apolar solvents.

The *para*-H, -*t*Bu, and -$SiMe_3$ substituted palladium and platinum complexes are soluble in dichloromethane, chloroform and THF, but to a lesser extent in benzene and diethyl ether. The introduction of protic *para*-substituents, *e.g.* COOH, PO(OH)(OEt), SO_3H, or NH_2, markedly lowers their solubility in aprotic solvents. Water-soluble and -stable NCN-pincer complexes are obtained upon the introduction of a sulfonate, a monoalkyl phosphonate, and to a lesser extent of a carboxylate substituent.

^{195}Platinum NMR studies

The chemical shift of the ^{195}Pt nucleus turned out to be a valuable tool for probing the electron density on the metal center of the various *para*-substituted pincer complexes. The ^{195}Pt chemical shift is highly sensitive towards subtle changes in geometry, oxidation state, and nature of the co-ordination sphere.[27] The magnetic shielding of the heavier nuclei contains contributions from both a paramagnetic and a diamagnetic shielding term. Both shielding terms are, to a different extent, sensitive towards σ and π contributions to the electronic charge on the metal center. In general, an increase in electron density on the metal leads to an increase in shielding of the nucleus. In 1976, a broad, but dated survey of the ^{195}Pt chemical shifts for a wide variety of platinum-complexes shows that no linear Hammett correlation is observed for several *para*-substituted diaryl platinum(II) complexes.[28] In contrast, Wu *et al.* later reported the synthesis and ^{195}Pt-NMR analysis of ferrocenyl based platinum complexes, for which a linear relation between the ^{195}Pt chemical shift and the σ_p Hammett substituent constants was found.[29]

Table 1. ^{195}Pt chemical shifts of the *para*-substituted NCN-pincer platinum(II) complexes [PtCl(NCN-Z)] and their corresponding Hammett substituent constants σ_p and σ_p^+.

Z	σ_p [a]	σ_p^+ [a]	**δ(^{195}Pt) / ppm** [b]
NO_2	0.81	1.23	-1802
CHO	0.47	1.04	-1843
COOH	0.44	0.73	-1899
I	0.28	0.13	-1923
H	0.0	0	-1959
$SiMe_3$	0.0	-0.03	-1963
*t*Bu	-0.15	-0.26	-1988
OH	-0.22	-0.92	-2009
NH_2	-0.3	-1.3	-2045

a) Taken from reference [30]; b) Referenced to H_2PtCl_6.

In order to study the influence of the para-substituent on the electron density of the pincer complexes by ^{195}Pt-NMR, all other structural features in the complex, *i.e.* halide and co-ordination geometry, were kept constant. ^{195}Pt chemical shifts were recorded for various para-

substituted pincer complexes in $CDCl_3$ (0.1 M) and referenced to H_2PtCl_6. The chemical shift data are collected in Table 1 and fit reasonably well (R=0.981) to the σ_p Hammett substituent constants reported by Exner (Figure 1).[30] Correlation of the chemical shift data with the σ_p^+ Hammett substituent constants results in a less good fit ($\delta(^{195}Pt) = 90.1 \cdot \sigma_p^+ - 1943.0$; R=0.969).

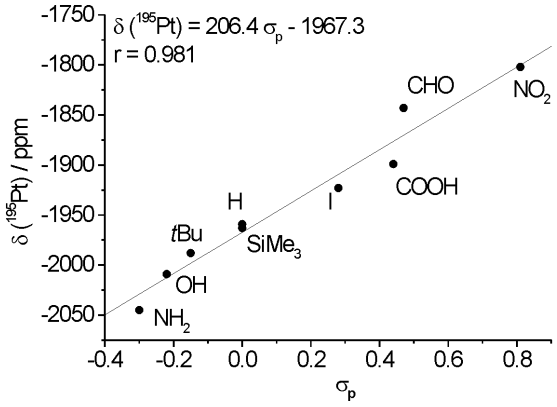

Figure 1. ^{195}Pt chemical shift of [PtCl(NCN-Z)] versus σ_p Hammett substituent constant and linear fit of the datapoints.

DFT-Calculations

The general increase in chemical shielding resulting from an increase in negative charge has been correlated in many studies with charge densities described by Mulliken population analysis.[27] In order to gain more insight in the influence of the substituent on the properties of the metal center, several *para*-substituted NCN-pincer platinum(II) chloride complexes [PtCl(NCN-Z)] were investigated by the density functional theory method B3LYP/LANL2DZ[31] as implemented in Gaussian 98.[32] Of specific interest in our calculations was the influence of the *para*-substituent on the Mulliken charges on the platinum center and the calculated structural features in comparison with single crystal X-ray structures.

Table 2. Selected bond distances [Å] and angles [°] for the experimental[17b] (X-ray) and calculated (DFT-B3LYP/LANL2DZ) geometry of [PtCl(NCN)].

	X-ray structure	**DFT-calculation**
Pt- C_{ipso}	1.907(5)-1.934(4)	1.94
Pt-Cl	2.41	2.53
Pt-N	2.082(8)-2.106(8)	2.13
N-Pt-N	160.5(3)-164.26(13)	165.0
Cl-Pt-C_{ipso}	173.14(11)-177.4(4)	180.0

Starting from structures calculated by MM2, further optimization took place with the DFT method B3LYP/LANL2MB (minimal basis set). These molecular structures were in turn used

as starting geometries for the calculations with the double-ζ basis set. The coordination environment, *i.e.* bond lengths and angles, of the platinum center were hardly affected by variations in the para-substituent. The calculated bond lengths and angles of pincer complex [PtCl(NCN)] together with earlier reported crystallographic data[17c] are given in Table 2.

The Mulliken charges on the platinum center are given in Table 3. These charges correlate well with the σ_p Hammett constants for the para-substituents ($Q_{Mulliken} = 0.055 \cdot \sigma_p + 0.22$; R = 0.9934), when the values for the substituents NH_2, NMe_2, and OH are omitted from the fitting procedure (Figure 2).

Table 3. The calculated Mulliken charges on platinum (DFT-B3LYP/LANL2DZ) of [PtCl(NCN-Z)], and their corresponding Hammett substituent constants σ_p.

Z	σ_p [a]	Mulliken population / e [b]
NO_2	0.81	0.2646
COOH	0.44	0.2434
I	0.28	0.2309
H	0.0	0.2190
SMe	0.06	0.2243
OH	-0.22	0.2281
NH_2	-0.3	0.2249
NMe_2	-0.32	0.2213

a) Taken from reference [30]; b) DFT-calculation with B3LYP/LANL2DZ

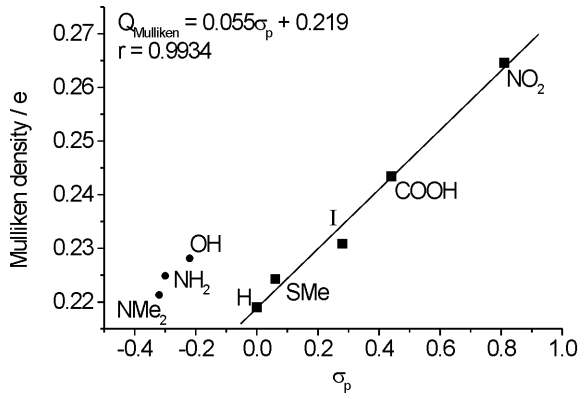

Figure 2. Calculated Mulliken charges (DFT-B3LYP/LANL2DZ) of [PtCl(NCN-Z)] versus σ_p Hammett substituent constant.

*Structures of **34** and **22a** in the solid state*

Crystal structures of various (*para*-functionalized) NCN-pincer palladium and platinum halide complexes have been determined earlier.[33] Crystals suitable for X-ray crystallographic structure determination of [PtI(NCN-COOH)] (**34**) were grown upon vapor diffusion of

pentane into a saturated solution of toluene-ether 1/1 (v/v). Upon crystallization from these apolar solvents, **34** crystallizes as the hydrogen bonded dimer. This in contrast with another crystal structure of **34** (not shown) obtained from a DMSO solution,[33a] and with a structurally related carboxylic acid functionalized CNN-pincer palladium complex.[34] Figure 3 shows its molecular structure in the crystal, together with a packing graph. Selected bond distances, angles and dihedral angles are collected in Table 4. The crystals contain disordered cocrystallized toluene solvent molecules.

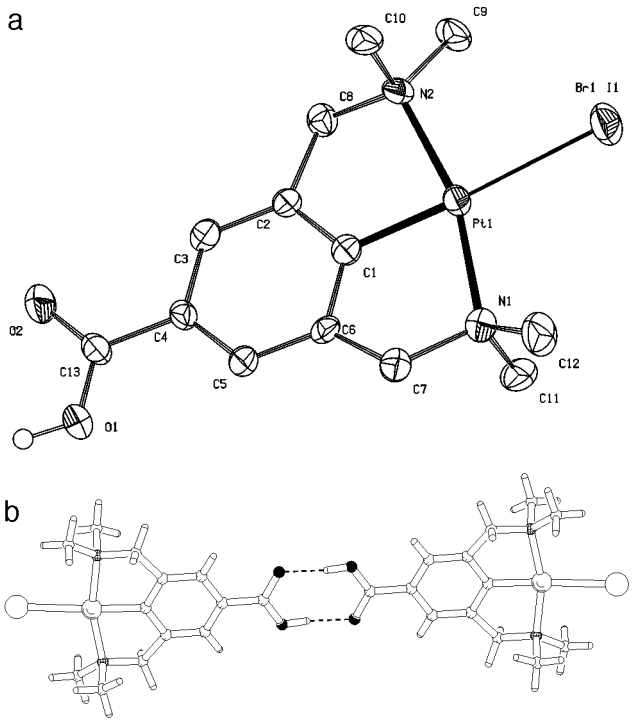

Figure 3. a) Displacement ellipsoid plot (50% probability level) of [PtI(NCN-COOH)] (**34**). The halogen position is occupied by 19% Br and 81% I, which were constrained to the same position and displacement parameters. Hydrogen atoms, except carboxylic acid, have been omitted for clarity. b) Packing graph of **34** showing the dimeric structure through hydrogen bonding.

Due to halogen scrambling on the platinum center, the crystal contained ~19% bromide and ~81% iodide on the metal center, as determined by a refinement of the occupancies. The Br1/I1 atoms were constrained on the same positions and displacement parameters. Therefore, the observed Pt1-Br1/I1 distance is a weighted average of both contributions. The metal center adopts a distorted square planar geometry with the coordination plane of platinum being almost coplanar with the plane of the aryl ring. The two five-membered metallacycles are puckered in the same direction with torsion angles Pt(1)-N(1)-C(7)-C(6) and Pt(1)-N(2)-C(8)-C(2) of 31.5(5)º and 30.0(5)º, respectively. The hydrogen bonds between both carboxylic acid residues have bond lengths H(10)-O(1), H(10)···O(2), and O(1)-O(2) of

0.89(8), 1.71(9), and 2.595(6) Å, respectively, with an almost linear O(1)-H(10)-O(2) angle of 173(8)°.

Crystals suitable for X-ray crystallographic structure determination of [PdCl(NCN-CH_2OH)] (**22a**) were grown upon slow vapor diffusion of diethyl ether into a concentrated dichloromethane solution of **22a**. Figure 4 shows the molecular structure, and a packing graph. In the solid state **22a** is self-assembled into dimers by hydrogen bonding interactions. Preliminary NMR-studies indicate that dimeric (or oligomeric) structures persist in $CDCl_3$-solution.

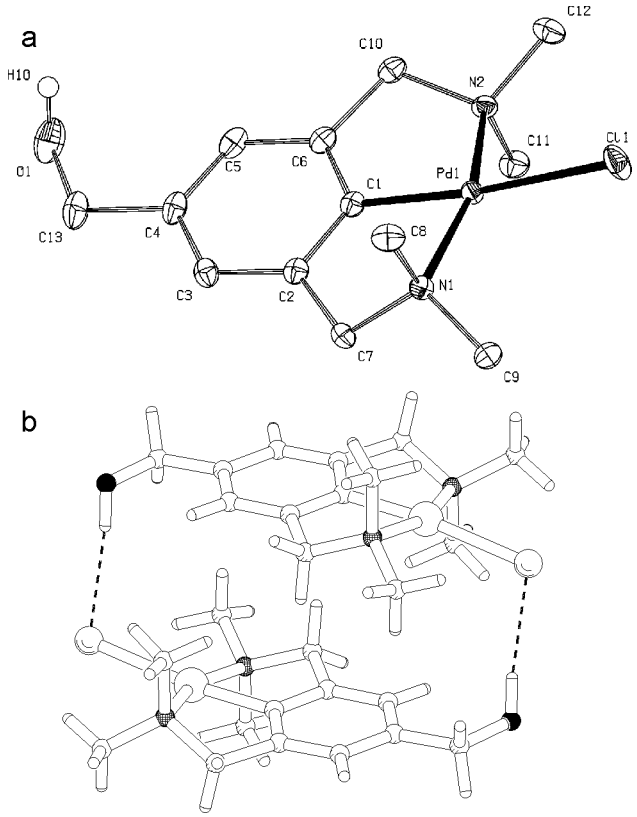

Figure 4. a) Displacement ellipsoid plot (50% probability level) of [PdCl(NCN-CH_2OH)] (**22a**). Hydrogen atoms, except hydroxyl, have been omitted for clarity. b) Packing graph of **22a** in which the hydrogen bonding in the dimeric substructure is shown.

The geometry around the palladium(II) center is distorted square planar, and the metal is bound to the chloride and the η^3-mer bonded NCN-ligand. The bond lengths and angles are similar to those generally encountered in NCN-pincer palladium(II) complexes. The five-membered metallacycles are puckered in the same direction with torsion angles Pd(1)-N(1)-C(7)-C(2) and Pd(1)-N(2)-C(10)-C(6) of -32.76(15)º and -32.64(15)º, respectively. Selected bond distances, angles and dihedral angles for **22a** are given in Table 4.

Table 4. Selected bond distances [Å], angles and torsion angles [°] of **22a** and **30**.

22a [PdCl(NCN-CH_2OH)]		**34** [PtI(NCN-COOH)]	
Pd1-C1	1.9174(18)	Pt1-C1	1.921(5)
Pd1-N1	2.1083(15)	Pt1-N1	2.088(5)
Pd1-N2	2.1066(15)	Pt1-N2	2.098(5)
Pd1-Cl1	2.4392(5)	Pt1-Br1/I1	2.7020(5)
C1-Pd1-N1	81.33(7)	C1-Pt1-N1	81.5(2)
C1-Pd1-N2	80.85(7)	C1-Pt1-N2	81.9(2)
C1-Pd1-Cl1	173.08(5)	C1-Pt1-Br1/I1	175.29(14)
N1-Pd1-N2	161.93(6)	N1-Pt1-N2	163.38(18)
Pd1-N1-C7-C2	-32.76(15)	Pt1-N1-C7-C6	31.5(5)
Pd1-N2-C10-C6	-32.64(15)	Pt1-N2-C8-C2	30.0(5)

2.3. Discussion

Synthesis

In general, direct modification of ligands in organometallic or coordination complexes is hampered by two major features. First, the complex is often kinetically not stable enough to allow organic transformations directly on a ligand bound to the metal. Secondly, metallation procedures can be incompatible with the type of substituent present on the ligand. This especially applies to the synthesis of organometallic complexes, in which a covalent metal-carbon bond has to be formed. Apparently these drawbacks are not encountered in the synthesis of *para*-functionalized NCN-palladium and -platinum complexes. Due to the exceptional stability of these complexes and the availability of various metallation procedures, we were able to synthesize a wide range of *para*-substituted NCN-pincer palladium and platinum complexes. The present organic transformations carried out directly on the pincer-metal complexes (strategy II), can be considered as particularly unconventional in organometallic synthesis and unexpected on the basis of their open structure, *i.e.* steric accessibility of the square planar aryl-palladium or -platinum starting materials. The preparation and isolation of pincer sulfonate complexes **24** (Pd) and **25** (Pt) illustrates the kinetic inertness of both the C_{ipso}-metal and N-metal bonds in the starting NCN-pincer complexes under the highly acidic and electrophilic reaction conditions employed in the aromatic sulfonation reaction. Moreover, the possibility to selectively lithiate NCN-pincer platinum complex **15** at the *para*-position shows that even the metal-halide bond can be kinetically stable under basic and nucleophilic conditions. These features open up a multitude of synthetic routes towards new ranges of ECE-Z pincer platinum derivatives.

The synthesis of [PdX(NCN-CH_2OH)] (**22**, X=Cl, Br) may serve to illustrate the synthetic flexibility offered by the NCN-pincer ligand framework. A straightforward route starts from

para-bromo NCN-pincer ligand **16** which can be synthesized in two steps from commercially available materials.[5b] However, this route involves lithiation of C_{ipso} limiting its scope to para-substituents which are either inert or can be protected during the lithiation step. It should be noted that after introduction of the inert $SiMe_3$-substituent on the C_{ipso} by lithiation, selective palladation can be performed directly, or after further transformations on the *para*-substituent. A second route starts from the bifunctional ligand **9**, which is only available from a multistep synthesis, but allows a broader range of substituents due to the mild oxidative addition procedures used in the metallation. In fact, it is the method of choice when targeting at protic or electrophilic *para*-substituents.

While in this study only selected *para*-substituted pincer complexes have been prepared, their syntheses represent the basic strategies available. This broadens the scope of possible *para*-substituents to virtually any organic functional group.[21,22,23,35] Extension of the presented synthetic routes to PCP- and SCS-pincer complexes can be envisaged, broadening the potential even more.

We found that several prerequisites should be taken into account when performing reactions on metallated pincer ligands. The palladium, and to a lesser extent the platinum pincer complexes, can decompose by reductive elimination and other processes upon prolonged heating or in highly concentrated solutions, leading to the formation of zerovalent metal particles. The cationic platinum complexes ($[Pt(OH_2)(NCN)]X$) can, in addition, add to activated alkyl halides (benzyl bromide, methyl iodide) leading in certain cases to the formation of either stable Wehland arenium intermediates or decomposition products.[36]

Properties

The influence of the *para*-substituent on the stability of the metal-to-carbon bond can be rationalized by considering substituent effects encountered in Hammett relations. Nitro-substituents of NCN-pincer complexes **10** and **11** withdraw electron density from the aromatic ring, thus polarizing the C_{ipso}-metal bond in the direction of C_{ipso} and consequently making the metal center more positive. The lowered electron density on the metal can be expected to make it less prone to reductive elimination, which would lead to the formation of zerovalent metal particles. On the other end, the amino-substituent in complexes **12** and **13** donates electron density to the aromatic ring, leading to a less polarised C_{ipso}-metal bond compared to **10** and **11**. A more electron rich metal center is expected to decompose more readily by reductive elimination. Indeed, this behavior is observed in the synthesis and handling of the metallated pincer systems. While palladium or platinum black is formed during the synthesis of **12** and **13**, and upon prolonged standing of their concentrated solutions, these reductive

elimination processes are never observed for the nitro-substituted pincers **10** and **11**. The palladium and platinum pincers bearing highly acidic groups, *e.g.* sulphonic acids **24** and **25** and phosphonic acids **41** and **42**, are highly hygroscopic and decompose slowly in moist air under the formation of palladium and platinum black, possibly *via* pathways involving protonation of the donor arms, followed by cleavage of the metal-carbon bond. Interestingly, these decomposition reactions were not observed in diluted aqueous solutions.

The solubility behavior of the *para*-functionalized pincer complexes is dominated by the *para*-substituent. The formation of intermolecular hydrogen bonding (arrays) between protic *para*-substituents and suitable Lewis bases such as the halide on the metal center, can give rise to the formation of oligomeric or polymeric structures, resulting in lower solubilities in common organic solvents. The formation of intermolecular hydrogen bonds is most pronounced in the solid state. Supramolecular assemblies of NCN-pincer complexes, through the formation of M-Cl···H hydrogen bonds, were earlier observed for the *para*-hydroxyl[17b] and *para*-ethynyl[20] functionalized platinum(II) complexes. These types of *para*-substituents induced the formation of infinite linear α-type networks. Despite the lower acidity of a benzylic hydroxyl functional group, compared to an aromatic one, it can still act as hydrogen bonding donor to the chloride ligand on the metal. The flexibility of the hydroxymethyl substituent in palladium(II) complex **22a** makes dimerization, instead of the formation of linear polymers, possible. Since the relative position of the aryl rings in the crystal lattice is not optimal for attractive π-stacking interactions, the origin of the dimerization can be completely attributed to the formation of the hydrogen bonds. Interestingly, similar M-Cl···HO dimerization was observed for the structurally related hydroxyl functionalized NCN-palladium complex [PdCl(NCN-$SiMe_2(CH_2)_6OH$]. This complex contains an extended spacer between the aryl ring and alcohol, giving rise to the formation of large hydrogen bonded squares.[37] Another hydrogen bonding motive is observed in the X-ray structure of the DMSO solvate of **34**. Whereas in this crystal structure the carboxylic acid is hydrogen bonded to a cocrystallized DMSO molecule, crystallization from apolar solvents afforded a molecular structure of **34** with the familiar hydrogen bonding motive for carboxylic acids. This hydrogen bonding motive is favored over others, such as hydrogen bonding to the halide, as can be expected on the basis of the poor hydrogen bond acceptor properties of the iodide, compared to the 'harder' chloride anion. IR-analysis (DRIFT) of amorphous **34** in KBr, confirmed that this dimeric structure is the predominant one in the solid state (broad absorption 2750-2270 cm^{-1}).

Hammett Relations

The linear correlation for the ^{195}Pt chemical shift with the σ_p Hammett substituent constants allows the use of NMR as a sensitive probe for the electron density on the metal center. Since all other structural features of the platinum complexes were found to remain constant (X-ray structures, DFT-calculations), changes in shielding can be attributed to the *para*-substituent solely. Similar linear correlations with σ_p were found for the Mulliken charges as calculated by DFT. It should be noted that the substituents NH_2, NMe_2 and OH, which can be considered as mesomeric electron donating substituents, deviate markedly from the other values. The offset of these charges with respect to the other values may be attributed to approximations used in the calculations, such as the effective core potential for the platinum nucleus. The calculated molecular structures of the pincer platinum complexes do resemble the experimental X-ray structures very well. All bond lengths and angles are in excellent agreement except for the Pt–Cl bond distance, which is overestimated by 5% in the calculation. This makes DFT an attractive method to study pincer complexes in more detail.[38]

2.4. Conclusions

The presented synthetic routes for the synthesis of *para*-functionalized NCN-palladium(II) and -platinum(II) complexes are highly versatile, and allow the functionalization with substituents covering the complete range of Hammett constants. The possibility to perform organic transformations on the metallated NCN-ligands makes their application as building blocks in the construction of new (macromolecular) organometallic materials facile. Additionally, both the transition metal(-halide) and selected substituents are able to participate in supramolecular assemblies by interactions such as hydrogen bonding, ligand coordination or π-π stacking. This is of especial interest for the application of NCN-pincer complexes as multifunctional building blocks for crystal engineering purposes. The direct and linear influence of the *para*-substituent on the platinum center as indicated by ^{195}Pt-NMR studies and the DFT-calculations can be extended to *para*-substituted pincer complexes of other metals. The catalytic and/or optical properties of these complexes can thus be optimized by choosing the appropriate *para*-substituent, based on its σ_p Hammett substituent constant.

2.5. Experimental

General

All reactions involving water/air-sensitive reagents were performed using standard Schlenk techniques unless stated otherwise. Benzene, pentane, hexane, THF and Et_2O were distilled from Na-benzophenone and CH_2Cl_2 from CaH_2 prior to use. $[Pd_2(dba)_3{\cdot}CHCl_3]$,[39] and $[Pt(tol\text{-}4)_2SEt_2]_2$[40] were synthesized according to literature procedures. All other reagents were obtained commercially and were used without further purification. Elemental Analyses were

performed by Kolbe, Mikroanalytisches Laboratorium (Müllheim, Germany). ^{1}H and ^{13}C{^{1}H} NMR spectra were recorded on a Varian Inova 300 spectrometer (operating at 300 and 75 MHz respectively) or a Varian Mercury 200 spectrometer (operating at 200 and 50 MHz respectively). Spectra were recorded in chloroform-*d* or benzene-d_6 at room temperature, unless stated otherwise, and were referenced to TMS (δ = 0.00 ppm). The syntheses of compounds **2** and **8**,[5b] **4**,[41] **5**,[41b] **16**,[42] **23**,[23b] **6**, **9** (alternative method), **14-15, 20-21, 28-29**, **32-33** and **37-38**[21] have been reported earlier.

1-Trimethylsilyl-2,6-bis[(dimethylamino)methyl]benzene (**3**)

1,3-Bis[(dimethylamino)methyl]benzene (**1**) (15.25 g, 79.4 mmol) was dissolved in 100 mL of hexane and cooled to -80 °C. To this solution was dropwise added 50 mL of *n*-butyllithium (1.6 M in hexane, 79.4 mmol) over 10 minutes. The reaction mixture was allowed to reach ambient temperature and stirred overnight. A freshly prepared solution of trimethylsilyl trifluoromethylsulphonate (15.4 mL, 87.4 mmol) in 50 mL THF was added at 0 °C. After stirring for an additional hour at room temperature all volatiles were evaporated *in vacuo*. Extraction with hexane (3 x 100 mL) afforded after evaporation of the solvent a yellow/brown oil. This was further purified by flash vacuum distillation yielding **3** as a colorless oil (16.12 g, 60 mmol, 77%). ^{1}H-NMR (benzene-d_6, 300 MHz) δ: 7.36 (d, 2H, $^{3}J_{HH}$=7.3 Hz, ArH), 7.20 (t, 1H, $^{3}J_{HH}$=7.3 Hz, ArH), 3.53 (s, 4H, CH_2N), 2.06 (s, 12H, NMe_2), 0.52 (s, 9H, $SiMe_3$). ^{13}C{^{1}H} (benzene-d_6, 75 MHz) δ: 146.8, 138.6, 129.7, 128.6 (Ar), 66.0 (CH_2N), 45.0 (NMe_2), 3.4 ($SiMe_3$). Anal. Calcd. for $C_{15}H_{28}N_2Si$: C 68.12, H 10.67, N 10.95; Found: C 68.20, H 10.58, N 10.83.

4-Nitro-1-trimethylsilyl-2,6-bis[(dimethylamino)methyl]benzene (**7**)

Compound **3** (3.88 g, 14.6 mmol) was added slowly during 1 hour to concentrated H_2SO_4 (10 mL) at 0 °C. Concentrated HNO_3 (2 mL) was added while maintaining the temperature below 10 °C. The mixture was allowed to reach ambient temperature and was stirred for 3 hours after which it was poured on 100 g of crushed ice. The acidic mixture was neutralized with KOH and subsequently extracted with CH_2Cl_2. The organic layer was washed with brine, dried over $MgSO_4$ and isolated after removal of the solvent *in vacuo* as a 20/80 mixture of **7** and 4-nitro-2,6-bis[(dimethylamino)methyl]benzene. Purification by column chromatography (Et_2O/hexanes 1/1, 3% TEA, basic alumina) yielded 0.64 g (2.1 mmol, 14%) of **7** as colorless crystals. ^{1}H-NMR (benzene-d_6, 300 MHz) δ: 8.17 (s, 2H, ArH), 3.28 (s, 4H, CH_2N), 1.86 (s, 12H, NMe_2), 0.34 (s, 9H, $SiMe_3$). ^{13}C{^{1}H} (benzene-d_6, 75 MHz) δ: 149.1, 148.5, 147.8, 122.5 (Ar), 65.0 (CH_2N), 44.8 (NMe_2), 2.8 ($SiMe_3$). Anal. Calcd. for $C_{15}H_{27}N_3O_2Si$: C 58.21, H 8.79, N 13.58, Si 9.08; Found: C 58.15, H 8.71, N 13.62, Si 8.94.

4-Nitro-NCN-palladium(II) chloride (**10a**)

To a solution of **7** (111.7 mg, 0.36 mmol) in freshly distilled methanol (10 mL) was added $Pd(OAc)_2$ (85.0 mg, 0.38 mmol) at once. The mixture was stirred for 2 h. followed by addition of LiCl (0.15 g, 3.6 mmol) resulting in the immediate formation of a white precipitate. The reaction mixture was stirred for 1 h., all volatiles were evaporated *in vacuo*, and the residue was dissolved in CH_2Cl_2 (60 mL), and washed with water. The dried ($MgSO_4$) organic phase was filtered over Celite and subsequent evaporation of the solvent *in vacuo* afforded pure **10** (132.8 mg, 0.35 mmol, 97%) as a yellowish solid. ^{1}H-NMR ($CDCl_3$, 200 MHz) δ: 7.61 (s, 2H, ArH), 4.02 (s, 4H, CH_2N), 2.88 (s, 12H, NMe_2). $^{13}C\{^1H\}$ ($CDCl_3$, 50 MHz) δ: 167.5, 145.6, 145.4, 115.0 (Ar), 74.0 (CH_2N), 52.9 (NMe_2). Anal. Calcd. for $C_{12}H_{18}ClN_3O_2Pd$: C 38.11, H 4.80, N 11.11; Found: C 38.19, H 4.91, N 11.02.

4-Nitro-NCN-platinum(II) bromide (**11**)

1-bromo-4-nitro-2,6-bis[(dimethylamino)methyl]benzene (**6**) (0.57 g, 1.80 mmol) was dissolved in benzene (10 mL) and added dropwise to a suspension of $[Pt(tol\text{-}4)_2(SEt)_2]_2$ (0.84 g, 0.90 mmol) in benzene (15 mL). The mixture was refluxed for 3 h. and upon cooling a yellow precipitate formed. Et_2O (75 mL) was added and the precipitate was isolated by centrifugation. The product was washed with Et_2O (2 x 90 mL) yielding pure **11** as a yellow solid (0.89 g, 1.73 mmol, 96%). ^{1}H-NMR ($CDCl_3$, 300 MHz) δ: 7.74 (s, 2H, ArH), 4.09 (s, $^3J_{HPt}$= 45.6 Hz, 4H, CH_2N), 3.13 (s, $^3J_{HPt}$= 38.4 Hz, 12H, NMe_2). $^{13}C\{^1H\}$ ($CDCl_3$, 75 MHz) δ: 157.5 (C_{para}), 144.7 (C_{ipso}), 143.9 ($^2J_{CPt}$= 81.1 Hz, C_{ortho}), 115.5 ($^3J_{CPt}$= 37.2 Hz, C_{meta}), 76.6 ($^2J_{CPt}$= 59.8 Hz, CH_2N), 55.0 ($^2J_{CPt}$= 13.4 Hz, NMe_2). Anal. Calcd. for $C_{12}H_{18}BrN_3O_2Pt$: C 28.19, H 3.55, N 8.22; Found: C 28.29, H 3.51, N 8.16.

4-Amino-NCN-palladium(II) bromide (**12**)

A solution of **8** (2.00 g, 7.0 mmol) in benzene (20 mL) was added to a solution of $[Pd_2(dba)_3{\cdot}CHCl_3]$ (5.66 g, 7.0 mmol) in benzene (50 mL). The mixture was stirred overnight and THF (5 mL) was added. After stirring for an additional hour all volatiles were removed *in vacuo*, and the material was redissolved in CH_2Cl_2 (10 mL). The dark brown solution was filtered over Celite and **12** precipitated upon addition of Et_2O (80 mL). The solid was washed four times with Et_2O (90 mL) and dried *in vacuo* affording **12** as a brown solid (2.09 g, 5.3 mmol, 76%). ^{1}H-NMR ($CDCl_3$, 300 MHz) δ: 6.20 (s, 2H, ArH), 3.89 (s, 4H, CH_2N), 2.94 (s, 12H, NMe_2). $^{13}C\{^1H\}$ ($CDCl_3$, 75 MHz) δ: 149.4, 145.8, 129.2, 107.4 (Ar), 74.7 (CH_2N), 54.0 (NMe_2). Anal. Calcd. for $C_{12}H_{20}BrN_3Pd$: C 36.71, H 5.13, N 10.70; Found: C 36.58, H 5.10, N 10.64.

4-Amino-NCN-platinum(II) bromide (**13**)

To a solution of **8** (0.80 g, 2.8 mmol) in benzene was added $[Pt(tol\text{-}4)_2SEt_2]_2$ (1.31 g, 1.4 mmol) at once. The solution was refluxed until a clear solution was obtained. The mixture was kept at reflux temperature for an additional 15 min. followed by evaporation of all volatiles. The resulting material was dissolved in CH_2Cl_2 (10 mL) and filtered over Celite. Precipitation with Et_2O (80 mL) and decantation afforded a brownish powder. This powder was washed twice with Et_2O (90 mL) and dried in vacuo to afford **13** as a light brown solid (1.10 g, 2.3 mmol, 82%). ^{1}H-NMR ($CDCl_3$, 300 MHz) δ: 6.26 (s, 2H, ArH), 3.10 (s, $^3J_{HPt}$= 45.8 Hz, 4H, CH_2N), 3.13 (s, $^3J_{HPt}$= 38.2 Hz, 12H, NMe_2). $^{13}C\{^1H\}$ ($CDCl_3$, 75 MHz) δ: 144.0, 143.1, 132.4, 107.0 (Ar), 77.4 (CH_2N), 55.1 (NMe_2). Anal. Calcd. for $C_{12}H_{20}BrN_3Pt$: C. 29.95, H. 4.19, N. 8.73; Found: C 29.78, H 4.23, N 8.56.

3,5-Bis[(dimethylamino)methyl]benzaldehyde (**17**)

To a solution of **16** (7.82 g, 29 mmol) in Et_2O (250 mL) was dropwise added *t*-BuLi (1.5 M in hexanes, 40 mL, 58 mmol) at a temperature of –78 °C. The reaction was stirred for 30 min. at –78 °C, and dimethylformamide (4.5 mL, 58 mmol) was added at once. The mixture was allowed to reach room temperature, stirred for an additional hour and carefully quenched with water (50 mL). The organic phase was washed with 1 M NaOH and brine. Subsequent drying over $MgSO_4$ and removal of all volatiles afforded **17** as a yellow oil (6.40 g, 29 mmol, 99%). ^{1}H-NMR ($CDCl_3$, 300 MHz) δ: 10.02 (s, 1H, CHO), 7.72 (s, 2H, ArH), 7.55 (s, 1H, ArH), 3.47 (s, 4H, CH_2N), 2.23 (s, 12H, NMe_2); $^{13}C\{^1H\}$-NMR (C_6D_6, 75 MHz) δ: 191.1 (CHO), 140.6, 136.9, 134.6, 128.4 (Ar), 63.3 (CH_2N), 44.8 (NMe_2). Elem. Anal. Calcd. for $C_{13}H_{20}N_2O$: C 70.87, H 9.15, N 12.72; Found: C 70.81, H 9.22, N 12.85.

1-Hydroxymethyl-3,5-bis[(dimethylamino)methyl]benzene (**18**)

$NaBH_4$ (1.21 g, 31.9 mmol) was added in portions to a solution of **17** (6.40 g, 29 mmol) in MeOH (100 mL). After addition, the mixture was stirred for 3 h. at room temperature, all volatiles were removed and the mixture was redissolved in Et_2O (100 mL). The organic layer was washed with water (2 x 50 mL) and brine and dried over $MgSO_4$. Removal of all volatiles *in vacuo* afforded **18** as a colourless oil (6.12 g, 27.6 mmol, 95%). ^{1}H-NMR ($CDCl_3$, 200 MHz) δ: 7.23 (s, 2H, ArH), 7.13 (s, 1H, ArH), 4,64 (s, 2H, CH_2O), 3.41 (s, 4H, CH_2N), 2.22 (s, 12H, NMe_2); $^{13}C\{^1H\}$-NMR ($CDCl_3$, 50 MHz) δ: 142.8, 135.7, 130.0, 128.1 (Ar), 63.9 (CH_2O), 62.9 (CH_2N), 44.8 (NMe_2). Elem. Anal. Calcd. for $C_{13}H_{22}N_2O$: C 70.23, H 9.97, N 12.60; Found: C 70.36, H 10.08, N 12.69.

1-Hydroxymethyl-4-trimethylsilyl-3,5-bis[(dimethylamino)methyl]benzene (**19**)

a) A mixture of *t*-butyldimethylsilyl chloride (1.91 g, 12.7 mmol) and imidazole (1.44 g, 21.1 mmol) in THF (50 mL) was stirred for 30 min. at room temperature. Benzyl alcohol **18** (2.35g, 10.6 mmol) in THF (20 mL) was added at once. The mixture was refluxed overnight and treated with freshly distilled MeOH (2 mL). All volatiles were evaporated in vacuo, and the residue was redissolved in hexane (150 mL), washed with water (2x 50 mL), and dried over $MgSO_4$. Removal of the solvent *in vacuo* afforded 3,5-bis[(dimethylamino)methyl]benyl *t*-butyldimethylsilyl ether as a yellow oil (2.64 g, 74%). ^{1}H-NMR ($CDCl_3$, 200 MHz) δ: 7.16 (s, 3H, ArH), 4.72 (s, 2H, CH_2O), 3.43 (s, 4H, CH_2N), 2.42 (s, 12H, NMe_2), 0.92 (s, 9H, *t*Bu), 0.09 (s, 6H, $SiMe_2$); $^{13}C\{^1H\}$-NMR ($CDCl_3$, 50 MHz) δ: 141.6, 138.1, 128.8, 126.2 (Ar), 64.9 (CH_2O), 64.0 (CH_2N), 45.1 (NMe_2), 26.0 ($C\underline{Me}_3$), 18.4 ($\underline{C}Me_3$), -5.2 ($SiMe_2$); Elem. Anal. Calcd. for $C_{19}H_{36}N_2OSi$: C 67.80, H 10.78, N 8.32, Si 8.34; Found: C 67.94, H 10.70, N 8.19, Si 8.46.

b) To a solution of 3,5-bis[(dimethylamino)methyl]benyl *t*-butyldimethylsilyl ether (2.64 g, 7.8 mmol) in hexane (50 mL) was added dropwise at –78 °C *n*-BuLi (1.6 M in hexanes, 4.9 mL, 7.8 mmol). The mixture was allowed to reach room temperature and was stirred for 6 hours. A solution of trimethylsilyl trifluoromethanesulfonate (2.27 mL, 11.8 mmol) in THF (25 mL) was added dropwise at 0 °C, and stirred for an additional hour. All volatiles were removed *in vacuo* and the product was extracted with hexane (3x 50 mL). The combined extracts were washed with water (50 mL), brine (50 mL) and dried over $MgSO_4$. Removal of the solvent afforded 4-trimethylsilyl-3,5-bis[(dimethylamino)methyl]benzyl *t*-butyldimethylsilyl ether as a yellow oil (2.48 g, 77%). ^{1}H-NMR ($CDCl_3$, 300 MHz) δ: 7.27 (s, 2H, ArH), 4.72 (s, 2H, CH_2O), 3.53 (s, 4H, CH_2N), 2.13 (s, 12H, NMe_2), 0.95 (s, 9H, *t*Bu), 0.38 (s, 9H, $SiMe_3$), 0.10 (s, 6H, $SiMe_2$); $^{13}C\{^1H\}$-NMR ($CDCl_3$, 75 MHz) δ: 146.4, 141.4, 136.9, 126.2 (Ar), 65.4 (CH_2O), 64.8 (CH_2N), 45.0 (NMe_2), 25.9 ($C\underline{Me}_3$), 18.4 ($\underline{C}Me_3$), 3.2 ($SiMe_3$), -5.2 ($SiMe_2$); Elem. Anal. Calcd. for $C_{22}H_{44}N_2OSi_2$: C 64.64, H 10.85, N 6.85, Si 13.74; Found: C 64.54, H 10.92, N 6.78, Si 13.65.

c) Triethylamine tris-hydrogenfluoride (2.97 mL, 18.2 mmol) was added to a solution of 4-trimethylsilyl-3,5-bis[(dimethylamino)methyl]benyl *t*-butyldimethylsilyl ether (2.48 g, 6.1 mmol) in THF (50 mL). The solution was stirred overnight at room temperature, after which all volatiles were removed *in vacuo*. The residue was redissolved in CH_2Cl_2 (250 mL), washed twice with aqueous NaOH (1 M, 50 mL), and once with brine. Removal of the solvent after treatment with $MgSO_4$, afforded **19** as a colourless oil (1.40 g, 4.8 mmol, 78%). ^{1}H-NMR ($CDCl_3$, 200 MHz) δ: 7.34 (s, 2H, ArH), 4.66 (s, 2H, CH_2O), 3.56 (s, 4H, CH_2N), 2.14 (s, 12H, NMe_2), 0.36 (s, 9H, $SiMe_3$); $^{13}C\{^1H\}$-NMR ($CDCl_3$, 50 MHz) δ: 146.4, 141.6, 130.4, 127.1 (Ar), 65.3 (CH_2O), 65.2 (CH_2N), 45.2 (NMe_2), 3.6 ($SiMe_3$); Elem. Anal. Calcd. for $C_{16}H_{30}N_2OSi$: C 65.25, H 10.27, N 9.51; Found: C 65.15, H 10.21, N 9.46.

4-Hydroxymethyl-NCN-palladium(II) chloride (**22a**)

$[Pd(OAc)_2]$ (0.47g, 2.1 mmol) was added to a stirred solution of **19** (0.59 g, 2.0 mmol) in MeOH (20 mL). The solution was stirred for 4 hours, and excess LiCl (0.85 g, 20 mmol) was added, resulting in a yellow suspension. The volatiles were removed *in vacuo*, the residue was redissolved in CH_2Cl_2 (20 mL), and carefully filtered over Celite. Addition of hexane (80 mL) to the filtrate resulted in precipitation of **22a** as a yellow solid (0.63 g, 1.7 mmol, 87%). ^{1}H-NMR ($CDCl_3$, 300 MHz) δ: 6.82 (s, 2H, ArH), 4.58 (s, 2H, CH_2O), 3.99 (s, 4H, CH_2N), 2.96 (s, 12H, NMe_2); $^{13}C\{^1H\}$-NMR ($CDCl_3$, 75 MHz) δ: 156.1, 145.3, 137.9, 119.2 (Ar), 74.8 (CH_2N), 65.6 (CH_2N), 53.3 (NMe_2); Elem. Anal. Calcd. for $C_{13}H_{21}ClN_2OPd$: C 42.99, H 5.83, N 7.71; Found: C 42.95, H 5.75, N 7.61.

4-SO_3H-NCN-palladium(II) chloride (**24**)

Chlorosulfonic acid (0.37 g, 3.14 mmol) was added to a cooled (0 ºC) solution of **4a** (0.95 g, 2.86 mmol) in CH_2Cl_2 (10 ml) and strirred at ambient temperature overnight. After evaporation of all volatiles *in vacuo*, the crude product was extracted with boiling acetonitrile. Slow precipitation upon cooling to room temperature afforded **24** as a brown solid (0.21 g, 0.51 mmol, 18%). ^{1}H-NMR (DMSO-d_6, 300 MHz) δ: 9.77 (broad s, 1H, SO_3H), 7.61 (s, 2H, ArH), 4.36 (s, 4H, CH_2N), 2.77 (s, 12H, NMe_2). $^{13}C\{^1H\}$ (DMSO-d_6, 75 MHz) δ: 150.3, 134.6, 131.4, 129.9 (Ar), 59.9 (CH_2N), 42.6 (NMe_2). Elem. Anal. Calcd. for $C_{12}H_{19}ClN_2O_3PdS$: C 34.88, H 4.63, N 6.78; Found: C 34.71, H 4.57, N 6.68.

4-SO_3H-NCN-platinum(II) chloride (**25**)

Chlorosulfonic acid (0.55 g, 4,74 mmol) was added to a cooled (0 ºC) solution of **5a** (1.01 g, 2.37 mmol) in CH_2Cl_2 (10 ml) and strirred at ambient temperature overnight. Evaporation of all volatiles *in vacuo* afforded a red solid which was analysed as a mixture of isomers. The *para*-isomer selectively precipitated from a boiling saturated solution of the crude product in methanol. Pure **25** was obtained after recrystallisation from methanol as a yellow solid (0.30 g, 0.59 mmol, 25%). ^{1}H-NMR (DMSO-d_6, 300 MHz) δ: 7.52 (s, 2H, ArH), 4.39 (s, $^3J_{HPt}$= 28.8 Hz, 4H, CH_2N), 2.91 (s, $^3J_{HPt}$= 28.8 Hz, 12H, NMe_2); $^{13}C\{^1H\}$-NMR (DMSO-d_6, 75 MHz) δ: 144.9, 140.9, 127.6, 123.1 (Ar), 76.2 (CH_2N), 56.5 (NMe_2). Elem. Anal. Calcd. for $C_{12}H_{19}ClN_2O_3PtS$: C 28.72, H 3.82, N 5.58; Found: C 28.79, H 3.90, N 5.49.

1-Bromo-2,6-bis((dimethyl)aminomethyl)phenyl methyl sulfide (**26**)

A solution of **9** (1.00 g, 2.5 mmol) in Et_2O was treated with *t*-BuLi (1.5M in pentane, 3.3 mL, 5 mmol) at –100 °C. The solution was stirred for 10 min. at –100 °C, and dimethyldisulfide (0.4 g, 3.8 mmol) was added at once. The mixture was allowed to reach room temperature and all volatiles were removed *in vacuo*. The residue was redissolved in pentane (50 mL), washed

with water (2 x 25 mL), and dried over $MgSO_4$. Removal of the volatiles afforded **26** as a colourless oil (0.65 g, 2.1 mmol, 82%). ^{1}H-NMR ($CDCl_3$, 300 MHz) δ: 7.51 (s, 2H, ArH), 3.48 (s, 4H, CH_2N), 2.10 (s, 12H, NMe_2), 2.06 (s, 3H, SMe). $^{13}C\{^1H\}$ ($CDCl_3$, 75 MHz) δ: 139.8, 138.3, 127.2, 122.9 (Ar), 63.8 (CH_2N), 45.5 (NMe_2), 15.4 (SMe). Elem. Anal. Calcd. for $C_{13}H_{21}BrN_2S$: C 49.21, H 6.67, N 8.83; Found: C 49.32, H 6.56, N 8.87.

1-Bromo-2,6-bis((dimethyl)aminomethyl)phenyl diethylphosphonate (**27**)

To a solution of **9** (1.2 g, 3.0 mmol) in Et_2O (25 mL) at –100 °C was added *t*-BuLi (1.5 M in pentane, 6.0 mmol, 4.0 mL) dropwise. After 10 min. at –100°C, chloro diethylphosphate (0.6 g, 3.5 mmol) was added at once. The solution was allowed to reach room temperature, and was stirred for 2 h. All volatiles were removed *in vacuo*, the residue was redissolved in hexane (50 mL), washed with water (2 x 25 mL), and dried over $MgSO_4$. Removal of the solvent *in vacuo* afforded **27** as a colourless oil (0.85 g, 2.1 mmol, 69%). ^{1}H-NMR (C_6D_6, 300 MHz) δ: 8.16 (d, $^3J_{P\text{-}H}$=13.2 Hz, 2H, ArH), 3.94 (m, 4H, O$\underline{CH_2}CH_3$), 3.42 (s, 4H, CH_2N), 2.04 (s, 12H, NMe_2), 1.00 (t, $^3J_{H\text{-}H}$=7.2 Hz, 6H, $OCH_2\underline{CH_3}$). $^{13}C\{^1H\}$ (C_6D_6, 75 MHz) δ: 140.1, 132.4, 131.2, 129.6 (Ar), 63.6 (CH_2N), 61.8 (OCH_2), 45.2 (NMe_2), 15.4 ($OCH_2\underline{CH_3}$). Elem. Anal. Calcd. for $C_{16}H_{28}N_2BrO_3P$: C 47.18, H 6.93, N 6.88, P 7.60; Found: C 46.96, H 7.14, N 6.95, P 7.38.

4-Methylthio-NCN-palladium(II) bromide (**30**)

$[Pd_2(dba)_3{\cdot}CHCl_3]$ (0.77 g, 0.95 mmol) was added to a solution of **26** (0.30 g, 0.95 mmol) in benzene (25 mL). The mixture was stirred overnight, and for an additional hour after the addition of 1 mL of THF. The solution was filtered over Celite, concentrated to 5 mL, after which **30** precipitated upon the addition of 25 mL of hexane. The resulting solid was washed with hexane (2 x 25 mL) and dried *in vacuo*, to afford **30** as a yellowish solid (0.34 g, 0.80 mmol, 85%). ^{1}H-NMR ($CDCl_3$, 300 MHz) δ: 6.73 (s, 2H, ArH), 3.95 (s, 4H, CH_2N), 2.95 (s, 12H, NMe_2), 2.41 (s, 3H, SMe). $^{13}C\{^1H\}$ ($CDCl_3$, 75 MHz) δ: 155.1, 145.8, 134.2, 119.6 (Ar), 74.6 (CH_2N), 54.0 (NMe_2), 17.4 (SMe). Elem. Anal. Calcd. for $C_{13}H_{21}BrN_2PdS$: C 36.85, H 5.00, N 6.61; Found: C 36.78, H 5.10, N 6.47.

4-PO(OEt)$_2$-NCN-palladium(II) bromide (**31**)

To a solution of **27** (1.30 g, 3.2 mmol) in benzene (25 mL) was added $[Pd_2(dba)_3{\cdot}CHCl_3]$ (2.58 g, 3.2 mmol) at once. The mixture was stirred overnight and THF (5 mL) was subsequently added. After filtration over Celite, the solution was concentrated to 10 mL, after which hexane (90 mL) was added to induce precipitation of **31**. The solid was washed with hexane (3 x 100 mL) which afforded pure **31** as an off-white solid (1.51 g, 2.94 mmol, 92%). ^{1}H-NMR ($CDCl_3$, 300 MHz) δ: 7.18 (d, $^3J_{HP}$=20.1 Hz, 2H, ArH), 4.06 (m, 4H, O$\underline{CH_2}CH_3$),

3.98 (s, 4H, CH_2N), 2.94 (s, 12H, NMe_2), 1.29 (t, $^3J_{HH}$=10.6 Hz, 6H, $OCH_2\underline{CH_3}$); $^{13}C\{^1H\}$ ($CDCl_3$, 75 MHz) δ: 164.3, 145.5, 125.4, 123.1 (Ar), 74.4 (CH_2N), 62.1 ($O\underline{CH_2}CH_3$), 53.8 (NMe_2), 16.5 ($OCH_2\underline{CH_3}$). Elem. Anal. Calcd. for $C_{16}H_{28}BrN_2O_3PPd$: C 37.41, H 5.49, N 5.45, P 6.03; Found: C 37.48, H 5.53, N 5.52, P 6.11.

4-COOH-NCN-platinum(II) iodide (**34**)

To a cooled (-100ºC) solution of **15** (1.06 g, 1.79 mmol) in THF (20 mL), was added *t*-BuLi dropwise (2.4 ml, 3.6 mmol, 1.5 M in pentane). The reaction was quenched after 2 min. by bubbling dry CO_2 (g) through the mixture. After reaching ambient temperature the CO_2 supply was stopped and the product was treated with a saturated aqueous NH_4Cl solution (1 mL). All volatiles were evaporated *in vacuo* and the crude mixture was redissolved in $CHCl_3$ (50 mL), washed with a saturated NH_4Cl solution (2x 5 mL) and dried over $MgSO_4$. After removal of the volatiles *in vacuo*, the product was redissolved in acetone (20 mL), treated with NaI (0.28 g, 1.85 mmol) for 30 min and filtered over Celite. Final traces of Na-salts were extracted with water from a $CHCl_3$ solution of the product. Pure **34** precipitated as an off-white solid upon slow addition of diethyl ether (90 mL) to a 10 mL solution in $CHCl_3$. Isolated yield: 0.89 g (1.59 mmol, 89%). ^{1}H-NMR (DMSO-d_6, 300 MHz) δ: 7.41 (s, 2H, ArH), 4.13 (s, $^3J_{HPt}$= 39.0 Hz, 4H, CH_2N), 3.07 (s, $^3J_{HPt}$= 28.8 Hz, 12H, $N(CH_3)_2$). $^{13}C\{^1H\}$ (DMSO-d_6, 75 MHz) δ: 168.2 (COOH), 156.0, 144.1, 125.6, 120.6, 75.4 (CH_2N), 55.6 ($N(CH_3)_2$). Elem. Anal. Calcd. for $C_{13}H_{19}N_2IO_2Pt$: C 28.02, H 3.44, N 5.03; Found: C 27.88, H 3.40, N 4.91; FT-IR (DRIFT, KBr) ν (cm^{-1}) (intensity in Kubelka-Munk units): 3100-2750 (0.18), 3211.6 (0.17), 2979.8 (0.20), 2922.3 (0.26), 2750-2300 (0.17), 1668.5 (0.59), 1587.7 (0.50), 1465.5 (0.26), 1452.5 (0.33), 1412.1 (0.25), 1345.3 (0.29), 1326.1 (0.37), 1308.0 (0.52), 1274.1 (0.34), 1231.1 (0.40).

4-Methylthio-NCN-platinum(II) bromide (**35**)

Method a) *t*-BuLi (1.5 M in pentane, 2.65 mL, 4.0 mmol) was added to a solution of **15** (1.2 g, 2.0 mmol) in THF (40 mL) at –100 °C. After stirring for 5 min at –100°C, dimethyl disulfide (0.30 g, 3 mmol) was added at once, and the mixture was allowed to reach room temperature. All volatiles were removed *in vacuo*, and the residue was redissolved in CH_2Cl_2 (25 mL). The solution was washed with water (2 x 25 mL, brine (25 mL), dried over $MgSO_4$, and concentrated to 10 mL. Compound **35** precipitated upon the careful addition of hexane (50 mL). The solid was washed with hexane (2 x 50 mL) and dried *in vacuo* to afford **35** as a off-white solid (0.61 g, 1.2 mmol, 60%).

Method b) To a solution of **26** (0.30 g, 0.95 mmol) in benzene (10 mL) was added $[Pt(tol\text{-}4)_2(SEt_2)]_2$ (0.44 g, 0.48 mmol) at once. The mixture was heated at reflux temperature until a clear solution was obtained. After cooling to room temperature, the solvent was evaporated *in*

vacuo and the resulting residue was redissolved in CH_2Cl_2 (5 mL). Compound **35** precipitated upon the addition of hexane (25 mL). The solid was washed with hexane (2 x 25 mL) and dried in vacuo to afford **35** as an off-white solid (0.46 g, 0.90 mmol, 95%). ^{1}H-NMR ($CDCl_3$, 300 MHz) δ: 6.81 (s, 2H, ArH), 3.99 (s, $^3J_{HPt}$= 45.4 Hz, 4H, CH_2N), 3.11 (s, $^3J_{HPt}$= 38.5 Hz, 12H, NMe_2), 2.44 (s, 3H, SMe). $^{13}C\{^1H\}$ ($CDCl_3$, 75 MHz) δ: 156.2, 144.3, 132.1, 120.1 (Ar), 77.4 (CH_2N), 55.3 (NMe_2), 18.0 (SMe). Elem. Anal. Calcd. for $C_{13}H_{21}BrN_2PtS$: C 30.47, 4.13, 5.47; C 30.59, H 4.26, N 5.36.

4-PO(OEt)$_2$-NCN-platinum(II) bromide (**36**)

Method a) To a cooled (−100ºC) solution of **15** (1.06 g, 1.79 mmol) in 25 ml THF was added dropwise *t*-BuLi (2.4 mL, 3.6 mmol, 1.5 M in pentane). After 2 min, the reaction mixture was quenched with (0.50 g, 2.70 mmol) chlorodiethylphosphate. The mixture was allowed to reach room temperature and all volatiles were evaporated *in vacuo*. The reaction mixture was redissolved in CH_2Cl_2 (50 mL) and washed with water (50 mL), 1M NaOH (50 mL) and brine. The CH_2Cl_2 solution was dried over $MgSO_4$ and evaporated to dryness. Pure **36** (0.86 g, 1.43 mmol, 80%) precipitated from a CH_2Cl_2 solution (10 mL) upon slow addition of hexane (90 mL).

Method b) To a solution of **27** (0.50 g, 1.2 mmol) in benzene (10 mL) was added $[Pt(tol\text{-}4)_2SEt_2]_2$ (0.56 g, 0.60 mmol) at once. The mixture was brought to reflux until a clear solution was obtained. After removal of the volatiles, the residue was redissolved in CH_2Cl_2 and precipitated with hexane (50 mL). The solid was washed with hexane (2 x 50 mL) to afford **36** as an off-white solid (0.69 g, 1.1 mmol, 95%).

^{1}H-NMR ($CDCl_3$, 300 MHz) δ: 7.23 (d, $^3J_{HP}$=13.5 Hz, 2H, ArH), 4.08 (m, 4H, OCH_2), 4.02 (s, $^3J_{HPt}$= 45.1 Hz, 4H, CH_2N), 3.16 (s, $^3J_{HPt}$= 38.4 Hz, 12H, NMe_2), 1.31 (t, $^3J_{HH}$=7.2 Hz, 6H, CH_3). $^{13}C\{^1H\}$ ($CDCl_3$, 75 MHz) δ: 156.2, 144.0, 123.0, 121.4 (Ar), 77.5 (CH_2N), 62.1 (OCH_2), 56.6 (NMe_2), 16.6 ($OCH_2\underline{CH_3}$). Anal. Calcd. for $C_{16}H_{28}IN_2O_3PPt$: C 29.59, H 4.35, N 4.31, P 4.77; Found: C 29.75, 4.28, 4.26, 4.59.

4-PO(OEt)(OH)-NCN-palladium(II) bromide (**39**) and *4-PO(OEt)(OH)-NCN-platinum(II) bromide* (**40**)

Both hydrolyses were performed under similar conditions. To a solution of the pincer diethylphosphonate (**31** or **36**) in CH_2Cl_2 (ca 0.1 M) were added 3 equivalents of trimethylsilyl bromide. The mixture was stirred overnight, MeOH (5 mL) was added, and all volatiles were removed *in vacuo*. The monoethylphosphonates **39** and **40** were isolated together with remaining **31** or **36** upon extractions with CH_2Cl_2. Careful precipitations of concentrated CH_2Cl_2 solutions with Et_2O afforded **39** and **40** as pure solids in yields of 15% and 23%, respectively.

39 (Pd): ^{1}H-NMR (DMSO-d_6/$CDCl_3$ 1/5, 200 MHz) δ: 6.87 (d, $^{3}J_{P-H}$=13.2 Hz, 2H, ArH), 3.70 (s, 4H, CH_2N), 3.64 (m, 2H, CH_2O), 2.61 (s, 12H, NMe_2), 0.93 (t, $^{3}J_{H-H}$=7.0 Hz, 3H, CH_3); $^{13}C\{^{1}H\}$ (DMSO-d_6/$CDCl_3$, 50 MHz) δ: 163.0, 145.5 (d), 125.5, 122.4 (d) (Ar), 74.1 (CH_2N), 61.1 (OCH_2), 53.6 (NMe_2), 16.5 ($OCH_2\underline{CH_3}$). Anal. Calcd. for $C_{14}H_{24}BrN_2O_3PPd$: C 34.62, H 4.98, N 5.77; Found: C 34.53, H 5.03, N 5.71.
40 (Pt): ^{1}H-NMR (DMSO-d_6/$CDCl_3$ 1/5, 300 MHz) δ: 6.85 (d, $^{3}J_{P-H}$=13.2 Hz, 2H, ArH), 3.68 (s, 4H, CH_2N), 3.61 (m, 2H, CH_2O), 2.72 (s, 12H, NMe_2), 0.90 (t, $^{3}J_{H-H}$=6.9 Hz, 3H, CH_3); Anal. Calcd. for $C_{14}H_{24}BrN_2O_3PPt$: C 29.28, H 4.21, N, 4.88; Found: C 29.72, H 4.52, N 4.80.

4-$PO(OH)_2$-NCN-palladium(II) bromide (**41**) and 4-$PO(OH)_2$-NCN-platinum(II) bromide (**42**) were not isolated as pure products, but were present in the crude hydrolysis products as indicated by $^{31}P\{^{1}H\}$-analysis.

Crystal structure determinations
Intensities were measured on a Nonius KappaCCD diffractometer with rotating anode and graphite monochromator (Mo-K_α, λ = 0.71073) up to a resolution of $(\sin\theta/\lambda)_{max}$ = 0.65 $Å^{-1}$. The structures were solved with Patterson methods (program DIRDIF97[43]) and refined with the program SHELXL97[44] against F^2 of all reflections. Non hydrogen atoms were refined freely with anisotropic displacement parameters. Hydrogen atoms were located in the difference Fourier map and refined as rigid groups. The hydrogen atom of the hydroxyl group in **22a** and the hydrogen atom of the carboxylic acid group in **34** were refined freely with isotropic displacement parameters. The drawings, structure calculations, and checking for higher symmetry were performed with the program PLATON[45].

*Crystal structure determination of **22a***
$C_{13}H_{21}ClN_2OPd$, FW = 363.17, yellow plate, 0.30 x 0.30 x 0.09 mm^3, T=125(2) K, monoclinic, $P2_1/c$ (No. 14), a = 9.1935(1), b = 10.5160(1), c = 15.9377(2) Å, β = 111.3489(7)°, V = 1435.11(3) $Å^3$, Z = 4, F(000) = 736, D_c = 1.681 gcm^{-3}, 29867 measured reflections, 3287 unique reflections (R_{int} = 0.066). Analytical absorption correction (PLATON[45], routine ABST, μ = 1.470 mm^{-1}, 0.62-0.86 transmission). 171 refined parameters, no restraints. R [I>2σ(I)]: R1 = 0.0205, wR2 = 0.0512. R [all data]: R1 = 0.0226, wR2 = 0.0522. S = 1.033. Residual electron density (min/max) = –0.72/0.62 e/$Å^3$.

*Crystal structure determination of **34***
$C_{13}H_{19}Br_{0.19}I_{0.81}N_2O_2Pt$ $0.5C_7H_8$, FW = 594.43, pale yellow plate, 0.06 x 0.06 x 0.02 mm^3, T = 150(2)K, monoclinic, $P2_1/c$ (No. 14), a = 21.0837(5), b = 6.0838(1), c = 14.7525(3) Å, β = 94.3916(6)°, V = 1886.73(7) $Å^3$, Z = 4, F(000) = 1118, D_c = 2.093 gcm^{-3}, 26659 measured

reflections, 4316 unique reflections (R_{int} = 0.064). An absorption correction was applied (PLATON[45], routine DELABS, μ = 9.173 mm^{-1}, 0.40-0.80 transmission). 216 refined parameters, 27 restraints. The atoms Br1 and I1 were constrained on the same position with the same displacement parameters. R [I>2σ(I)]: R1 = 0.0327, wR2 = 0.0648. R [all data]: R1 = 0.0554, wR2 = 0.0704. S = 1.043. Residual electron density (min/max) = −1.17/0.86 e/$Å^3$.

2.6. References and Notes

1. van Koten, G. *Pure Appl. Chem.* **1989**, *61*, 1681.
2. Rietveld, M. P. H.; Grove, D. M.; van Koten, G. *New J. Chem.* **1997**, *21*, 751-771.
3. Albrecht, M; van Koten, G. *Angew. Chem. Int. Ed.* **2001**, *40*, 5000-5031, *Angew. Chem*., **2001**, *113*, 3866-3898.
4. Complexation with these d^8 metals (Ni(II), Pd(II), Pt(II)) affords NCN-pincer complexes with terdentate meridional η3-NCN bonding to the metal, affording two five-membered metallacycles. The ligand acts as a monoanionic 6-electron donor with both N-donor atoms positioned *trans* with respect to each other. The d^8 metals Ni(II), Pd(II), and Pt(II) adopt a square planar geometry with the co-ordination plane of the metal being almost coplanar with the phenyl ring of the pincer ligand (*C*2-symmetric). The remaining co-ordination site can be filled with either a halogen or a Lewis basic ancillary ligand.
5. a) Gossage, R. A.; van de Kuil, L. A.; van Koten, G. *Acc. Chem. Res.,* **1998**, 31, 423-431. b) van de Kuil, L. A.; Luitjes, H.; Grove, D. M.; Zwikker, J. W.; van der Linden, J. G. M.; Roelofsen, A. M.; Jenneskens, L. W.; Drenth, W.; van Koten, G. *Organometallics* **1994**, *13*, 468-77; c) van de Kuil, L. A.; Grove, D. M.; Gossage, R. A.; Zwikker, J. W.; Jenneskens, L. W.; Drenth, W.; van Koten, G. *Organometallics* **1997**, *16*, 4985-4994.
6. van Manen, H-. J.; Nakashima, K.; Shinkai, S.; Kooijman, H.; Spek, A. L.; van Veggel, F. C. J. M.; Reinhoudt, D. N. *Eur. J. Inorg. Chem.,* **2000**, *12*, 2533-2540.
7. Bergbreiter, D. E.; Osburn, P. L.; Liu, Y.-S. *J. Am. Chem. Soc.* **1999**, *121*, 9531-9538.
8. Bergbreiter, D. E.; Osburn, P. L.; Frels, J. D. *J. Am. Chem. Soc.* **2001**, *123*, 11105-11106.
9. van de Kuil, L. A.; Grove, D. M.; Zwikker, J. W.; Jenneskens, L. W.; Drenth, W.; van Koten, G. *Chem. Mater*. **1994**, *6*, 1675-83.
10. a) Dijkstra, H. P.; Meijer, M. D.; Patel, J.; Kreiter, R.; van Klink, G. P. M.; Lutz, M.; Spek, A. L.; Canty, A. J.; van Koten, G. *Organometallics*, **2001**, *20*, 3159-3168. b) Dijkstra, H. P.; Steenwinkel, P.; Grove, D. M.; Lutz, M.; Spek, A. L.; van Koten, G. *Angew. Chem. Int. Ed.* **1999**, *38*, 2186-2188; *Angew. Chem.,* **1999**, *111*, 2322-2324 c) Beletskaya, I. P.; Chuchurjukin, A. V.; Dijkstra, H. P.; van Klink, G. P. M; van Koten, G. *Tetrahedron Lett.* **2000**, *41*, 1075-1079. d) Beletskaya, I. P.; Chuchurjukin, A. V.; Dijkstra, H. P.; van Klink, G. P. M; van Koten, G. *Tetrahedron Lett.* **2000**, *41*, 1081-1085.
11. Schlenk, C.; Kleij, A. W.; Frey, H.; van Koten, G., *Angew. Chem. Int. Ed.*, **2000**, *39*, 3445; *Angew. Chem.,* **2000**, *112*, 3587-3589.
12. Knapen, J. W. J.; van der Made, A. W.; de Wilde, J. C.; van Leeuwen, P. W. N. M.; Wijkens, P.; Grove, D.; van Koten, G. *Nature* **1994**, *327*, 659.
13. a) Kleij, A.W.; Gossage, R. A.; Jastrzebski, J. T. B. H.; Boersma, J.; van Koten, G. *Angew. Chem. Int. Ed.* **2000**, *39*, 176-178; *Angew. Chem.* **2000**, *112*, 179-181. b) Kleij, A.W.; Kleijn, H.; Jastrzebski, J. T.

B. H.; Spek, A. L.; van Koten, G. *Organometallics* **1999**, *18(2)*, 277-285. c) Kleij, A.W.; Kleijn, H.; Jastrzebski, J. T. B. H.; Smeets, W. J. J.; Spek, A. L.; van Koten, G. *Organometallics* **1999**, *18*, 268-276. d) Kleij, A. W.; Gossage, R. A.; Klein Gebbink, R. J. M.; Brinkmann, N.; Reijerse, E. J.; Lutz, M; Spek, A. L.; van Koten, G. *J. Am. Chem. Soc.* **2000**, *122*, 12112-12124.

14. a) Albrecht, M.; Hovestad, N. J.; Boersma, J.; van Koten, G. *Chem. Eur. J.* **2001**, *7*, 1289-1294. b) Albrecht, M.; Gossage, R. A.; Lutz, M.; Spek, A. L.; van Koten, G. *Chem. Eur. J.* **2000**, *6*, 1271 and 1431-1445. c) Albrecht, M.; van Koten, G. *Adv. Mater.* **1999**, *11*, 171-174. d) Albrecht, M.; Gossage, R. A.; Spek, A. L.; van Koten, G. *Chem. Commun.* **1998**, 1003-1004.
15. a) Meijer, M. D.; van Klink; G. P. M.; de Bruin, B; van Koten, G. *Inorg. Chim. Act*. **2002**, *327*, 31-40. b) Meijer, M. D.; Ronde, N.; Vogt, D.; van Klink; G. P. M.; van Koten, G. *Organometallics* **2001**, *20*, 3993-4000.
16. Giminez, R.; Swager, T.M. *J. Mol. Cat. A*. **2001**, *166*, 265-273.
17. a) van de Coevering, R.; Kuil, M.; Klein Gebbink, R. J. M.; van Koten, G. *Chem. Commun.* **2002**, 1636-1637; b) Albrecht, M.; Lutz, M.; Spek, A. L.; van Koten, G. *Nature* **2000**, *406*, 970-974. c) Albrecht, M.; Lutz, M.; Schreurs, A. M. M.; Lutz, E. T. H.; Spek, A. L.; van Koten, G. *J. Chem. Soc., Dalton Trans*. **2000**, 3797-3804. d) Davies, P. J.; Veldman, N.; Grove, D. M.; Spek, A. L.; Lutz, B. T. G.; van Koten, G. *Angew. Chem. Int. Ed.* **1996**, *35*, 1959-1961.
18. For example: a) Huisman, B-.H.; Schönherr, H.; Huck, W. T. S.; Friggeri, A.; Van Manen, H. W. J.; Menozzi, E.; Vancso, G. J.; Van Veggel, F. C. J. M.; Reinhoudt, D. N. *Angew. Chem. Int. Ed.* **1999**, *38*, 2248-2251; *Angew. Chem.* **1999**, *111*, 2385-2389. b) Huck, W. T. S.; Prins, L. J.; Fokkens, R. H.; Nibbering, N. M. M.; Van Veggel, F. C. J. M.; Reinhoudt, D. N. *J. Am. Chem. Soc.* **1998**, *120*, 6240-6246. c) Huck, W. T. S.; Van Veggel, F. C. J. M.; Reinhoudt, D. N. *Angew. Chem. Int. Ed.* **1996**, *35*, 1213-1215; *Angew. Chem.* **1996**, *108*, 1304-1306.
19. Steenwinkel, P.; Kooijman, H.; Smeets, W. J. J.; Spek, A. L.; Grove, D. M.; van Koten, G. *Organometallics* **1998**, *17*, 5411-5426.
20. a) Back, S.; Gossage, R. A.; Lutz, M.; del Rio, I.; Spek, A. L.; Lang, H.; van Koten, G. *Organometallics* **2000**, *19*, 3296-3304. b) Back, S.; Gossage, R. A.; Lang, L.; van Koten, *G. Eur. J. Inorg. Chem*. **2000**, 1457-1464. c) Back, S.; Frosch, W.; del Rio, I.; van Koten, G.; Lang, H. *Inorg. Chem. Comm. 2* **1999**, 584-586. d) Back, S.; Gossage, R. A.; Rheinwald, G.; Lang, H.; van Koten, G. *J. Organometal. Chem.* **1999**, *582*, 126-138.
21. Rodríguez, G.; Albrecht, M.; Schoenmaker, J.; Ford, A.; Lutz, M.; Spek, A. L.; van Koten, G. *J. Am. Chem. Soc.* **2002**, *124*, 5127-5138.
22. Guillena, G.; Rodríguez, G.; van Koten, G. *Tetrahedron Lett.* **2002**, *43*, 3895-3898
23. a) Suijkerbuijk, B. M. J. M.; Slagt, M. Q.; Klein Gebbink, R. J. M.; Lutz, M.; Spek, A. L.; van Koten, G. *Tetrahedron Lett.* **2002**, *43*, 6565-6568; b) Albrecht, M.; Rodríguez, G.; Schoenmaker, J.; van Koten, G. *Org. Lett.* **2000**, *22*, 3461-3464.
24. a) Lau, M.-K.; Zhang, Q.-F.; Chim, J. L. C.; Wong, W.-T.; Leung, W.-A. Chem. Commun. 2001, 1478-1479; b) Clark, A. M.; Rickard, C. E. F.; Roper, W. R.; Wright, L. J. J. Orgmet. Chem. 2000, 598, 262-275; c) Clark, A. M.; Rickard, C. E. F.; Roper, W. R.; Wright, L. J. Organometallics 1999, 18, 2813-2820; d) Coudret, C.; Fraysse, S.; Launay, J.-P. Chem. Commun. 1998, 663-664; e) Clark, A. M.; Rickard, C. E. F.; Roper, W. R.; Wright, L. J. Organometallics 1998, 17, 4535-4537; f) Clark, G. R.; Rickard, C. E. F.; Roper, W. R.; Wright, L. J.; Yap, P. D. Inorg. Chim. Acta 1996, 251, 65-74; g) Clark, G. R.; Headford, C. E. L.; Roper, W. R.; Wright, L. J. Inorg. Chim. Acta 1994, 220, 261-272.

25. a) Steenwinkel, P.; Gossage, R. A.; van Koten, G. *Chem. Eur. J.* **1998**, *4*, 759-762. b) Steenwinkel, P.; Jastrzebski, J. T. B. H.; Deelman, B.-J.; Grove, D. M.; Kooijman, H.; Veldman, N.; Smeets, W. J. J.; Spek, A. L.; van Koten, G. *Organometallics* **1997**, *16*, 5486-5498. c) Valk, J.-M.; van Belzen, R.; Boersma, J.; Spek, A. L.; van Koten, G. *J. Chem. Soc., Dalton Trans.* **1994**, 2293-2302. d) Valk, J.-M.; Boersma, J.; van Koten, G. *J. Organomet. Chem.* **1994**, *483*, 213-216.
26. Rodríguez, G.; van Koten; unpublished results.
27. Jameson, C. J.; Mason, J. *Multinuclear NMR* (Ed. J. Mason), **1987**, Plenum Press, New York, London, chapters 3, 20 and references cited.
28. Kennedy, J. D.; McFarlane, W.; Puddephat, R. J.; Thompson, P. J. *J. Chem. Soc., Dalton Trans.* **1976**, 874-879, and references cited.
29. Ding, L.; Wu, Y. J.; Zhou, D. P. *Polyhedron* **1998**, *17*, 1725-1728.
30. Exner, O. in *Correlation Analysis in Chemistry; Recent Advances*, Plenum Press, New York, **1978** and references cited.
31. The DFT-B3LYP/LANL2DZ method uses density functional theory combined with effective core potentials. The basis sets used for chlorine and platinum are the Los Alamos National Laboratory sets (LANL) for effective core potentials (ECP) of double ζ type, consisting of a small core ECP with 3s and 3p orbitals in the valence space. The functional form used is the B3LYP, and the relativistic correlations for heavy atoms are considered in ECP.
32. Frisch, M. J. *et al*., Gaussian 98, Revision A.6, Gaussian Inc., Pittsburgh PA, **1998**.
33. Examples of *para*-functionalized NCN-pincer palladium and platinum crystal structures: a) Slagt, M. Q.; Klein Gebbink, R. J. M.; Lutz, M.; Spek, A. L.; van Koten, G. *J. Chem. Soc., Dalton Trans.* **2002**, 2591; b) Dijkstra, H. P.; Meijer, M. D.; Patel, J.; Kreiter, R.; van Klink, G. P. M.; Lutz, M.; Spek, A. L.; Canty, A. J.; van Koten, G. *Organometallics* **2001**, *20*, 3159; c) Albrecht, M.; Gossage, R. A.; Spek, A. L.; van Koten, G. *Chem. Commun.* **1998**, 1003; d) Lagunas, M.-C.; Gossage, R. A.; Spek, A. L.; van Koten, G. *Organometallics* **1998**, *17*, 731; e) James, S. I.; Verspui, G.; Spek, A. L.; van Koten, G. *Chem. Commun.* **1996**, 1309; .
34. Neve, F.; Crispini, A.; Di Pietro, C.; Campagna, S. *Organometallics* **2002**, *21*, 3511-3518.
35. Meijer, M. D.; de Wolf, E. W.; Lutz, M.; Spek, A. L.; van Klink, G. P. M.; van Koten, G. *Organometallics* **2001**, *20*, 4198-4206.
36. a) Albrecht, M.; Spek, A. L.; van Koten, G. *J. Am. Chem. Soc.* **2001**, *123*, 7233-7246. b) Albrecht, M.; Gossage, R. A.; Spek, A. L.; van Koten, G. *J. Am. Chem. Soc.* **1999**, *121*, 11898-11899.
37. van de Coevering, R.; Klein Gebbink, R. J. M.; van Koten, G. manuscript in preparation.
38. For DFT-calculations on NCN- and PCP-pincer complexes, see Stadler, C.; de Lacey, L.; Hernández, B.; Fernández.; Conesa, J. C. *Inorg. Chem.* **2002**, *41*, 4417-4423; Fan, H.-J.; Hall, M. B. *J. Mol Cat. A, Chem.* **2002**, *189*, 111-118.
39. Komiya, S. *Synthesis of Organometallic Compounds*, Wiley, Winchester, **1997**.
40. (a) Canty, A. J.; Patel, J.; Skelton, B. W.; White, A. H. *J. Organomet. Chem.* **2000**, *599*, 195-199. (b) Steele, B. R.; Vrieze, K. *Transition Met. Chem.* **1977**, *2*, 140-144.
41. (a) Steenwinkel, P.; Gossage, R. A.; Maunula, T.; Grove, D. M.; Van Koten, G. *Chem. Eur. J.* **1998**, *4*, 763-768. (b) Terheijden, J.; Van Koten, G.; Grove, D. M.; Vrieze, K.; Spek, A. L. *J. Chem. Soc., Dalton Trans.* **1987**, *6*, 1359-1366. (c) Alsters, P. L.; Baesjou, P. J.; Janssen, M. D.; Kooijman, H.; Sicherer-Roetman, A.; Spek, A. L.; van Koten, G. *Organometallics* **1992**, *11*, 4124-4135.

42. Steenwinkel, P.; James, S. L.; Grove, D. M.; Veldman, N.; Spek, A. L.; van Koten, G. *Chem. Eur. J.* **1996**, *2*, 1440-1445.
43. Beurskens, P. T.; Admiraal, G.; Beurskens, G.; Bosman, W. P.; Garcia-Granda, S.; Gould, R. O.; Smits, J. J. M.; Smykalla, C. *The DIRDIF97 program system*, Technical Report of the Crystallography Laboratory, University of Nijmegen, The Netherlands, **1997**.
44. Sheldrick, G. M. *SHELXL97, Program for crystal structure refinement*, University of Göttingen, Germany, **1997**.
45. Spek, A. L. *PLATON, a multipurpose crystallographic tool*, Utrecht University, The Netherlands.

Chapter Three

Self-assembly of *para*-nitro NCN-pincer palladium complexes into dimers through electron donor-acceptor interactions

Abstract

Para-nitro substituted pincer palladium(II) complexes [PdX(NCN-NO_2)] (X = Cl, Br, NO_2) were found to self assemble into dimers in the solid state. It is proposed that the monomeric units are held together by electron donor-acceptor (EDA) interactions, with the palladium(II) atom acting as a Lewis acid and the nitro-substituent as a Lewis base. The analogous platinum complex [PtBr(NCN-NO_2)] forms no such dimers in the solid state, but is capable of η^1-Pt–SO_2 binding with the platinum(II) centre acting as a Lewis base.

3.1. Introduction

Ligand functionalization offers an important tool for electronic fine-tuning of organometallic complexes. The anionic terdentate ECE ligating 'pincer' complexes, in particular, have attracted attention, since both variations in the *trans* coordinating donor atoms (E) and the introduction of substituents on the phenyl ring *para* to the C_{ipso}–metal bond, allow the manipulation of the properties and reactivities of the resulting complexes.[1,2] The square planar d^8-metal pincer complexes [MX(ECE)] with M = Pd, Pt offer a variety of interesting structural possibilities, acting either in the monocationic $[M(ECE)]^+$ forms as Lewis acids or in their neutral forms as Lewis bases.[1a] In this chapter we report the unexpected dimerization of the *para*-nitro substituted NCN-pincer palladium(II) complexes [PdX(NCN-NO_2)] with X = Cl (**1a**) and Br (**1b**) through electron donor-acceptor (EDA) interactions. A related interaction is observed for the pincer palladium(II) complex [Pd(NO_2)(NCN-NO_2)] (**1c**). However, it is not observed for the analogous platinum(II) complex [PtBr(NCN-NO_2)] (**2**), nor for other *para*-substituted pincer palladium complexes. The non-covalent EDA interaction between palladium and the nitro-substituent described here, is a new structural motif in supramolecular organometallic chemistry.

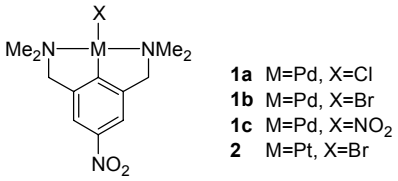

Chart 1. *para*-Nitro substituted NCN-pincer complexes **1a-c** and **2**.

3.2. Results and Discussion

Crystals of **1a** were grown by slow vapor diffusion of diethyl ether into a concentrated dichloromethane solution, while suitable crystals of **1b** were obtained by slow concentration of a dichloromethane solution. Both complexes are isostructural and have approximate, non-crystallographic C_S-symmetry in the solid state. The palladium(II) metal centers have distorted square planar geometries comparable with those found for C_2-symmetric NCN-pincer palladium complexes.[3] In the crystal **1a** and **1b** form a closely packed dimeric structure (see Figure 1).

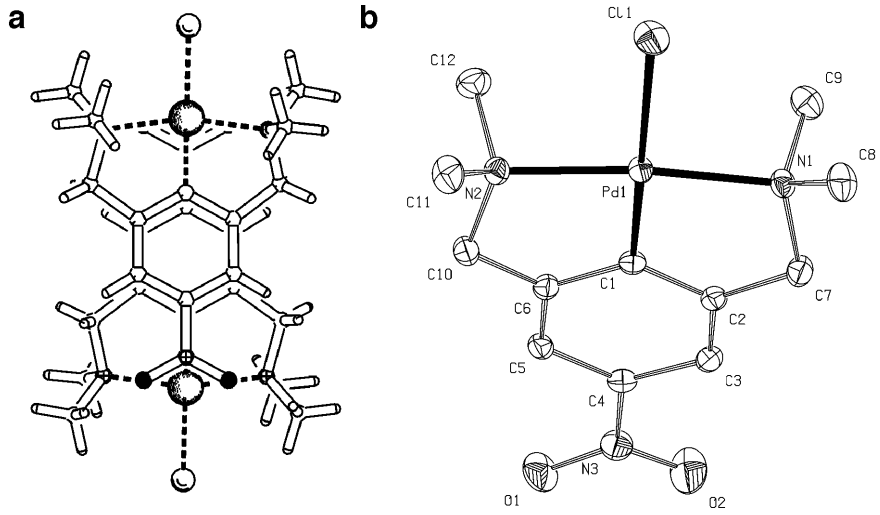

Figure 1. (a) Packing diagram of [PdCl(NCN-NO_2)] (**1a**) showing the dimeric substructure; (b) Displacement ellipsoid plot (50% probability level) of **1a**. Hydrogen atoms have been omitted for clarity.

As a consequence of the C_s-symmetry, both five-membered metallacycles are puckered in the same direction with Pd1-N1-C7-C2 and Pd1-N2-C10-C6 torsion angles of 23.75(18)º and -17.72(17)º, respectively, for compound **1a**. The dimeric structure is centrosymmetric; consequently both participating aryl rings are parallel and are positioned directly on top of one another (Table 1). The face-to-face centre-to-centre arrangement of the aryl rings in the dimer is typical for π-stacked donor-acceptor pairs.[4] The disposition of the amino methyl groups C8 and C11 leaves enough space to accommodate the nitro-substituent of the other molecule in the dimer. The dimer is additionally stabilized by weak hydrogen bonds between aromatic, benzylic and aliphatic C–H hydrogens as donors and halogenide and nitro groups as acceptors. However, the presence of these weak hydrogen bonds cannot solely account for the dimeric structure encountered.

Table 1. Relative orientation of the participating aryl rings in the dimeric structures of **1a**, **1b**, and **1c** (residues 1 and 2).

	1a	**1b**	**1c_1**[a]	**1c_2**[b]
Interplane distance (Å)[c]	3.516	3.503	3.540/3.397	3.557
Distortion (°)[d]	8.62	10.63	17.29/23.64	24.20
Interplane dihedral angle (°)	0.00	0.00	8.22	0.00

a) For the dimer between residues 1 and 2; b) For the dimer between residues 3 and 3^i [1-x, 1-y, 1-z]; c) Perpendicular distance from the ring centroid to the plane of the other ring. d) Angle between the plane normal and the vector connecting the two ring centroids

Interestingly, the short intermolecular contacts between the palladium atoms, and the nitro substituents, indicate the presence of an additional interaction. The distance between the

palladium atoms and the NO_2-nitrogens is slightly shorter (Pd1...N3^i 3.818(2) Å for **1a** than the sum of the Van der Waals radii, 3.85 Å (Table 2). While the coordination of positively charged metals to nitro-substituents is generally considered to involve mainly the negatively charged oxygen atoms, the palladium atoms in **1a** and **1b** are clearly in closer contact with the nitrogen atom than the NO_2-oxygen atoms.

Table 2. Short intramolecular contacts between the Pd-atom and the NO_2-substituent in the dimeric structures of **1a**, **1b** and **1c**.

	1a (Å)	**1b** (Å)	**1c_1** (Å)[a]	**1c_2** (Å)[b]	Sum of Van der Waals radii (Å)[c]
Pd...N3^i	3.818(2)	3.851(3)	3.724(2)/4.051(2)	4.0301(19)	3.85
Pd...O1^i	3.8753(19)	3.863(3)	3.5853(16)/4.2149(19)	4.0006(16)	3.82
Pd...O2^i	3.8759(19)	3.973(3)	3.6930(18)/3.8208(16)	3.9847(18)	3.82

a) For the palladium atoms of residues 1 and 2, respectively; b) For the palladium atoms of residues 3 and 3^i [1-x, 1-y, 1-z] respectively; c) see reference [5]; Symmetry operations i: (**1a**): 1-x, -y, -z; (**1b**): 1-x, -y, -z; (**1c_1**): x, y, z; (**1c_2**): 1-x, 1-y, 1-z.

In fact, we propose the presence of an electron donor-acceptor (EDA) interaction to be responsible for this close contact between the two [PdX(NCN–NO_2)] units in the dimer. This type of EDA interaction can be rationalized using the qualitative orbital model, proposed by Alvarez *et al*. for the description of M···M interactions in dimers and stacks of square planar d^8-ML_4 complexes.[6] Both the filled d_z^2 and the empty p_z frontier orbitals of the metal center possess the correct symmetry for binding along the z-axis. The relative energies of these orbitals can be tuned by choosing appropriate ligands (L) in the xy-plane. The use of better σ-donor ligands stabilizes the filled d_z^2-orbital and enlarges its size. The presence of π-acceptor ligands stabilizes the empty p_z-orbital by making this orbital less contracted, while π-donor ligands do the opposite.[6a,b] Colorful examples of the bonding of Lewis basic NCN-pincer platinum(II) complexes to Lewis acidic SO_2- and I_2-ligands have been reported previously.[1a] Based on the qualitative orbital description (*vide supra*) and the observation that NCN-pincer palladium complexes do not bind to Lewis acids like their platinum analogues,[7] we propose that the palladium(II) atom acts as a Lewis acid in the formation of the dimeric structures observed for **1a** and **1b**. The *para*-nitro substituent on the NCN-pincer ligand withdraws electron density, rendering the pincer ligand a poorer σ-donor, resulting in a destabilized and more contracted filled palladium d_z^2-orbital. Simultaneously, the aryl ligand becomes a better π-acceptor, thereby stabilizing the empty p_z-orbital. These combined effects make the metal less prone to act as a Lewis base, but instead improve its Lewis acidic properties. These Lewis acidic palladium(II) atoms can have attractive interactions with the filled π-orbitals of the nitro-substituent of the neighboring complex. Comparison of **1a** and **1b** indicates that the

influence of the halide on the dimeric structure is only marginal, since the intermolecular distances are similar (Table 2). The somewhat longer Pd···N3 contacts in **1b** compared to **1a** might be ascribed to destabilization of the p_z-orbital by the more π-basic bromide ligand. Replacement of the halide by π-acidic nitrite anion (NO_2^-), to afford complex **1c**, was expected to influence the dimerisation behavior. Interestingly, the crystal structure of **1c** contains three independent molecules. Residues 1 and 2 form a dimer with one another, while residue 3 assembles into a dimer with a symmetry generated molecule of itself (see Figure 2). The pincer complex of residue 3 has approximate C_2-symmetry with the chelate rings puckered in opposite directions. The metal complexes of residues 1 and 2 have their chelate rings puckered in the same direction (approximate C_s-symmetry), as in **1a** and **1b**. The nitrite anion coordinates to the metal via its nitrogen atom and is oriented such that the NO_2 plane is nearly orthogonal with respect to the coordination plane of the palladium atom. The relative arrangement of the interacting complexes in the dimers differs markedly from that in **1a** and **1b**. The aryl rings are shifted sidewards (Table 1), and, here, the oxygen atoms of the nitro-substituent are in close contact with the palladium atom of the neighboring complex (Table 2).

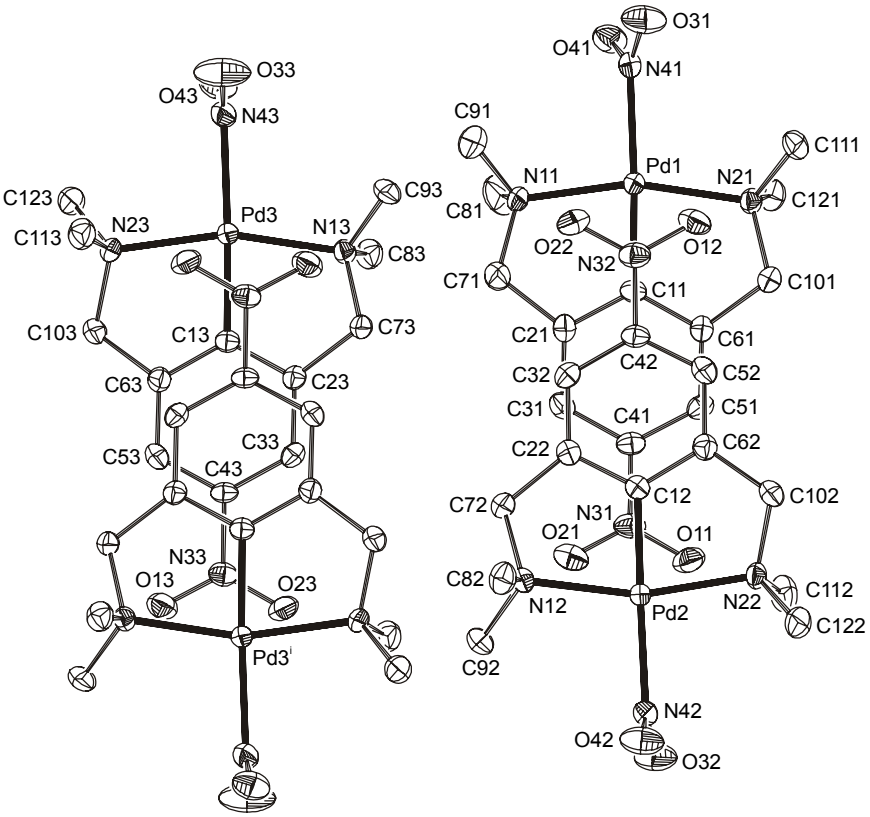

Figure 2. Displacement ellipsoid plot (50% probability level) of [Pd(NO_2)(NCN-NO_2)] (**1c**), showing both dimeric units as they exist next to each other in the solid state. Hydrogen atoms have been omitted for clarity. Symmetry operation i: 1-x, 1-y, 1-z.

As a result of the nearly orthogonal orientation of the nitrite ligand, the effect of its π-system on the relative energies of the metal d_z^2- or p_z-orbitals is small.[8] Hence, these orbitals are mainly influenced by the σ-donating properties of the ligand. We therefore ascribe the differences in the geometry of the dimers in **1c** compared to **1a,b**, mainly to steric factors imposed by the nitrite ligand.

The nitro-substituted NCN-pincer platinum(II) complex **2** was crystallized by vapor diffusion of diethyl ether in a concentrated dichloromethane solution. The crystal structure of **2** contains two independent molecules of comparable geometry. Interestingly, no dimers are formed here, rather the molecules display monomeric structures as normally encountered in d^8-metal pincer complexes (Figure 3). The molecules have approximate C_2-symmetry, with both five-membered metallacycles puckered in opposite directions.

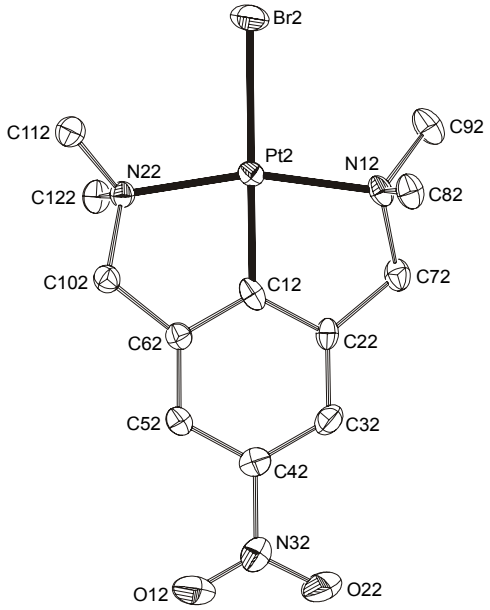

Figure 3. Displacement ellipsoid plot (50% probability level) of one of the independent molecules of [PtBr(NCN-NO_2)] (**2**). Hydrogen atoms have been omitted for clarity.

Obviously, the attractive NO_2...Pd binding interactions, that lead to dimers in the solid state structures of **1a** and **1b** are less pronounced for platinum complex **2**. Most likely, the Lewis acidity of the p_z-orbital is to a greater extent countered by the filled d_z^2-orbital on platinum, leading to an overall repulsive interaction with the filled π-orbitals of the nitro-substituent. It should be noted that the d_z^2-orbital of the platinum(II) centre in **2** is still able to act as a Lewis base for reversible η^1-Pt–SO_2 binding, as was confirmed by ^{1}H- and ^{195}Pt-NMR and IR-spectroscopy. SO_2-binding leads to the typical downfield shift of all signals in ^{1}H-NMR, an upfield shift of 500 ppm in ^{195}Pt-NMR, and characteristic (ν_{ass} = 1248 cm^{-1}, ν_s = 1086 cm^{-1}) SO_2 absorbances in IR-spectroscopy. Similar to other NCN-pincer palladium complexes,[7]

both **1a** and **1b** do not form such adducts with SO_2. We are currently studying the supramolecular structure of other *para*-substituted NCN-pincer metal complexes both in solution and in the solid state.

3.3. Experimental

General

The syntheses of complexes **1a**, **1b** and **2** is described in chapter 2. ^{1}H-NMR spectra were recorded on a Varian Inova 300 spectrometer (operating at 300 MHz), and UV/Vis spectra were recorded on an Inova Cary 1 spectrophotometer.

*[Pd(NO$_2$)(NCN-NO$_2$)] (**2**)*

To a solution of **1a** (200 mg, 0.53 mmol) in wet acetone (10 mL) was added solid $AgBF_4$ (108 mg, 0.56 mmol) at once. An off-white precipitate was formed immediately and the mixture was stirred for 1 h at room temperature. The suspension was carefully filtered over Celite. An excess of $NaNO_2$ (0.5 g, 7.2 mmol) was added to the filtrate and the suspension was stirred for 1 h. The solids were removed by filtration over Celite and **1c** was precipitated from the solution by the addition of hexane (90 mL) as a yellowish solid (177 mg, 0.46 mmol, 86%)

Crystal Structure Determinations

1a: $C_{12}H_{18}ClN_3O_2Pd$, FW = 378.14, pale yellow block, 0.18 x 0.18 x 0.15 mm^3, T=150(2) K, monoclinic, $P2_1/c$ (No. 14), a = 8.9737(1), b = 10.7287(2), c = 16.5569(3) Å, β = 117.170(1)°, V = 1418.14(4) Å^3, Z = 4, F(000) = 760, D_c = 1.771 gcm^{-3}, 14018 measured reflections, 3246 unique reflections (R_{int} = 0.037). Absorption correction based on multiple measured reflections (PLATON, routine MULABS, μ = 1.498 mm^{-1}, 0.69-0.74 transmission). 176 refined parameters, no restraints. R (I > 2σ(I)): R1 = 0.0204, wR2 = 0.0466. R (all data): R1 = 0.0237, wR2 = 0.0479. S = 1.066. Residual electron density (min/max) = -0.61/0.38 e/Å^3. Selected bond lengths (Å), angles and dihedral angles (°) for **1a**: Pd1-C1 1.9131(18), Pd1-N1 2.1018(15), Pd1-N2 2.1007(15), Pd1-Cl1 2.4277(5), C1-Pd1-N1 82.48(7), C1-Pd1-N2 82.49(7), C1-Pd1-Cl1 172.81(5), N1-Pd1-N2 163.56(6), Pd1-N1-C7-C2 23.75(18), Pd1-N2-C10-C6 -17.72(17).

1b: $C_{12}H_{18}BrN_3O_2Pd$, FW = 422.60, pale yellow block, 0.30 x 0.24 x 0.21 mm^3, T=150(2) K, monoclinic, $P2_1/c$ (No. 14), a = 8.9419(1), b = 10.7870(1), c = 16.6640(2) Å, β = 116.1940(6)°, V = 1442.28(3) Å^3, Z = 4, F(000) = 832, D_c = 1.946 gcm^{-3}, 18411 measured reflections, 3293 unique reflections (R_{int} = 0.048). Absorption correction based on multiple measured reflections (PLATON, routine MULABS, μ = 4.058 mm^{-1}, 0.36-0.43 transmission). 176 refined parameters, no restraints. R (I > 2σ(I)): R1 = 0.0264, wR2 = 0.0618. R (all data):

R1 = 0.0331, wR2 = 0.0644. S = 1.061. Residual electron density (min/max) = -1.41/0.86 e/Å^3.
Selected bond lengths (Å), angles and dihedral angles (°) for **1b**: Pd1-C1 1.913(2), Pd1-N1 2.107(2), Pd1-N2 2.105(2), Pd1-Br1 2.5516(3), C1-Pd1-N1 82.41(9), C1-Pd1-N2 82.33(9), C1-Pd1-Br1 172.10(7), N1-Pd1-N2 163.58(8), Pd1-N1-C7-C2 -25.0(2), Pd1-N2-C10-C6 17.4(2).

1c: $C_{12}H_{18}N_4O_4Pd$, FW = 388.70, yellow block, 0.09 x 0.09 x 0.03 mm^3, T=150(2) K, monoclinic, $P2_1/n$ (No. 14), a = 13.8395(1), b = 12.4601(1), c = 26.6584(3) Å, β = 102.9047(6)°, V =4480.91(7) Å^3, Z = 12, F(000) = 2352, D_c = 1.729 gcm^{-3}, 77494 measured reflections, 10202 unique reflections (R_{int} = 0.050). Absorption correction based on multiple measured reflections (PLATON, routine MULABS, μ = 1.263 mm^{-1}, 0.91-0.97 transmission). The crystal structure contains three independent residues, which are related by pseudo translational symmetry (1/3 in *c* direction), which is 87% fulfilled. The major difference between these residues is the conformation of the nitrite ligand and the puckering of the pincer chelate rings. As a consequence there are weak, but non-negligible superstructure reflections with the pseudo extinction condition (hkl, l=3n). 580 refined parameters, no restraints. R (I > 2σ(I)): R1 = 0.0292, wR2 = 0.0666. R (all data): R1 = 0.0512, wR2 = 0.0741. S = 0.997. Residual electron density (min/max) = -0.70/0.65 e/Å^3.
Selected bond lengths (Å), angles and dihedral angles (°) for **1c**. Residue 1: Pd1-C11 1.919(2), Pd1-N11 2.0908(17), Pd1-N21 2.1054(17), Pd1-N41 2.1184(19), C11-Pd1-N11 82.45(8), C11-Pd1-N21 82.06(8), C11-Pd1-N41 177.50(8), N11-Pd1-N21 162.79(7), Pd1-N11-C71-C21 -23.6(2), Pd1-N21-C101-C61 21.6(2), N11-Pd1-N41-O41 -67.11(17). Residue 2: N12-Pd2-N42-O42 –83.13(17). Residue 3: Pd3-C13 1.917(2), Pd3-N13 2.1052(16), Pd3-N23 2.0968(17), Pd3-N43 2.1250(19), C13-Pd3-N13 81.49(8), C13-Pd3-N23 82.09(8), C13-Pd3-N43 177.43(8), N13-Pd3-N23 163.45(7), Pd3-N13-C73-C23 25.61(19), Pd3-N23-C103-C63 27.9(2), N13-Pd3-N43-O43 94.42(17).

2: $C_{12}H_{18}BrN_3O_2Pt$, FW = 511.29, yellow plate, 0.36 x 0.27 x 0.06 mm^3, T=150(2) K, monoclinic, C2/c (No. 15), a = 31.5588(4), b = 15.6312(2), c = 8.9960(1) Å, β = 98.8412(6)°, V = 4385.01(9) Å^3, Z = 12, F(000) = 2880, D_c = 2.323 gcm^{-3}, 31967 measured reflections, 5015 unique reflections (R_{int} = 0.041). Analytical absorption correction (PLATON, routine ABST, μ = 12.335 mm^{-1}, 0.09-0.60 transmission). 266 refined parameters, no restraints. R (I > 2σ(I)): R1 = 0.0202, wR2 = 0.0396. R (all data): R1 = 0.0288, wR2 = 0.0417. S = 1.046. Residual electron density (min/max) = -1.12/1.56 e/Å^3.
Selected bond lengths (Å), angles and dihedral angles (°) for **2** (residue 2): Pt2-C12 1.937(4), Pt2-N12 2.105(3), Pt2-N22 2.099(2), Pt2-Br12 2.5211(4), C12-Pt2-N12 81.78(11), C12-Pt2-

N22 81.46(11), C12-Pt2-Br12 175.56(8), N12-Pt2-N22 163.20(11), Pt2-N12-C72-C22 -31.5(3), Pt2-N22-C102-C62 -34.0(3).

*SO_2-absorption of [PtBr(NCN-NO_2)] (**2**)*

2: ^{1}H-NMR (300 MHz, 0.1 M, $CDCl_3$) δ (ppm): 7.74 (s, 2H, ArH), 4.09 (s, 4H, $^3J_{Pt-H}$ 46.2 Hz, CH_2N), 3.13 (s, 12H, $^3J_{Pt-H}$ 38.1 Hz, NMe_2); ^{195}Pt-NMR (64.3 MHz, 0.1 M, $CDCl_3$) δ (ppm): -1819.

2(SO_2): ^{1}H-NMR (0.1 M, $CDCl_3$ sat. with SO_2) δ (ppm): 7.77 (s, 2H, ArH), 4.19 (s, 4H, $^3J_{Pt-H}$ 43.8 Hz, CH_2N), 3.19 (s, 12H, $^3J_{Pt-H}$ 36.3 Hz, NMe_2); ^{195}Pt-NMR (0.1 M, $CDCl_3$ sat. with SO_2) δ (ppm): -1324. IR (CH_2Cl_2) ν (cm^{-1}): 1248 ($\nu_{as}(SO_2)$, $PtSO_2$-adduct), 1086 ($\nu_s(SO_2)$, $PtSO_2$-adduct).

3.4 References and Notes

1. For reviews see: (a) Albrecht, M; van Koten, G. *Angew. Chem. Int. Ed.* **2001**, *40*, 5000-5031, *Angew. Chem*., **2001**, *113*, 3866-3898; (b) Rybtchinski, R.; Milstein, D. *Angew. Chem. Int. Ed.* **1999**, *38*, 870-883; (c) Rietveld, M. P. H.; Grove, D. M.; van Koten, G. *New J. Chem.* **1997**, *21*, 751-771. (d) van Koten, G. *Pure Appl. Chem.* **1989**, *61*, 1681.
2. (a) Grimm, J. C.; Nachtigal, C.; Mack, H.-G.; Kaska, W. C.; Mayer, H. A. *Inorg. Chem. Comm.* **2001**, *3*, 511-514. (b) Gossage, R. A.; van de Kuil, L. A.; van Koten, G. *Acc. Chem. Res.* **1998**, 31, 423-431; and chapter 2 of this thesis.
3. For example: (a) Albrecht, M.; Lutz, M.; Schreurs, A. M. M.; Lutz, E. T. H.; Spek, A. L.; van Koten, G. *J. Chem. Soc., Dalton Trans*. **2000**, 3797-3804. b) Lagunas, M.-C.; Gossage, R. A.; Spek, A. L.; van Koten, G. *Organometallics* **1998**, *17*, 731.
4. Rathore, R.; Lindeman, S. V.; Kochi, J. K. *J. Am. Chem. Soc.* **1997**, *119*, 9393-9404.
5. Bondi, A. *J. Phys. Chem.* **1964**, *68*, 441.
6. (a) Aullón, G.; Ujaque, G.; Lledós, A.; Alvarez, S.; Alemany, P. *Inorg. Chem.* **1998**, *37*, 804-813. (b) Aullón, G.; Alvarez, S. *Chem. Eur. J.* **1997**, *3*, 655-664. (c) Aullón, G.; Alemany, P.; Alvarez, S. *Inorg. Chem.* **1996**, *35*, 5061-5067. (d) Aullón, G.; Alvarez, S. *Inorg. Chem.* **1996**, *35*, 3137-3144. (e) Novoa, J. J.; Aullón, G.; Alemany, P.; Alvarez, S. *J. Am. Chem. Soc.* **1995**, *117*, 7169-7171.
7. Gossage, R. A.; Ryabov, A. D.; Spek, A. L.; Stufkens, D. J.; van Beek, J. A. M.; van Eldik, R.; van Koten, G. *J. Am. Chem. Soc.* **1999**, *121*, 2488-2497.
8. The π-system of the orthogonally oriented nitrite ligand has the correct symmetry for constructive overlap with the $d_{x^2-y^2}$ orbital on the palladium atom.

Chapter Four

NCN-Pincer Palladium(II) - Pyrenoxy based Molecular Tweezers: Synthesis, Properties in Solution and Catalysis

Abstract

A highly flexible molecular tweezer **1a**, constructed from a para-hydroxyl functionalized NCN-pincer palladium(II) complex (NCN-Z = [2,6-$(CH_2NMe_2)_2C_6H_2$-4-Z]), a pyrenoxy unit and a xylyl spacer, was synthesized and immobilized on a G_2-carbosilane dendrimer (**1b**). The binding affinity of picric acid towards the pyrenoxy moiety was studied by ^{1}H-NMR titrations, revealing association constants K_a in the order of 10^1-10^2 M^{-1}. X-ray analysis of the structure of **10**, a precursor ligand of **1a** and **1b**, showed a completely flattened conformation in the solid state, imposed by favorable intramolecular π-stacking interactions. The molecular structure of **1a** in solution proved to be fluxional on the NMR-timescale. UV/Vis and (time-resolved) fluorescence spectroscopy revealed that in spite of the high flexibility, the catalyst and pyrenoxy unit are in close proximity due to cation-π interactions. This was further supported by conformer searches using molecular mechanics (MM2). Tweezer **1a** shows small rate enhancements in aldol condensations of aromatic aldehydes with methyl isocyanoacetate compared to complex **2**, which lacks the pyrenoxy unit.

4.1. Introduction

The use of NCN-pincer complexes (NCN = 2,6-bis[(dimethylamino)methyl]phenyl anion) as building blocks in the construction of multisite or dendritic catalysts, of supramolecular assemblies and of sensor materials, has attracted considerable attention.[1] An important issue in their construction is the synthetic flexibility for the introduction of functional groups, combined with the variety of metallation procedures available.[2] Whereas ligand substitution allows immobilization of transition metal complexes on various support systems,[3] the introduction of functional groups in the vicinity of a metal site can alter its catalytic properties. Both features are represented in a system published earlier in our group. Catalytic palladium(II) sites were encapsulated by strategic placement of diphenylsilane moieties, and subsequently immobilized on a dendritic backbone.[4] This rather rigid encapsulation of the catalytic site resulted in enhanced reaction rates, but hardly influenced the selectivity of the studied aldol reaction catalyzed by the cationic NCN-pincer palladium(II) complex. This approach, where functional groups are introduced in the vicinity of the metal site to modify its (catalytic) properties by secondary interactions, has motivated us to construct new molecular tweezers (**1a** and **1b**) based on a pincer palladium(II) complex and a pyrenoxy moiety, as shown in Chart 1.

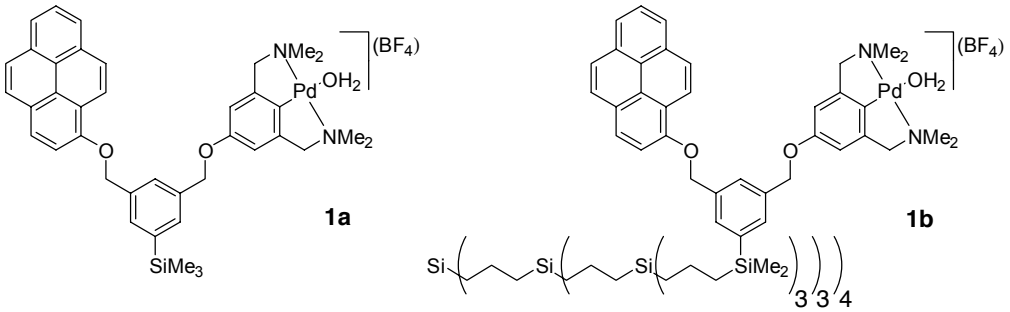

Chart 1. (Dendritic) NCN-palladium(II) complexes **1a** and **1b** functionalized with pyrenoxy units.

In this chapter we report the synthesis of **1a, 1b** and their relevant variations **2-4** (Chart 2), following a minimalistic approach where the separately prepared building blocks are assembled on the xylyl spacer group by highly flexible ether linkages. This spacer has an additional reactive site, which allows immobilization on suitable (dendritic) support systems. In **1a**, a trimethylsilyl substituent is attached at this anchoring point, serving as a mimic for dimethylsilyl functionalized carbosilane dendrimers. The dendrimer immobilized multisite catalyst **1b** contains 36 NCN-palladium pyrenoxy moieties attached to an inert carbosilane dendrimer. Anchoring of these systems to dendrimers makes recycling of the catalyst possible by employing nano-filtration techniques to separate the catalyst from the reaction products.[5] The molecular flexibility of **1a** in solution is studied by spectroscopic techniques using the

pyrenoxy group as fluorescent probe, and by molecular modeling studies. Furthermore, the influence of the pyrenoxy moiety on the application of **1a** as homogeneous catalysts in aldol reactions is described, together with its binding properties to aromatic molecules.

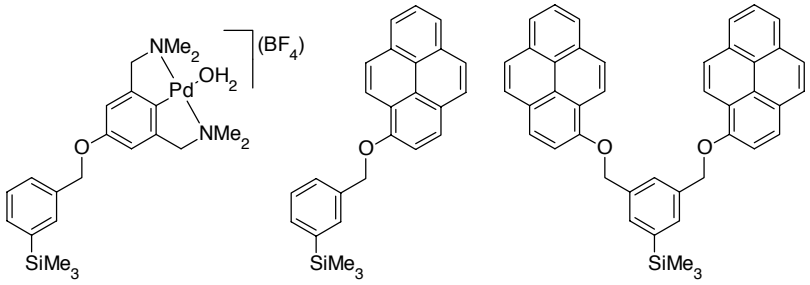

2 **3** **4**

Chart 2. NCN-palladium(II) complex **2** and pyrenyl ethers **3** and **4**.

4.2. Results

Synthesis

Precursor ligand **10** has been synthesized by combining three building blocks, *i.e.* pyren-1-ol (**6**) and the NCN-pincer ligand (**9**) were connected to the 3,5-bis(bromomethyl)phenyl bromide linker (**5**) via ether syntheses (Scheme 1). An excess of tribromide **5** was reacted with pyrenoxy unit **6** to afford a 1:2:1 mixture of unreacted **5**, monofunctionalized **7**, and bisfunctionalized **8**. Selective extraction of **5** from the reaction mixture with refluxing pentane afforded a 2:1 mixture of pyrenyl ethers **7** and **8**. This unresolved mixture was used in the subsequent coupling with 4-trimethylsilyl-3,5-bis[(dimethylamino)methyl]phenoxide, which was prepared in situ from **9** by deprotection with tetrabutylammonium fluoride. Purification of the coupling products by careful precipitation of the bispyrenyl ether **8** from dichloromethane/pentane afforded pure **10** in the mother liquor. Precursor ligand **10** was subsequently attached to either a trimethylsilyl substituent to prepare **11a**, or to a G_2 carbosilane dendrimer to produce **11b**. Reaction of **10** with *t*-BuLi followed by treatment with trimethylsilyl chloride or a chlorosilane functionalized G_2-carbosilane dendrimer afforded ligands **11a** and **11b**, respectively (Scheme 1). Ligand **14**, the trimethylsilyl precursor of complex **2**, and pyrenyl ethers **3** and **4** were obtained via similar synthetic procedures, using 3-(bromomethyl)phenyl bromide as anchoring point for either NCN-ligand **9** or pyrenoxy unit **6**.

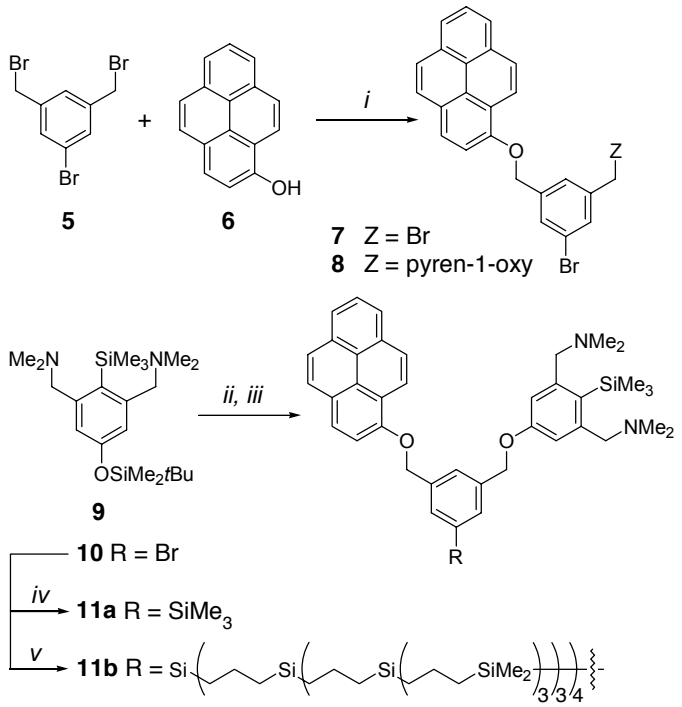

Scheme 1. Synthesis of precursor ligands, *i)* K_2CO_3, 18-crown-6; *ii)* Bu_4NF; *iii)* **7**, K_2CO_3, 18-crown-6; *iv)* *t*BuLi, $SiMe_3Cl$; *v)* *t*-BuLi, $Si((CH_2)_3Si((CH_2)_3Si((CH_2)SiMe_2Cl)_3)_3)_4$.

Earlier work of Valk[6] *et al.* and Steenwinkel *et al.*[7] had demonstrated that in R_2NCH_2-substituted aromatic systems replacement of an *ortho*-aryl-H by a trimethylsilyl-substituent can steer the regioselectivity of the palladation reaction. Thus, treatment of **11a**, **11b** and **14** with $Pd(OAc)_2$ and subsequent addition of LiCl led to the formation of the corresponding palladium(II) chloride complexes **12a**, **12b** and **15**, respectively. Noteworthy is the quantitative metallation of the dendritic polyligand **11b**, by applying this mild and selective method. The cationic catalytically active palladium(II) complexes **1a** and **1b** were prepared by electrophilic palladation and subsequent halide abstraction starting from their ligand precursors **11a** and **11b** (Scheme 2). Complex **2** was prepared from NCN-ligand **14** in a similar manner. This approach offers the advantage that a wide number of chemical reactions (*e.g.* lithiation at the linker) can be performed on the system, while regioselective introduction of the palladium(II) center under relatively mild conditions is feasible as the final step in the synthesis. All palladium(II) chloride complexes **12a**, **12b** and **15**, and their corresponding cationic complexes **1a, 1b** and **2**, are air and water stable. However, in concentrated solutions slow decomposition, *i.e.* the formation of Pd(0), is observed for all complexes. Furthermore, the somewhat less stable cationic complexes are prepared freshly when applied in catalysis.

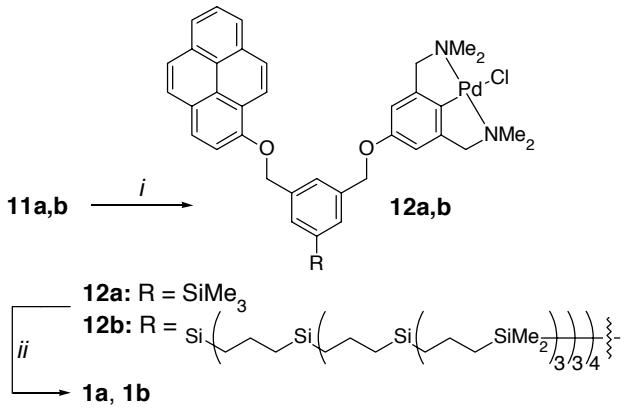

Scheme 2. Synthesis of **1a** and **1b** by site-selective palladation and subseqent halide abstraction, *i)* $Pd(OAc)_2$, LiCl; *ii)* $AgBF_4$.

*Crystal Structure of **10**.*

All attempts to obtain suitable crystals for X-ray analysis of cationic complex **1a** or its chloropalladium(II) analogue **12a** failed. Crystallization of the precursor ligand **10**, afforded suitable crystals for structure determination. The molecular and crystal structure, together with selected bond lengths and angles, are given in Figures 1 and 2, and Table 1.

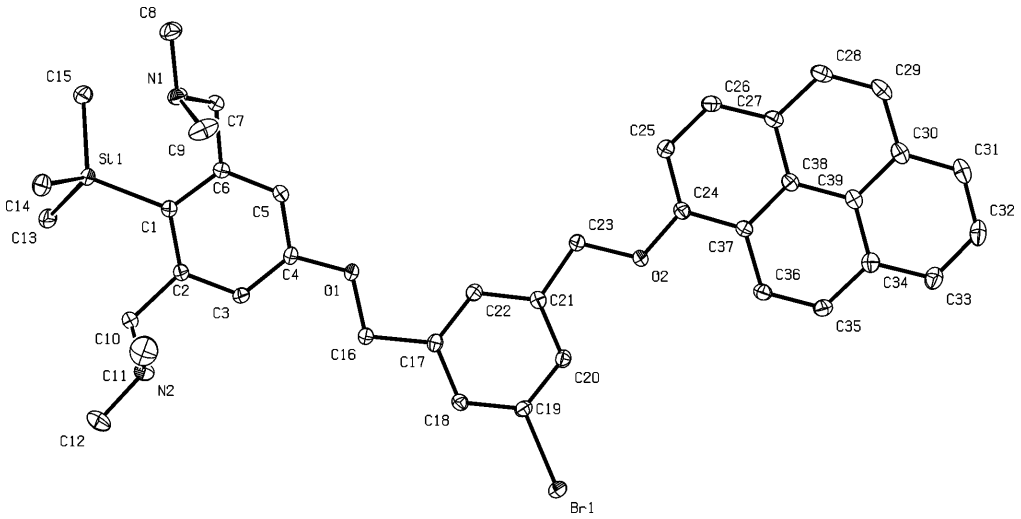

Figure 1. ORTEP representation of **10** (displacement ellipsoids with 30% probability). Hydrogen atoms are omitted for clarity.

The structure of **10** shows the full integrity of the molecule. Interesting aspects of the structure include the silicon center which is σ-bonded to three methyl groups, C_{ipso} (C(1)) of the ligand, and in addition has an interaction with one of the *ortho*-CH_2NMe_2 groups. The Si(1)...N(1) distance is 3.264(2) Å, which is substantially smaller than the sum of the Van der Waals radii of nitrogen and silicon (3.65 Å). As a consequence of this interaction, the methyl groups on silicon are distorted from a true tetrahedral geometry, with the Si(1)-C(13) bond

being significantly longer than the Si(1)-C(14) and Si(1)-C(15) bonds. An even shorter N...Si contact of 3.040 Å has been reported by Steenwinkel et al.[7b]

Table 1. Selected bond lengths [Å], bond angles [deg] and dihedral angles [deg] of **10**; the numbering refers to Figure 1.

Bond Distances (Å)			
Br(1)-C(19)	1.903 (2)	O(1)-C(16)	1.371 (3)
N(1)- C(7)	1.460 (3)	O(2)-C(23)	1.419 (3)
N(1)- C(8)	1.463 (3)	O(2)-C(24)	1.372 (3)
N(1)- C(9)	1.455 (3)	Si(1)-C(1)	1.909 (2)
N(2)-C(10)	1.467 (3)	Si(1)-C(13)	1.886 (2)
N(2)-C(11)	1.458 (4)	Si(1)-C(14)	1.870 (3)
N(2)-C(12)	1.467 (4)	Si(1)-C(15)	1.879 (3)
O(1)-C(4)	1.371 (3)	Si(1)-N(1)	3.264 (2)
Bond Angles (deg)			
C(4)-O(1)-C(16)	117.9 (2)	C(13)-Si(1)-C(14)	110.0 (1)
C(7)-N(1)-C(8)	110.3 (2)	C(13)-Si(1)-C(15)	101.1 (1)
C(7)-N(1)-C(9)	111.5 (2)	C(14)-Si(1)-C(1)	112.4 (1)
C(8)-N(1)-C(9)	109.6 (2)	C(14)-Si(1)-C(15)	109.1 (1)
C(10)-N(2)-C(11)	110.2 (2)	C(15)-Si(1)-C(1)	114.9 (1)
C(10)-N(2)-C(12)	109.1 (2)	C(21)-C(23)-O(2)	110.2 (2)
C(11)-N(2)-C(12)	110.9 (2)	C(23)-O(2)-C(24)	117.1 (2)
C(13)-Si(1)-C(1)	108.7 (2)	O(1)-C(16)-C(17)	108.1 (2)
Dihedral Angels (deg)			
C(3)-C(2)-C(10)-N(2)	46.0 (3)	C(22)-C(21)-C(23)-O(2)	-175.3 (2)
C(4)-O(1)-C(16)-C(17)	-173.4 (2)	C(23)-O(2)-C(24)-C(37)	189.1 (2)
C(5)-C(6)-C(7)-N(1)	-123.6 (2)	C(24)-O(2)-C(23)-C(21)	179.9 (2)
C(16)-O(1)-C(4)-C(5)	171.6 (2)	O(1)-C(16)-C(17)-C(18)	177.0 (2)

In the crystal lattice, the molecule is completely flattened out as a result of crystal packing (Figure 2). The bulky substituents on the ligand, *i.e.* the $SiMe_3$ and *ortho*-Me_2NCH_2-substituents, are placed in the crystal lattice in such a way that optimal stacking between the aromatic parts can take place. The requirements[8] for good FFCE (face-to-face, edge-to-edge) stacking are fulfilled for several intermolecular ring-ring interactions. For example, the interaction between the aromatic ring containing C(17)-C(22) and the ring C(34)-C(39) of the neighboring molecule, has the following stacking parameters: $\alpha = 2.9°$, x = 1.8 Å and z = 3.5 Å, which all lay within the boundaries for good FFCE stacking.

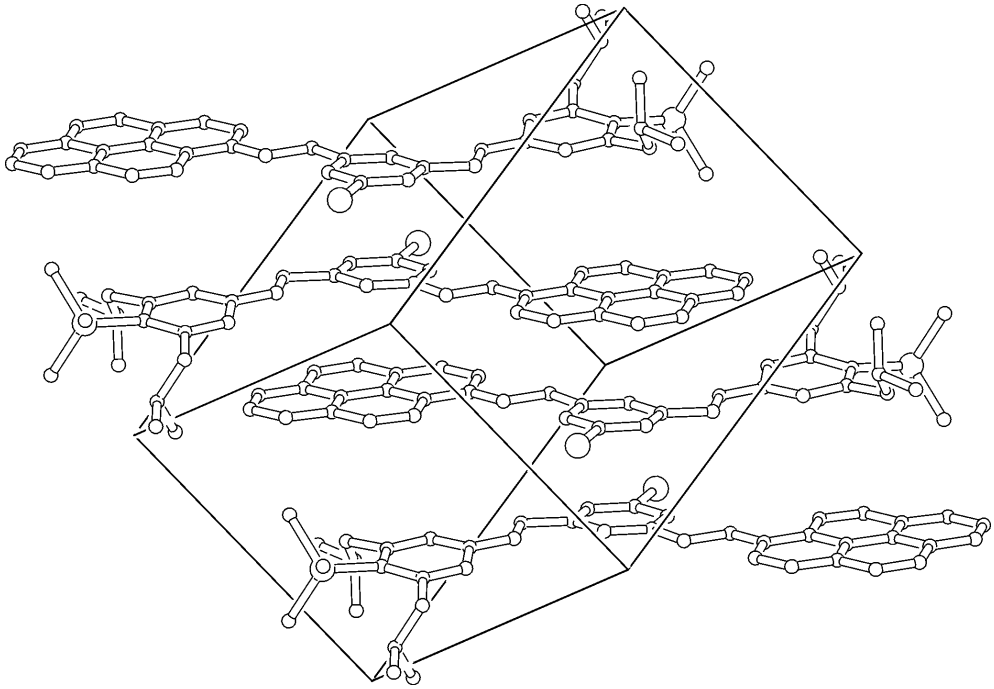

Figure 2. Packing plot of **10** with unit cell, showing the π-stacked layered structure.

UV/Vis-, fluorescence-, and ^{1}H-NMR-spectroscopic studies.

As a result of relatively unhindered rotation around the ether linkages, a wide range of conformations can be adopted by complex **1a** in solution. To obtain an indication for the preferred conformation(s) in solution, **1a** was subjected to UV/Vis, fluorescence and variable-temperature ^{1}H-NMR studies. The highly fluorescent pyrenoxy moiety offers an excellent probe to study the conformational behavior of this cationic palladium complex. Conformational molecular mechanics studies were performed to obtain more insight.

Variable temperature ^{1}H-NMR studies were performed on a solution of **1a** in $CDCl_3$ between -60 °C and 40 °C. Although the resonances of the benzylic protons from the spacer broadened upon cooling down, no conformation could be frozen out. At higher temperatures sharpening of the signals occurred, but no other significant changes in the ^{1}H-NMR spectrum were observed. The electronic absorption spectrum of cationic palladium(II) complex **1a** shows small batochromic shifts for the longer wavelength bands and significant hypochroism compared to its non-metallated analogue **11a**. Besides this, the fluorescence bands of **1a** show a batochromic shift of approximately 5 nm and a decrease in fluorescence intensity by a factor of 10. The optical properties of the G_2-carbosilane immobilized complex (**1b**) and ligand (**11b**) were not studied in detail, since their fluorescence was quenched. Fluorescence lifetime measurements revealed that the decay curves of **1a** and **11a** were both due to one-component systems. In dichloromethane, the fluorescence lifetime for **1a** is 1.8 ns while the lifetime of its non-metallated analogue **11a** is 10.6 ns (Figure 3).

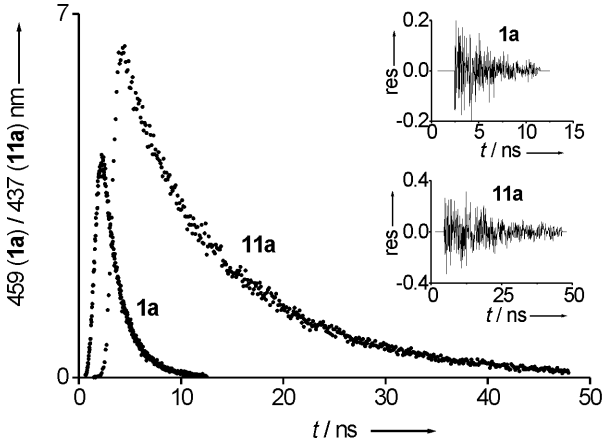

Figure 3. Fluorescence decay curves for **1a** (τ=1.8 ns) and **11a** (τ=10.6 ns).

To gain more insight in the flexibility of the 1,3-bis-(hydroxymethyl)benzene ethers, bis-pyrenoxy ether **8** was subjected to time-resolved fluorescence spectroscopy. A new emission band (λ_{max}=450 nm) appeared apart from the monomer emission in the steady-state fluorescence spectrum of **8** (Figure 4a). This band was attributed to excimer emission, owing to the proximity of two pyrenoxy fragments. The formation of this intramolecular excimer was studied by multiwavelength time-resolved fluorescence spectroscopy using a streak camera in solvents varying in polarity and viscosity.

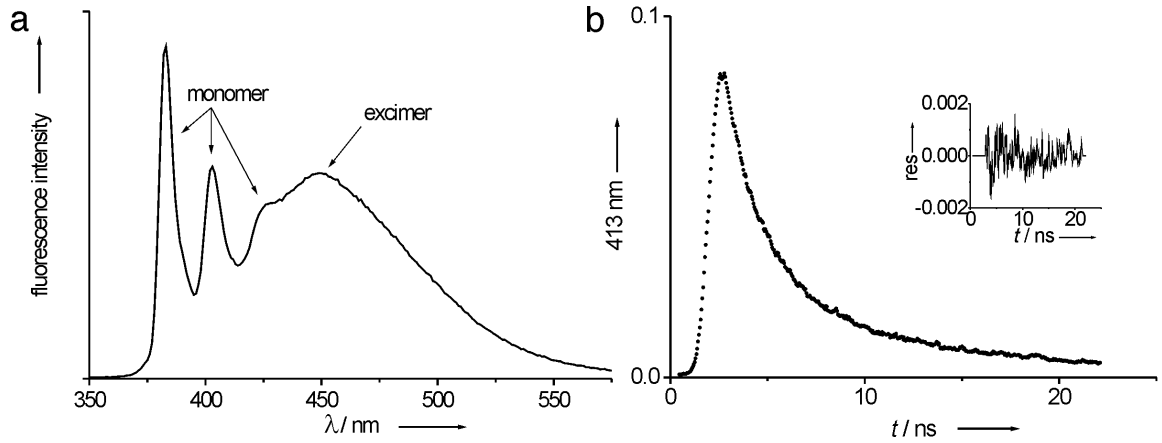

Figure 4. a) Steady state fluorescence spectrum and b) fluorescence decay curve of **8** (τ_1=10.2 ns, τ_2=1.8 ns) in cyclohexane.

The fluorescence trace of **8** in cyclohexane could be fitted to a bi-exponential decay with lifetimes of τ_1=10.2 ns and τ_2=1.8 ns attributed to the local (monomer) and the excimer emission, respectively (Figure 4b). Formation of the excimer from the excited monomer could

however not be observed. In more polar benzonitril, similar results were obtained (τ_1=13.5 ns and τ_2=3.8 ns), albeit with a lower relative intensity of the excimer band. Since no growth of monomer into excimer fluorescence could be observed, possibly as a result of the speed of excimer formation with respect to detection limits, the solvent was changed to the highly viscous sucrose-octa-acetate (SOA). Measurements in SOA in the temperature range from 30 to 150 ºC showed a decrease in excimer emission intensity as compared to the local fluorescence at higher temperatures. Furthermore, the fine structure in the local fluorescence band was lost. The lifetimes of local and excimer fluorescence were found to be in the same order as in non-viscous solvents (τ_1=20.0 ns and τ_2=2.3 ns at 30 ºC to τ_1=15.5 ns and τ_2=4.8 ns at 110 ºC) and as in the previous cases no growth of monomer into excimer fluorescence was observed.

Molecular Mechanics

The preferred conformations of complex **1a** were calculated by conformer searches, allowing stepwise rotation around the six bonds connecting the NCN-ligand and pyrenoxy unit to the linker followed by a Molecular Mechanics optimization of the structure. All optimized conformers of **1a** showed a close proximity (< 5 Å) of the cationic palladium ion and the pyrenoxy unit. In similar conformer searches of **11a**, the proximity between the NCN-ligand ($SiMe_3$-substituent) and pyrenoxy moiety was not observed as a major conformation. A representation of the structure of the functionalized dendrimer **11b** (26 kD) was also calculated by molecular mechanics, showing a densely crowded dendrimer with an average diameter of 5.3 nm.

Binding studies with picric acid.

The binding affinities of **1a**, **3** and the bispyrenyl ether **4** towards aromatic molecules were studied by ^{1}H-NMR titrations with picric acid (2,4,6-trinitrophenol) as guest molecule. Picric acid is known for its ability to form π-stacking complexes with a wide variety of aromatic molecules. Furthermore, the diagnostic ^{1}H-resonances of picric acid are situated in an isolated region of the spectrum. The titration experiments were performed in $CDCl_3$ at constant guest concentrations in the order of 0.5 K_a^{-1} to obtain optimal results.[9] In these experiments the upfield shift of the aromatic proton resonance of picric acid was monitored as a function of host/guest ratio. The titration curves were fitted to obtain the association constants and complexation induced shift values (Table 2). The stoichiometry of the stacking complexes was determined by Job's method of continuous variation for species in rapid exchange.[10] Job plots of $\Delta\delta^*X_G$ versus X_G ($\Delta\delta$: induced shift, X_G: molefraction guest) for the supramolecular complexes of picric acid with pyrenoxy NCN-palladium(II) complex **1a**, monopyrenoxy receptor **3** and the bispyrenoxy compound **4** are shown in Figure 5. The maxima in the curves

for **1a** and **3** are found at $X_G = 0.5$ revealing the formation of 1:1 complexes. The maximum of the curve in the Job plot of **4** is found at $X_G = 0.7$ indicating the formation of a 2:1 complex with picric acid.

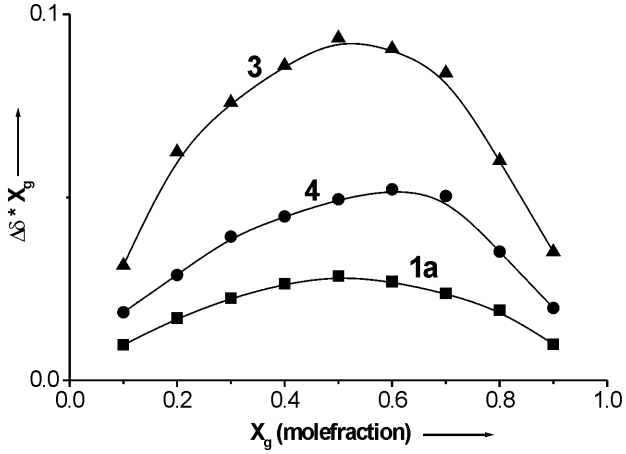

Figure 5. Job plots for complexes between picric acid and pyrenoxy hosts **1a**, **3**, and **4**.

Table 2. Association constants and complexation induced shift values (CIS) of supramolecular complexes between picric acid and hosts **1**, **3**, and **4**.

	K_a (M^{-1})[a]	CIS (ppm)
1a	94	-0.67
3	44	-1.08
4	81[b]	-0.64

a) Estimated error of 10%; b) $K_{a1}=K_{a2}=81\ M^{-1}$.

Catalysis - Aldol Condensations

The cationic NCN-palladium(II) complexes **1a**, **1b** and **2** can be applied as Lewis acidic catalysts. These types of cationic palladium(II) salts, amongst several other late transition metal salts, have been successfully applied as catalysts in aldol reactions between aldehydes and methyl isocyanoacetate (Scheme 3).[11]

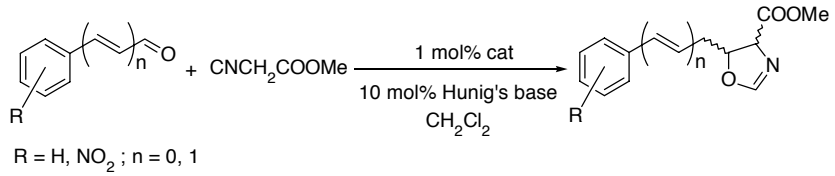

Scheme 3. Aldol condensation of methyl isocyanoacetate with aromatic aldehydes or cinnemaldehydes.

Complexes **1a** and **2** were tested as catalysts in this aldol condensation with several aromatic substrates. All aldol reactions were also performed with a mixture of equimolar amounts of **2** and the pyrenyl ether **3**. Furthermore, multisite catalyst **1b** was applied in the aldol condensation of benzaldehyde to study the effect of immobilization on catalytic performance. The results from the catalytic experiments are collected in Table 3.

Table 3. Results from aldol condensations between methyl isocyanoacetate and (nitro-substituted) aldehydes and cinnemaldehydes in dichloromethane in the prescence of Hunig's base at ambient temperature.

		Conversion[a] (%)				cis/trans[b]
Substrate	**time/h**	**1a**	**2**	**2 + 3**	**1b**	
PhCHO	6	48	25	27	11	1.82
	24	95	91	92	76	
4-NO_2PhCHO	3	42	41	43	n.d.	1.98
	24	>99	>99	>99		
PhCH=CHCHO	5	50	34	30	n.d.	1.40
	24	>99	95	96		
2-NO_2PhCH=CHCHO	3	49	38	38	n.d.	1.43
	24	>99	97	96		

a) Determined by ^{1}H-NMR; b) Cis/trans-ratios were identical for catalysts **1a**,**b**, **2**, and **2**+**3**; Conditions: 1.2 mmol substrate, 1 mol% catalyst, 10 mol% Hunig's base, 5 ml CH_2Cl_2, room temperature.

4.3. Discussion

The approach in which distinct building blocks are assembled on a multisite linker has been shown successful for the synthesis of complex **1a**. The strategic positioning of the virtually inert trimethylsilyl substituent on C_{ipso} of the NCN-pincer ligand allows regioselective metallation of the ligand at a later stage in the synthesis. Further modifications, such as immobilization on a carbosilane dendrimer (see **1b**) appeared to be feasible even after introduction of the ligand, which makes ligand **9** a versatile building block for the construction of complex (multimetallic) structures. With this in mind a synthetic route is available which allows the placement of various other functional groups in the vicinity of the cationic NCN-pincer palladium(II) site, apart from the pyrenoxy fluorescent probe in **1a**. The third attachment point on the xylyl linker, which in this study has been used for immobilization purposes, can be used for the selective introduction of a third functional moiety on the molecule.

Knowledge about the favored conformations of **1a** in solution is of interest in order to be able to assess the influence of the pyrenoxy unit on the catalytic properties of the cationic complex. The polycyclic flat aromatic surface of a pyrenoxy moiety can exhibit interactions

with other π-systems. The π-π stacking interactions observed in the crystal packing **10** are a clear example of this (see Figure 2). This crystal structure also shows that the NCN-pincer moiety itself can be part of stacking interactions. For the catalysis experiments it is of importance to know whether the π-π stacking found in the solid state is also present in dilute solution. In the case of pure **1a**, ^{1}H-NMR dilution experiments showed no evidence for significant formation or break-up of di- or oligomeric intermolecularly assembled species around concentrations used in catalysis (10^{-3} M). Complexation experiments of **1a** and **3** with picric acid show binding of the aromatic guest molecule to the pyrenoxy moiety by π-π stacking interactions in a 1:1 ratio, with typical association constants of 10^{1}-10^{2} M^{-1}. The bispyrenoxy compound **4** can be expected to bind picric acid in two distinct manners. Firstly, complexation of one picric acid molecule in the cleft of the tweezer, in which it would interact with both pyrenoxy moieties at the same time, would result in the formation of a 1:1 complex. Secondly, complexation of two picric acid molecules each with one of the pyrenoxy groups would result in the formation of a 2:1 complex. The titration curve and Job plots clearly show that 2:1 complexation occurs, which indicates that there is no significant synergic binding of picric acid by the to pyrenoxy units of **4**.

The flexibility of complex **1a** was probed by low temperature NMR studies, revealing that rotations around the benzyl ether linkages are fast on the NMR timescale, and that preferred conformations could not be frozen out. However, the broadening of these benzylic proton resonances at low temperatures pointed at hindered rotation. This broadening could result from an attractive interaction between the NCN-palladium moiety and the pyrenoxy unit, such as a cation-π interaction, bringing the substituents on the xylyl linker in a tweezer-type arrangement. Immobilization of 36 of these units on a G_2 carbosilane dendrimer results in a dendrimer with a sterically congested periphery, undoubtly influencing the flexibility and conformation of the individual units. Interestingly, severe broadening of all proton signals was observed already at room temperature in the polyfunctionalized dendrimers **1b** and **11b**. This can be attributed to the crowded structure of the dendrimer with substituents in various conformations, with ample π-π stacking interactions. This densely crowded periphery and the formation of various intramolecular (interbranch) π-π stacking contacts was also observed in molecular mechanics optimized structures of **11b**, and further supported by the quench of fluorescence in both **1b** and **11b**.

Optical spectroscopic methods offer the possibility to study flexibility and conformation of the system on a smaller timescale. Close proximity between the pyrenoxy and cationic palladium(II) site, resulting from cation-π interactions, would influence the optical properties of the fluorescent pyrenoxy unit in **1a** compared to **11a**, which lacks the palladium cation.

The NCN-palladium complex and pyrenoxy moiety are electronically isolated from each other by the linker, hence the influence of the palladium ion on the electronic spectra can only arise from a through space interaction either inter- or intramolecularly. Since the fluorescence studies were performed at high dilution, we excluded the presence of significant intermolecular interactions. The batochromic shifts in combination with the observed hypochroism in UV/Vis spectra of **1a** compared to **11a** imply that the cationic palladium(II) ion is in close vicinity of the pyrenoxy site. The prescence of this interaction is further supported by fluorescence spectroscopy. The fluorescence decay curves of **1a** and **11a** differ markedly. While not only the fluorescence intensity is decreased by a factor 10, also its lifetime is significantly reduced. Interactions between the pyrenoxy π-system and the palladium(II) cation result in (partial) quenching of the pyrenoxy fluorescence. The influence of cation-π interactions on the adopted structure of **1a** was further supported by molecular mechanics conformation searches. While for **1a** all conformations showed a close proximity of the palladium(II) cation and the π-system, no such preferred conformations were found for the trimethylsilyl analogue **11a**. The NCN-palladium(II) complex and the pyrenoxy moiety connected to the xylyl linker preferentially adopt a tweezer-type arrangement. The behavior of bis-pyrenoxy compound **8** in time-resolved fluorescence spectroscopy was indicative for a relation between the solvent polarity, and the preferential formation of either an 'open' or 'closed' (tweezer) conformation. While both local (monomer) and excimer bands are observed in the fluorescence spectrum, no interconversion of the excited monomer in the excimer is observed. This behavior can be explained by considering two distinct conformations. First, the pyrenoxy fragments can be in close proximity, resulting in excimer fluorescence upon excitation. Alternatively, when the groups are further apart a rearrangement is necessary to form the excimer after excitation. This rearrangement processes are apparently too slow to occur within the lifetime of the monomer fluorescence (10-20 ns). The relative intensity of the excimer emission compared to the local emission, which decreases upon higher solvent polarity, indicates that in less polar solvents **8** indeed possesses a more closed conformation with the pyrenoxy surfaces close together. The structural relationship between **8** and **1a**, *i.e.* the tweezer-type arrangement of substituents, can allow an extension of these results to the conformation of **1a** in solvents of different polarity.

Catalytic behavior in Aldol Condensations

The aldol condensation between methyl isocyanoacetate and aromatic aldehydes or cinnemaldehydes is especially useful to study the effect of modifications on the catalyst on its performance. The formation of a mixture of two pairs of diastereoisomers allows monitoring of both (stereo)selectivity and activity of the catalyst. These condensations are assumed to occur via coordination of the isocyanoacetate to the metal ion upon replacement of the weakly

coordinating water ligand, followed by deprotonation of the coordinated isocyanoacetate to its corresponding enolate. The enolate subsequently reacts with the aldehyde in the rate-determining step to form the product oxazolines as a mixture of the *cis*- and *trans*-isomers.[11e,12]

Enhancements of up to two times in the initial reaction rates are found for complex **1a** compared to complex **2**. In addition, the presence of pyrenyl ether **3** does not affect the reaction rate of the aldol reaction catalyzed by **2**, ruling out an independent effect of the pyrenoxy unit on the catalysis. In the case of 4-nitrobenzaldehyde (entry 2) no influence of the pyrenoxy unit on catalytic performance is observed. The electron withdrawing nitro-substituent activates the aldehyde for nucleophilic attack of the palladium-coordinated isocyanoacetate enolate. A change in rate-determining step resulting from this substrate-activation can make the presence or absence of the pyrenoxy unit irrelevant for catalytic performance. The small, but reproducible, rate enhancements observed in the aldol reactions of the other substrates with complex **1a**, may be explained by several aspects of this tweezer. First, the cation-π interaction activates the catalyst by allowing faster ligand exchange on the metal ion, *i.e.* exchange of water for methyl isocyanoacetate. Secondly, the presence of the pyrenoxy unit stabilizes one or more of the transition states or intermediates in the catalytic cycle. Stabilization of the protonated ammonium cocatalyst (Hunig's base) by cation-π interactions can be envisaged. Thirdly, complexation of the aromatic substrate molecules to the pyrenoxy unit by π-π stacking interactions would increase their local molarity near the active site. The increased local molarity would facilitate the rate-determining step, resulting in an increased reaction rate. Dendritic multisite complex **1b** shows a dramatic 4-fold drop in rate in comparison with complex **1a**. This decreased activity can be attributed to the steric crowding, making various catalytic sites inaccessible for substrate molecules. The selectivity, *e.g.* the *cis/trans* ratio of the product oxazolines, was found to be independent of the catalyst applied. The pyrenoxy unit does not influence the orientation of the substrate in a (stereo)specific manner towards the coordinated enolate.

4.4. Conclusions

The availability of mild site-selective palladation procedures for NCN-pincer ligands, in combination with their facile *para*-functionalisation, allowed us to use them as building block in the construction of organometallic tweezer **1a**. The applied reaction sequence in assembling the pyrenoxy, NCN-pincer and xylyl-spacer building blocks was flexible enough to allow immobilization of the tweezer on a G_2-carbosilane dendrimer, followed by site-selective metallation to produce **1b**. The non-immobilized tweezer **1a** is highly flexible and can bind to aromatic substrates (picric acid) by π-π stacking interactions. It preferentially

adopts a tweezer-type conformation in solution as a result of cation-π interactions between the palladium(II) ion and the pyrenoxy unit. The abundance of this conformation, compared to a more open one with no interaction between the pyrenoxy and NCN-palladium unit, appears to be higher in apolar solvents. The minimalistic design approach, with the building blocks simply combined on a flexible linker, leads to observable effects in catalysis. The presence of the pyrenoxy unit in **1a** was beneficial for its performance as catalyst in the aldol reaction between methyl isocyanoacetate and aromatic aldehydes. Both complex **2**, which is devoid of a pyrenoxy site, as well as to **2** in the presence of pyrenyl ether **3** show lower activities in the aldol condensations compared to **1a**. It seems apparent that the close proximity of the pyrenoxy unit and the catalytic palladium(II) site is responsible for the observed rate enhancements.

4.5. Experimental Section

All experiments were conducted in a dry nitrogen atmosphere using standard Schlenk techniques, when using air- and/or water-sensitive reagents. Solvents were dried over appropriate agents and distilled prior to use. The reagent 3,5-bis{(dimethylamino)methyl}phenyl *t*-butyldimethylsilyl ether was prepared according to literature procedures.[13] Elemental analyses were performed by H. Kolbe, Mikroanalytisches Laboratorium, Mülheim, Germany. ^{1}H and ^{13}C NMR spectra were recorded at 298 K on a Varian Inova 300 or Mercury 200 spectrometer. UV/Vis spectra were recorded on a Varian Cary I spectrophotometer.

*3-{(Pyrenoxy)methyl}-5-(bromomethyl)phenyl bromide (**7**)*

K_2CO_3 (10 g, 130 mmol) was added to a stirred solution of pyren-1-ol (**6**) (3.0 g, 14 mmol), 3,5-*bis*(bromomethyl)phenyl bromide (**5**) (5.30 g, 15 mmol) and 18-crown-6 ether (0.3 g, 1.3 mmol) in THF (75 mL) and the mixture was stirred at room temperature for 18 h. The volatiles were evaporated in vacuo and the residue was extracted with dichloromethane (3x50 mL). The combined dichloromethane extracts were evaporated in vacuo resulting in a brownish solid which contained unreacted **5**, the desired mono substituted 3-{(pyrenoxy)methyl}-5-(bromomethyl)phenyl bromide (**7**) and the double substituted 3,5-bis{(pyrenoxy)methyl}phenyl bromide (**8**) in a ratio of approximately 1:2:1. This mixture was extracted with pentane until all 3,5-*bis*(bromomethyl)phenyl bromide was removed (ca 10x100 mL), yielding 4.23 g of a 2:1 mixture of the mono (**7**) and double (**8**) substituted products according to ^{1}H-NMR integration. This mixture was used in the subsequent step without further purification.

*3,5-Bis{(dimethylamino)methyl}-4-(trimethylsilyl)phenyl t-butyldimethylsilyl ether (**9**)*

n-BuLi (10.4 mL, 1.6 M in hexanes, 16.5 mmol) was added dropwise over a period of 5 minutes to a cooled (-78 °C) solution of 3,5-bis[(dimethylamino)methyl]phenyl *t*-butyldimethylsilyl ether (5.16 g, 16 mmol) in hexane (20 mL). The reaction mixture was allowed to warm to room temperature and was stirred for an additional 4 h. After cooling the reaction mixture to 0 °C, a solution of trimethylsilyl trifluoromethylsulfonate (3.71 mL, 19.2 mmol) in THF (20 mL) was added dropwise over a period of 10 minutes and stirring was continued for 1 hour at room temperature. The volatiles were evaporated in vacuo and the residue was subjected to flash chromatography (CH_2Cl_2, basic Al_2O_3) to afford 3,5-bis{(dimethylamino)methyl}-4-(trimethylsilyl)phenyl-*t*-butyldimethylsilyl ether (**9**) as a yellow oil. Yield: 5.64 g (89%), ^{1}H-NMR (C_6D_6, 300 MHz): 7.14 (s, 2H, ArH), 3.45 (s, 4H, CH_2N), 2.01 (s, 12H, NMe_2), 0.99 (s, 9H, *t*-BuSi), 0.46 (s, 9H, $SiMe_3$), 0.18 (s, 6H, $SiMe_2$); ^{13}C-NMR (C_6D_6, 75 MHz): 156.4, 148.9, 130.5, 120.7 (Ar), 65.8 (CH_2N), 45.0 (NMe_2), 25.9, -0.4 (*t*-BuSi), -3.6 ($SiMe_3$), -4.2 ($SiMe_2$). Anal. Calcd for $C_{21}H_{42}N_2OSi_2$: C, 63.90; H, 10.72; N, 7.10. Found: C 63,70, H 10.80, N 6.98.

*3-{(Pyrenoxy)methyl}-5-{4-trimethylsilyl-3,5-bis(dimethylaminomethyl)phenyloxy}-phenyl bromide (**10**)*

To a stirred solution of **9** (2.22 g, 6 mmol) in 30 mL of THF was added NBu_4F (6 mL, 1M in THF, 6 mmol). After 30 min. K_2CO_3 (5.0 g, 30 mmol), 18-crown-6 (0.15 g, 0.6 mmol), and the above mentioned 2:1 mixture of **7** and **8** (4.23 g, contains 5.4 mmol of **7**) were added and the reaction mixture was stirred for an additional 18 h. The volatiles were removed in vacuo and subjected to flash chromatography (CH_2Cl_2, basic Al_2O_3) resulting in a yellow solid (5.61 g). The product mixture was redissolved in CH_2Cl_2 and careful precipitation of **8** with pentane followed by filtration afforded pure **10** in the mother liquor. Evaporation of the volatiles in vacuo yielded 1.34 g of **10** as a white solid. ^{1}H-NMR ($CDCl_3$, 300 MHz): 8.51 (d, 1H, $^3J_{HH}$=9.2 Hz, pyrenyl), 8.15-7.85 (m, 7H, pyrenyl), 7.69 (s, 1H, Ar), 7.63 (s, 1H, Ar), 7.58 (s, 1H, Ar), 7.53 (d, 1H, $^3J_{HH}$=8.2 Hz, pyrenyl), 7.05 (s, 2H, Ar), 5.37 (s, 2H, CH_2O), 5.09 (s, 2H, CH_2O), 3.51 (s, 4H, CH_2N), 2.15 (s, 12H, NMe_2), 0.37 (s, 9H, $SiMe_3$); ^{13}C ($CDCl_3$, 75 MHz): 158.5, 151.9, 148.3, 139.6, 139.2, 131.3, 131.4, 129.8, 129.6, 129.1, 127.0, 126.3, 125.9, 125.5, 125.3, 125.1, 125.0, 124.6, 124.3, 124.2, 124.1, 122.6, 120.9, 120.1, 114.3, 108.9 (Ar), 69.2, 68.2 (CH_2O) 65.2 (CH_2N), 45.0 (NMe_2), 3.4 ($SiMe_3$). Anal. Calcd. for $C_{39}H_{43}BrN_2O_2Si$: C 68.91, H 6.38, N 4.12, Si 4.13. Found: C 68.83, H 6.46, N 3.98, Si 4.23. ES-MS: calculated for $C_{39}H_{43}BrN_2O_2Si$ $(M+H)^+$: 679.2; found: 680.2.

*1-{Trimethylsilyl}-3-{(pyrenoxy)methyl}-5-{4-trimethylsilyl-3,5-bis(dimethylaminomethyl)phenyloxymethyl}benzene (**11a**)*

To a precooled (-100°C) solution of **10** (0.84 g, 1.25 mmol) in 10 mL of THF was added *t*-BuLi (1.66 mL, 1.5M in pentane, 2.50 mmol) dropwise. The reaction mixture was stirred at -100°C for an additional hour and trimethylsilyl chloride (0.32 mL, 2.55 mmol) was added at once. The reaction mixture was allowed to warm to room temperature and al volatiles were evaporated in vacuo. After purification by column chromatography (hexane/Et_2O 3/1, 3% TEA, basic Al_2O_3) pure **11a** was obtained as an off-white solid (0.81 g, 96%). ^{1}H-NMR ($CDCl_3$, 300 MHz): 8.53 (d, 1H, $^3J_{HH}$=9.2 Hz, pyrenyl), 8.11-8.01 (m, 4H, pyrenyl), 7.96-7.84 (m, 3H, pyrenyl), 7.70 (s, 1H, Ar), 7.69 (s, 1H, Ar), 7.62 (s, 1H, Ar), 7.56 (d, 1H, $^3J_{HH}$=8.3 Hz, pyrenyl), 7.08 (s, 2H, Ar), 5.39 (s, 2H, CH_2O), 5.14 (s, 2H, CH_2O), 3.51 (s, 4H, CH_2N), 2.14 (s, 12H, NMe_2), 0.38 (s, 9H, $SiMe_3$), 0.33 (s, 9H, $SiMe_3$); ^{13}C ($CDCl_3$, 75 MHz): 159.0, 152.8, 148.4, 141.3, 136.8, 136.6, 132.3, 132.0, 131.6, 129.6, 127.4, 127.2, 126.4, 126.0, 125.8, 125.5, 125.4, 125.1, 124.9, 124.3, 124.2, 121.3, 120.6, 114.5, 109.6 (Ar), 71.0 (CH_2O), 69.6 (CH_2O), 65.4 (CH_2N), 45.1 (NMe_2), 3.4 ($SiMe_3$), -1.1 ($SiMe_3$). Elem. Anal. Calcd. for $C_{42}H_{52}N_2O_2Si_2$: C 74.95, H 7.79, N 4.16, Si 8.35. Found: C 74.86, H 7.88, N 4.20, Si, 8.26.

*[1-{Trimethylsilyl}-3-{(pyrenoxy)methyl}-5-{3,5-bis(dimethylaminomethyl)phenyl-4-(chloropalladium(II))-1-oxymethyl}benzene] (**12a**)*

To a suspension of **11a** (0.15 g, 0.22 mmol) in freshly distilled methanol (5 mL) was added $Pd(OAc)_2$ (52 mg, 0.23 mmol). The reaction mixture was stirred for 3 h at room temperature after which an excess of LiCl (42 mg, 1 mmol) was added and stirring was continued for an additional hour. After evaporation of all volatiles in vacuo, the residue was extracted with CH_2Cl_2 (3x 10 mL). The combined CH_2Cl_2 extracts were filtered over celite and evaporation of the solvent afforded 0.16 g (99%) of pure **12a** as an off-white solid. ^{1}H-NMR ($CDCl_3$, 300 MHz): 8.51 (d, 1H, $^3J_{HH}$=9.2 Hz, pyrenyl), 8.14-8.04 (m, 4H, pyrenyl), 8.00-7.85 (m, 3H, pyrenyl), 7.70 (s, 1H, Ar), 7.65 (s, 1H, Ar), 7.63 (d, 1H, $^3J_{HH}$=8.3 Hz, pyrenyl), 7.56 (s, 1H, Ar), 6.44 (s, 2H, Ar), 5.41 (s, 2H, CH_2O), 5.00 (s, 2H, CH_2O), 3.82 (s, 4H, CH_2N), 2.87 (s, 12H, NMe_2), 0.34 (s, 9H, $SiMe_3$); ^{13}C ($CDCl_3$, 75 MHz): 157.0, 152.5, 145.2, 141.2, 138.6, 136.6, 136.5, 132.0, 131.9, 131.5, 131.4, 127.1, 127.0, 126.3, 126.0, 125.6, 125.3, 125.2, 124.9, 124.6, 124.2, 124.0, 121.0, 120.3, 113.3, 109.4, 106.9 (Ar), 74.4 (CH_2N), 70.7 (CH_2O), 70.4 (CH_2O), 52.8 (NMe_2), -1.2 ($SiMe_3$). Elem. Anal. Calcd for $C_{39}H_{43}ClN_2O_2PdSi$: C 63.15, H 4.78, N 3.78; Found: C 62.97, H 4.90, N 3.72; ES-MS: calculated for $C_{39}H_{43}ClN_2O_2PdSi$ $(M\text{-}Cl)^+$: 705.2; found: 705.3.

*[1-{Trimethylsilyl}-3-{(pyrenoxy)methyl}-5-{3,5-bis(dimethylaminomethyl)phenyl-4-(aqua-palladium(II))-1-oxymethyl}benzene] tetrafluoroborate (**1a**)*

To a solution of **12a** (0.16 g, 0.22 mmol) in wet acetone was added $AgBF_4$ (45.4 mg, 0.23 mmol) which resulted in the immediate formation of a white precipitate. The reaction mixture was stirred at room temperature for 1 hr. and was filtered over celite. Evaporation of the acetone in vacuo afforded pure **1a** as an off-white solid (0.18 g, >99%). ^{1}H-NMR ($CDCl_3$, 200 MHz): 8.50 (d, 1H, $^3J_{HH}$=9.2 Hz, pyrenyl), 8.16-7.85 (m, 7H, pyrenyl), 7.69 (s, 1H, Ar), 7.64 (s, 1H, Ar) , 7.62 (d, 1H, $^3J_{HH}$=8.3 Hz, pyrenyl), 7.53 (s, 1H, Ar), 6.46 (s, 2H, Ar), 5.46 (s, 2H, CH_2O), 5.01 (s, 2H, CH_2O), 3.87 (s, 4H, CH_2N), 2.85 (s, 12H, NMe_2), 0.31 (s, 9H, $SiMe_3$); ^{13}C ($CDCl_3$, 50 MHz): 157.6, 152.6, 145.2, 143.6, 141.3, 136.6, 136.5, 132.1, 132.0, 131.6, 131.5, 127.2, 127.1, 126.3, 126.0, 125.7, 125.4, 125.3, 125.0, 124.7, 124.2, 124.1, 121.2, 120.5, 109.7, 107.5 (Ar), 73.8 (CH_2N), 70.9, 70.5 (CH_2O), 52.7 (NMe_2), -1.1 ($SiMe_3$). Anal. Calcd. for $C_{39}H_{45}BF_4N_2O_3PdSi$: C 57.75, H 5.59, N 3.45, Si 3.46. Found: C 57.71, H 5.62, N 3.35, Si 3.53. FAB-MS: calculated for $C_{39}H_{45}BF_4N_2O_3PdSi$ (M -BF_4 -H_2O)$^+$: 705.2; found: 705.1.

*1-{3-(Bromo)benzyloxy}-3,5-bis{(dimethylamino)methyl}-4-(trimethylsilyl)benzene (**13**)*

To a stirred solution of **9** (0.64 g, 1.6 mmol) in 15 mL of THF was added NBu_4F (1.6 mL, 1M in THF, 1.6 mmol) at once. After 30 minutes K_2CO_3 (2.0 g, 14,5 mmol), 18-crown-6 (50 mg, 0.2 mmol) and 3-bromobenzyl bromide (0.40 g, 1.6 mmol) were added and the reaction mixture was stirred for an additional 18 h. The volatiles were evaporated in vacuo and the residue was extracted with hexane (3x 20 mL). Purification by chromatography (hexane/Et_2O 3/1, 3% TEA, basic Al_2O_3) afforded **13** as a colorless oil (0.41 g, 60%). ^{1}H-NMR ($CDCl_3$, 200 MHz): 7.63 (s, 1H, Ar), 7.44 (d, 1H, $^3J_{HH}$=8.3 Hz), 7.36 (d, 1H, $^3J_{HH}$=7.3 Hz) 7.23 (dd, 1H, $^3J_{HH}$=8.3 Hz, $^3J_{HH}$=7.3 Hz), 7.02 (s, 2H, Ar), 5.05 (s, 2H, CH_2O), 3.50 (s, 4H, CH_2N), 2.14 (s, 12H, NMe_2), 0.37 (s, 9H, $SiMe_3$); ^{13}C ($CDCl_3$, 50 MHz): 158.6, 148.4, 139.6, 130.8, 130.4, 130.0, 129.9, 125.9, 122.5, 114.3 (Ar), 68.6 (CH_2O), 65.3 (CH_2N), 45,1 (NMe_2), 3.5 ($SiMe_3$). Anal. Calcd. for $C_{22}H_{33}BrN_2OSi$: C 58,78, H 7.40, N 6.23, Si 6.25. Found: C 59.02, H 7.34, N 6.21, Si 6.33.

*1-{3-(Trimethylsilyl)benzyloxy}-3,5-bis{(dimethylamino)methyl}-4-(trimethylsilyl)benzene (**14**)*

To a precooled (-100°C) solution of **13** (0.41 g, 0.91 mmol) in diethyl ether (15 mL) was added dropwise *t*-BuLi (1.21 mL, 1.5M in pentane, 1.82 mmol) and the reaction mixture was stirred for 1 hour at -100°C. Trimethylsilyl chloride (0.23 mL, 1.82 mmol) was added dropwise to the yellow solution and the reaction mixture was allowed to warm to room temperature. The volatiles were evaporated in vacuo and the residue was extracted with

dichloromethane and filtered over celite. Purification by chromatography (hexane, 2% TEA and Et_2O, 2% TEA, basic Al_2O_3) afforded 0.22 g (55%) pure **14** as a colorless oil. ^{1}H-NMR ($CDCl_3$, 200 MHz): 7.64 (s, 1H, Ar), 7.57-7.37 (m, 3H, Ar) ,7.09 (s, 2H, Ar), 5.13 (s, 2H, CH_2O), 3.55 (s, 4H, CH_2N), 2.18 (s, 12H, NMe_2), 0.42 (s, 9H, $SiMe_3$) 0.33 (s, 9H, $SiMe_3$); ^{13}C ($CDCl_3$, 50 MHz): 159.0, 148.3, 140.6, 136.2, 132.8, 132.6, 129.5, 128.2, 127.8, 114.5 (Ar), 69.8 (CH_2O), 65.4 (CH_2N), 45.5 (NMe_2), 3.4 ($SiMe_3$), -1.1 ($SiMe_3$). Anal. Calcd. for $C_{25}H_{42}N_2OSi_2$: C 67.81, H 9.56, N 6.33, Si 12.69. Found: C 67.75, H 9.49, N 6.28, Si 12.48.

*[1-{3-(Trimethylsilyl)benzyloxy}-3,5-bis{(dimethylamino)methyl}phenyl-4-(chloropalladium(II))] (**15**)*

To a suspension of **14** (0.22 g, 0.5 mmol) in freshly distilled methanol was added $Pd(OAc)_2$ (0.12 g, 0.52 mmol). The reaction mixture was stirred for 45 min. during which a yellow precipitate was formed. To the reaction mixture LiCl (0.21 g, 5.0 mmol) was added at once and stirring continued for an additional 30 min. Evaporation of the volatiles in vacuo followed by extraction with dichloromethane (3x50 mL), and filtration over celite afforded the yellow solid **15** in a 90% yield (0.23 g). ^{1}H-NMR ($CDCl_3$, 200 MHz): 7.54-7.32 (m, 4H, Ar), 6.50 (s, 2H, Ar), 4.96 (s, 2H, CH_2O), 3.97 (s, 4H, CH_2N), 2.92 (s, 12H, NMe_2), 0.27 (s, 9H, $SiMe_3$). ^{13}C ($CDCl_3$, 50 MHz): 156.9, 146.5, 145.1, 140.4, 135.8, 132.6, 132.1, 127.9, 127.8, 127.6, 106.7 (Ar), 74.3 (CH_2N), 70.4 (CH_2O), 52.7 (NMe_2), -1.4 ($SiMe_3$) Anal. Calcd. for $C_{22}H_{33}ClN_2OPdSi$: C 51.66, H 6.50, N, 5.48. Found: C 51.70, H 6.57, N 5.52. ES-MS: calculated for $C_{22}H_{33}ClN_2OPdSi$ $(M\text{-}Cl)^+$: 475.1; found: 474.8.

*[1-{3-(Trimethylsilyl)benzyloxy}-3,5-bis{(dimethylamino)methyl}phenyl-4-(aqua-palladium(II))] tetrafluoroborate (**2**)*

To a solution of 0.10 g (0.20 mmol) **15** in wet acetone (5 mL) was added 42 mg (0.21 mmol) $AgBF_4$. A white precipitate was formed instantaneously. The reaction mixture was stirred at room temperature for an addtional hour and was filtered over celite. Evaporation of the acetone in vacuo afforded 0.12 g (>99%) pure **2** as a yellow solid. ^{1}H-NMR ($CDCl_3$, 200 MHz): 7.55-7.36 (m, 4H, Ar), 6.51 (s, 2H, Ar), 4.96 (s, 2H, CH_2O), 3.98 (s, 4H, CH_2N), 2.92 (s, 12H, NMe_2), 0.27 (s, 9H, $SiMe_3$). ^{13}C ($CDCl_3$, 50 MHz): 157.9, 149.5, 145.2, 140.9, 135.9, 133.0, 132.4, 128.1, 127.9, 127.8, 107.7 (Ar), 73.7 (CH_2N), 70.7 (CH_2O), 52.7 (NMe_2), -1.1 ($SiMe_3$). Anal. Calcd. for: $C_{22}H_{35}BF_4N_2O_2PdSi$: C 45.49, H 6.07, N 4.82; Found: 45.38, H 6.16, N 4.75.

*1-{(Pyrenoxy)methyl}-3-bromobenzene (**16**)*

K_2CO_3 (3.45 g, 25 mmol) was added to a stirred solution of pyren-1-ol (**6**) (1.09 g, 5 mmol), 3-bromobenzyl bromide (1.22 g, 4.9 mmol) and 18-crown-6 (0.13 g, 0.5 mmol) in THF (30

mL) and the mixture was stirred at room temperature for 36 h. The volatiles were evaporated in vacuo and the residue was extracted with dichloromethane (3x50 mL). The combined dichloromethane extracts were evaporated in vacuo. Purification by flash chromatography (CH_2Cl_2, basic Al_2O_3) afforded 1.70 g (90%) of pure **16** as a yellow oil. ^{1}H-NMR ($CDCl_3$, 200 MHz): 8.51 (d, 1H, $^3J_{HH}$=9.2 Hz, pyrenyl), 8.12-7.87 (m, 7H, pyrenyl), 7.77 (s, 1H, Ar), 7.57-7.47 (m, 3H, pyrenyl), 7.30 (dd, 1H, Ar), 5.40 (s, 2H, CH_2O). ^{13}C ($CDCl_3$, 50 MHz): 152.0, 139.2, 131.5, 131.4, 130.8, 130.0, 129.9, 127.2, 127.0, 126.4, 126.0, 125.5, 125.5, 125.1, 125.0, 124.6, 124.2, 124.1, 122.5, 120.9, 120.2, 109.1 (Ar), 69.4 (CH_2O). Anal. Calcd. for $C_{23}H_{15}BrO$: C 71.33, H 3.90. Found: C 71.39, H 3.92. ES-MS: calculated for $C_{23}H_{15}BrO$ $(M)^+$: 386.0; found: 386.6.

*1-{(Pyrenoxy)methyl}-3-(trimethylsilyl)benzene (**3**)*

To a precooled (-100°C) solution of **16** (0.48 g, 1.24 mmol) in THF (15 mL) was added dropwise *t*-BuLi (1.65 mL, 1.5M in pentane, 2.48 mmol) and the reaction mixture was stirred for 1 h at -100°C. Trimethylsilyl chloride (0.30 mL, 2.50 mmol) was added dropwise to the dark red solution and the reaction mixture was allowed to warm to room temperature. The volatiles were evaporated in vacuo and the residue was extracted with dichloromethane and filtered over celite 521. Evaporation of the dichloromethane in vacuo afforded 0.44 g (93%) 1-{(pyrenoxy)methyl}-3-(trimethylsilyl)benzene (**3**) as a yellow oil. ^{1}H-NMR ($CDCl_3$, 200 MHz): 8.52 (d, 1H, $^3J_{HH}$=9.2 Hz, pyrenyl), 8.08-7.80 (m, 7H, pyrenyl, Ar), 7.74 (s, 1H, pyrenyl) 7.58-7.38 (m, 4H, Ar), 5.33 (s, 2H, CH_2O), 0.33 (s, 9H, $SiMe_3$). ^{13}C ($CDCl_3$, 50 MHz): 152.6, 140.7, 132.9, 132.3, 131.6, 131.5, 130.9, 128.0, 127.9, 127.7, 127.1, 126.3, 125.9, 125.7, 125.3, 124.9, 124.8, 124.1, 124.0, 121.2, 120.4, 109.3 (Ar), 70.9 (CH_2O). Anal. Calcd. for $C_{26}H_{24}OSi$: C 82.06, H 6.36, Si 7.38. Found: C 81.89, H 6.38, Si 7.26. ES-MS: calculated for $C_{26}H_{24}OSi$ $(M)^+$: 380.2; Found: 380.7.

*3,5-Bis{(pyrenoxy)methyl}-1-(trimethylsilyl)benzene (**4**)*

To a precooled (-100°C) solution of **8** (0.20 g, 0.32 mmol) in THF (5 mL) was added dropwise *t*-BuLi (0.41 mL, 1.5M in pentane, 0.62 mmol) and the reaction mixture was stirred for 30 min. at -100°C. Excess trimethylsilyl chloride (0.30 mL, 2.50 mmol) was added dropwise to the dark red solution and the reaction mixture was allowed to warm to room temperature. The volatiles were evaporated in vacuo and the residue was extracted with dichloromethane and filtered over celite. Evaporation of the solvent in vacuo afforded 0.18 g (92%) **4** as a yellowish solid. ^{1}H-NMR ($CDCl_3$, 300 MHz): 8.58 (d, 2H, $^3J_{HH}$=9.6 Hz, pyrenyl), 8.25-7.91 (m, 14H, pyrenyl), 7.89 (s, 1H, Ar), 7.83 (s, 2H, Ar) , 7.59 (d 1H, $^3J_{HH}$=8.1 Hz, pyrenyl), 5.47 (s, 4H, CH_2O), 0.48 (s, 9H, $SiMe_3$); ^{13}C ($CDCl_3$, 75 MHz): 141.8, 138.0, 132.3, 132.0, 131.9, 127.7, 127.5, 127.4, 126.8, 126.4, 126.1, 125.8, 125.7, 125.4,

125.2, 124.6, 124.5, 121.6, 121.0, 109.9 (Ar), 71,2 (CH_2O), -0.7 ($SiMe_3$). Anal. Calcd. for $C_{436}H_{34}O_2Si$: C 84.55, H 5.61; Found: 84.67, H 5,70; ES-MS: calculated for $C_{43}H_{34}O_2Si$ $(M+H)^+$: 611.2; Found: 611.1.

Fluorescence spectroscopy

Steady state fluorescence measurements were carried out on a SPEX Fluorolog 3-22 with a 450W Xe excitation source and a Peltier cooled R636-10 photomultiplier from Hamamatsu, operating in photon counting mode. For time resolved emission measurements we used a Chromex IS250 spectrograph coupled to a Hamamatsu streak camera (C5680-21 with M5677 Low-Speed Single Sweep Unit and C4742-95 CCD camera). For excitation an LTB MSG400 nitrogen laser (337 nm, fwhm≈0.6 ns) was used.

*Crystal data and data collection for **10***

Formula $C_{39}H_{43}BrN_2O_2Si{\bullet}CH_2Cl_2$, M_r = 764.68, triclinic, space group $P\bar{1}$ (no. 2), a = 9.9388(2), b = 13.2651(3), c = 14.7898 Å, α = 84.512(1)°, β = 80.614(1)° γ = 74.891(1)°, V = 1854.38(7) Å^3, F(000) = 796, Z = 2, $\rho_{calcd.}$=1.370 Mg/m^3, $\mu(Mo_{K\alpha})$ = 1.322 mm^{-1}, $2\theta_{max}$=55.0°. 19551 reflections measured, 8432 independent, R_{int} = 0.0349. Refinement converged at a *w*R2 value of 0.1054 (S = 1.023), R = 0.0408 [for 7064 reflections with $F_o>4\sigma(F_o)$]. Maximum residual electron density 0.44 e/Å^3. A pale yellow plate crystal measuring (0.36 x 0.21 x 0.09 mm) was mounted under the nitrogen stream (150 K), on a Nonius Kappa CCD area detector diffractometer with a graphite monochromator (λ = 0.71073 Å), and a rotating anode source. Lorentz, polarisation, and an absorption correction, the latter using multiple measured equivalent reflections), were applied (PLATON/MULABS[14a]). The structure was solved with the DIRDIF97[14c] program and refined with SHELXL-97[14b] using full matrix least squares on F^2. All non-hydrogen atoms were refined with anisotropic displacement parameters, hydrogen atoms were located at calculated positions and refined riding on their carrier atoms. The dichloromethane is equally disordered across two positions. Crystallographic data (excluding structure factors) for the structure of **10** reported in this paper have been deposited with the Cambridge Crystallographic Data Centre as supplementary publication no. CCDC-165285. Copies of the data can be obtained free of charge on application to CCDC, 12 Union Road, Cambridge CB21EZ, UK (fax: (+44)1223-336-033; e-mail: deposit@ccdc.cam.ac.uk).

Computational details

Results were obtained utilizing the multiple conformer search as implemented in the SPARTAN 5.1.1 (UNIX) package, with a MMFF94 mechanics force field.[15] The input data used in the conformer searches of both **1** and **11** were imported in the program by using the

builder routine in the molecular modelling package followed by a geometry optimisation with the MMFF94 mechanics force field. The conformer searches were performed using Monte Carlo and systematic stepwise rotation around the six bonds connecting the NCN-ligand and the pyrenoxy unit to the linker, both leading to similar results.

4.6. References and Notes

1. For overviews on NCN-pincer chemistry see: (a) Albrecht, M.; van Koten, G. *Angew. Chem., Int. Ed.* **2001**, *40*, 3750-3781; (b) Steenwinkel, P.; Gossage, R. A.; van Koten, G. *Chem. Eur. J.* **1998**, *4*, 759-763. (c) Gossage, R. A.; van de Kuil, L. A.; van Koten, G. *Acc. Chem. Res.* **1998**, *31*, 423-431; (d) Rietveld, M. H. P.; Grove, D. M.; van Koten, G. *New J. Chem.* **1997**, *21*, 751; (e) van Koten, G. *Pure and Appl. Chem*. **1989**, *61*, 1681.
2. G. Rodriguez, G.; Albrecht, M.; Schoenmaker, J.; Ford, A.; Lutz, M.; Spek, A. L.; van Koten, G. *J. Am. Chem. Soc.* **2002**, *124*, 5127-5138; and chapter 2 of this thesis.
3. See for overviews on catalytically active metallodendritic complexes: (a) Kreiter, R.; Kleij, A. W.; Klein Gebbink, R. J. M.; van Koten, G. *Top. Curr. Chem.* **2001**, *217*, 163-199. (b) Oosterom, G. E.; Reek, J. N. H.; Kamer, P. C. J.; van Leeuwen, P. W. N. M. *Angew. Chem. Int. Ed.* **2001**, *40*, 1828-1849. (c) Astruc, D.; Chardac, F. *Chem. Rev.* **2001**, *101*, 2991-2023.
4. Rodríguez, G.; Lutz, M.; Spek, A. L.; van Koten, G. *Chem. Eur. J.* **2002**, *8*, 45-57.
5. (a) Dijkstra, H. P.; van Klink, G. P. M.; van Koten, G. *Acc. Chem. Res.* **2002**, in press.
(b) Kleij, A. W.; Gossage, R. A.; Jastrzebski, J. T. B. H.; Boersma, J.; van Koten, G. *Angew. Chem.* **2000**, *39*, 176-178. (c) Wijkens, P.; Jastrzebski, J. T. B. H.; van der Schaaf, P.A.; Kolly, R.; Hafner, A.; van Koten, G. *Org. Lett.* **2000**, *11*, 1621-1624. (d) Kragl, U.; Dreisbach, C.; *Angew. Chem. Int. Ed. Engl.* **1996**, *35*, 342. (e) Kragl, U.; Dreisbach, C.; Wandrey, C. in *Membrane Reactors in Homogeneous Catalysis, "Applied Homogeneous Catalysis with Organometallic Compounds"*, Eds Cornils, B.; Herrmann, W. A., VCH Weinheim, **1996**, 833-843.
6. (a) Valk, J.-M.; van Belzen, R.; Boersma, J.; Spek, A. L.; van Koten, G. *J. Chem. Soc., Dalton Trans.* **1994**, 2293. (b) Valk, J.-M.; Boersma, J.; van Koten, G. *J. Organomet. Chem.* **1994**, *483*, 213.
7. (a) Steenwinkel, P.; Gossage, R. A.; van Koten, G. *Chem. Eur. J.* **1998**, *4*, 759-762. (b) Steenwinkel, P.; Jastrzebski, J. T. B. H.; Deelman, B.-J.; Grove, D. M.; Kooijman, H.; Veldman, N.; Smeets, W. J. J.; Spek, A. L.; van Koten, G. *Organometallics* **1997**, *16*, 5486-5498.
8. Good FFCE (face-to-face, centre-to-edge) stacking is present in cases where the stacking parameters fulfil the following requirements: $\alpha < 45°$, 1.4 Å < x < 2.7 Å and 3.3 Å < z < 4.0 Å (α = angle between planes, x = horizontal displacement, z = vertical displacement). See also: Martin, C. B.; Mulla, H. R.; Willis, P. G.; Cammers-Goodwin, A. *J. Org. Chem.* **1999**, *64*, 7802-7806.
9. Granot, J. *J. Magn. Res.* **1983**, *55*, 216.
10. Connors, K. A. *Binding Constants, The Measurement of Molecular Complex Stability*; Wiley-Interscience: New-York, **1987**, 24-28.
11. Examples of Pd^{II} and Pt^{II} catalyzed aldol condensations: (a) Dijkstra, H. P.; Meijer, M. D.; Patel, J.; Kreiter, R.; van Klink, G. P. M.; Lutz, M.; Spek, A. L.; Canty, A. J.; van Koten, G. *Organometallics* **2001**, *20*, 3159-3168. (b) Stark, M. A.; Richards, C. J. *Tetrahedron Lett.* **1997**, *38*, 5881-5884. (c) Longmire, J. M.; Zhang, X. *Organometallics* **1998**, *17*, 4374-4379. (d) Fujimura, O. *J. Am. Chem. Soc.* **998**, *120*, 10032-10039. (e) Gorla, F.; Togni, A.; Venanzi, L. M.; Albinati, A.; Lianza, F.

Organometallics **1994**, *13*, 1607-1616. (f) Nesper, R.; Pregosin, P. S.; Püntener, K.; Wörle, M. *Helv. Chim. Acta* **1993**, *76*, 2239; see also reference [4].

12. (a) Hayashi, T.; Sawamura, M.; Ito, Y. *Tetrahedron* **1992**, *48*, 1999-2012. (b) Soloshonok V. A.; Hayashi, T. *Tetrahedron Lett.* **1994**, *35*, 2713-2716. (c) Togni, A.; Pastor, S. D. *J. Org. Chem.* **1990**, *55*, 1649.
13. (a) Davies, P. J., Grove, D. M., van Koten, G. *Organometallics* **1997**, *16*, 800-802. (b) Huck, W. T. S., van Veggel, F. C. J. M., Kropman, B. L., Blank, D. H. A., Keim, E. G., Smithers, M. M. A., Reinhoudt, D. N. *J. Am. Chem. Soc.* **1995**, *117*, 8293.
14. (a) Spek, A. L., *PLATON*. A multipurpose crystallographic tool. Utrecht University, The Netherlands, **2000**. (b) Sheldrick, G. M., *SHELXL97*. Program for crystal structure refinement. University of Göttingen, Germany, **1997**. (c) Beurskens, P. T.; Admiraal, G.; Beurskens, G.; Bosman, W. P.; Garcia-Granda, S.; Gould, R. O.; Smits, J. M. M.; Smykalla, C., *DIRDIF97* Program System, Technical Report. Crystallography Laboratory, University of Nijmegen, The Netherlands, **1997**.
15. SPARTAN SGI Version 5.1.1, Wavefunction, Inc., 18401 Von Karman Ave., Ste. 370 Irvine, CA 92612 U.S.A.

Chapter Five

NCN-Pincer Palladium Complexes with Multiple Anchoring Points for Functional Groups

Abstract

para-Substituted NCN-pincer palladium(II) complexes (NCN-Z = [2,6-$(CH_2NMe_2)_2C_6H_2$-4-Z]$^-$) of the type [Pd(OH_2)(NCN-CHZ-$C_6H_4SiMe_3$)](BF_4) (with Z = OH, OAc, $OSiMe_2$t-Bu, $(C_5H_5N)(BF_4)$ have been synthesized and used as catalysts in the aldol reaction between methyl isocyanoacetate and several benzaldehydes. The substituent Z, placed on a distal position from the palladium(II) site, does not significantly influence the catalytic activity and selectivity of the resulting complexes, but offers a useful starting point for further functionalization.

5.1. Introduction

The use of functionalized ligands in organometallic or coordination chemistry is a common tool to immobilize a complex, alter its solubility, and tune the metal center electronically. Our interest is focused on the *para*-functionalization of NCN-pincer metal complexes (NCN = 2,6-bis[(dimethylamino)methyl]phenyl anion)[1] with multiple anchoring points that allow further modifications.[2] The NCN-pincer palladium and platinum complexes are especially suitable in this respect, since they are highly stable, even allowing functionalisation after metallation of the ligand.[3] This makes them excellent building blocks for the construction of new (catalytic) organometallic materials.[1a] Especially successful has been the immobilization of NCN-pincer complexes on dendritic support systems for (catalyst) recycling purposes.[1c,3,4] Here, we report the synthesis of catalytically active cationic NCN-pincer palladium(II) complexes **1-4** functionalized with two anchoring points, thus allowing both immobilization and the introduction of additional functional groups, *e.g.* hydroxyl, acetyl, and pyridinium, in the vicinity of the metal complex (Chart 1). These complexes were tested as catalysts in C–C coupling reactions between methyl isocyanoacetate and several functionalized benzaldehydes.

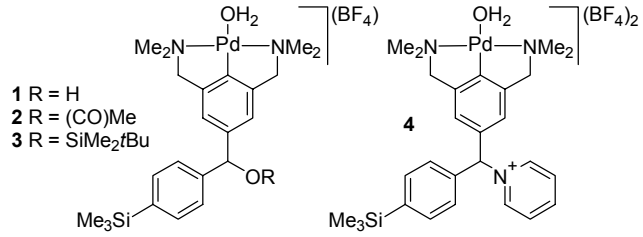

Chart 1. Hydroxyl (**1**), acetyl (**2**), siloxy (**3**), and pyridinium (**4**) functionalized NCN-pincer palladium(II) complexes.

Complexes **1-4** are all substituted with a trimethylsilyl group. This trimethylsilyl group is used as a mimic for carbosilane dendritic support systems. Earlier results (see also chapter 4) indicated that once attachment to trimethylsilyl chloride is feasible, the method holds for attachment to dimethylchlorosilyl functionalized carbosilane dendrons.[4d,e]

5.2. Results

Synthesis

Complexes **1-4** were synthesized from a single ligand precursor (**9**), which was obtained according to the route depicted in Scheme 1. Lithiation of 1-bromo-3,5-bis-[(dimethylamino)methyl]benzene (**5**) with two equivalents of *t*-BuLi, followed by a quench with 4-bromobenzaldehyde, afforded the *para*-substituted ligand **6**. Protection of the benzylic alcohol with a *t*-butyldimethylsilyl group (TBDMS) proceeded quantitatively in THF. The resulting silyl ether **7** was reacted with two equivalents of *t*-BuLi and subsequently quenched

with trimethylsilyl chloride. This reaction afforded compound **8** in good yield. A second trimethylsilyl substituent was introduced on the position *ortho* with respect to both nitrogen donor atom-containing substituents, by selective deprotonation with *n*-BuLi in hexanes, and subsequent treatment with Me_3SiOTf (OTf = trifluoromethylsulfonate) in THF, affording **9** as a single product in an overall yield of 67% based on **5**.

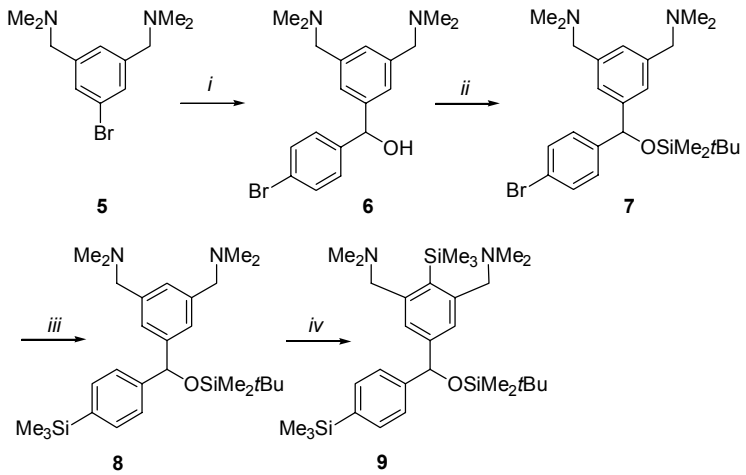

Scheme 1. Synthesis of ligand **9**: *i)* 2 *t*-BuLi, 4-bromobenzaldehyde, NH_4Cl; *ii)* $SiMe_2tBuCl$, imidazole; *iii)* 2 *t*-BuLi, $SiMe_3Cl$; *iv) n*-BuLi, $SiMe_3OTf$.

Complexes **11**, **12** and **13** were obtained from **9**, as depicted in Scheme 2. Direct palladation of **9** with $Pd(OAc)_2$ in methanol followed by treatment with LiCl, afforded complex **13** as the only product, isolated in 92% yield. Deprotection of the benzylic alcohol function of **9** with NBu_4F in THF to obtain ligand **10** proceeded smoothly and in high yield (94%). Palladation of **10** afforded complex **11**, containing a hydroxyl group, in a satisfactory 89% yield. The high stability[3] of the NCN-pincer palladium complex enabled us to react the benzylic hydroxyl group with acetic anhydride in the presence of pyridine to obtain the acetyl functionalized complex **12** in a 87% yield, without observable decomposition of the organometallic moiety.

Attempts were made to functionalize the benzylic alcohol of palladium complex **11** with a diethylphosphate moiety. Reaction of complex **11** with chloro diethylphosphate in the prescence of various bases, *i.e.* triethylamine or diisopropylethylamine, yielded the desired diethylphosphate. Attempted isolation of the product by aqueous work-up led to the quantitative removal of the phosphate giving back alcohol **11**. The use of pyridine as solvent and internal base in the esterification of **11** with chloro diethylphosphate, led to an unexpected reaction, generating exclusively pyridinium complex **14** (Scheme 3).

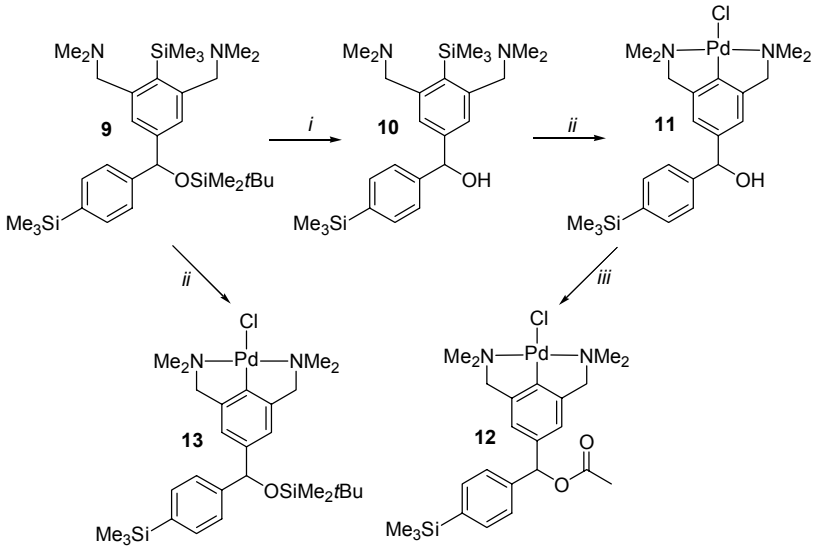

Scheme 2. Synthesis of palladium complexes **11-14**: *i)* NBu_4F; *ii)* $Pd(OAc)_2$, LiCl; *iii)* Ac_2O/pyridine.

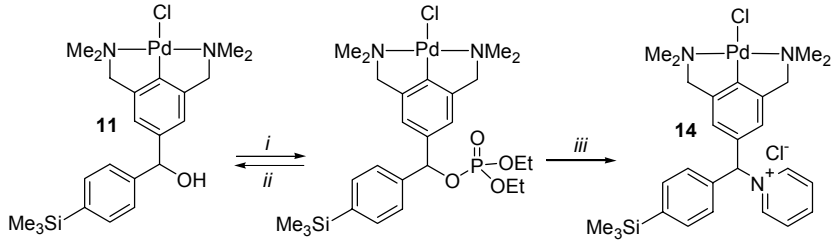

Scheme 3. Reversible formation of the diethylphosphate substituted NCN-palladium complex, and formation of **14**: *i)* $ClPO(OEt)_2$, base; *ii)* H_2O; *iii)* pyridine.

Catalysis

Complexes **11-14** were converted into their corresponding cationic aqua complexes by treatment with $AgBF_4$, resulting in the formation of complexes **1-4**, respectively (Scheme 4). The additional chloride present in pyridinium complex **14** was removed by adding an additional equivalent of $AgBF_4$ to obtain the dicationic complex **4**.

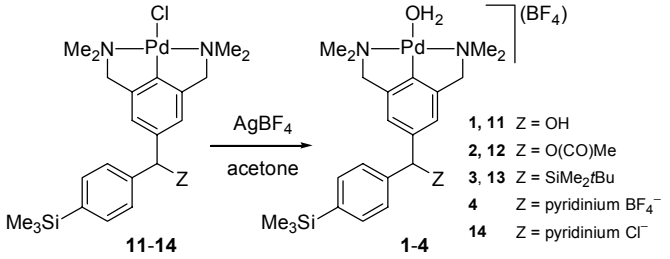

Scheme 4. Dehalogenation of **11-14** to obtain the catalytically active cationic palladium-aqua complexes **1-4**.

Cationic NCN-pincer palladium(II) aqua complexes can serve as catalyst in Lewis acid catalyzed aldol type reactions, such as the addition of methyl isocyanoacetate to benzaldehydes, to produce a diastereomeric mixture of oxazolines (Scheme 5).[5,6]

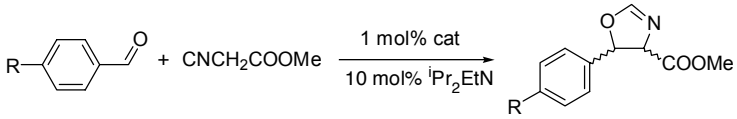

Scheme 5. Aldol condensation catalyzed by NCN-palladium complexes between methyl isocyanoacetate and *para*-substituted benzaldehydes; R = H, CH_2OH, OH.

The catalytic activity of cationic complexes **1-4** was tested in this aldol reaction, applying initially dichloromethane as the commonly used solvent.[5] However, the low solubility of 4-hydroxymethyl- and 4-hydroxybenzaldehyde in this solvent led to extremely slow conversions. Hence, these reactions were carried out in THF to solubilize the substrate. The results from the experiments are collected in Table 1.

Table 1. Results from the aldol reaction of methyl isocyanoacetate and several para-substituted benzaldehydes catalyzed by complexes **1-4**.[a]

Complex	k (10^{-3} h^{-1})[b]	Conversion (%, after 24hrs)
Benzaldehyde (R=H)		
1 (Z = OH)	314	93
2 (Z =OAc)	259	95
3 (Z = OTBDMS)	340	93
4 (Z = pyridinium)	132	80
4-Hydroxymethylbenzaldehyde (R=CH_2OH)[c]		
1	108	80
2	102	77
3	114	81
4	192	99
4-Hydroxybenzaldehyde (R=OH)[c]		
1	90	58
2	78	55
3	90	60
4	118	72

a) Conditions: see experimental section; b) initial rate of methyl isocyanoacetate consumption, determined for conversions < 40%. c) in THF.

The product distributions of the formed oxazolines were similar for all catalysts. The use of benzaldehyde and 4-hydroxybenzaldehyde as substrates led to the formation of oxazolines with cis/trans ratios amounting to 60/40 and 70/30, respectively. The cis/trans ratios were not determined for the products obtained from 4-hydroxybenzaldehyde, due to the gradual build up of various side-products upon prolonged reaction times.

5.3. Discussion

Synthesis

The selective and quantitative introduction of a trimethylsilyl substituent by a lithiation-transmetallation procedure to produce intermediate **8**, opens the way to immobilize the system on carbosilane dendrimers for catalyst recovery and recycling purposes.[4] An important factor in dendrimer synthesis is the necessity to have high conversions and selectivities for all reactions performed on dendrimers, to prevent the formation of extensive defects in the products. Thus, reactions performed on **8** and products obtained from it should be selective and quantitative. Indeed, the introduction of a trimethylsilyl substituent to C_{ipso} (**9**), the deprotection of the alcohol (**10**), the palladation (**11**), and all subsequent transformations proceeded quantitatively, although loss of material during work-up procedures can lead in certain cases to reduced isolated yields.

The above-mentioned findings strongly indicate that the performed transformations can be used to selectively synthesize the dendritic analogues of **1-4**. Interesting to note is that the used two-step palladation route, involving lithiation and silylation of C_{ipso} and subsequent electrophilic aromatic palladation,[7] is preferred over a direct lithiation-transpalladation route.[8] The latter does not lead to quantitative palladation of the NCN-pincer ligand. An additional advantage of the first route is the inertness of the trimethylsilyl group towards a wide variety of reaction conditions, allowing various modifications on the ligand prior to palladation, when desired. Functionalization of benzylic hydroxyl NCN-pincer palladium(II) complex **11** with a diethylphosphate group results in a material that is unstable towards (weak) nucleophiles such as water. This reactivity is incompatible with the presence of nucleophiles in the envisaged catalytic experiments (aldol reactions), making the diethyl phosphate functionalized complex an unsuitable catalyst, but offers a suitable starting material for further functionalizations. Finally, it is noteworthy that the routes to **11**, **12** and **14** involve organic functionalization steps on the ligand of the organometallic complex itself.

Catalysis

Of interest in the study of the catalytic properties of complexes **1**, **2** and **4**, is the influence of the hydroxyl, acetyl, or pyridinium substituents on catalysis. These substituents are, in principle, capable of hydrogen bonding or attractive coulombic interactions with selected substrates.[9] These interactions can be excluded for silyl functionalized complex **3**, which is therefore used as reference catalyst. Interesting to note for the application of **1-4** in catalysis is that a chiral center is formed on the *para*-position of the NCN-pincer ligand during the first

step of the synthesis. However, no attempts were made to separate and isolate the compounds in their enantiomerically pure form.

Complexes **1-3** have similar activities and product distributions in the aldol reaction with benzaldehyde, 4-hydroxymethylbenzaldehyde, and 4-hydroxybenzaldehyde. Pyridinium functionalized complex **4** is significantly less active in the aldol reaction with benzaldehyde, whereas in the reaction with 4-hydroxymethylbenzene a two-fold increase in activity is found. Low activities are observed for all catalysts in aldol reactions with 4-hydroxybenzaldehyde, albeit that **4** has a somewhat enhanced activity. This increased activity of **4** in the aldol reactions with hydroxyl-functionalized benzaldehydes, indicates a positive effect of the cationic pyridinium site on the catalytic performance of the NCN-palladium complex. One might speculate on the origin of this enhanced catalytic activity for the hydroxyl functionalized substrates. Hydrogen bonding interactions between the co-catalyst ($^{i}Pr_2EtN$) and the alcohol, leading to a build up of negative charge on the oxygen atom, could result in an attractive interaction with the pyridinium cation of **4**. This interaction brings the aldehyde in the vicinity of the catalytic site, possibly resulting in enhanced reaction rates.[10] Such an interaction between the amine and the alcohol, which is more pronounced for the more acidic phenolic alcohol, could also account for the low rates and conversions observed for 4-hydroxybenzaldehyde. Protonation of large amounts of the base by the acidic phenolic hydrogen inhibits its activity as cocatalyst.[11] No effect of the hydroxyl and acetyl group on the catalytic activity of **1** and **2** was observed. Apparently, the capability of the alcohol or ester moiety to participate in hydrogen bond formation with the substrate does not lead to observable effects in the catalytic performance of **1** and **2**.

5.4. Conclusions

The construction of multi-functionalized NCN-pincer complexes **1-4**, illustrates the potential of the NCN-pincer moiety in the construction of new organometallic materials. Extension of the presented synthetic methodologies would allow the introduction of a variety of functional groups to tune and optimize the catalytic behavior of the resulting complexes. These functional groups can act as cocatalyst (a sterically hindered amine base), as supramolecular receptor sites for substrate molecules, or as steric bulk to encapsulate the catalyst. The additional possibility to immobilize the presented systems on (dendritic) supports, can be advantageous for recycling purposes.

5.5. Experimental Section

All experiments using air and water sensitive reagents were conducted in a dry nitrogen atmosphere using standard Schlenk techniques. Solvents were dried over appropriate agents

and distilled prior to use. The reagent 1-bromo-3,5-bis((dimethylamino)methyl)benzene (**5**)[12] was prepared according to previously reported procedures. Elemental analyses were performed by H. Kolbe, Mikroanalytisches Laboratorium, Mülheim, Germany. ^{1}H and ^{13}C NMR spectra were recorded at 298 K on a Varian Inova 300 or Mercury 200 spectrometer.

4-[2,6-(NMe_2CH_2)$_2$$C_6H_3$-4-CH(OH)]$C_6H_4Br$ (**6**)

To a precooled (-90°C) solution of **5** (4.11 g, 15.18 mmol) in Et_2O (50 mL) was added *t*-BuLi (20.2 ml, 1.5 M in pentane, 30.3 mmol) dropwise. The reaction mixture was stirred at -90°C for an additional 30 min. and 4-bromobenzaldehyde (3.37 g, 18.21 mmol) in Et_2O (20 mL) was added dropwise. The reaction mixture was allowed to warm to room temperature and was stirred for an additional 2 hours. The mixture was quenched with water and the organic phase was extracted with 1M HCl (2 x 30 mL). The combined aqueous extracts were washed with Et_2O (30 mL), neutralized with K_2CO_3 and extracted with Et_2O (2 x 50 mL). The organic layer was dried and concentrated *in vacuo*, to afford **6** as a white solid. Yield: 4.96 g (87%), ^{1}H-NMR ($CDCl_3$, 200 MHz) δ: 7.42 (d, 2H, $^{3}J_{HH}$ = 8.0 Hz, ArH), 7.28 (s, 2H, ArH), 7.26 (d, 2H, $^{3}J_{HH}$ = 8.0 Hz, ArH), 7.13 (s, 1H, ArH), 5.74 (s, 1H, ArCH), 3.41 (s, 4H, CH_2N), 2.20 (s, 12H, NMe_2); $^{13}C\{^{1}H\}$ ($CDCl_3$, 50 MHz) δ: 144.5, 143.9, 138.6, 131.3, 129.2, 128.1, 126.1, 120.8 (Ar), 75.1 (CH(OH)), 64.1 (CH_2N), 45.2 (NMe_2); Anal. Calcd. for $C_{19}H_{25}BrN_2O$: C 60.48, H 6.68, N 7.42; Found: C 60.29, H 6.58, N 7.32.

4-[2,6-(NMe_2CH_2)$_2$$C_6H_3$-4-CH(OTBDMS)]$C_6H_4Br$ (**7**)

To a stirred solution of TBDMSCl (4.09 g, 27.16 mmol) and imidazole (3.08 g, 45.27 mmol) in THF (50 mL) was added dropwise a solution of **6** (8.54 g, 22.63 mmol) in THF (15 mL). The mixture refluxed temperature overnight and after cooling to room temperature methanol (3 mL) was added, followed by removal of all volatiles *in vacuo*. The residue was redissolved in Et_2O (50 mL), washed with water and brine. The etheral layer was dried over $MgSO_4$, and then concentrated *in vacuo* to afford **7** as a yellow oil. Yield: 10.47 g (94%), ^{1}H-NMR ($CDCl_3$, 200 MHz) δ: 7.39 (d, 2H, $^{3}J_{HH}$ = 8.4 Hz, ArH), 7.23 (d, 2H, $^{3}J_{HH}$ = 8.4 Hz, ArH), 7.17 (s, 2H, ArH), 7.13 (s, 1H, ArH), 5.69 (s, 1H, ArCH), 3.44 (d, 2H, $^{2}J_{HH}$ = 11.4 Hz, CH_2N), 3.35 (d, 2H, $^{2}J_{HH}$ = 11.4 Hz, CH_2N), 2.21 (s, 12H, NMe_2), 0.89 (s, 9H, *t*-BuSi), -0.04 (d, 6H, $SiMe_2$); $^{13}C\{^{1}H\}$ ($CDCl_3$, 50 MHz) δ: 144.5, 144.4, 138.9, 131.1, 128.8, 127.8, 125.7, 120.5 (Ar), 76.0 (CH(OTBS)), 64.2 (CH_2N), 45.3 (NMe_2), 25.7 ($C(\underline{C}H_3)_3$), 18.2 ($\underline{C}(CH_3)_3$), -4.8, -4.9 ($SiMe_2$); Anal. Calcd. for $C_{25}H_{39}N_2OSi$: C 61.08, H 8.00, N 5.70; 5.71; Found: C 61.20, H 8.04, N 5.42, Si 5.60.

4-[2,6-(NMe_2CH_2)$_2C_6H_3$-4-CH(OTBDMS)]$C_6H_4SiMe_3$ (**8**)

To a precooled (-78°C) solution of **7** (1.25 g, 2.54 mmol) in Et_2O (15 mL) was added *t*-BuLi (3.4 ml, 1.5M in pentane, 5.1 mmol) dropwise. The reaction mixture was stirred at -78°C for an additional 30 min., and trimethylsilyl chloride (1.6 mL, 12.7 mmol) was added at once. The reaction mixture was allowed to warm to room temperature and all volatiles were evaporated *in vacuo*. The residue was redissolved in Et_2O (25 mL) and the solution was washed with brine. The etheral layer was dried over $MgSO_4$ and then concentrated to afford **8** as a yellow oil. Yield: 1.11 g (90%). ^{1}H-NMR ($CDCl_3$, 200 MHz) δ: 7.43 (d, 2H, $^3J_{HH}$ = 8.0 Hz, ArH) 7.33 (d, 2H, $^3J_{HH}$ = 8.0 Hz, ArH), 7.20 (s, 2H, ArH), 7.13 (s, 1H, ArH), 5.73 (s, 1H, ArCH), 3.45 (d, 2H, $^2J_{HH}$ = 11.4 Hz, CH_2N), 3.36 (d, 2H, $^2J_{HH}$ = 11.4 Hz, CH_2N), 2.21 (s, 12H, NMe_2), 0.90 (s, 9H, *t*-BuSi), 0.22 (s, 9H, $SiMe_3$), -0.04 (d, 6H, $SiMe_2$); $^{13}C\{^1H\}$ ($CDCl_3$, 50 MHz) δ: 145.8, 145.0, 138.6, 138.4, 133.1, 128.6, 126.1, 125.3 (Ar), 76.6 (CH(OTBS)), 64.3 (CH_2N), 45.3 (NMe_2), 25.8 (C($\underline{C}H_3$)$_3$), 18.3 ($\underline{C}(CH_3)_3$), -1.1($SiMe_3$), -4.7, -4.9 ($SiMe_2$); Anal. Calcd. for $C_{28}H_{48}N_2OSi_2$: C 69.36, H 9.98, N 5.78, Si 11.58; Found: C 69.46, H 10.01, N 5.71, Si 11.39.

4-[1-$SiMe_3$-2,6-(NMe_2CH_2)$_2C_6H_2$-4-CH(OTBDMS)]$C_6H_4SiMe_3$ (**9**)

*n*BuLi (3.1 mL, 1.6 M in hexanes, 4.9 mmol) was added dropwise over a period of 5 minutes to a precooled (-78°C) solution of **8** (2.37 g, 4.89 mmol) in hexane (20 mL). The reaction mixture was allowed to warm to room temperature and was stirred for an additional 4 h. After cooling the reaction mixture to 0°C, a solution of trimethylsilyl trifluoromethylsulfonate (1.42 mL, 7.33 mmol) in THF (20 mL) was added dropwise over a period of 10 min. and stirred for 16 h. at room temperature. All volatiles were removed in vacuo, and the residue was extracted with hexane (3 x 50 mL). The combined hexane extracts were flushed over basic Al_2O_3 and then concentrated to afford **9** as a yellow oil. Yield: 2.49 g (91%), ^{1}H-NMR ($CDCl_3$, 200 MHz) δ: 7.42 (d, 2H, $^3J_{HH}$ = 8.0 Hz, ArH), 7.34 (d, 2H, $^3J_{HH}$ = 8.0 Hz, ArH), 7.32 (s, 2H, ArH), 5.74 (s, 1H, ArCH), 3.60 (d, 2H, $^2J_{HH}$ = 13.2 Hz, CH_2N), 3.40 (d, 2H, $^2J_{HH}$ = 13.2 Hz, CH_2N), 0.91 (s, 9H, *t*-BuSi), 0.33 (s, 9H, $SiMe_3$), 0.22 (s, 9H, $SiMe_3$), -0.04 (d, 6H, $SiMe_2$) ; $^{13}C\{^1H\}$ ($CDCl_3$, 50 MHz) δ: 146.4, 145.8, 145.0, 138.3, 137.2, 133.1, 128.0, 126.6, 126.0 (Ar), 76.5 (CH(OTBS)), 65.6 (CH_2N), 45.1 (NMe_2), 25.9 (C($\underline{C}H_3$)$_3$), 18.3, ($\underline{C}(CH_3)_3$), 3.2 ($SiMe_3$), -1.0 ($SiMe_3$), -4.6, -4.9 ($SiMe_2$); Anal. Calcd. for $C_{31}H_{56}N_2OSi_3$: C 66.84, H 10.13, N 5.03; Found: C 66.73, H 10.29, N 4.91

4-[1-$SiMe_3$-2,6-(NMe_2CH_2)$_2C_6H_2$-4-CH(OH)]$C_6H_4SiMe_3$ (**10**)

To a stirred solution of **9** (1.04 g, 1.87 mmol) in THF (15 mL) was added NBu_4F (1.9 mL, 1 M in THF, 1.9 mmol) at once. The mixture was stirred at room temperature for one hour. All volatiles were evaporated, and the residue was extracted with hexane (3x 100 mL). The

combined fractions were washed with brine. The hexane layer was dried over $MgSO_4$ and concentrated to afford **10** as a yellow oil. Yield: 0.87 g (94%). ^{1}H-NMR ($CDCl_3$, 200 MHz) δ: 7.48 (d, 2H, $^3J_{HH}$ = 7.4 Hz, ArH), 7.38 (d, 2H, $^3J_{HH}$ = 7.4 Hz, ArH), 7.37 (s, 2H, ArH), 5.80 (s, 1H, ArCH) 3.52 (s, 4H, CH_2N), 2.11 (s, 12H, NMe_2), 0.36 (s, 9H, $SiMe_3$), 0.25 (s, 9H, $SiMe_3$); $^{13}C\{^1H\}$ ($CDCl_3$, 75 MHz) δ: 146.4, 144.9, 144.2, 139.2, 137.6, 133.4, 126.2, 125.9 (Ar), 76.1 (CH(OH)), 65.3 (CH_2N), 45.0 (NMe_2), 3.3 ($SiMe_3$), -1.1 ($SiMe_3$); Anal. Calcd. for $C_{25}H_{42}N_2OSi_2$: C 67.81, H 9.56, N 6.33; Found: C 67.69, H 9.51, N 6.24.

[1-PdCl-2,6-(NMe_2CH_2)$_2$$C_6H_2$-4-CH(OH)($C_6H_4SiMe_3$)] (**11**)

To a suspension of **10** (1.20 g, 2.71 mmol) in freshly distilled methanol (30 mL) was added $Pd(OAc)_2$ (0.67 g, 2.98 mmol) at once. The reaction mixture was stirred for 3 h. at room temperature, excess LiCl (0.75 g, 17.77 mmol) was added at once, and stirring was continued for an additional hour. All volatiles were evaporated *in vacuo* and the residue was extracted with dichloromethane (3x 30 mL). The combined dichloromethane extracts were filtered over Celite, and removal of the volatiles afforded **11** as an orange solid. Yield: 1.23 g (89%), ^{1}H-NMR ($CDCl_3$, 200 MHz) δ: 7.49 (d, 2H, $^3J_{HH}$ = 8.0 Hz, ArH), 7.35 (d, 2H, $^3J_{HH}$ = 8.0 Hz, ArH), 6.80 (s, 2H, ArH), 5.71 (s, 1H, ArCH) 3.95 (s, 4H, CH_2N), 2.91 (s, 12H, NMe_2), 0.25 (s, 9H, $SiMe_3$). $^{13}C\{^1H\}$ ($CDCl_3$, 75 MHz) δ: 156.2, 145.3, 144.6, 140.7, 140.0, 133.8, 125.9, 118.5 (Ar), 76.6 (CH(OH)), 74.9 (CH_2N), 53.4 (NMe_2), -0.8 ($SiMe_3$); Anal. Calcd. for $C_{22}H_{33}ClN_2OPdSi$: C 51.66, H 6.50, N 5.48. Found: C 51.46, H 6.45, N 5.36.

[1-PdCl-2,6-(NMe_2CH_2)$_2$$C_6H_2$-4-CH(OAc)($C_6H_4SiMe_3$)] (**12**)

To a solution of **11** (155 mg, 2.71 mmol) in pyridine (1 mL) was added Ac_2O (0.5 mL) at once. The mixture was stirred at room temperature for 16 hours, and subsequently poured into an ice/water mixture. The aqueous layer was extracted with dichloromethane (3x) and the combined fractions were washed with an aqueous 1 M $NaHCO_3$ solution, dried over $MgSO_4$, and concentrated to afford **12** as a light yellow solid. Yield: 146 mg (87%). ^{1}H-NMR ($CDCl_3$, 200 MHz) δ: 7.48 (d, 2H, $^3J_{HH}$ = 8.0 Hz, ArH), 7.29 (d, 2H, $^3J_{HH}$ = 8.0 Hz, ArH), 6.75 (s, 2H, ArH), 6.72 (s, 1H, ArH) 3.95 (s, 4H, CH_2N), 2.91 (s, 12H, NMe_2), 2.13 (s, 3H, OAc), 0.24 (s, 9H, $SiMe_3$). $^{13}C\{^1H\}$ ($CDCl_3$, 75 MHz) δ: 170.2 (CO), 156.8, 145.3, 140.9, 140.3, 137.0, 133.7, 126.3, 119.1 (Ar), 77.4 (C*H*OAc), 74.9 (CH_2N), 53.3 (NMe_2), 21.6 (CO*C*H_3) –0.9 ($SiMe_3$); Anal. Calcd. for $C_{24}H_{35}ClN_2O_2PdSi$: C 52.08, H 6.37, N 5.06. Found: C 51.92, H 6.31, N 4.95.

*[1-PdCl-2,6-(NMe_2CH_2)$_2$$C_6H_2$-4-CH(OTBDMS)($C_6H_4SiMe_3$)] (**13**)*

A similar procedure as described for **11** was used, with **9** as starting material (yield 92%). ^{1}H-NMR ($CDCl_3$, 300 MHz) δ: 7.43 (d, 2H, $^3J_{HH}$ = 7.5 Hz, ArH), 7.30 (d, 2H, $^3J_{HH}$ = 7.5 Hz,

ArH), 6.75 (s, 2H, ArH), 5.60 (s, 1H, ArCH) 3.93 (s, 4H, CH_2N), 2.91 (s, 12H, NMe_2), 0.89 (s, 9H, *t*Bu), 0.24 (s, 9H, $SiMe_3$), -0.05, -0.07 ($SiMe_2$); $^{13}C\{^1H\}$ (acetone-d_6, 75 MHz) δ: 156.2, 146.8, 145.5, 142.1, 138.5, 133.4, 125.7, 117.7 (Ar), 77.2 (CH(OTBS)), 74.7 (CH_2N), 52.6 (NMe_2), 25.7 ($C(\underline{C}H_3)_3$), 18.3 ($\underline{C}(CH_3)_3$) –1.5 ($SiMe_3$), -5.1 ($SiMe_2$); Anal. Calcd. for $C_{28}H_{47}ClN_2OPdSi_2$: C 53.75, H 7.57, N 4.48; Found: C 53.60, H 7.51, N 4.33.

[1-PdCl-2,6-(NMe_2CH_2)$_2$$C_6H_2$-4-CH($C_5H_5N^+$)($C_6H_4SiMe_3$)] ***(14)***

A solution of **11** (240 mg, 0.47 mmol) in 5 mL of pyridine was treated with chloro diethylphosphate (120 mg ,0.70 mmol). The reddish solution was stirred for 16 hours at room temperature. All volatiles were removed *in vacuo*, and the residue was redissolved in CH_2Cl_2 (50 mL). This solution was washed with water (50 mL) and brine (50 mL), and dried over $MgSO_4$. The organic layer was concentrated to 5 mL, followed by precipitation with Et_2O, to afford **13** as a orange yellow solid (277 mg, 0.40 mmol) in 85% yield. ^{1}H-NMR ($CDCl_3$, 300 MHz) δ: 9.18 (br d, 2H, pyridinium), 8.54 (br t, 1H, pyridinium), 8.17 (m, 2H, pyridinium), 8.16 (s, 1H, C*H*(NC_5H_5)), 7.47 (d, 2H, $^3J_{HH}$ = 8.1 Hz, ArH), 7.16 (d, 2H, $^3J_{HH}$ = 8.0 Hz, ArH), 6.84 (s, 2H, ArH), 3.94 (s, 4H, CH_2N), 2.85 (s, 12H, NMe_2), 0.19 (s, 9H, $SiMe_3$). $^{13}C\{^1H\}$ ($CDCl_3$, 75 MHz) δ: 146.6, 144.9, 128.8 (pyridinium), 159.7, 146.2, 142.8, 136.3, 134.6, 131.6, 127.9, 121.4 (Ar), 77.2 ($\underline{C}H(NC_5H_5)$), 74.8 (CH_2N), 53.4 (NMe_2), –1.0 ($SiMe_3$); Anal. Calcd. for $C_{25}H_{31}Cl_2N_2PdSi$: C 53.15, H 5.53, N 4.96; Found: C 53.09, H 5.60, N 4.88.

General procedure for cationic palladium complexes **1-4**

$AgBF_4$ (39 mg, 0.20 mmol) was added at once to a solution of the palladium halides **11-14** (0.20 mmol) in wet acetone, resulting in immediate precipitation of a yellowish solid. The mixture was stirred for 30 min. followed by removal of all volatiles. The residue was extracted with CH_2Cl_2 (2 x 5 mL), and the combined extracts were filtered carefully over Celite. Evaporation of the volatiles afforded **1-4** as yellow to orange solids in near quantitative yields (> 95%). The cationic complexes were prepared freshly prior to catalysis.

Catalyst Screening

To a solution of the catalyst (1 mol%, 8 μmol) in 2.5 mL of CH_2Cl_2 or THF, was added the (substituted) benzaldehyde (0.8 mmol), *i*PrEtN (10 mol% 80 μmol), and methyl isocyanoacetate (0.8 mmol). The mixture was stirred at room temperature in air in a closed reaction vessel. Samples (100 μl) for ^{1}H-NMR (200 MHz) analysis were stripped from the solvent in a stream of nitrogen gas, and redissolved in $CDCl_3$ (0.5 mL). Conversions (methyl isocyanoacetate consumptions) were calculated from the intensity of the CNC*H*$_2$COOMe protons versus the combined methyl ester signals.

5.6. References and Notes

1. For overviews on NCN-pincer chemistry see: (a) M. Albrecht, G. van Koten, *Angew. Chem., Int. Ed.* **2001**, *40*, 3750-3781; (b) P. Steenwinkel, R. A. Gossage, G. van Koten, *Chem. Eur. J.* **1998**, *4*, 759. (c) R. A. Gossage, L. A. van de Kuil, G. van Koten, *Acc. Chem. Res*. **1998**, *31*, 423; (d) M. H. P. Rietveld, D. M. Grove, G. van Koten, *New J. Chem.* **1997**, *21*, 751; (e) G. van Koten, *Pure & Appl. Chem*. **1989**, *61*, 1681.
2. Rodríguez, G.; Lutz, M.; Spek, A. L.; van Koten, G. *Chem. Eur. J.* **2002**, *8*, 45-57; and chapter 4 of this thesis.
3. G. Rodriguez, G.; Albrecht, M.; Schoenmaker, J.; Ford, A.; Lutz, M.; Spek, A. L.; van Koten, G. *J. Am. Chem. Soc*. **2002**, *124*, 5127-5138; and chapter 2 of this thesis.
4. (a) Dijkstra, H. P.; Kruithof, C. A.; Ronde, N.; van de Coevering, R.; Ramon, D. J.; Vogt, D.; van Klink, G. P. M.; van Koten, G. *J. Org. Chem*. **2002**, ASAP Article. (b) Dijkstra, H. P.; Meijer, M. D.; Patel, J.; Kreiter, R.; van Klink, G. P. M.; Lutz, M.; Spek, A. L.; Canty, A. J.; van Koten, G.; *Organometallics* **2001**, *20*, 3159-3168; (c) Albrecht, M.; Hovestad, N. J.; Boersma, J.; van Koten, G. *Chem. Eur. J.* **2001**, *7*, 1289-1294; (d) Kleij, A. W.; Gossage, R. A.; Klein Gebbink, R. J. M.; Brinkmann, N.; Reijerse, E. J.; Kragl. U.; Lutz, M.; Spek, A. L.; van Koten, G. *J. Am. Chem. Soc.* **2000**, *122*, 12112-12124. (e) Schlenk, C.; Kleij, A. W.; Frey, H.; van Koten, G. *Angew. Chem. Int. Ed.* **2000**, *39*, 3445-3447. (f) Kleij, A. W.; Gossage, R. A.; Jastrzebski, J. T. B. H.; Lutz, M.; Spek, A. L.; van Koten, G. *Angew. Chem. Int. Ed.* **2000**, *39*, 176. (g) Dijkstra, H. P.; Steenwinkel, P.; Grove, D. M.; Lutz, M.; Spek, A. L.; van Koten, G. *Angew. Chem. Int. Ed.* **1999**, *38*, 2186; (h) Albrecht, M.; van Koten, G. *Adv. Mater*. **1999**, *11*, 171. (i) Knapen, J. W. J.; van der Made, A. W.; de Wilde, J. C.; van Leeuwen, P. W. N. M.; Wijkens, P.; Grove, D. M.; van Koten, G. *Nature* **1994**, *372*, 659.
5. (a) Williams, B. S.; Dani, P.; Lutz, M.; Spek, A. L.; van Koten, G. *Helvetica Chimica Acta* **2001**, 84, 3519-3530. (b) Meijer, M. D.; Ronde, N.; Vogt, D.; van Klink, G. P. M.; van Koten, G. *Organometallics* **2001**, *20*, 3993-4000. (c) Gimenez, R.; Swager, T. M. *J. Mol. Catal. A: Chem.* **2001**, *166*, 265-273. (d) Dijkstra, H. P.; Meijer, M. D.; Patel, J.; Kreiter, R.; van Klink, G. P. M.; Lutz, M.; Spek, A. L.; Canty, A. J.; van Koten, G. O*rganometallics* **2001**, *20*, 3159-3168. (e) Stark, M. A.; Richards, C. J. *Tetrahedron Lett.* **1997**, *38*, 5881. (f) Longmire, J. M.; Zhang, X.; Shang, M. *Organometallics* **1998**, *17*, 4374-4379. (g) Fujimura, O. *J. Am. Chem. Soc.* **1998**, *120*, 10032-10039. (h) Gorla, F.; Togni, A.; Venanzi, L. M.; Albinati, A.; Lianza, F.; O*rganometallics* **1994**, *13*, 1607-1616. (i) Nesper, R.; Pregosin, P. S.; Püntener, K.; Wörle, M. *Helv. Chim. Acta* **1993**, *76*, 2239-2249.
6. (a) Ohkouchi, M.; Masui, D.; Yamaguchi, M.; Yamagishi, T. *J. Mol. Cat. A: Chem.* **2001**, *170*, 1-15. (b) Johnson, J. S.; Evans, D. A. *Acc. Chem. Res.* **2000**, *33*, 325-335. (c) Evans, D. A.; Murry, J. A.; Kozlowski, M. C. *J. Am. Chem. Soc.* **1996**, *118*, 5814. (d) Evans, D. A.; Kozlowski, M. C.; Tedrow, J. S. *Tetrahedron Lett.* **1996**, *37*, 7481. (e) Sawamura, M.; Nakayama, Y.; Kato, T.; Ito, Y. *J. Org. Chem.* **1995**, *60*, 1727-1732.
7. Steenwinkel, P.; Gossage, R. A.; van Koten, G. *Chem. Eur. J.* **1998**, *4*, 759-762, and references cited.
8. Alsters, P. L.; Baesjov, P. J.; Janssen, M. D.; Kooijman, H.; Sicherer-Roetman, A.; Spek, A. L.; van Koten, G. *Organometallics* **1992**, *11*, 4124-4135.
9. For example, para-hydroxymethyl substituted NCN-pincer palladium(II)chloride complexes are known to dimerize by O–H....Cl hydrogen bonding interactions; see X-ray structure of **22a** in chapter 2.

10. The reaction between the aldehyde the palladium-coordinated methyl isocyanoacetate enolate is considered to be the rate determining step in this aldol reaction; see references 5i and 6.
11. The pKa's of phenols and trialkylammonium ions are both located around 10, with the phenolic aldehyde concentration being ten times higher under catalytic conditions.
12. Steenwinkel, P.; James, S. L.; Grove, D. M.; Veldman, N.; Spek, A. L.; van Koten, G.; *Chem. Eur. J.*, **1996**, 2, 1440.

Chapter Six

Encapsulation of Hydrophilic NCN-Pincer Platinum Complexes in Amphiphilic Hyperbranched Polyglycerol Nanocapsules

Abstract

Hydrophilic NCN-pincer platinum(II) complexes with sulfonate groups are encapsulated in amphiphilic hyperbranched polyglycerols with a core-shell structure (‘nanocapsules’). In apolar solvents, these macromolecules exhibit a reverse micelle-type architecture. The maximum loading of the polar NCN-pincer complexes in the nanocapsules depends on the molecular weight of the hyperbranched polymers. The non-covalently encapsulated Pt(II) complexes show catalytic activity in double Michael additions, albeit with decreased activities compared to the free NCN-pincer complex. Hyperbranched polymer based microenvironments are promising supports with respect to the application of homogeneous NCN-pincer catalysts in membrane reactors.

6.1. Introduction

The study of catalytically active dendritic materials has become an attractive subject of interest.[1] Such materials can be obtained either upon attachment of the appropriate catalyst (precursor) at the core or periphery of dendrimers, or by the immobilization of metal nanoclusters in dendritic compartments.[2] Unfortunately, the preparation of dendrimers requires multi-step syntheses, which limits their large-scale (industrial) application. In contrast, hyperbranched polymers are conveniently prepared on large scales in one-pot procedures via polymerization of AB_m-type monomers.[3] Controlled polymerization of glycidol by anionic ring-opening multibranching polymerization results in the formation of highly hydrophilic hyperbranched polyglycerols.[4] Esterification of a certain fraction (40-60%) of the hydroxyl groups of these hyperbranched polyether polyols with hydrophobic alkyl chains yields amphiphilic molecular nanocapsules with a reverse micelle-type architecture. These low polydispersity ($1.3<M_w/M_n<1.5$) amphiphilic molecular nanocapsules are soluble in apolar organic solvents and irreversibly encapsulate various polar, water-soluble dye molecules in their hydrophilic interior by liquid-liquid extraction.[5] Our interest in the immobilization of homogeneous transition metal catalysts by soluble support systems has motivated us to prepare hydrophilic transition metal complexes which can be encapsulated inside these amphiphilic nanocapsules in a noncovalent manner. Due to their chemical integrity, metal complexes of the pincer-ligand (3,5-bis[(dimethylamino)methyl]phenyl anion) have proven to be especially potent candidates for immobilization purposes.[6,7] The introduction of suitable substituents at the *para*-postition of these NCN-pincer complexes permits to tailor their solubility in solvents ranging from apolar to highly polar and protic (see chapter 2). This chapter describes the noncovalent encapsulation of sulfonated pincer platinum(II) complexes in readily available amphiphilic nanocapsules based on hyper-branched polyglycerol (Scheme 1). The encapsulated platinum(II) complexes have been applied as catalyst in double Michael additions to demonstrate their potential as homogeneous catalysts in continous membrane reactors.

6.2. Results and Discussion

Synthesis

The nanocapsules $P(G_{25}C16_{0.5})$ **1** and $P(G_{106}C16_{0.6})$ **2** investigated in this study, were synthesized by partial esterification of hyperbranched polyglycerols with molecular weights of M_n= 2,000 and M_n= 8,000, respectively.[8] Esterifications were performed with palmitoyl chloride in a mixture of pyridine and toluene,[5a] and the products were characterized by ^{1}H- and ^{13}C-NMR spectroscopy, IR-spectroscopy, and SEC analysis. While nanocapsule **1** possesses a molecular weight of M_n= 5,200 (M_w/M_n= 1.2), with a degree of substitution of

50%, nanocapsule **2** has a molecular weight of M_n= 23,500 (M_w/M_n= 1.3) with 60% degree of substitution with palmitoyl tails. Polymers **1** and **2** are completely and homogeneously soluble in apolar solvents such as dichloromethane, chloroform and toluene. It should be emphasized that the analogous linear polyglycerols after partial esterification (60%) afford chloroform-soluble materials unable of transporting polar guest molecules.[9]

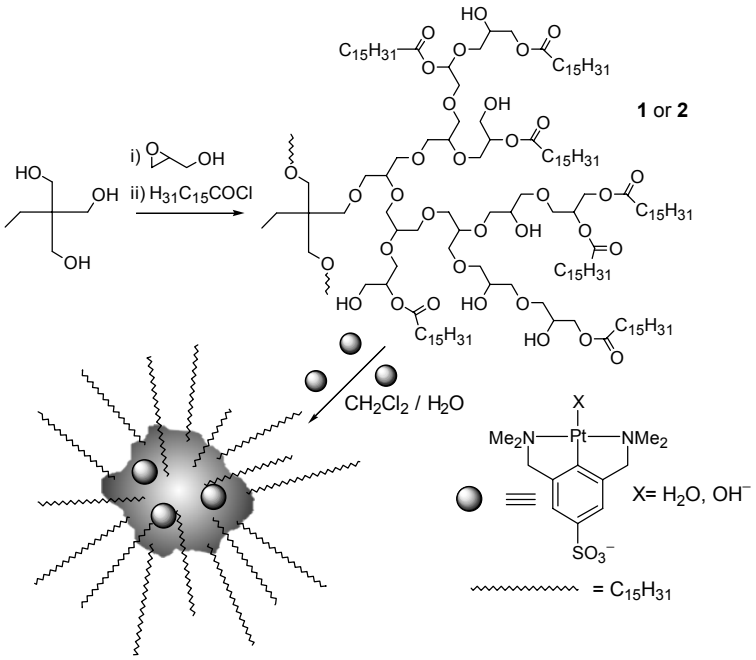

Scheme 1. Molecular nanocapsule synthesis, structure, and non-covalent encapsulation of NCN-pincer platinum complexes.

Hydrophilic NCN-platinum complexes

The hydrophilic pincer-platinum(II) complexes **3** and **4** (Chart 1) can be dissolved in polar (protic) solvents such as water, methanol or DMSO. Their solubility in aqueous solvents can be enhanced by the addition of base.

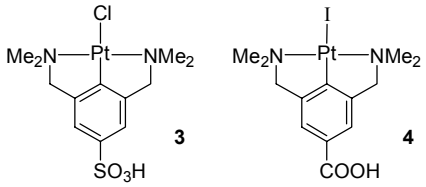

Chart 1. Structures of hydrophilic NCN-platinum complexes.

Since encapsulation of **3** and **4** by liquid-liquid extraction involves solubilization of the organometallic complexes in aqueous solution, we investigated their behaviour in aqueous solution in more detail. Carboxylic acid complex **4** is slightly soluble, and sulphonic acid **3** is reasonably soluble in water. However, their solubility is enhanced in aqueous solutions with

pH >7 due to more efficient deprotonation of the acidic functional group. A ^{1}H-NMR spectrum of a saturated solution of platinum complex **3** in D_2O shows, apart from the aromatic and benzylic resonances, a large signal from the NMe_2 protons at 2.99 ppm, corresponding with the sulfonate. In a saturated 0.5M NaOH/D_2O solution this resonance disappears, and two new signals appear for the NMe_2 protons at higher field (2.88 ppm and 2.59 ppm). ^{195}Pt-NMR in 0.5M NaOH/D_2O shows two signals located at -1795 and -1849 ppm. These shifts correspond to the dehalogenation of **3**, as confirmed by halide abstraction with $AgBF_4$, followed by the formation of an equilibrium between presumably the aqua and the hydroxyl analogues of **3,** in a ratio dependent on the pH of the solution (Scheme 2).[10] In D_2O, the solubility of **3** is too low for observation by ^{195}Pt-NMR. Similar behaviour, *i.e.* dehalogenation under basic aqueous conditions, was observed for platinum complex **4**.

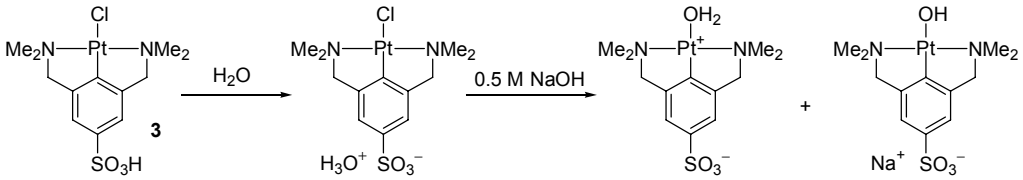

Scheme 2. Dehalogenation of NCN-platinum complex **3** under basic aqueous conditions.

Non-covalent Encapsulation

Using UV/Vis spectroscopy, we monitored the extent to which molecular nanocapsules **1** and **2** were able to encapsulate the platinum complexes **3** (*p*-SO_3H) and **4** (*p*-COOH) by extraction from aqueous solutions (0.5 M NaOH) into dichloromethane solutions. Dichloromethane solutions of the nanocapsules (c = 5 x 10^{-5} M) were shaken thoroughly with aqueous solutions of the pincer complexes **3** and **4**, respectively, with various concentrations in the range of 10^{-5}-10^{-4} M. The clear organic phase obtained after phase separation was studied by UV/Vis spectroscopy. While the sulfonated complex **3** shows very little solubility in neat dichloromethane, it could be extracted from the aqueous phase into dichloromethane solutions of the amphiphilic polyglycerols **1** and **2**. UV/Vis spectra from solutions of **3** in the nanocapsules showed two strong bands ($\varepsilon_{\pi\text{-}\pi^*} \approx 10^4$ $M^{-1}cm^{-1}$) at 262 and 275 nm. The intensity of these bands increased at higher ratios of [**3**]/[nanocapsule]. Selected UV/Vis spectra from the extractions of **3** by nanocapsules **1** and **2**, together with the corresponding titration curves, are depicted in Figure 1. The corresponding UV/Vis spectra from the aqueous phase, showing incomplete uptake of **3** by the nanocapsules, are given in Figure 2.

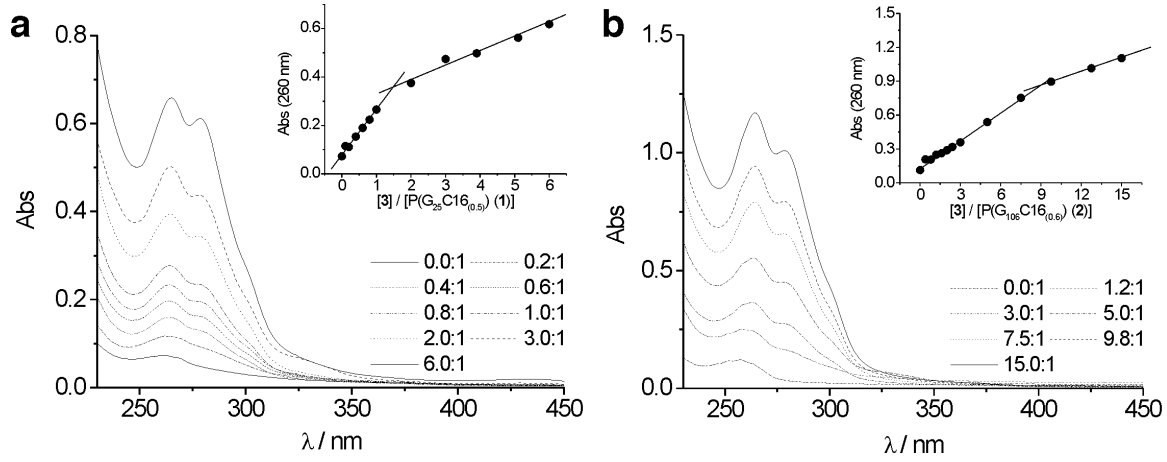

Figure 1. UV/Vis spectra (organic phase) and titration curves (insets) of the extractions of NCN-platinum complex **3** by nanocapsules (a) **1** and (b) **2** at various [**3**]/[nanocapsule] ratios.

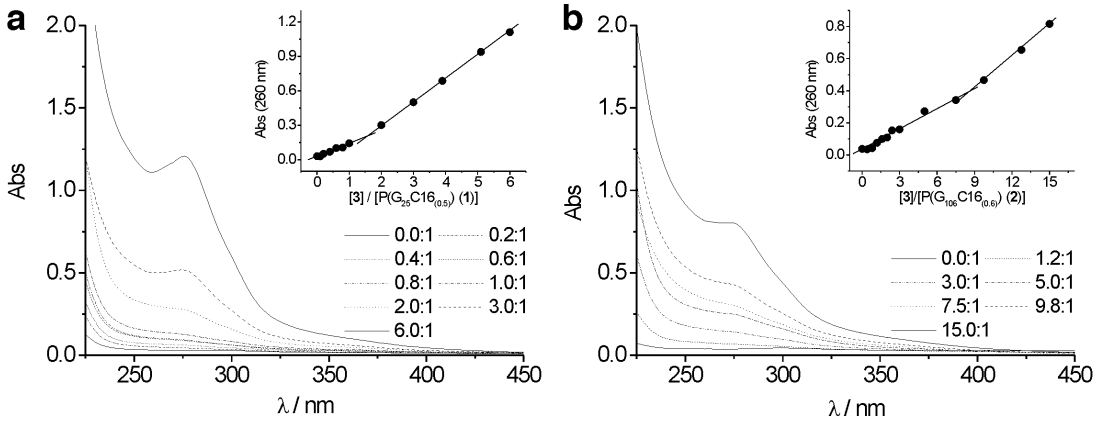

Figure 2. UV/Vis spectra from the aqueous phase for extractions with nanocapsules (a) **1** and (b) **2**, corresponding to Figure 1.

A change in slope of absorbance versus concentration ratio (inflection point) was reached at ratios of 1.5 ([**3**]/[**1**]) and 9.0 ([**3**]/[**2**]), clearly demonstrating the effect of molecular weight on the loading capacity of the amphiphilic hyperbranched polyglycerol. The incorporation behavior of **3** in the molecular nanocapsules is similar to that observed for sulfonated organic dyes.[5] At concentrations above the inflection point the nanocapsules take up more **3** from the aqueous solution, but clearly by a different mechanism. This behavior deviates from the sulfonated dyes reported previously,[5a] and we explain this tentatively by the aggregation of nanocapsules to form larger micelle-type structures, most probably assembled around the polar NCN-platinum complex, which possesses two polar moieties (SO_3^- and HO^-) and a Lewis-acidic center. It should be pointed out that all our observations to date suggest that the unimolecular nature of the solvating nanocapsules depends on the nature of the guest

molecule studied. UV/Vis analysis of the aqueous phase showed that at concentrations exceeding the inflection point, **3** is not extracted quantitatively into the organic phase any more. Preparative loading of nanocapsules **1** and **2** with NCN-pincer platinum complex **3** was carried out using concentration ratios of [**3**]/[nanocapsule] equal to 1.5 and 9, respectively. The resulting yellowish solids were analyzed by ^{1}H-, ^{13}C-, and ^{195}Pt-NMR, and SEC-chromatography. ^{1}H-NMR integration of the NMe_2 signals ($\delta(CH_3)$= 3.02 ppm) originating from complex **3** and hydrophobic shell protons ($\delta(CH_3)$= 0.84 ppm) of the nanocapsule afforded an estimate for the loading of the nanocapsules. Nanocapsule **1** was found to encapsulate 0.9-1.1, and nanocapsule **2** 3.8-4.1 molar equivalents of **3**. More accurate loadings of 1.3 for **1** and 2.4 for **2** were determined based on the platinum content quantified by elemental analysis. The loaded nanocapsules will be denoted as **1·3$_{1.3}$** and **2·3$_{2.4}$**.

The carboxylate platinum(II) NCN-pincer **4** is not encapsulated in the hyperbranched nanocapsules. Dichloromethane solutions of **1** and **2** remained unchanged after shaking them with aqueous (0.5M NaOH) solutions of **4**. UV/Vis-spectra of the organic phase showed no phase transfer of the complex. Furthermore, the band at 308 nm in the spectrum of **4** in the aqueous phase did not decrease upon repeated extractions with the nanocapsules. Attempts to encapsulate **4** with other counterions, *e.g.* in 0.5 M KOH and CsOH, were also unsuccessful. It should be noted that the encapsulation behavior observed for the carboxylate pincer complexes is similar to that of carboxylate-substituted organic dye molecules, which have a low affinity for the polyether-polyol interior of the nanocapsules compared to sulfonate substituted dyes.[11]

Double Michael Additon

The isolated loaded nanocapsules **1·3$_{1.3}$** and **2·3$_{2.4}$** were applied as catalyst in the double Michael addition of methyl vinyl ketone to ethyl cyanoacetate. Although cationic NCN-pincer platinum complexes are, in contrast to their highly active palladium analogues, not considered to be catalytically active in Lewis-acid catalysed processes,[6] they do accelerate selected examples to some extent. This offers the opportunity for a model-study of the non-covalently assembled system towards catalysis. The platinum loadings determined by elemental analysis were used to calculate the amount of catalyst applied in the double Michael addition. The results from the catalysis experiments are summarized in Table 1.

Table 1. Catalytic results of the double Michael addition, catalyzed by the encapsulated complexes.[a]

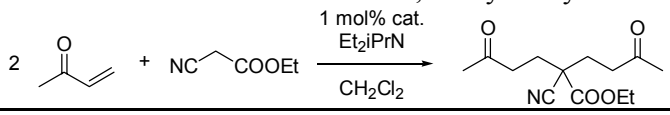

Entry	Catalyst	k (10^{-3} h^{-1})	Conversion (%, after 40 h)
a	[Pt(OH_2)NCN](BF_4)	280	99
b	none	28	38
c	**1**	35	45
d	**2**	29	40
e	**1·3$_{1.3}$**	73	95
f	**2·3$_{2.4}$**	62	81

a) for conditions see experimental section.

Amphiphilic polyglycerols P($G_{25}C16_{0.5}$) and P($G_{106}C16_{0.6}$) without encapsulated catalyst do not result in a significant rate enhancement compared to the blank reaction (entries b,c,d).[12] The loaded nanocapsules **1·3$_{1.3}$** as well as **2·3$_{2.4}$** considerably increased the reaction rate compared to the blank reaction (entries e,f), albeit that the observed activity is lower than observed for the unsubstituted NCN-pincer platinum(II) complex (entry a). This may be due to the fact that the catalysts are shielded from the environment by the core of the nanocapsules, their fatty acid substituents preventing fast exchange of products and substrates. Interactions between the hydroxyl groups of the polyglycerol core and the platinum cation can also render the catalyst less accessible for the coordination of ethyl cyanoacetate. The catalytic activity of **1·3$_{1.3}$** and **2·3$_{2.4}$** supports the finding that **3** is dehalogenated in 0.5M NaOH, prior to the encapsulation, since the halide platinum(II) pincers are not Lewis acidic and not active in the Michael addition.[13] Due to the size of the nanocapsules, we were able to separate the products from the encapsulated catalysts by dialysis, and recover >97% of the catalytic material.[14] These results shows the suitability of the presented hyperbranched systems as catalyst carriers in continuous membrane reactors.[15]

6.3. Conclusion

In conclusion, hydrophilic NCN-pincer platinum(II) complexes have been encapsulated in amphiphilic nanocapsules based on hyperbranched polyglycerols, possessing a reverse micelle-type architecture. The loading of the pincer complexes in the nanocapsules depends on the molecular weight of the hyperbranched polymer as well as on the functionality of the pincer. The incorporated platinum(II) complexes show catalytic activity in a double Michael addition, albeit with decreased activities compared to the parent NCN-pincer complex. To our knowledge this is the first example of the use of a hyperbranched polymer-based micro-environment for homogenous catalysis in a non-covalent strategy. This strategy is also promising with respect to the application of catalysts in a membrane reactor set-up.

6.4. Experimental

General

All solvents were distilled from and stored over molsieves (4Å) under a dry nitrogen or argon atmosphere. All other reagents were obtained commercially and were used without further purification. Elemental Analyses were performed by Kolbe, Mikroanalytisches Laboratorium (Müllheim, Germany). ^{1}H and $^{13}C\{^{1}H\}$ NMR spectra were recorded on a Varian Inova 300 spectrometer (operating at 300 and 75 MHz respectively) or a Varian Mercury 200 spectrometer (operating at 200 and 50 MHz respectively). Spectra were recorded in chloroform-d or benzene-d_6 at room temperature, unless stated otherwise, and were referenced to TMS (δ = 0.00 ppm). The syntheses of NCN-platinum complexes **3** and **4** is described in chapter 2.

*Synthesis of nanocapsules **1** and **2**.*

Partially esterified polyglycerols P($G_{25}C16_{0.5}$) (**1**) and P($G_{106}C16_{0.6}$) (**2**) were prepared as followed: To a pyridine solution (80 mL) of hyperbranched polyglycerol (DP_n= 25; 1.52 g; 20.51 mmol of OH groups), was added dropwise a toluene solution (100 mL) of palmitoyl chloride (3.6 mL; 12 mmol) at 80°C within 1h. The mixture was refluxed for 20h at 130°C. A stoichiometric amount of $NaHCO_3$ (10.28 mmol; 1.03 g) was added to the cold solution and most of the volatiles were removed in vacuo. Residual pyridine was removed by azeotropic distillation in 100 mL of toluene. The remaining solution was filtered and concentrated in vacuo. The residue was washed several times with ethyl acetate to remove traces of free palmitoyl carboxylic acid and was further purified by dialysis (MWCO 1000) in $CHCl_3$. The polymer was obtained as a white solid.

Polymer P($G_{25}C16_{0.5}$) (1): Yield 85%. ^{1}H NMR ($CDCl_3$): 0.81 (t, $\underline{CH_3}$), 1.11-1.25 (br , 24H, $\underline{CH_2}$), 1.53 (m, $COCH_2\underline{CH_2}$), 2.24-2.28 (m, CH_2, $\underline{CH_2}CO$), 3.44-4.03 (br , 5H, glycerol moiety), 5.04 (br, OH). ^{13}C NMR ($CDCl_3$): 14.08, 22.66, 24.88, 29.16, 29.51, 29.64, 31.90, 34.10, 65.12, 68.65, 69.81, 70.16, 173. IR (NaCl) υ= 1738.43 (C=O), 3441.81 (O-H). α (Degree of substitution per hydroxyl group)= 50%; M_n= 5,230; M_w/M_n= 1.2.

Polymer P($G_{106}C16_{0.6}$) (2): Dried hyperbranched polyglycerol (DP_n=106; 10g, 134.95 mmol of OH groups) and palmitoyl chloride (24.54 mL; 80.97 mmol) were reacted following the same procedure as polymer **1**, to give polymer P($G_{106}C16_{0.6}$), **2** as a white solid. Yield: 90%. ^{1}H NMR ($CDCl_3$): 0.84 (t, CH_3), 1.21 (br, 24H, CH_2), 1.57 (m, 2H, $\underline{CH_2}CH_2CO$), (m, 2H, $\underline{CH_2}CO$), 2.26-2.3 (m, CH_2, CH_2CO), 3.52-4.07 (br , 5H, glycerol), 5.10 (br, OH). ^{13}C NMR ($CDCl_3$): 14.10, 22.67, 24.94, 29.13, 29.43, 29.66, 31.91, 34.10, 65.12, 68.65, 69.81, 70.16, 173. IR (NaCl)= 1636.76 (C=O), 3388.06 (O-H). α (Degree of substitution per hydroxyl group)= 60%; M_n= 23506; M_w/M_n= 1.3.

UV/Vis-titrations

Solutions of **3** and **4** in aqueous 0.5 M NaOH were prepared in concentrations ranging from 10^{-5}-10^{-4} M. Nanocapsules **1** and **2** were dissolved in dichloromethane with concentrations in the range of 10^{-5} M. In a typical UV/Vis experiment, 3 mL of the aqueous solution was mixed thoroughly for 1 hour with 3 mL of the dichloromethane solution. The phases were allowed to settle completely en were subsequently separated and both analysed by UV/Vis-spectroscopy.

*Loading of Nanocapsules **1** and **2***

Equivolumetric amounts (50 mL) of an aqueous solution of **3** (5.0 mM, 0.5 M NaOH) and dichloromethane solutions of **1** (3.3 mM) or **2** (0.6 mM) were mixed vigorously for 30 minutes. The phases were allowed to settle overnight and subsequently separated. The organic phase was dried over $MgSO_4$, filtered and dried *in vacuo* to obtain the loaded nanocapsules as yellowish solids in near quantitative yields. **1·3$_{1.3}$**: ^{1}H NMR ($CDCl_3$): 0.83 (t, $\underline{CH_3}$), 1.24 (br, $\underline{CH_2}$), 1.58 (br. m, $COCH_2\underline{CH_2}$), 2.28 (br. m, CH_2, $\underline{CH_2}CO$), 3.00-3.18 (NMe_2 pincer), 3.40-4.13 (br, glycerol moiety), 4.01 (CH_2N pincer), 5.04 (br, OH). 7.60 (ArH pincer); ^{13}C NMR ($CDCl_3$): 174.0-173.0, 123.4, 119.4, 80.0-78.0, 74.0-68.0, 66.0-63.0, 54.6, 34.5, 32.1, 30.0-29.0, 25.1, 22.9, 14.3; Elem. Anal.: C 65.64, H 10.37, Pt 4.45. **2·3$_{2.4}$**: ^{1}H NMR ($CDCl_3$): 0.84 (t, $\underline{CH_3}$), 1.24 (br, $\underline{CH_2}$), 1.59 (br. m, $COCH_2\underline{CH_2}$), 2.29 (br. m, CH_2, $\underline{CH_2}CO$), 3.00-3.20 (NMe_2 pincer), 3.40-4.20 (br, glycerol moiety), 4.01 (CH_2N pincer), 5.06 (br, OH). 7.62 (ArH pincer); ^{13}C NMR ($CDCl_3$): 174.0-173.0, 143.5, 123.4, 119.4, 80.0-78.0, 74.0-68.0, 66.0-63.0, 54.6, 34.5, 32.1, 30.0-29.0, 25.1, 22.9, 14.3; Elem. Anal.: C 64.52, H 10.63, Pt 3.25.

Double Michael Addition

General conditions for the double Michael addition:1.6 mmol ethyl cyanoacetate, 4.8 mmol methyl vinyl ketone, 0.16 mmol EtN^iPr_2, 1 mol% catalyst based on its platinum content, 5 ml CH_2Cl_2, room temperature. The reaction was followed by ^{1}H-NMR, and the products were characterized by ^{1}H-NMR and GC-MS. Lewis acidic palladium(II) and platinum(II) pincer complexes of the type $[M(OH_2)NCN](BF_4)$ can be applied as catalyst in aldol-type reactions.

6.5. References and Notes

1. (a) Hecht, S.; Fréchet, J. M. J. *Angew. Chem. Int. Ed. Engl.* **2001**, *40*, 74-91. (b) Crooks, R. M.; Zhao, M.; Sun, L.; Chechik, V.; Yeung, L. K. *Acc. Chem. Res.* **2001**, *34*, 18. (c) Fischer, M.; Vögtle, F. *Angew. Chem. Int. Ed. Engl.* **1999**, *38*, 884. (d) Newkome, G. R.; He, E.; Moorefield, C. N. *Chem. Rev.* **1999**, *99*, 1689 (e) Bosman, A. W.; Janssen, H. M.; Meijer, E. W. *Chem. Rev*. **1999**, *99*, 1665. (f) Zeng, F. W.; Zimmerman, S. C. *Chem. Rev*. **1997**, *97*, 1681. (g) Tomalia, D. A.; Durst, H. D. *Top. Curr.*

Chem. Weber, E., Springer-Verlag: Berlin, **1993**; Vol. 165, p 193. (h) Newkome, G. R.; Moorefield, C. N.; Vögtle, F. *Dendrimers and Dendrons*; WILEY-VCH: Weinheim, **2001.**

2. (a) Kreiter, R.; Kleij, A. W.; Klein Gebbink, R. J. M.; van Koten, G., *Top. Curr. Chem.* **2001**, *217*, 163 (b) Oosterom, G. E.; Reek, J. N. H.; Kamer, P. C. J.; van Leeuwen, P. W. N. M. *Angew. Chem., Int. Ed. Engl.* **2001**, *40*, 1828. (c) Hearshaw, M. A.; Moss, J. R. *Chem. Commun*. **1999**, 1. (d) Mecking, S.; Thomann, R.; Frey, H.; Sunder, A., *Macromolecules* **2000**, *33*, 3958.
3. (a) Voit, B. I. J. *Polym. Sci., Polym. Chem.* **2000**, 38, 2505. (b) Kim, Y. H. J. *Polym. Sci., Polym. Chem.* Ed. **1998**, 36, 1685. (c) Flory, P. J. *J. Am. Chem. Soc.* **1952**, 74, 2718. Conceptual overview: (d) Sunder, A.; Heinemann, J.; Frey, H. *Chem. Eur. J.* **2000**, 6, 2499.
4. Sunder, A.; Hanselmann, H.; Frey, H.; Mülhaupt, R. *Macromolecules* **1999**, *32*, 4240.
5. (a) Sunder, A.; Krämer, M.; Hanselmann, R.; Mülhaupt, R.; Frey, H. *Angew. Chem.* **1999**, *111*, 3758; *Angew. Chem. Int. Ed. Engl.* **1999**, *38*, 3552; (b) Haag, R.; Stumbé, J.-F.; Sunder, A.; Frey, H.; Hebel, A. *Macromolecules* **2000**, *33*, 8158.
6. For a recent overview on pincer chemistry: Albrecht, M.; van Koten, G. *Angew. Chem. Int. Ed. Engl.* **2001**, *40*, 3750.
7. Pincer complexes from the nickel triad (Ni, Pd, Pt) are applicable as catalyst in various carbon-carbon coupling reactions, such as the Kharasch addition, the Heck reaction and aldol condensations.
8. Nomenclature $P(G_xCY_z)$: x= DP_n of polyglycerol, Y: number of carbon atoms of the palmitoyl acid, z: degree of alkyl substitution per hydroxyl group.
9. Stiriba, S.-E.; Kautz, H.; Frey, H. *J. Am. Chem. Soc.* **2002**, *124*, 9698-9699.
10. For pK_a studies on platinum pincer aqua complexes: Schmülling, M.; Grove, G. M.; van Koten, G.; van Eldrik, R.; Veldman, N.; Spek, A. L. *Organometallics* **1996**, *15*, 1384-1391.
11. Stiriba, S.-E.; Kautz, H.; Frey, H. *J. Am. Chem. Soc.* **2002**, *124*, 1698-1699.
12. Neat dichloromethane, shaken thoroughly with an aqueous solution of **3**, was also not catalytically active in the double Michael addition.
13. In a control experiment, the encapsulated pincer systems were treated with AgBF4, which is a normal procedure for dehalogenation. The resulting materials did not show significant rate enhancements compared to **1·3$_{1.3}$** and **2·3$_{2.4}$**.
14. Benzoylated dialysis tubing (D-7884 Sigma) in dichloromethane/methanol 95/5, overnight stirring at room temperature has been used.
15. Catalyst recycling by nanofiltration techniques: a) Dijkstra, H. P.; van Klink, G. P. M.; van Koten, G. *Acc. Chem. Res.* **2002**, *35*, 798-810; b) Kragl, U. *Industrial Enzymology,* 2nd ed (Eds.: Godfrey, T.; West, S.), Macmillan, Hampshire, **1996**, 275-283 and references cited therein.

Chapter Seven

Synthesis and Visualization of Immobilized NCN-Pincer Platinum(II) Complexes on Hyperbranched Polyglycerol supports

Abstract

Pertosylation of hyperbranched polyglycerol (M_n= 2000; M_w/M_n = 1.3) followed by partial displacement of the tosyl groups with carboxylic acid functionalized NCN-pincer platinum(II) complexes [PtI-2,6-$(CH_2NMe_2)_2C_6H_2$-4-COOH], results in covalent attachment of the NCN-pincer complexes to the polyglycerol. These functionalized hyperbranched macromolecules were characterized by ^{1}H-, ^{13}C- ^{195}Pt-NMR, UV/Vis and IR spectroscopy. The presence of Pt and I atoms renders them directly visible by TEM without staining procedures, offering the first images of hyperbranched macromolecules. TEM micrographs show disk-shaped structures with a small size distribution (15-20 nm) and characteristic core-shell ring structures. The thickness of the corona observed in TEM are correlated with the substitution degree with pincer platinum moieties.

7.1. Introduction

Immobilization of functional molecules on dendritic scaffolds - in either covalent or non-covalent fashion - has been a subject of intense research in the last decade.[1] Application of transition metal complexes in dendrimer chemistry, as building blocks or as functional moieties, has attracted specific interest.[2] Dendrimers and hyperbranched polymers functionalized with catalytically active transition metal complexes are promising with respect to catalyst recovery.[3] Furthermore, they are interesting for the design of materials with new optical or electrochemical properties as well as for diagnostic applications in medicine.[4] Since dendrimers have to be prepared in tedious multistep syntheses, which is a limiting factor for most (large scale) applications, hyperbranched polymers offer a promising alternative.[5] These hyperbranched polymers are obtained in a one-pot synthesis from branched AB_m-type monomers, resulting in a randomly branched globular polymeric structure with a broad molecular weight distribution.[5a-e] Important recent progress in this field has been made with the development of slow monomer addition strategies, allowing control over the molecular weights of the polymers, determined by the monomer to initiator ratio. The anionic ring-opening multibranching polymerization (ROMBP) of glycidol results in a hyperbranched polyglycerol, which can be tailored in terms of core functionality and molecular weight.[6] The narrow polydispersity of these materials ($1.3<M_w/M_n<1.5$) as well as the flexibility of the chemically inert polyether structure allows further specific functionalization of the polyglycerol.[7] To date, there are only few reports on the attachment of catalytically active transition metal complexes to hyperbranched polymers.[1c] In previous work, an approach to hyperbranched polycarbosilanes functionalized with aryldiamine palladium (II) complexes has been established by us.[8] The soluble macromolecular multisite catalyst obtained was as catalytically active as its carbosilane dendrimer analogue, and suitable for continuous membrane applications.

Apart from being catalytically active compounds or sensor materials, organometallic NCN-pincer complexes (NCN-pincer = 2,6-bis[(dimethylamino)methyl]phenyl anion) are attractive building blocks since they can be prepared with various *para*-substituents as anchoring moieties for immobilization purposes (see Chapter 2).[9] Covalent introduction of these transition metal complexes is of interest in view of visualization and imaging of dendritic polymers by transmission electron microscopy (TEM). The electron rich metal ions in the polymer structure create enhanced contrast and should permit visualization of isolated polymer molecules.[10] To date, only few molecular images of dendritic macromolecules have been published, because their size range (2-10 nm for dendrimers) and non-contrasting organic composition renders resolution by TEM very difficult. Moreover, the application of

staining techniques to such small structures is not trivial.[11] Here, we report the synthesis of NCN-pincer platinum(II) substituted polyglycerols obtained via nucleophilic displacement of a tosylated polyglycerol by the potassium carboxylate of a platinated NCN-pincer precursor. The platinated hyperbranched polyglycerols have been studied by TEM and compared to shape-persistent multi NCN-pincer platinum complexes with respect to their size and structure.

7.2. Results

Synthesis

Tosylation of the hydroxyl groups of PG_{25} **1** (M_n= 2000; M_w/M_n = 1.3) was carried out at 80°C using two equivalents of *para*-tosyl chloride for each hydroxyl group, resulting in the pertosylated polyglycerol $P(G_{25}Tos_1)$ **2** (Scheme 1).[12] This compound was further purified by dialysis in chloroform. The purity as well as molecular weight were confirmed by ^{1}H-, $^{13}C\{^1H\}$-, IR, UV/Vis spectroscopy and elemental analysis. The tosylated material was, in contrast to the hydrophilic starting material, completely and homogenously soluble in apolar solvents.

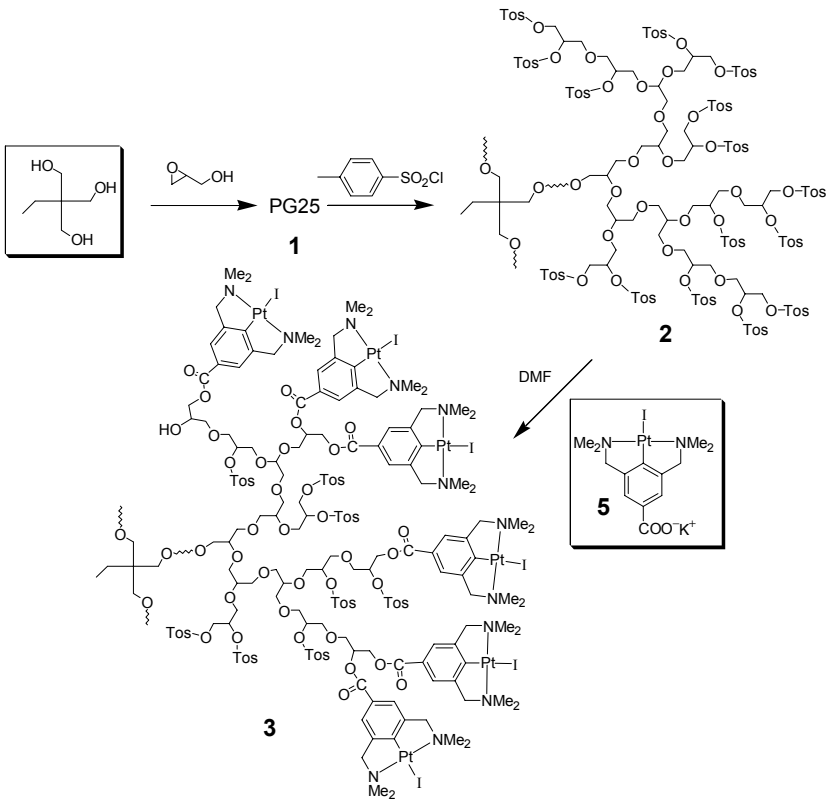

Scheme 1. Synthesis of the pertosylated hyperbranched polyglycerol **2** followed by partial substitution of its tosyl groups with NCN-pincer platinum(II) carboxylates to afford **3**.

Grafting of the NCN-pincer platinum(II) complexes was achieved by nucleophilic displacement of the tosylate groups by carboxylated NCN-platinum(II) complexes. The platinated NCN-pincer carboxylic acid **4**, reported in chapter 2, was deprotonated for this purpose by treatment with potassium *t*-butoxide (*t*-BuOK) in THF (Scheme 2). The potassium carboxylate **5** immediately precipitated from the solution.

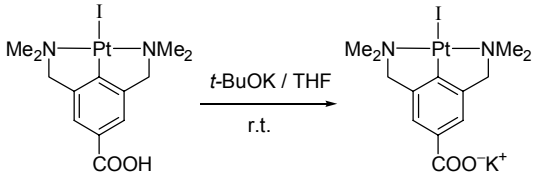

4 **5**

Scheme 2. Synthesis of the potassium carboxylate NCN-pincer platinum complex **5**.

Based on the number of tosylate groups per polyglycerol, which is approximately equal to its DP_n, we treated **2** with an excess of **5** in DMF at 80 °C (Scheme 1). Irrespective of the excess of **5** (10-100%) employed in the substitution reactions, only 50% of the available tosylate groups could be replaced by the organometallic carboxylate, affording the modified hyperbranched polymers **3** (Scheme 1). Organometallic polymer **3** is constructed from 25 monomer units, with 50% of its hydroxyl groups substituted by NCN-pincer platinum iodide units, and 50% remaining tosyl groups. Thus, each modified polyglycerol molecule contains on average 12.5 platinum sites and 12.5 tosylate groups. Unreacted **5** was removed from **3** by repeated liquid-liquid extractions with water, and subsequent dialysis (MWCO = 1000 D) against chloroform.

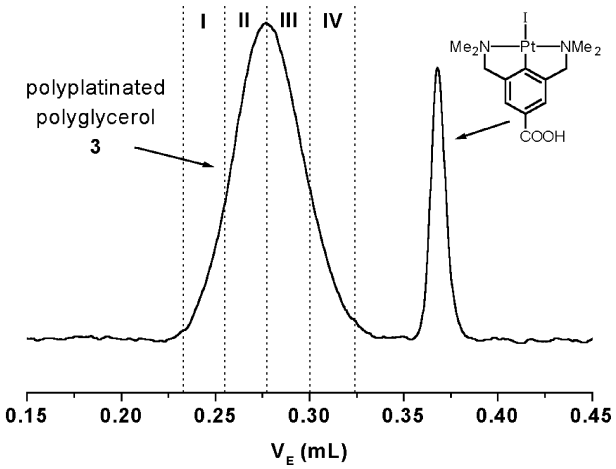

Figure 1. Preparative GPC traces of the separation and fractionalization of **3**.

Finally, separation by preparative SEC equipped with an UV/Vis monitor was performed in order to investigate the fractions of different molecular weight with respect to their degree of

NCN-pincer platinum substitution and visualization. The corresponding SEC diagram with the fractions sampled is shown in Figure 1. Apparently, both aqueous extractions, and dialysis of the crude coupling product were not sufficient to remove unreacted **5** completely.

The immobilized platinum(II) iodide complexes could be converted in their cationic aqua complexes by dehalogenation upon treatment with $AgBF_4$. The activity of dehalogenated **3**[13] in the double Michael addition of two equivalents of methyl vinylketone to ethyl cyanoacetate was tested as a model reaction. The observed reaction rate for macromolecule **3** ($191 \cdot 10^{-3}$ h^{-1}) was comparable to that of a non-immobilized pincer complex [$Pt(OH_2)NCN$](BF_4) ($280 \cdot 10^{-3}$ h^{-1}). Separation of products and catalyst **3** after full conversion was achieved conveniently by dialysis against neat dichloromethane. The catalytic material (7.3 mg, 0.65 μmol) was recovered in near quantitative yields (92%).

TEM characterization

TEM-images of the platinum(II) containing macromolecules (**5**) were obtained by depositing its dilute THF-solution on carbon-coated electron microscopy grids, followed by evaporation of the solvent. The presence of the platinum and iodine atoms in the hyperbranched materials renders them directly visible by TEM and leads to the possibility to study their shape and size distribution in more detail. Figure 2 gives the TEM image obtained for a sample of **5** prior to fractionation, showing the presence of particles in the size range of 10-25 nm.

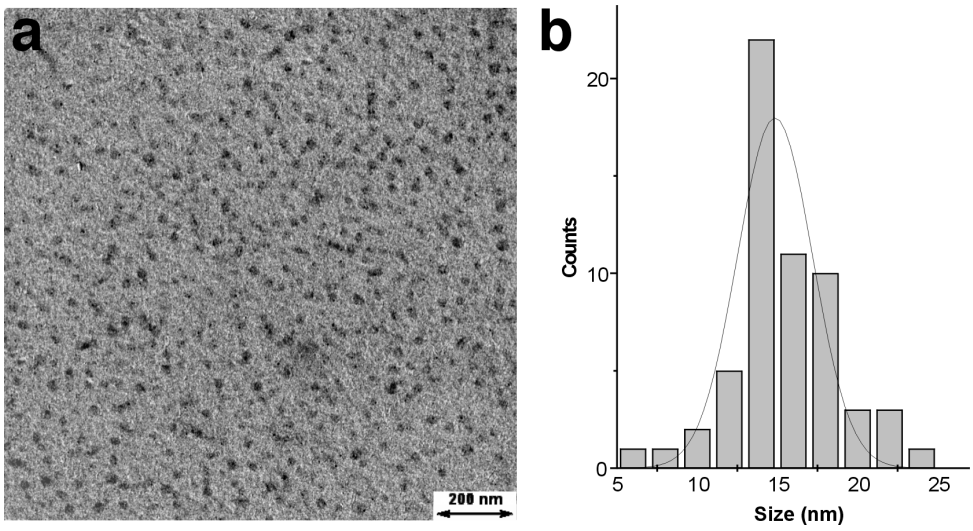

Figure 2. (a) TEM image of **3** before SEC fractionalization; (b) histogram of particle size distribution.

In order to obtain more detailed insight into the size and structure of the hyperbranched platinum(II)-loaded macromolecules, the fractions obtained from preparative SEC were

employed in the TEM studies.[14] Figures 3a and 3b show the non-contrasted images of two typical fractions (fraction II and fraction IV, see figure 1) of the hyperbranched polymers.

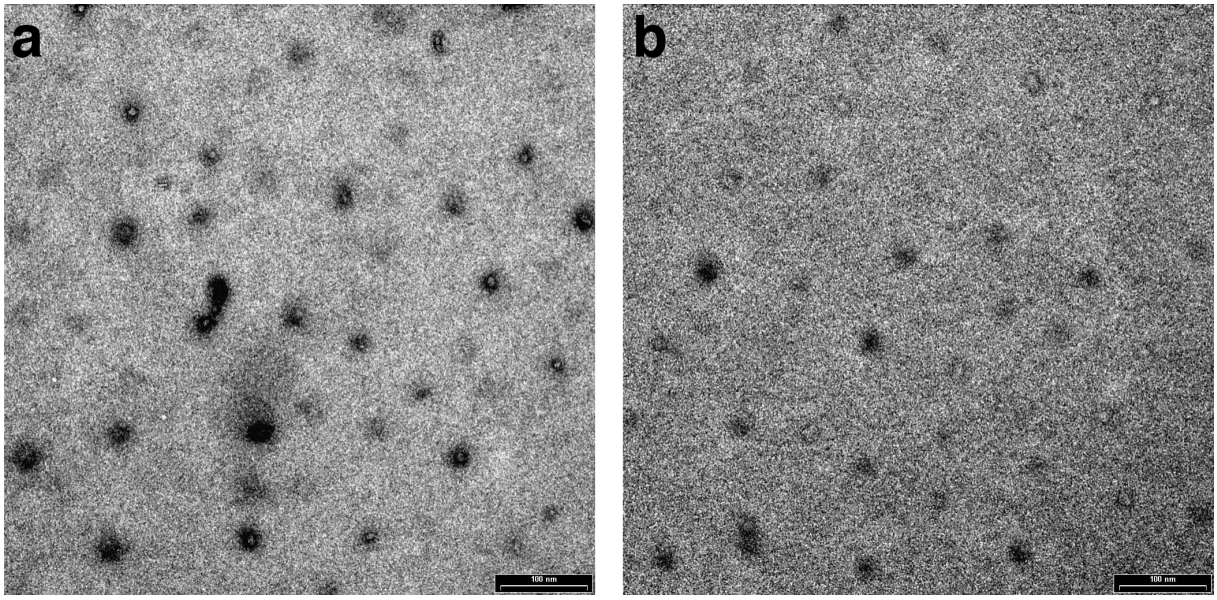

Figure 3. a) TEM image of fraction II after SEC; b) TEM image of fraction IV after SEC.

For comparison in the TEM studies, we chose the earlier reported[15] rigid dodeca-platinated NCN-pincer complex **6** (Chart 1). This complex has a calculated diameter of 3.2 nm (MM2-calculations) and is a single compound, in contrast to the hyperbranched polymers that possess small molecular weight distributions. A TEM-image of **6**, together with the corresponding size histogram is shown in Figure 4.

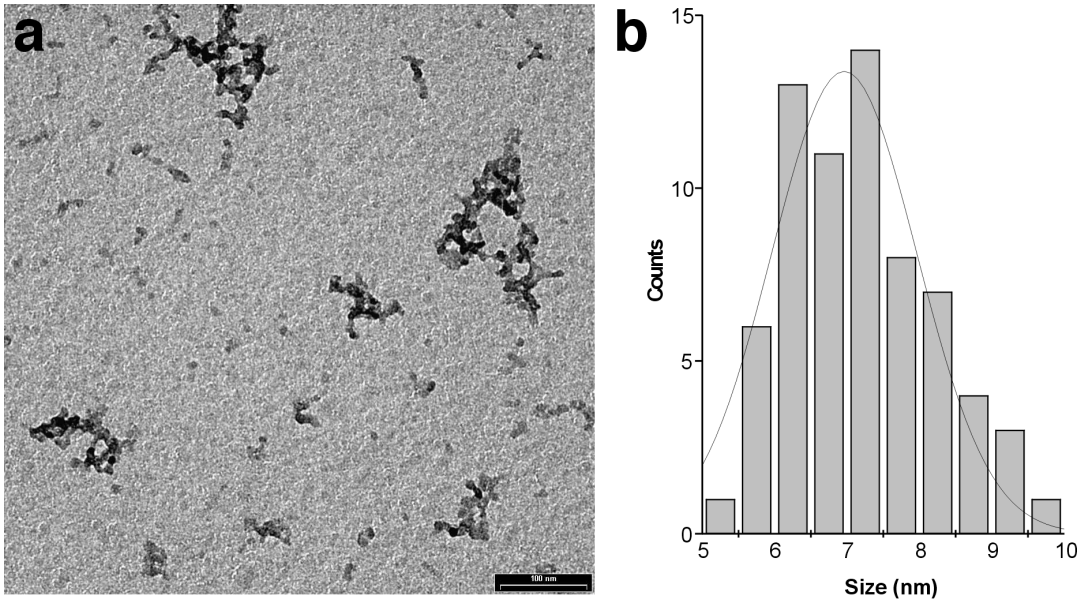

Figure 4. (a) TEM image of the dodecaplatinum(II) pincer **6**; (b) Histogram of particle size distribution.

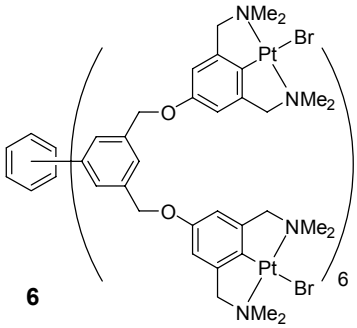

6

Chart 1. Structure of the dodecaplatinum (II) pincer dendrimer **6**.

7.3. Discussion

Synthesis

Hyperbranched polyglycerols possess terminal and internal hydroxyl groups, which can be functionalized *via* several routes.[7] Esterification with acyl chlorides in a mixture of pyridine/toluene affords the partially esterified polyglycerols that have been demonstrated to act as "nanocapsules" for the encapsulation of polar guest molecules (see Chapter 6).[7a] This direct substitution route turned out to be impractical for the introduction of the pincer complexes, since the corresponding acyl chloride of **4** could only be prepared in low yields, and had to be reacted with the polyglycerol under harsh reaction conditions. We therefore turned to an alternative strategy, *i.e.* the preparation of an activated polygylcerol derivative with easily displaceable tosyl groups. Surprisingly, substitution of the tosylate groups on **2** with **5**, did not result in the formation of a fully platinated polyglycerol polymer. No evidence was found for preferential substitution of either primary or secondary tosylate groups of the tosylated hyperbranched polyglycerols. We tentatively explain the incomplete substitution to excessive steric crowding of the bulky pincer system, preventing complete substitution.

^{1}H-, ^{195}Pt-NMR and UV/Vis Analysis

^{1}H-NMR spectra of **3** clearly demonstrate partial replacement of the tosylate groups by NCN-pincer platinum groups. While the intensity of the signals originating from the tosylate groups, located at 7.78, 7.36 ppm (ArH) and 2.45 ppm (CH_3) decreased, new signals appeared at 7.56 ppm (ArH), 4.07 ppm (CH_2N), and 3.19 ppm (NMe_2), typical of platinated NCN-pincer complexes. The degree of substitution was determined to be 50% by the relative intensity ratios of these signals. The $^{3}J_{Pt\text{-}H}$ couplings of **4** with the NMe_2 (28.8 Hz) and CH_2N (39.0 Hz) protons in the ^{1}H-NMR spectra, were not fully resolved in spectra of **3**, due to broadening of the signals caused by the immobilization on a polymeric support system. ^{195}Pt-NMR clearly showed the presence of one discrete platinum(II) site, originating from the immobilized NCN-pincer complexes as a single resonance at –1914 ppm. For comparison,

carboxylic acid **4** showed a singlet located at -1899 ppm in ^{195}Pt-NMR. UV/Vis spectroscopic analysis of tosylated polyglycerol **2** in chloroform showed an absorption band at 262 nm ($\varepsilon \approx 10^5$ M^{-1}). In UV/Vis spectra of **3** an additional band shows up at 324 nm ($\varepsilon \approx 10^5$ M^{-1}), originating from the NCN-pincer platinum moieties covalently linked to the polymer. For comparison, the NCN-pincer platinum carboxylate **4** has an absorption band located at 326 nm ($\varepsilon \approx 10^4$ M^{-1}). Furthermore, in UV/Vis-spectra of **2** and the polyplatinated polymer **3**, the shoulder of an additional absorption band with its maximum located below 225 nm was visible.

TEM characterization

In contrast to dendrimers, molecular images of single hyperbranched macromolecules have not yet been reported. The introduction of heavy atoms (Pt, I) on the polyglycerol backbone permits imaging of molecular or defined supramolecular structures of the materials by transmission electron microscopy (TEM) without staining procedures. The platinum(II) atoms are covalently bonded to the aryl carbon atom in the stabilizing coordination environment of the NCN-pincer ligand. This in turn is covalently connected to the polyglycerol backbone, thereby ensuring that the metal is attached to the hyperbranched polyglycerol support and cannot leach from the material without cleavage of the ester bond.

In the TEM image of **3** (Figure 2) prior to fractionation by SEC the functionalized hyperbranched polymers appear as dark spots in the range of 21-30 nm. Since the size of single hyperbranched macromolecules is expected to be in the range of 5-10 nm based on molecular modeling (MM2) of their three dimensional structures, these metal rich particles must be agglomerates of the macromolecules, not unimolecular species. Size exclusion chromatography revealed that this sample still contained unreacted **5**, which is expected to be accomodated in the polyglycerol core of the hyperbranched polymeric aggregates, based on the difficulty of its removal by dialysis and repeated washings with aqueous solutions. The TEM-images of the SEC fractions II and IV (Figures 3a and 3b) show particles of varying size with, in many cases, an unusual core-shell type substructure with lighter cores and darker coronas. In view of the lower size of the single hyperbranched molecule, we interpret the core-shell structures as micellar aggregates of the amphiphilic functionalized hyperbranched polymers. Whether these aggregates are disk shaped or globular cannot be concluded based on the TEM results. Furthermore, the agglomerates can be flattened out as a result of the TEM sample preparation and do not necessarily represent their structure in solution. The observed core-shell separated structure can be attributed to differences in polarity between the polyglycerol backbone and the NCN-pincer platinum(II) moieties. In the less contrasting core of the structures only the polyether-scaffold is present, while in the dark corona of the core-

shell assemblies the NCN-pincer platinum(II) complexes dominate. An intuitive two-dimensional model that can account for the orbserved core-shell separated structure is given in Scheme 3. Alternatively, a similar three-dimensional aggregate can be envisaged.

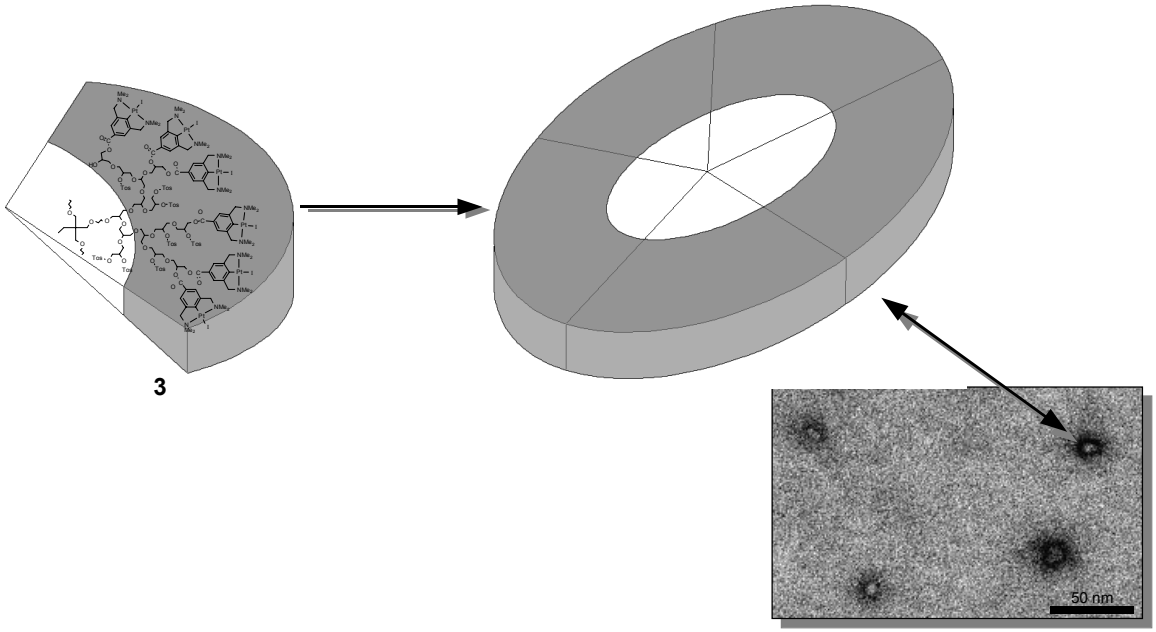

Scheme 3. A speculative model for the formation of two-dimensional supramolecular aggregates of **3** to explain the observed TEM images.

An additional feature shown in Figures 3a and 3b is the increase in the size of the dark corona for the higher molecular weight fractions. The TEM image of Fraction II (Figure 3a) shows dense coronas, while for the lower molecular weight fraction IV (Figure 3b) less contrasted coronas are observed. The molecular weight of the functionalized polyglycerol (molecular weight of **2** amounts to 5800 D) is highly dependent on the substitution degree with the relatively heavy NCN-pincer complexes (molecular weight of **5** equals 557.3). The thickness of the corona can thus be correlated with the substitution degree on the polyglycerol. With an increase in substitution degree, the size of the NCN-pincer platinum(II) rich corona increases. In order to rationalize the behaviour of NCN-pincer platinum species in TEM studies, a previously described NCN-pincer platinum loaded scaffold **6** was also investigated. The TEM image of **6** (Figure 4a) shows this dodeca-platinated NCN-pincer species as roughly spherical dark spots, that in certain cases assemble to irregular shaped aggregates. This irregular aggregation most likely has to be attributed to TEM sample preparation. The particle size of the individual black dots, as can be deduced from the histogram (Figure 4b), is in the range of 5-10 nm. As shown in Figure 4, no core-shell type supramolecular organization similar to **3** is observed. Both TEM studies show clearly that the NCN-pincer platinum species can be

applied conveniently for the imaging of small (dendritic) molecules by TEM without the necessity of staining procedures. The broad range of available *para*-substituted NCN-pincer complexes (see chapter 2) makes their (covalent) attachment to virtually any (organic) scaffold feasible, allowing electron microscopic studies.

7.4. Conclusion

Activation of hyperbranched polyglycerols *via* tosylation was found to be an efficient method to produce suitable starting materials for further functionalisation. In fact, nucleophilic displacement of the tosyl groups by NCN-pincer platinum(II) carboxylates (**5**) gives excess to a new poly-organometallic polyglycerol polymer **3** with discrete platinum(II) sites. The presence of the covalently bound heavy atoms platinum and iodine in this poly-organometallic material, allowed their direct visualization by TEM without the necessity of staining techniques, showing core-shell type aggregates. To the best of our knowledge, this is the first time that transition metal complexes have been linked to a hyperbranched polyether backbone and TEM has been applied to study the size and shape of individual hyperbranched polyglycerol molecules.

7.5. Experimental Section

General

All the reactions were performed under an inert Argon atmosphere. Polyglycerol **1** (DP_n= 25, M_n = 2000, M_n/M_w = 1.3) was prepared as reported previously,[6a] using trimethylpropane (TMP) as initiator. NCN-pincer platinum complex **4** and the dodecaplatinum(II) pincer dendrimer **6**[15] were prepared according to literature procedures. Pyridine was distilled from KOH, toluene and DMF were distilled from calcium hydride; all other solvent were used without further purification. *p*-Tosyl chloride and *t*-butoxide potassium were purchased from Aldrich. Benzoylated cellulose tubing for dialysis (MWCO = 1000 D) was obtained from SIGMA. ^{1}H NMR and ^{13}C{^{1}H} NMR spectra were obtained from solutions in $CDCl_3$ on a Bruker ARX 300 spectrometer operating at 300 and 75.4 MHz, respectively. ^{159}Pt{^{1}H} NMR spectra were measured using a Varian Inova 300 from solutions in $CDCl_3$. IR spectra were recorded on a Bruker Vector 22 spectrophotometer, using thin polymer films on KBr disks. UV/Vis spectra were carried out on a Perkin-Elmer Lambda 2 spectrophotometer. Preparative GPC was carried out on MZ-Gel Sd*plus* column (250 x 40 mm) using analytical tetrahydrofuran as eluent. Separation of samples using a variable wavelength monitor at 320 nm with a flow of 5mL/mn.

TEM Measurements

TEM analysis were carried out on a LEO 912 Omega apparatus using an acceleration voltage of 120 kV. Samples were prepared by applying a drop of the THF solvated organometallic macromolecule **3** to a carbon-coated grid, followed by drying of the sample in air. Samples were not stained.

Tosylated Polyglycerol **2**

To a solution of dried hyperbranched polyglycerol (DP_n= 25) **1** (5 g, 67.5 mmol of OH groups) in pyridine (100 mL) was added dropwise a solution of *p*-toluene sulfonic acid chloride (25.7 g, 135 mmol) in pyridine (150 mL) at 50°C. The resulting mixture was stirred at 80°C for 3h. After cooling to room temperature chloroform (200 mL) was added and the solution was poured on a mixture of ice and 100 mL of 10N HCl solution. The organic layer was separated, washed three times with water and dried over Na_2SO_4. The product was transferred to benzoylated cellulose tubing for dialysis in chloroform overnight. Chloroform was removed under vacuum pressure and the product was dried under vacuum, yielding a yellowish oil (70%). ^{1}H NMR (300 MHz, $CDCl_3$): δ = 1.19 (t, 3H, CH_3, initiator TMP), 2.32 (s, 3H, CH_3, tosylate), 2.34 (s, 3H, CH_3, tosylate), 3.37-3.95 (m, br, polyether scaffold), 3.97-4.04 (q, 2H, CH_2, initiator TEM), 4.45-4.58 (m, br, polyether scaffold), 7.23-7.26 (m, 4H, tosylate), 7.64-7.70 (m, 4H, tosylate). ^{13}C{^{1}H} NMR (75.4 MHz, $CDCl_3$): δ = 14.5 (CH_3, TEM), 21.5 (CH_3, tosylate), 66.7, 67.1, 67.26, 68.0, 68.7, 69.7, 71.4, 77.2, 77.4, 127.6, 128.5, 129.8, 132.0, 132.5, 132.8, 132.9, 133.1, 133.6, 139.2, 143.4, 144.5, 144.8, 145.1. IR (KBr) υ (cm^{-1}) = 1595 (C─H aromatic), 1494 (C─H aromatic), 1453 (C─H sat), 1420-1330 (S═O), 1200-1145 (S═O), 1170 (C─O). UV/Vis ($CHCl_3$): λ_{max} = 334 nm. Anal. Calcd: C, 52.38; H, 5.71; S, 13.98 %. Found: C, 52.33; H, 5.15, S, 12.85 %.

Synthesis of pincer complex ***5***

To a solution of **4** (0.50 g, 0.90 mmol) in THF (50 mL) was added a stoichiometric amount of KO*t*Bu (0.10 g, 0.90 mmol) in THF (20 mL) at once. A solid precipitated immediately upon addition. The product was isolated by centrifugation and washed twice with THF (15 mL), to afford **5** as an off-white solid. The solid was applied directly in the substitution reactions with the tosylated polyglycerols.

Synthesis of poly-organometallic polyglycerols ***3***

To a solution of the tosylated polyglycerol (0.2-0.5 g) in DMF (20 mL) was added **4** (1.1-2.0 equivalents per DP_n) at once. The solution was heated at 80 °C for 16 hours, followed by removal of all volatiles *in vacuo*. The brownish residue was redissolved in dichloromethane and washed twice with NaOH (1M) and with brine. The solution was dried over $MgSO_4$,

concentrated to 5 mL, filtered over Celite, and dialyzed against neat dichloromethane (250 mL) to afford a brownish solid. The product was then dissolved in THF and purified with preparative GPC using THF as eluent. A yellow fraction was first isolated which correspond to compound **5** with 50% tosylated and 50% substituted with **4** (50%). the second fraction was discarded, since it corresponded to free platinum pincer complex **4**. (**3**): M_n= 10541; ^{1}H NMR (300 MHz, $CDCl_3$) δ = 2.41 (3H, CH_3 tosylate), 3.19 ppm (12H, NMe_2 pincer), 4.07 (4H, CH_2N pincer), 5.4-3.0 (m, PG), 7.32 (2H, ArH tosylate), 7.56 ppm (2H, ArH pincer), 7.77 (2H, ArH tosylate). $^{13}C\{^1H\}$ NMR (75.4 MHz, $CDCl_3$) δ = 130.2, 155.0, 144.1, 127.9, 125.2, 120.1, 77.3, 81-78, 74-68, 55.1, 42.7. $^{159}Pt\{^1H\}$ NMR (64.4 MHz, $CDCl_3$) δ = –1914. IR (KBr) υ (cm^{-1})= 1720 (C═O), 1420-1330 (S═O). UV/Vis ($CHCl_3$): λ_{max} = 262, 324 nm.

Conditions for double Michael addition

To a solution of 4.8 mmol methyl vinyl ketone, 0.16 mmol Et*i*Pr_2N, and 1 mol% catalyst based on its [Pt] content (12.5 sites for **3**) in 5 ml CH_2Cl_2 was added 1.6 mmol ethyl cyanoacetate at once. The mixture was stirred at room temperature, and 100 µL aliquots for ^{1}H-NMR-analysis were taken in the course of the reaction. After full conversion **3** was recovered from the product mixture by dialysis against neat dichloromethane (250 mL) for 48 hours. The catalytic materials and products were recovered separately in near quantitative yields (92%).

7.6. References and Note

1. For comprehensive reviews on dendrimers see: a) J. M. J. Fréchet, *Science* **1994**, *263*, 1710-1715; b) F. Zeng, S. C. Zimmerman, *Chem. Rev.* **1997**, *97*, 1681-1712; c) H. Frey, C. Lach, K. Loranz, *Adv. Mater.* **1998**, *10*, 279-293; d) *Dendrimers I-IV* (Ed. F. Vögtle), *Top. Curr. Chem.* **1998**, *197*, 1-228; **2000**, *210*, 1-308; **2001**, *212*, 1-194; **2001**, *217*, 1-238; e) A. W. Bosman, H. M. Hanssen, E. W. Meijer, *Chem. Rev.* **1999**, *99*, 1665-1689; f) G. R. Newkome, C. N. Moorefield, F. Vögtle, *Dendritic Molecules: Concepts, Syntheses, Perspectives*, VCH, Weinheim, **2001**; g) S. M. Garyson, J. M. J. Fréchet, *Chem. Rev.* **2001**, *101*, 3819-3867;
2. For specific reviews on metallodendrimers, see: a) E. C. Constable, *Chem. Commun*. **1997**, 1073-1080; b) G. R. Newkome, E. He, C. N. Moorefield, *Chem. Rev.* **1999**, *99*, 1689-1746; c) M. A. Hearshaw, J. R. Moss, *Chem. Commun.* **1999**, 1-8; (c) H.-J. van Maanen, F. C. J. M. van Veggel, D. N. Reinhoudt, *Top. Curr. Chem.* **2001**, 121-162; (d) R. Kreiter, A. W. Kleij, R. J. M. Klein Gebbink, G. van Koten, *Top. Curr. Chem.* **2001**, *217*, 163-199; (e) G. E. Oosterom, J. N. H. Reek, P. C. J. Kamer, P. W. N. M. van Leeuwen, *Angew. Chem. Int. Ed.* **2001**, *40*, 1828-1849; Astruc, D.; Chardac, F. *Chem. Rev.* **2001**, *101*, 2991-2023; For reports on non-covalent incorporation of catalytically active metal complexes, see: f) van de Coevering, R.; Kuil, M.; Klein Gebbink, R. J. M.; van Koten, G. *Chem. Commun.* **2002**, 1636-1637; g) D. de Groot, B. F. M. de Waal, J. N. H. Reek, A. P. H. J. Schenning, P. C. J. Kamer, E. W. Meijer, P. W. N. M. Leeuwen, *J. Am. Chem. Soc.* **2001**, 123, 8453; and chapter 6 of this thesis; for

encapsulation of zerovalent metal particles, see: h) R. M. Crooks, M. Zhao, L. Sun, V. Chechik, L. K. Yeung, *Acc. Chem. Res.* **2001**, *34*, 18 and references cited therein.

3. a) H. P. Dijkstra; G. P. M. van Klink; G. van Koten, *Acc. Chem. Res.* **2002**, in press; b) M. Albrecht, N. J. Hovestad, J. Boersma, G. van Koten, *Chem. Eur. J.* **2001**, 7, 1289-1294 c) Kragl, U. *Industrial Enzymology,* 2nd ed (Eds.: Godfrey, T.; West, S.), Macmillan, Hampshire, **1996**, 275-283.
4. (a) M. Venturi, S. Serroni, A. Juris, S. Campagna, V. Balzani, *Top. Curr. Chem.* **1998**, *197*, 193; (b) M. Fischer, F. Vögtle, *Angew. Chem.* **1999**, *111*, 934-955; *Angew. Chem. Int. Ed.* **1999**, *38*, 884-905; (c) S. Hecht, J. M. J. Fréchet, *Angew. Chem. Int. Ed.* **2001**, *40*, 74; (d) S.-E. Stiriba, F. Holger, R. Haag, *Angew. Chem.* **2002**, *114*, 1385-1390; *Angew. Chem. Int. Ed.* **2002**, *41*, 1329-1334.
5. a) P. J. Flory, *J. Am. Chem. Soc.* **1952**, *74*, 2718; b) M. Jikei, M. Kakimoto, *Prog. Polym. Sci.* **2001**, *26*, 1233; c) Y. H. Kim, *J. Polym. Sci., Polym. Chem. Ed.* **1998**, *36*, 1685; d) B. I. Voit, *J. Polym. Sci., Polym. Chem.* **2000**, *38*, 2505; e) A. Sunder, J. Heinemann, H. Frey, *Chem. Eur. J.* **2000**, *6*, 2499; f) L. J. Markoski, J. S. Moore, I. Sendijarevic, A. J. McHugh, *Macromolecules* **2001**, *34*, 2695.
6. a) A. Sunder, R. Hanselman, H. Frey, R. Mülhaupt, *Macromolecules* **1999**, *32*, 4240-4246; b) A. Sunder, R. Mülhaupt, R. Haag, H. Frey, *Macromolecules* 2000, *33*, 253-254; c) A. Sunder, H. Türk, R. Haag, H. Frey, *Macromolecules* 2000, *33*, 7682-7692.
7. a) A. Sunder, M. Krämer, R. Hanselmann, R. Mülhaupt, H. Frey, *Angew. Chem.* **1999**, *111*, 3758; *Angew. Chem. Int. Ed.* **1999**, *38*, 3552-3555; b) A. Sunder, M.-F. Quincy, R. Mülhaupt, H. Frey, *Angew. Chem., Int. Ed.* **1999** , *38* , 2928; c) R. Haag, J.-F. Stumbé, A. Sunder, H. Frey, A. Hebel, *Macromolecules* **2000**, *33*, 8158-8166; for a general overview, see: d) A. Sunder, R. Mülhaupt, R. Haag, H. Frey, *Adv. Mater.* **2000**, 12, 235-239
8. C. Schlenk, A. W. Kleij, H. Frey, G. van Koten, *Angew. Chem. Int. Ed.* **2000**, *39*, 3445-3447.
9. For key publications on NCN-pincer chemistry see: (a) M. Albrecht, G. van Koten, *Angew. Chem., Int. Ed.*, **2001**, *40*, 3750-3781; (b) P. Steenwinkel, R. A. Gossage, G. van Koten, *Chem. Eur. J.* **1998**, *4*, 759. (c) R. A. Gossage, L. A. van de Kuil, G. van Koten, *Acc. Chem. Res*. **1998**, *31*, 423; (d) M. H. P. Rietveld, D. M. Grove, G. van Koten, *New J. Chem*. **1997**, *21*, 751; (e) G. van Koten, *Pure & Appl. Chem*. **1989**, *61*, 1681.
10. Earlier accounts on the concept of direct observation of linear polymer molecules involving platinum, see: a) M. J. Richardson, *Proc. R. Soc. London, A.* **1964**, *279*, 50; b) L. C. Sawyer, D. T. Grubb, *Polymer Microscopy*, Chapman and Hall: London, **1987**; c) D. A. Tomalia, A. M. Naylor, W. A. Goddard, *Angew. Chem. Int. Ed. Engl*. **1990**, 29, 138.
11. Reports on the visualization of dendrimers with TEM technique: a) D. A. Tomalia, H. Baker, J. Dewald, M. Hall, G. Kallos, S. Martin, J. Roeck, J. Ryder, P. Smith, *Macromolecules* **1986**, *19*, 2466; b) G. Newkome, C. N. Moorefield, G. R. Backer, M. J. Saunders, S. H. Grossman, *Angew. Chem. Int. Ed.* Engl. **1991**, *30*, 1178; c) S. Bonaccio, M. Wessicken, D. Berti, P. Walde, P. L. Luisi, *Langmuir* **1996**, *12*, 4976; d) M. F. Ottaviani, P. Matteini, M. Brustolon, N. J. Turro, S. Jockusch, D. A. Tomalia, J. *Phys. Chem. B.* **1998**, *102*, 6029; e) C. L. Jackson, H. D. Chanzy, F. P. Booy, B. J. Drake, D. A. Tomalia, B. J. Bauer, E. J. Amis, *Macromolecules*, **1998**, *31*, 6259; f) Bosman, A. W.; Schenning, A. P. H. J.; Janssen, R. A. J.; Meijer, E. W. *Chem. Ber.* **1997**, *130*, 725-728.
12. Nomenclature: $P(G_xTos_y)$, x= DP_n of polyglycerol, y= degree of tosylate substitution per hydroxyl group.

13. Although cationic NCN-pincer platinum complexes are, in contrast to their highly active palladium analogues, not considered to be catalytically active in Lewis-acid catalysed processes, they do accelerate selected examples to some extent.
14. EDX analysis of the samples failed due to the detection limits of this method, combined with the sensitivity of the material towards electron induced damage.
15. H. P. Dijkstra, C. A. Kruithof, N. Ronde, R. van de Coevering, D. J. Ramón, D. Vogt, G. P. M. van Klink, G. van Koten, *J. Org. Chem.* **2002**, published on the web.

Chapter Eight

Chiral Hyperbranched Polyglycerol as Scaffolds for the Covalent and Non-Covalent Immobilization of *para*-COOH and *para*-SO_3H NCN-pincer Platinum(II) Complexes

Abstract

NCN-platinum complexes have been immobilized in both a covalent and non-covalent manner on chiral hyperbranched polyglycerols obtained by ROMBP of either *(S)*- or *(R)*-glycidol. Chiral nanocapsules *(S)*-$PG_{40}C16_{(0.53)}$ and *(R)*-$PG_{73}C16_{(0.55)}$ were found to encapsulate 1.6 and 2.4 molar equivalents of [PtX(NCN-SO_3H)] (X = OH_2 or OH^-) respectively. A partially tosylated chiral hyperbranched polyglycerol *(S)*-$PG_{40}Tos_{(0.5)}$ was reacted with [PtI(NCN-COOK)] affording the covalently modified polyglycerol $P(G_{40}Tos_{(0.15)}PtI(NCN\text{-}COO)_{(0.35)})$. The chirality of the organometallic materials was probed by circular dichroism. Model studies towards the catalytic efficiency of the immobilized NCN-platinum complexes showed that the chiral support does not lead to chiral induction in an asymmetric Michael addition.

8.1 .Introduction

Dendritic macromolecules are promising materials for a range of applications.[1] Of particular interest is their use as molecular scaffolds for the immobilization of organometallic complexes or coordination compounds.[2] Targeted functionalization of the core, shells or periphery of the dendrimer has made them suitable materials for non-covalent immobilization of transition metal complexes.[2f-h] Alternatively, dendritic materials have been covalently functionalized with organometallic complexes.[1d,3] Hyperbranched polymers offer a promising alternative for the many applications encountered in dendrimer chemistry. In contrast to dendrimers, hyperbranched polymers can be synthesized in a controlled one-step polymerization of AB_m-type monomers, resulting in randomly branched globular polymers of low polydispersity.[4] Anionic ring-opening multibranching polymerization (ROMBP) of glycidol results in hyperbranched polyglycerols which can be tailored in terms of their core (initiator) functionality and molecular weight affording highly flexible, hydrophilic, polyetherpolyols, which exhibit unusual narrow polydispersities (M_w/M_n = 1.2 - 1.5).[5] Their globular shape, and well-defined structure allows targeted functionalisation and the possibility to construct core-shell type architectures.

Chapters 6 and 7 of this thesis report on the use of these hyperbranched polyglycerols as macromolecular scaffolds for the immobilization of *para*-substituted NCN-pincer platinum(II) complexes (NCN-pincer = 2,6-bis[(dimethylamino)methyl]phenyl anion). Partial esterification (40-60%) of the hydroxyl groups from the polyglycerol with fatty acid chains affords nanocapsules with an inverted micelle type structure applicable for the non-covalent immobilization of sulfonated NCN-pincer platinum(II) complexes (see Chapter 6). Alternatively, hyperbranched polyglycerols were activated by tosylation to introduce NCN-pincer platinum carboxylic acids *via* covalent bonding (see Chapter 7). This allowed direct visualization of the hyperbranched polyglycerols loaded with NCN-platinum iodides by transmission electron microscopy (TEM). Anionic ROMB polymerization of enantiomerically pure *(R)*- or *(S)*-glycidol affords chiral hyperbranched polyglycerols.[6] The availability of these chiral hyperbranched polyglycerols motivated us to apply them in both the covalent and non-covalent immobilization of NCN-pincer platinum complexes, using similar methodologies as described in the previous chapters for the achiral polyglycerols.

8.2. Results

Synthesis of nanocapsules based on chiral hyperbranched polyglycerol

Chiral nanocapsules were synthesized by ROMB polymerization of either *(S)*- or *(R)*-glycidol, followed by partial functionalisation of the hydroxyl groups with palmitoyl tails (Scheme 1). Esterifications were performed with palmitoyl chloride in a mixture of pyridine and toluene, and the products were characterized by ^{1}H- and ^{13}C-NMR spectroscopy, IR-spectroscopy, and SEC analysis. The resulting nanocapsules *(S)*-$PG_{40}C16_{(0.53)}$ (*(S)*-**1**) and *(R)*-$PG_{73}C16_{(0.55)}$ (*(R)*-**2**)[7] had molecular weights of M_n = 8140 (M_w/M_n = 1.19) and 15270 (M_w/M_n= 1.42), respectively, with approximately 55% of the hydroxyl groups functionalized by palmitoyl chains. Polymers *(S)*-**1** and *(R)*-**2** are completely and homogeneously soluble in apolar solvents such as dichloromethane, chloroform, and toluene.

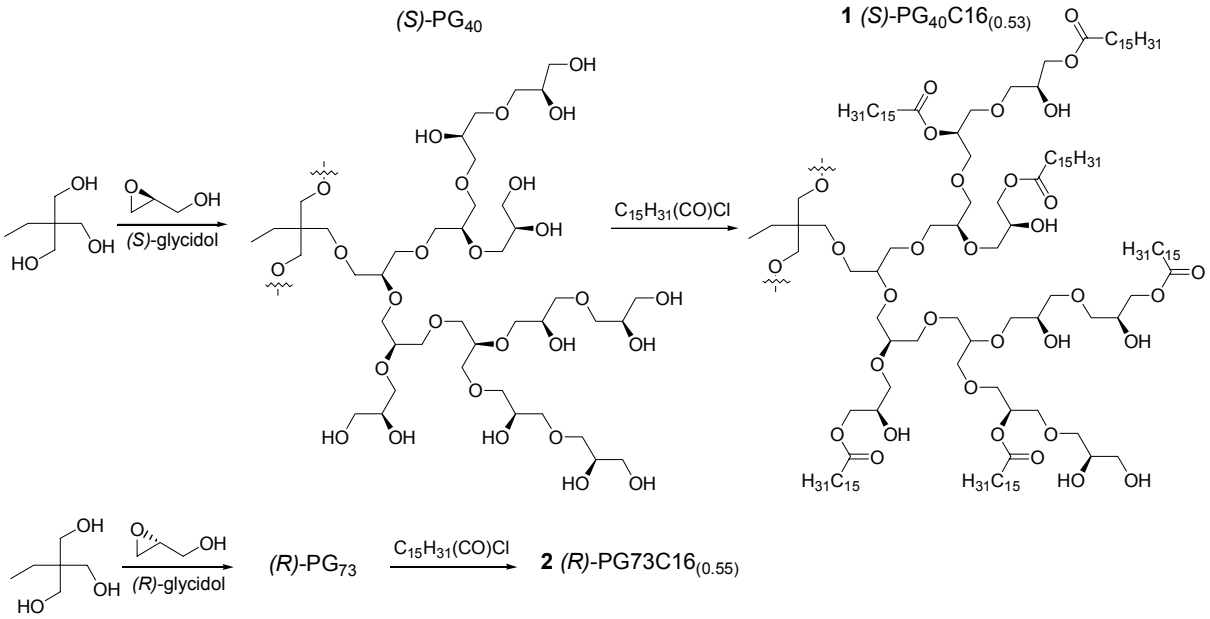

Scheme 1. Preparation of chiral nanocapsules *(S)*-**1** and *(R)*-**2** by ROMBP followed by partial esterification.

*Non-covalent immobilization of NCN-pincer platinum complexes in chiral nanocapsules (S)-**1** and (R)-**2***

In earlier studies towards the loading of the nanocapsules with water-soluble dyes[5] or with NCN-pincer platinum complexes as described in Chapter 6, extraction took place from an aqueous solution into an organic phase containing the nanocapsule. This methodology was also applied for the non-covalent loading of the chiral nanocapsules *(S)*-**1** and *(R)*-**2** with water-soluble sulfonated NCN-platinum complex **3** (Scheme 2).

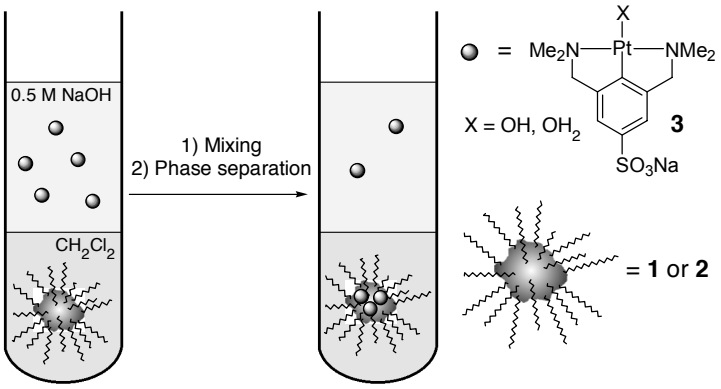

Scheme 2. Non-covalent loading of nanocapsules *(S)*-**1** and *(R)*-**2** with NCN-platinum complexes.

Hydrophilic NCN-pincer platinum complex **3** was encapsulated by liquid-liquid extractions from an aqueous solution (0.5 M NaOH)[8] into a dichloromethane solution of nanocapsule *(S)*-**1** or *(R)*-**2**. The affinity of **3** for the polyglycerol interior, and the loading capacities of the nanocapsules were investigated by performing the encapsulation experiments at various NCN-platinum to polyglycerol molar ratios, monitoring both phases by UV/Vis-spectroscopy. While *(S)*-**1** and *(R)*-**2** contain no active chromophores in the range of 220-800 nm, sulfonate **3** shows a broad absorption located at 275 nm ($\varepsilon \approx 10^4$ $M^{-1}cm^{-1}$) in 0.5 M NaOH. Aqueous solutions of **3** (10^{-5}-10^{-4} M in 0.5 M NaOH) were prepared and mixed thoroughly with solutions of *(S)*-**1** and *(R)*-**2** (5.0 x 10^{-5} M in dichloromethane). After careful phase separation, both layers were subjected to UV/Vis spectroscopy. UV/Vis spectra from solutions of the nanocapsules non-covalently loaded with **3** showed two absorption bands ($\varepsilon \approx 10^4$ $M^{-1}cm^{-1}$) at 262 and 275 nm. Selected UV/Vis spectra of the organic phase, obtained from the encapsulation experiments of **3** with nanocapsule *(S)*-**1,** together with the corresponding titration curve, are depicted in Figure 1.

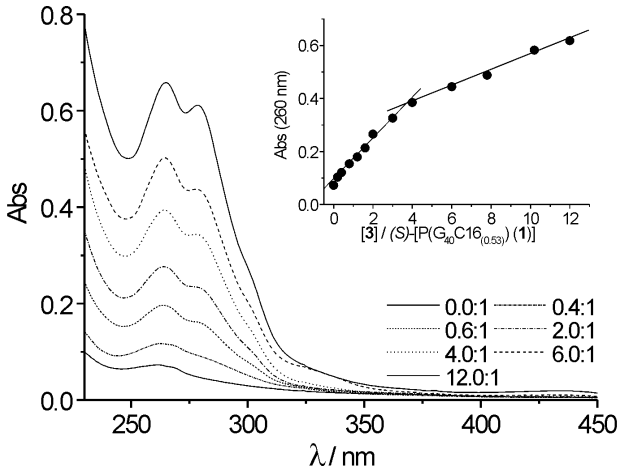

Figure 1. UV/Vis spectra (organic phase) and titration curve (inset) of the extractions of NCN-platinum complex **3** by nanocapsule *(S)*-**1** at various [**3**]/[nanocapsule] ratios.

Upon increasing the concentration of **3** in the aqueous phase, the nanocapsule takes up more of this NCN-platinum complex, until an infliction point is reached (shown for *(S)*-**1** in Figure 1). For the smaller *(S)*-$PG_{40}C16_{(0.53)}$ (*(S)*-**1**) this point was located at a molar ratio [**3**]/[nanocapsule] of about 4, while for the larger *(R)*-$PG_{73}C16_{(0.55)}$ (*(R)*-**2**) it was located at a molar ratio of 7. UV/Vis analysis of the aqueous phases showed that platinum sulfonate **3** is not extracted quantitatively into the organic phase, similar as described in Chapter 6 for the achiral nanocapsules. Since part of the complex remains in the aqueous phase, the ratios found for the saturation points (*vide supra*) are consequently not equal to the actual loading of the nanocapsules.

The chiral nanocapsules were loaded on a preparative scale by shaking up dichloromethane solutions of *(S)*-**1** and *(R)*-**2** thoroughly with a 0.5 M NaOH solution of **3** at ratios equal to the infliction points found in the UV/Vis-titrations. ^{1}H-NMR integration of the NMe_2 (**3**) and CH_3 (palmatoyl endgroup of *(S)*-**1** or *(R)*-**2**) resonances showed the encapsulation of 1.6-1.8 and 2.5-2.8 equivalents of **3** in nanocapsules *(S)*-**1** and *(R)*-**2**, respectively. According to elemental analysis the loaded chiral nanocapsules *(S)*-**1** and *(R)*-**2** had encapsulated 1.6 and 2.4 equivalents of **3**, respectively, which is in agreement with the data obtained from ^{1}H-NMR analysis. Consequently, NCN-platinum loaded chiral polyglycerols were obtained, which according to their stoichiometries are denoted as *(S)*-**1·3$_{1.6}$** and *(R)*-**2·3$_{2.4}$**.

Covalent immobilization of NCN-pincer platinum complexes on chiral hyperbranched polyglycerol

The chiral hydrophilic hyperbranched polyglycerols *(S)*-PG_{40} and *(R)*-PG_{73} were tosylated in a mixture of pyridine and toluene by treatment with tosyl chloride at elevated temperatures (Scheme 3).

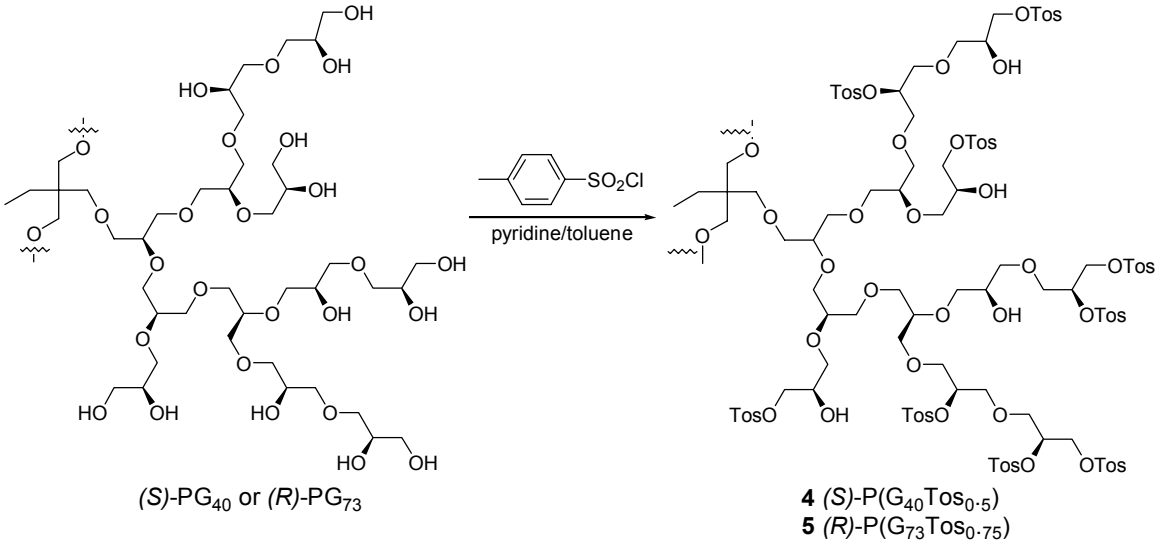

Scheme 3. Partial tosylation of chiral hyperbranched polyglycerols to obtain *(S)*-**4** and *(R)*-**5**.

This tosylation procedure afforded partially tosylated chiral polyglycerols *(S)*-P($G_{40}Tos_{0.5}$) (*(S)*-**4**) and *(R)*-P($G_{73}Tos_{0.75}$) (*(R)*-**5**). Low molecular weight impurities were removed by dialysis against neat dichloromethane, using a membrane with a molecular weight cut off (MWCO) of 1000 D. The tosylated materials were, in contrast to the hydrophilic starting material, completely and homogeneously soluble in apolar solvents. Subsequent covalent modification of the tosylated materials with NCN-pincer platinum complexes was performed using similar procedures as described in Chapter 7. To this purpose NCN-pincer platinum(II) carboxylic acid [PtI(NCN-COOH)] (**6**) was deprotonated by treatment with potassium *t*-butoxide to afford carboxylate **7** (Scheme 4). Based on the number of tosylate groups per polyglycerol, which is approximately equal to the average number of monomer units (DP_n) in the polymer, we treated *(S)*-**4** and *(R)*-**5** with an excess of **7** in DMF at 80 °C (Scheme 4).

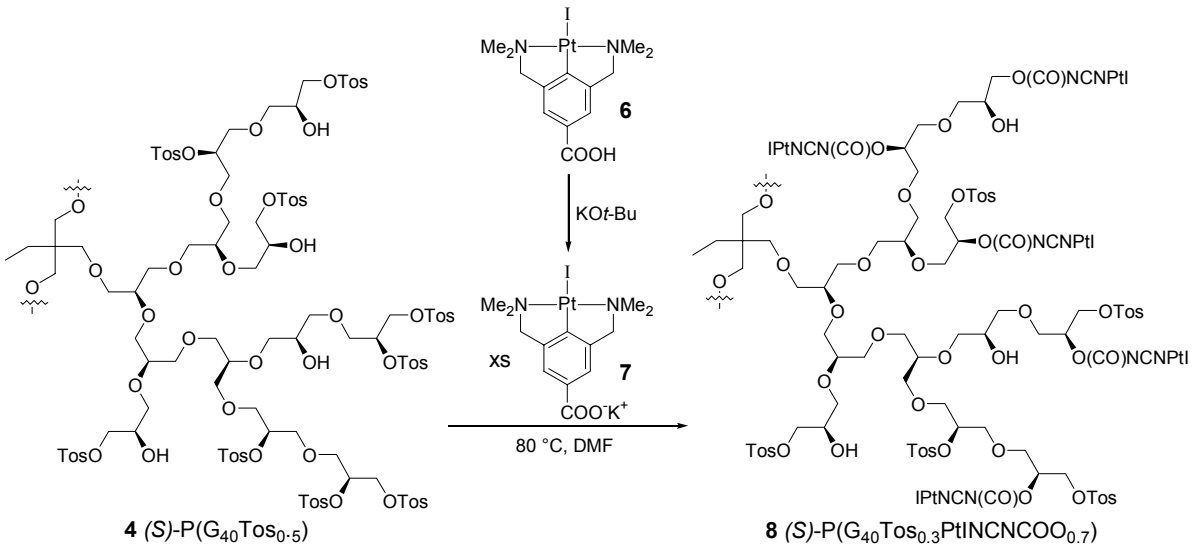

4 *(S)*-P($G_{40}Tos_{0.5}$) **8** *(S)*-P($G_{40}Tos_{0.3}$PtINCNCOO$_{0.7}$)

Scheme 4. Substitution of tosylates for [PtI(NCN-COO)] moieties.

Irrespective of the excess of **7** (10-100%) employed in the case of tosylated *(S)*-polyglycerol *(S)*-**4**, only 70% of the available tosylate groups could be substituted, affording the modified chiral hyperbranched polyglycerol P($G_{40}Tos_{(0.15)}$PtI(NCN-COO)$_{(0.35)}$) (*(S)*-**8**). Various attempts in the substitution of the tosylate groups of *(R)*-**5** with NCN-platinum complex **7** resulted in the formation of a mixture of products. Whether this was the result of its size (DP_n =73) or other factors, is unclear at the moment. However, unreacted **7** could be removed from *(S)*-**8** by liquid-liquid extraction with water, and subsequent dialysis (MWCO = 1000 D) against neat dichloromethane.

^{1}H-NMR analysis of *(S)*-**8** clearly shows the (partial) substitution of the tosylate groups by NCN-pincer platinum(II) carboxylic complexes. While the intensities of the signals originating from the tosylate groups, located at 7.78, 7.36 ppm (ArH) and 2.45 ppm (CH_3)

were decreased, new signals appeared at 7.56 ppm (ArH), 4.07 ppm (CH_2N), and 3.19 ppm (NMe_2), all typical of the NCN-platinum carboxylic complex. The degree of substitution could be based on the relative intensity ratios of these signals. The UV/Vis-spectrum of *(S)*-**4** in dichloromethane shows an absorption band at 262 nm ($\varepsilon \approx 10^5$ M^{-1}), while in the UV/Vis-spectrum of *(S)*-**8** an additional band appears at 324 nm ($\varepsilon \approx 10^5$ M^{-1}). The latter band, which matches that of NCN-pincer platinum carboxylic acid **6** (326 nm, $\varepsilon \approx 10^4$ M^{-1}), points to the presence of NCN-pincer platinum moieties in the polymer.

Circular Dichroism

The chiral nanocapsules *(S)*-**1·3$_{1.6}$** and *(R)*-**2·3$_{2.4}$**, loaded with sulfonated NCN-platinum complexes, were subjected to circular dichroism (CD) in order to investigate the chiral properties of the materials. Unloaded nanocapsules *(S)*-**1** and *(R)*-**2** show optical rotations in polarimetry,[6] but are CD-silent in the region 220-800 nm. Non-covalent loading with the NCN-pincer platinum moieties in their interior renders these materials CD-active (Figure 2). The CD-spectrum of the achiral analogue of *(S)*-**1·3$_{1.6}$** and *(R)*-**2·3$_{2.4}$**, nanocapsule $PG_{106}C16_{(0.6)}$**·3$_{4.3}$**, shows a broad signal around 270 nm (Figure 2a). This CD-spectrum was subtracted from the spectra obtained for loaded chiral nanocapsules *(S)*-**1·3$_{1.6}$** and *(R)*-**2·3$_{2.4}$**, to isolate the chiral contributions from the CD-spectrum.[9] The difference spectra for *(S)*-**1·3$_{1.6}$** and *(R)*-**2·3$_{2.4}$** are depicted in Figure 2b. Around 320 nm, low intensity bands of opposite sign (+0.4 mdeg and -0.5 mdeg) appear for the chiral nanocapsules *(S)*-**1·3$_{1.6}$** and *(R)*-**2·3$_{2.4}$**, respectively.

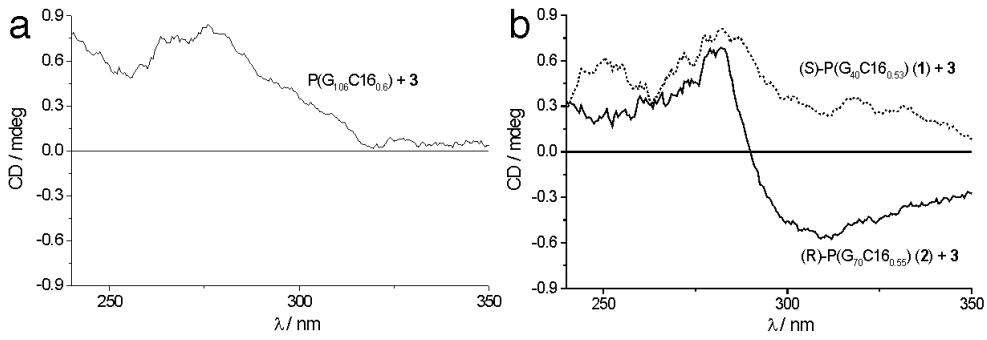

Figure 2. (a) CD spectrum of achiral nanocapsule $PG_{106}C16_{(0.5)}$ and (b) difference spectra of *(S)*-**1·3$_{1.6}$** and *(R)*-**2·3$_{2.4}$** with $PG_{106}C16_{(0.5)}$.

The CD-spectra of the covalently modified chiral hyperbranched polymers *(S)*-**4**, *(R)*-**5** and *(S)*-**8** are also presented as difference spectra with their achiral analogues $PG_{25}Tos_{(1.0)}$ and $P(G_{25}Tos_{(0.5)}PtI(NCN\text{-}COO)_{(0.5)})$, respectively.[9] Figure 3a shows the difference spectra of the tosylated hyperbranched chiral polyglycerols *(S)*-**4** and *(R)*-**5**, having signals with opposite

signs at 265 nm with intensities of –1.8 and +2.0 mdeg respectively. Figure 3b shows the CD-spectrum of *(S)*-**8**, from which the spectrum of its achiral analogue $P(G_{25}Tos_{(0.25)}PtI(NCN\text{-}COO)_{(0.25)})$ has been subtracted. The absorption band at 265 nm, which has decreased in intensity compared to *(S)*-**4** (Figure 3a), is ascribed to the presence of the remaining tosylate groups in *(S)*-$P(G_{40}Tos_{(0.15)}PtI(NCN\text{-}COO)_{(0.35)})$. Apart from this band, two new bands with opposite signs appeared at 305 nm (-0.15 mdeg) and 335 nm (+0.45 mdeg). These must originate from the presence of the NCN-platinum units in the material, which has a broad absorption band located at 326 nm in its UV/Vis absorption spectrum.

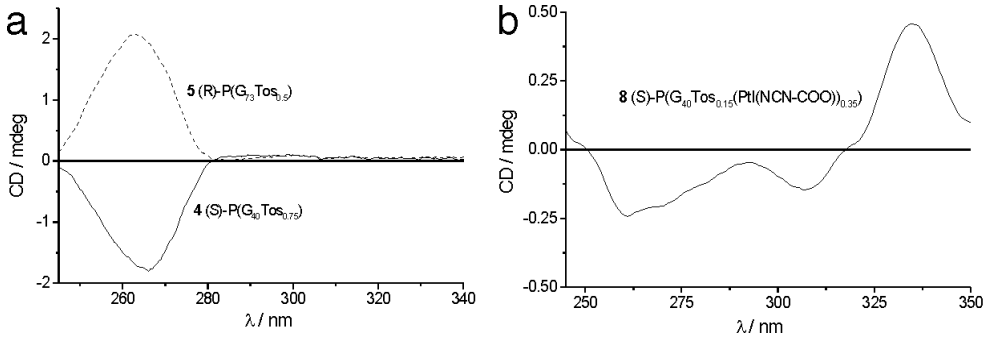

Figure 3. (a) CD difference spectra of *(S)*-**4** and *(R)*-**5** with $PG_{106}Tos_{(1.0)}$ and (b) difference spectrum of *(S)*-**8** with $P(G_{25}Tos_{(0.5)}PtI(NCN\text{-}COO)_{(0.5)})$.

Asymmetric Michael additions

Lewis acidic cationic NCN-pincer complexes of the type $[Pt(OH_2)NCN](BF_4)$ can be applied as model catalyst in aldol type reactions, such as the asymmetric Michael addition between methyl vinyl ketone to ethyl *(R/S)*-α-cyanopropionate (Scheme 5).[10] Chiral nanocapsules *(S)*-**1·3$_{1.6}$** and *(R)*-**2·3$_{2.4}$**, non-covalently loaded with the sulfonated NCN-platinum complexes, were tested as catalysts in this asymmetric addition.

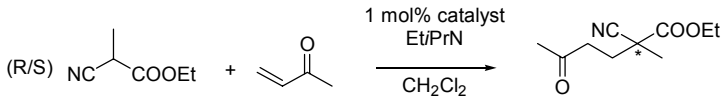

Scheme 5. Asymmetric Michael addition between α-methyl cyanopropionate and methyl vinyl ketone.

The results were compared with the performance of the unloaded chiral nanocapsules *(S)*-**1** and *(R)*-**2**, the blank, as well as with parent complex $[Pt(OH_2)NCN](BF_4)$. The results from these experiments are collected in Table 1. After full conversion, both products and loaded nanocapsules could be separated and isolated in near quantitative yields (>96% for the nanocapsule) by dialysis. Polarimetric analysis of the product revealed that in all cases racemic mixtures were obtained.

Table 1. Catalytic results from the asymmetric Michael addition of methyl vinyl ketone to ethyl α-cyanopropionate with chiral nanocapsules *(S)*-**1** and *(R)*-**2**.[a]

	Catalyst	k (10^{-3} h^{-1})[b]	Conversion (%, 24 hrs)	ee (%)
a	$[Pt(OH_2)NCN]^+BF_4^-$	207	99	0
b	none	17	38	0
c	*(S)*-**1**	21	42	0
d	*(R)*-**2**	18	37	0
e	*(S)*-**1**·$\mathbf{3}_{1.6}$	86	75	0
f	*(R)*-**2**·$\mathbf{3}_{2.4}$	57	63	0

a) for conditions see experimental section; b) initial rate, determined at conversions < 40%.

The activity and selectivity of *(S)*-**8**, containing the covalently attached NCN-platinum units was tested in the same Michael addition. As 70% of the, in total 20, tosylate groups were substituted by NCN-pincer platinum units, the polyglycerol contains, on average, 14 platinum sites per polymer. The results from the catalytic experiments, carried out with material activated with $AgBF_4$, are collected in Table 2. After full conversion, the products were separated from *(S)*-**8** by dialysis (11.0 mg, 0.60 μmol, 89% recovered). Polarimetry revealed that also in this case racemic product mixtures were obtained.

Table 2. Results from catalytic experiments in the asymmetric Michael addition.[a]

Catalyst	k (10^{-3} h^{-1})[b]	Conv. (%, after 20 hrs)	ee (%)
$[Pt(OH_2)NCN]^+BF_4^-$	207	99	0
none	17	38	0
(S)-**8**	189	80	0

a) conditions: see experimental section; b) determined at conversions < 40%.

8.3. Discussion

The ability of chiral nanocapsules **1** and **2** to immobilize NCN-platinum complex **3** by non-covalent interactions is similar as described in Chapter 6 for their achiral analogues, showing a dependence of the encapsulation capacity on the molecular weight of the hyperbranched polymer and incomplete extraction of **3** from the aqueous phase. This correspondence between the chiral and achiral materials was also observed in the covalent modification of tosylated hyperbranched polyglycerols with NCN-platinum units. Although *(S)*-**4** was incompletely tosylated (50%), treatment with the NCN-platinum complex resulted in the substitution of 70% of the available tosyl groups. In contrast, treatment of tosylated polymer *(R)*-**5** with NCN-platinum complex **7** did not react to produce the desired material. Instead, a mixture of unreacted **7** and various unidentified (partially substituted) polymeric materials was obtained.

Chirality of the hyperbranched materials

The synthesis of optically active polymers is an important field in polymer science, offering a wide variety of applications based on the chiral structure. Applications involve chiral recognition toward racemic compounds, asymmetric catalysis and liquid crystal formation.[11] Optically active catalysts have been anchored to achiral polymers for asymmetric organic synthesis with varying success. However, a significant decrease in enantioselectivity is generally observed compared to the monomeric complex. This indicates that the microenvironment of the polymer has a pronounced influence on the stereoselectivity of the catalyst.[11c] Although main chain chiral polymers such as polypeptides have also been applied in asymmetric catalysis, these investigations are more rare.[11d] Stereo-irregularity and flexibility of the chiral polymers functionalized with catalytic sites leads to an underdefined microenvironment of the catalytic site. In general it is difficult to systematically modify this chiral microenvironment, unless a large amount of rigidity is introduced in the polymeric structure.[11c] The chiral hyperbranched polymers used in this study were obtained by controlled polymerization of enantiomerically pure monomers and are considered to be highly flexible. The polyglycerols, non-covalently or covalently modified with NCN-platinum units were studied by circular dichroism to probe their configuration and conformation. Interesting to note is the CD-activity, albeit small, of the achiral reference materials, indicating the presence of ordered domains within the polymeric material.

CD-spectra of the chiral nanocapsules non-covalently loaded with NCN-pincer platinum(II) complexes *(S)*-**1·3**$_{1.6}$ and *(R)*-**2·3**$_{2.4}$ show signals with opposite sign. This indicates that the macromolecular chirality of *(S)*-**1** and *(R)*-**2** is translated, to some extent, on a molecular level to the absorption features of the encapsulated NCN-pincer platinum complexes. The low intensity of this signal might be attributed to the non-uniformity in binding interactions between **3** and the polyglycerol interior of the nanocapsules, or to the frugal translation of chirality.

The opposite signals for the tosylated chiral hyperbranched polymers *(S)*-**4** and *(R)*-**5** observed in their CD-spectra confirm the retention of chirality during the ROMB polymerization of *(S)*- and *(R)*-glycidol respectively, as was earlier observed by polarimetry.[6] The conditions employed in the tosylation of the chiral hyperbranched polyglycerols are not expected to influence the chirality, *e.g.* to cause racemization, of the material. However, the nucleophilic displacement of tosylates on secondary alkyl groups can proceed *via* a borderline nucleophilic replacement mechanism, resulting in partial racemization of the configuration.[12] For substitutions on tosylate *(S)*-**4** this would result in partial racemization of the product *(S)*-**8**. Indeed, the overall decrease in intensity of the bands when compared to *(S)*-**4** might be

attributed this. On the other hand, comparing different materials quantitatively by CD-spectroscopy, might not hold. Overall, substitution of the tosylate groups by the NCN-pincer moieties leads to organometallic materials with at least part of the chiral information retained in the macromolecule.

Asymmetric Michael Additions

The catalytic behavior of the non-covalently loaded nanocapsules *(S)*-**1·3**$_{1.6}$ and *(R)*-**2·3**$_{2.4}$, compared to the control experiments is similar to that observed for the double Michael addition with achiral nanocapsules. The initial reaction rate is enhanced by a factor 3-4 with respect to the blank reaction for both *(S)*-**1·3**$_{1.6}$ and *(R)*-**2·3**$_{2.4}$, but is decreased when compared to [Pt(OH_2)NCN](BF_4). The unloaded nanocapsules *(S)*-**1** and *(R)*-**2** did not show any significant catalytic activity when compared to the blank. The activity of the covalently immobilized NCN-pincer platinum(II) groups in *(S)*-**8** is comparable to that of the parent complex [Pt(OH_2)NCN](BF_4), as was the case for its achiral analogue (Chapter 7). The reduced catalytic activity of the non-covalently immobilized complexes, compared to the parent and the covalently immobilized complexes, might be attributed to steric shielding of the catalytic site in the nanocapsule core. Additionally, competitive coordination between hydroxyl or ether functionalities and the α-cyanopropionate substrate to the platinum site can reduce the catalytic activity further.

The usage of the chiral micro-environment of the polyglycerol nanocapsule or polyglycerol backbone to perform catalysis can be compared to the application of chiral solvents in asymmetric synthesis. These chiral solvents generally yield products of low optical purity (0-10%).[13] Functionalization of chiral hyperbranched polyglycerol, either in a covalent or non-covalent manner with NCN-platinum moieties did not influence the stereoselective outcome of the catalyzed reaction. A racemic product mixture is obtained after full conversion. For successful chiral induction in this asymmetric Michael addition, either one of the substrates *(R)*- or *(S)*-ethyl α-cyanopropionate should react faster, without loss of chiral information. Alternatively, chiral induction can occur during the nucleophillic attack of methyl vinyl ketone, after the ethyl α-cyanopropionate is deprotonated in the catalytic cycle to afford an achiral enolate intermediate. The lack of chirality in the Michael addition product after full conversion can be attributed to either non-transfer of chirality, or to racemization *via* a retro-aldol reaction. However, these results do not exclude the possibility of chiral induction at low conversion (kinetic resolution), which could be monitored using a continuous membrane reactor set-up.[14] The applicability of both covalently and non-covalently modified polyglycerols in such a reactor was demonstrated by their facile separation from the product mixtures using a dialysis membrane, which was successful even on very small scales.

8.4. Conclusions

The immobilization of NCN-platinum complexes on chiral hyperbranched polyglycerols, either in a covalent or non-covalent manner, affords CD active chiral materials. Application of these organometallic materials as model catalyst in an asymmetric Michael addition revealed, however, that the chirality in the backbone was not able to induce an enantioselective outcome of the reaction after full conversion.

8.5. Experimental Section

Solvents were dried over appropriate agents and distilled prior to use. Benzoylated dialysis tubing (Sigma D-7884, cut-off mass = 1500 $gmol^{-1}$) was stored in methanol prior to use. Elemental analyses were performed by H. Kolbe, Mikroanalytisches Laboratorium, Mülheim, Germany. ^{1}H and ^{13}C NMR spectra were recorded at 298 K on a Varian Inova 300 or Mercury 200 spectrometer. UV/Vis spectra were recorded on a Varian Cary I spectrophotometer. CD-spectra were recorded on a Jasco J-810 spectropolarimeter. The syntheses of the hyperbranched polyglycerols,[6] NCN-platinum complexes **3** and **6**, $P(G_{106}(C16)_{(0.6)})$ and **7**, $P(G_{25}Tos_{(1.0)})$ and $P(G_{25}Tos_{(0.5)}PtI(NCN\text{-}COO)_{(0.5)})$ have been described in previous chapters.

*Nanocapsule (S)-$PG_{40}C16_{(0.53)}$; (S)-**1***

To a pyridine solution (80 mL) of hyperbranched (S)-polyglycerol (DP_n= 40; 2.00 g, 27.0 mmol of OH groups), was added drop wise a toluene solution (100 mL) of palmitoyl chloride (4.8 mL; 16 mmol) at 80°C within 1h. The mixture was refluxed for 20h at 130°C. A stoichiometric amount of $NaHCO_3$ (16 mmol; 1.35 g) was added to the cold solution and most of the volatiles were removed in vacuo. Residual pyridine was removed by azeotropic distillation in 100 mL of toluene. The remaining solution was filtered and concentrated in vacuo, the residue was washed three times with ethyl acetate (30 mL) to remove traces of free palmitoyl carboxylic acid and was further purified by dialysis in $CHCl_3$. The polymer was obtained as a white solid in a yield of 85%. ^{1}H NMR ($CDCl_3$): 0.84 (t, CH_3), 1.21 (br, 24H, CH_2), 1.57 (m, 2H, $\underline{CH_2}CH_2CO$), (m, 2H, $\underline{CH_2}CO$), 2.26-2.3 (m, CH_2, CH_2CO), 3.52-4.07 (br, 5H, glycerol), 5.10 (br, OH). ^{13}C NMR ($CDCl_3$): 14.10, 22.67, 24.94, 29.13, 29.43, 29.66, 31.91, 34.10, 65.12, 68.65, 69.81, 70.16, 173.8; IR (NaCl)= 1636.76 (C=O), 3388.06 (O-H). α (Degree of substitution per hydroxyl group) = 60%; M_n= 8140; M_w/M_n= 1.19; Elem. Anal.: C 66.96, H 10.76.

*Nanocapsule (R)-$PG_{70}C16_{(0.55)}$; (R)-**2***

Dried *(R)*-polyglycerol (DP_n = 70; 2.2 g, 29.7 mmol of OH groups) and palmitoyl chloride (5.34 mL, 17.8 mmol) were reacted using the same procedure as described for *(S)*-**1**, affording

(R)-**2** as a white solid in a 78% yield. ^{1}H NMR ($CDCl_3$): 0.81 (t, $\underline{CH_3}$), 1.11-1.25 (br, $\underline{CH_2}$), 1.53 (m, $COCH_2\underline{CH_2}$), 2.24-2.28 (m, CH_2, $\underline{CH_2}CO$), 3.44-4.03 (br, glycerol moiety), 5.04 (br, OH). ^{13}C NMR ($CDCl_3$): 14.08, 22.66, 24.88, 29.16, 29.51, 29.64, 31.90, 34.10, 65.12, 68.65, 69.81, 70.16, 173. IR (NaCl) ν= 1738.43 (C=O), 3441.81 (O-H). α (Degree of substitution per hydroxyl group) = 55%; M_n= 15270; M_w/M_n= 1.42; Elem. Anal.: C 68.59, H 11.41.

UV/Vis-titrations

Solutions of **3** in aqueous 0.5 M NaOH were prepared in concentrations ranging from 10^{-5}-10^{-4} M. Nanocapsules *(S)*-**1** and *(R)*-**2** were dissolved in dichloromethane with concentrations in the range of 10^{-5} M. In a typical UV/Vis experiment, 3 mL of the aqueous solution was mixed thoroughly for 1 hour with 3 mL of the dichloromethane solution. The phases were allowed to settle completely en were subsequently separated and both analyzed by UV/Vis-spectroscopy.

*Loading of Chiral Nanocapsules (S)-**1** and (R)-**2***

Equivolumetric amounts (50 mL) of an aqueous solution of **3** (5.0 mM, 0.5 M NaOH) and dichloromethane solutions of *(S)*-**1** (1.2 mM), or *(R)*-**2** (0.7 mM) were mixed vigorously for 30 minutes. The phases were allowed to settle overnight and subsequently separated. The organic phase was dried over $MgSO_4$, filtered and dried *in vacuo* to obtain the loaded nanocapsules as yellowish solids in near quantitative yields. *(S)*-**1·6$_{1.6}$**: ^{1}H NMR ($CDCl_3$): 0.85 (t, $\underline{CH_3}$), 1.25 (br, $\underline{CH_2}$), 1.57 (br. m, $COCH_2\underline{CH_2}$), 2.31 (br. m, CH_2, $\underline{CH_2}CO$), 3.00-3.15 (NMe_2 pincer), 3.40-4.20 (br, glycerol moiety), 4.01 (CH_2N pincer), 5.07 (br, OH). 7.60 (ArH pincer); ^{13}C NMR ($CDCl_3$): 174.0-173.0, 123.4, 119.4, 80.0-78.0, 74.0-68.0, 66.0-63.0, 54.6, 34.5, 32.1, 30.0-29.0, 25.1, 22.9, 14.3; Elem. Anal.: C 66.94, H 10.51, Pt 3.51. *(R)*-**2·6$_{2.4}$**: ^{1}H NMR ($CDCl_3$): 0.87 (t, $\underline{CH_3}$), 1.26 (br, $\underline{CH_2}$), 1.58 (br. m, $COCH_2\underline{CH_2}$), 2.30 (br. m, CH_2, $\underline{CH_2}CO$), 3.00-3.20 (NMe_2 pincer), 3.40-4.20 (br, glycerol moiety), 4.01 (CH_2N pincer), 5.04 (br, OH). 7.60 (ArH pincer); ^{13}C NMR ($CDCl_3$): 174.0-173.0, 123.4, 119.4, 80.0-78.0, 74.0-68.0, 66.0-63.0, 54.6, 34.5, 32.1, 30.0-29.0, 25.1, 22.9, 14.3; Elem. Anal.: C 66.50, H 10.45, Pt 2.84.

*Synthesis of (S)-**4** and (R)-**5**, tosylation of hyperbranched polyglycerols*

To a solution of the dried hyperbranched polyglycerol (1-3 g, with DP_n equivalents of OH groups) in pyridine (1 mmol/ml) was added tosyl chloride (2 x DP_n equivalents) in portions. The mixture was heated at 130 °C for 20 hours and excess $NaHCO_3$ was added to the cooled solution. All volatiles were removed *in vacuo*, and residual pyridine was removed by azeotropic distillation in toluene. The solution was filtered and washed twice with NaOH (1M), dried over $MgSO_4$ and concentrated *in vacuo* to afford the tosylated polyglycerols as colorless sticky solids. *(S)*-**4**: DP_n=40; 50% tosylated; M_n= 6084; M_w/M_n= 1.2; ^{1}H-NMR

($CDCl_3$) δ (ppm): 7.75 (2H, ArH tosylate), 7.32 (2H, ArH tosylate), 5.4-3.0 (m, PG), 2.41 (3H, CH_3 tosylate); ^{13}C-NMR ($CDCl_3$); ^{13}C-NMR ($CDCl_3$) δ (ppm):130.3, 128.0, 81-78, 74-68, 42.8; Elem. Anal.: C H; *(R)*-**5**: DP_n=95; 75% tosylated; M_n= 18371; M_w/M_n= 1.4; ^{1}H-NMR ($CDCl_3$) δ (ppm): 7.77 (2H, ArH tosylate), 7.33 (2H, ArH tosylate), 5.5-3.1 (m, PG), 2.43 (3H, CH_3 tosylate); ^{13}C-NMR ($CDCl_3$); ^{13}C-NMR ($CDCl_3$) δ (ppm):130.2, 128.2, 81-78, 74-68, 42.8.

*Synthesis of P(G_{40}Tos$_{(0.15)}$PtI(NCN-COO)$_{(0.35)}$) (S)-**8***

To a solution of the tosylated polyglycerol *(S)-**4*** (0.2-0.5 g) in DMF (20 mL) was added **7** (1.1-2.0 equivalents per DP_n) at once. The solution was heated at 80 °C for 16 hours, followed by removal of all volatiles *in vacuo*. The brownish residue was redissolved in dichloromethane and washed twice with NaOH (1M) and with brine. The solution was dried over $MgSO_4$, concentrated to 5 mL, filtered over Celite, and dialyzed against neat dichloromethane (250 mL) to afford *(S)*-**8** as brownish solids (50-70%). **8**: DP_n=40; 50% free OH, 15% tosylated, 35% substituted with **7;** M_n= 11475; ^{1}H-NMR ($CDCl_3$) δ (ppm): 7.78 (2H, ArH tosylate), 7.56 ppm (2H, ArH pincer), 7.34 (2H, ArH tosylate), 5.4-3.0 (m, PG), 4.05 (4H, CH_2N pincer), 3.18 ppm (12H, NMe_2 pincer), 2.44 (3H, CH_3 tosylate); ^{13}C-NMR ($CDCl_3$); ^{13}C-NMR ($CDCl_3$) δ (ppm): 130.3, 155.0, 144.0, 128.2, 125.3, 120.2, 77.5, 81-78, 74-68, 55.2, 42.8;

Conditions for the asymmetric Michael addition

To a solution of 1.2 mmol methyl vinyl ketone, 0.08 mmol EtN^iPr_2, and 1 mol% catalyst based on its [Pt] in 2.5 ml CH_2Cl_2 was added 0.8 mmol racemic ethyl α-cyanopropionate at once. The mixture was stirred at room temperature, and 100 μL aliquots for ^{1}H-NMR-analysis were taken in the course of the reaction. After full conversion, the catalytic material was removed from the product mixture by dialysis against neat dichloromethane (250 mL) for 48 hours, and the chirality of the product mixture was determined by polarimetry.

8.6. References and Notes

1. For comprehensive reviews on dendrimers and their application: *Topics in Current Chemistry:* (a) *Dendrimers* **1998**, *vol. 197*, 1-228; (b) *Dendrimers II - Architecture, Nanostructure and Supramolecular Chemistry* **2000**, *210*, 1-308; (c) *Dendrimers III - Design, Dimension, Function* **2001**, *212*, 1-194; (d) *Dendrimers IV - Metal Coordination, Self Assembly, Catalysis* **2001**, *217*, 1-238.
2. For specific reviews on metallodendrimers, see: a) Constable, E. C. *Chem. Commun*. **1997**, 1073-1080; b) Newkome, G. R.; He, E.; Moorefield, C. N. *Chem. Rev.* **1999**, *99*, 1689-1746; c) Hearshaw, M. A.; Moss, J. R. *Chem. Commun.* **1999**, 1-8; (c) van Maanen, H.-J.; van Veggel, F. C. J. M.; Reinhoudt, D. N. *Top. Curr. Chem.* **2001**, 121-162; (d) R. Kreiter, R.; Kleij, A. W.; Klein Gebbink, R. J. M.; van

Koten, G. *Top. Curr. Chem.* **2001**, *217*, 163-199; (e) Oosterom, G. E.; Reek, J. N. H.; Kamer, P. C. J.; van Leeuwen, P. W. N. M. *Angew. Chem. Int. Ed.* **2001**, *40*, 1828-1849; For reports on non-covalent incorporation of catalytically active metal complexes, see: f) van de Coevering, R.; Kuil, M.; Klein Gebbink, R. J. M.; van Koten, G. *Chem. Commun.* **2002**, 1636-1637; g) de Groot, D.; de Waal, B. F. M.; Reek, J. H. N.; Schenning, A. P. H. J.; Kamer, P. C. J.; Meijer, E. W.; Leeuwen, P. W. N. M. *J. Am. Chem. Soc.* **2001**, 123, 8453; h) Slagt, M. Q.; Stiriba, S.-E.; Klein Gebbink, R. J. M.; Kautz, H.; Frey, H.; van Koten, G. *Macromolecules* **2002**, *35*, 5734-5737; for encapsulation of zerovalent metal particles, see: i) Crooks, R. M.; Zhao, M.; Sun, L.; Chechik, V.; Yeung, L. K. *Acc. Chem. Res.* **2001**, *34*, 18 and references cited therein.

3. (a) Liao, Y. -H.; Moss, J. R. *Organometallics* **1996**, *15*, 4307. (b) Knapen, J. W. J.; van der Made, A. W.; de Wilde, J. C.; van Leeuwen, P. W. N. M.; Wijkens, P.; Grove, D. M.; van Koten, G. *Nature* **1994**, *372*, 659. (c) Kleij, A. W.; Kleijn, H.; Jastrzebski, J. T. B. H.; Smeets, W. J. J.; Spek, A. L.; van Koten, G. *Organometallics* **1999**, *18*, 268. (d) Kleij, A. W.; Kleijn, H.; Jastrzebski, J. T. B. H.; Smeets, W. J. J.; Spek, A. L.; van Koten, G. *Organometallics* **1999**, *18*, 277. (e) Gossage, R. A.; Jastrzebski, J. T. B. H.; van Ameijde, J.; Mulders, S. J. E.; Brouwer, A. J.; Liskamp, R. J. M.; van Koten, G. *Tetrahedron Lett.* **1999**, *40*, 1413. For the more abundant ferrocene-based organometallic dendrimers see: (f) Astruc, D.; Blais, J. -C.; Cloutet, E.; Djakovitch, L.; Rigaut, S.; Ruiz, J.; Sartor, V.; Valério, C. *Top. Curr. Chem.* **2000**, *210*, 229-259.
4. (a) Voit, B. J. Polym. *Sci., Polym. Chem.* **2000**, *38*, 2505. (b) Kim, Y. H. J. *Polym. Sci., Polym. Chem. Ed.* **1998**, *36*, 1685. (c) Flory, P. J. *J. Am. Chem. Soc.* **1952**, *74*, 2718. Conceptual overview: (d) Sunder, A.; Heinemann, J.; Frey, H. *Chem. Eur. J.* **2000**, *14*, 2499.
5. (a) Haag, R.; Stumbé, J.-F.; Sunder, A.; Frey, H.; Hebel, A. *Macromolecules* **2000**, *33*, 8158. (b) Sunder, A.; Krämer, M.; Hanselmann, R.; Mülhaupt, R.; Frey, H. *Angew. Chem*. **1999**, *111*, 3758; *Angew. Chem. Int. Ed.* **1999**, *38*, 3552. (c) Sunder, A.; Hanselmann, R.; Frey, H.; Mülhaupt, R. *Macromolecules* **1999**, *32*, 4240.
6. Sunder, A.; Mülhaupt, R.; Haag, R.; Frey, H. *Macromolecules*, **2000**, *33*, 253.
7. Nomenclature P(GxXy): x = DPn of polyglycerol, X = substituent on hydroxyl group. y = degree of substitution on hydroxyl groups.
8. Solubilization of **3** in 0.5 M NaOH results in dehalogenation of the metal, affording a mixture of the zwitterionic aqua complex and the anionic hydroxy NCN-pincer platinum complex; see Chapter 6 for more details.
9. The CD-spectra of the achiral loaded polyglycerol $PG_{106}C16_{(0.6)}$**·3**$_{4.3}$ and the chiral loaded polyglycerols **1·3**$_{1.6}$ and **2·3**$_{2.4}$ were recorded at concentrations with equal absorbance intensities in the UV/Vis-region prior to substraction. The same methodology was applied in the CD-analyses of *(S)*-**4** and *(R)*-**5** with $PG_{25}Tos_{(1.0)}$ and *(S)*-**8** with $P(G_{25}Tos_{(0.5)}PtI(NCN\text{-}COO)_{(0.5)})$.
10. Although cationic NCN-pincer platinum complexes are, in contrast to their highly active palladium analogues, not considered to be catalytically active in Lewis-acid catalysed processes, they do accelerate selected examples to some extent.
11. (a) Nakano, T.; Okamoto, Y. *Macromol. Rapid Commun.* **2000**, *21*, 603-612; (b) Okamoto, Y. *Prog. Polym. Sci.* **2000**, *25*, 159-162; (c) Pu, L. *Chem. Eur. J.* **1999**, *5*, 2227-2232; (d) Pu, L. *Tetrahedron Assym.* **1998**, *9*, 1457-1477 and references cited; (e) Okamoto, Y.; Nakano, T. *Chem. Rev.* **1994**, *94*, 349-372; (f) Wulff, G. *Angew. Chem. Int. Ed.* **1989**, *28*, 21.

12. Carey, F. A.; Sundberg, R. J. *Advanced Organic Chemistry, Part A,* 3rd ed., Plenum Press, New York **1993**, 257-270.
13. Morrison, J. D.; Mosher, H. S. in 'Asymmetric Organic Reactions', Pentice-Hall, New Jersey, **1970**, Ch. 10, p. 411.
14. a) Dijkstra, H. P.; van Klink, G. P. M.; van Koten, G. *Acc. Chem. Res.* **2002**, *35*, 798-810; b) Kragl, U. *Industrial Enzymology,* 2nd ed. (Eds.: Godfrey, T.; West, S.), Macmillan, Hampshire, **1996**, 275-283 and references cited therein.

Graphical Abstract

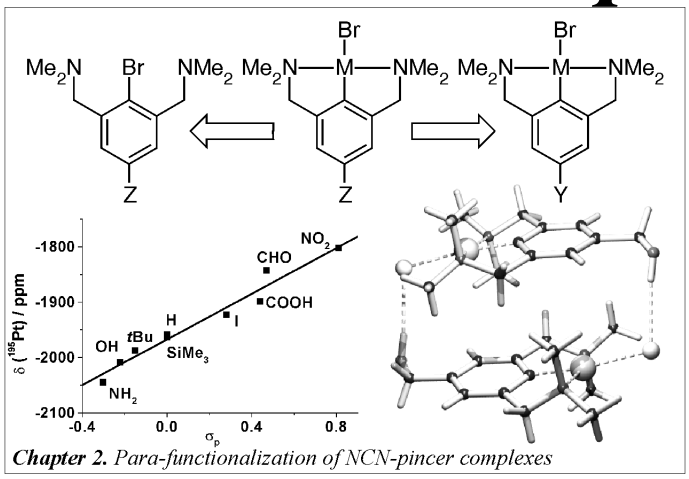

Chapter 2. *Para-functionalization of NCN-pincer complexes*

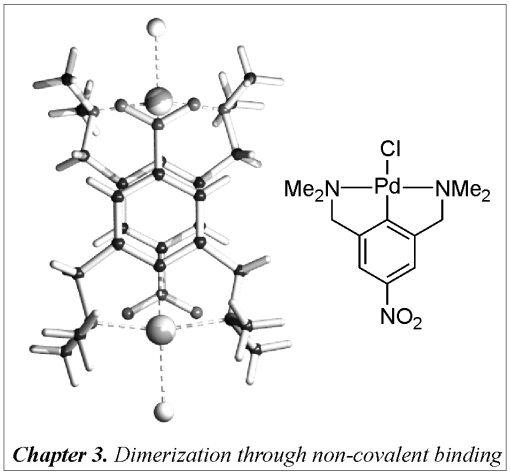

Chapter 3. *Dimerization through non-covalent binding*

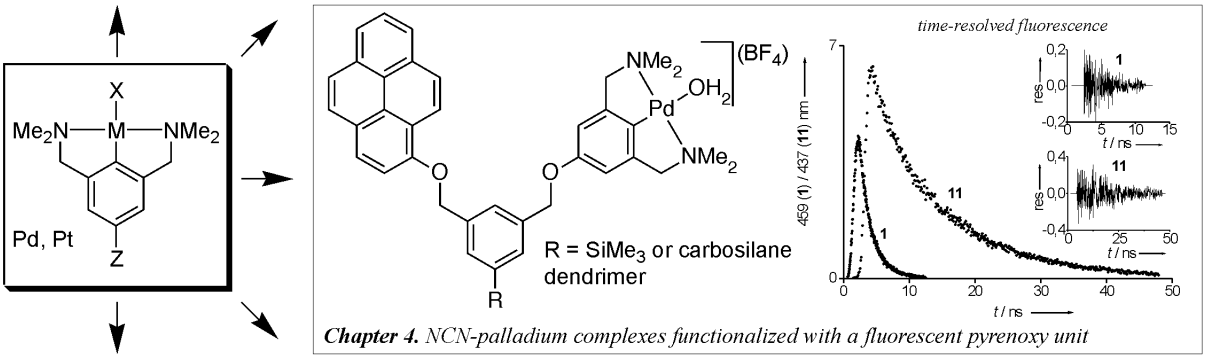

Chapter 4. *NCN-palladium complexes functionalized with a fluorescent pyrenoxy unit*

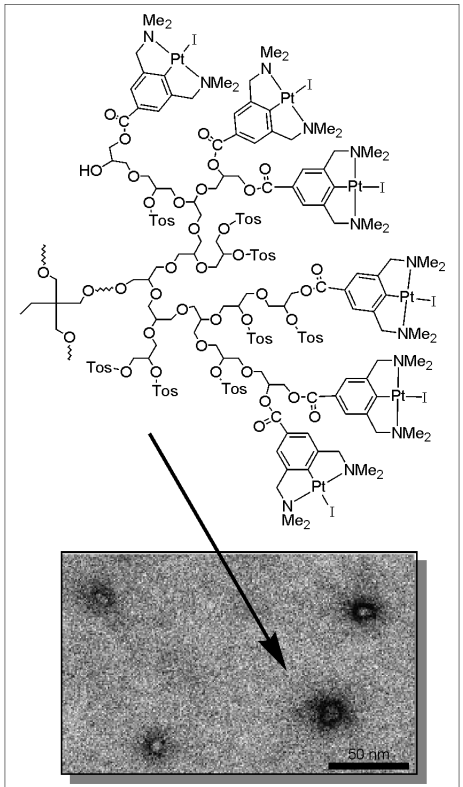

Chapters 7 and 8. *Covalent immobilization of NCN-platinum complexes*

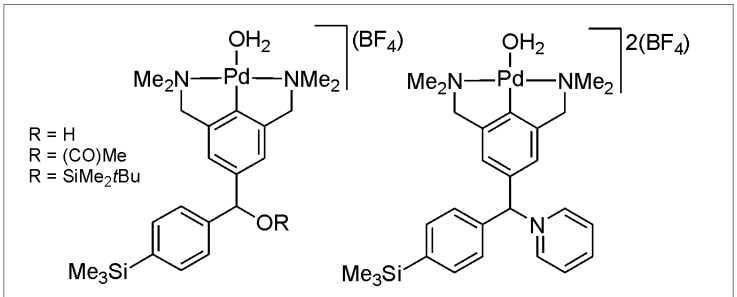

Chapter 5. *NCN-palladium complexes with multiple anchoring points.*

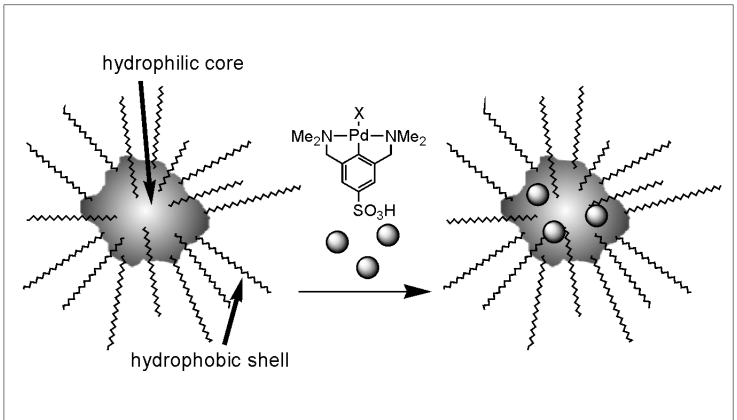

Chapters 6 and 8. *Non-covalent encapsulation of NCN-platinum complexes in nanocapsules based on hyperbranched polyglycerol*

Summary

A rapidly evolving field in chemistry is the application of organometallic and coordination complexes as building blocks or active components for the construction of new materials exhibiting specific catalytic, redox, optical or sensor activities. A central theme in the construction of these inorganic building blocks is the targeted functionalization of ligands, either prior to or, less conventionally, after the metallation step. Ligand functionalization enables the immobilization of the transition-metal complexes on macromolecular or inorganic supports, the regulation of their solubility, the introduction of additional functional moieties, as well as the electronic tuning of the metal. Furthermore, the functionalized complexes can be applied in inorganic crystal engineering or for targeted (supramolecular) assembly in solution. The NCN-pincer ligand (NCN = 2,6-bis[(dimethylamino)methyl]phenyl anion) is a versatile building block for these purposes. NCN-pincer palladium(II) and platinum(II) complexes (Chart 1) are air- and water-stable, and find widespread applications in the field of catalysis and as sensor materials. *Para*-functionalization of these complexes offers an anchoring point, while leaving the structural integrity of the metal center intact.

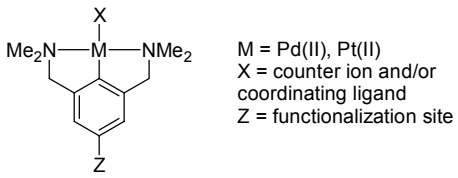

Chart 1

This thesis describes the synthesis and application of new, *para*-functionalized NCN-pincer palladium(II) and platinum(II) complexes and their use as building blocks in the covalent and non-covalent assembly of functional organometallic materials. Chapter 1 gives a brief overview on the use of transition metal complexes as building blocks for the construction of various functional materials. In chapters 2 and 3, the synthesis of *para*-functionalized NCN-pincer complexes is described, together with the influence of the substituents on various properties of the resulting complexes. The modification of NCN-pincer palladium complexes with a variety of molecular anchoring points, together with the influence of the added functional moieties on catalysis is outlined in chapters 4 and 5. Immobilization of these complexes on carbosilane dendrimers, and mimics thereof, is also presented. Chapters 6, 7, and 8 deal with the immobilization of NCN-platinum complexes by either covalent or non-covalent interactions, onto polymeric supports based on hyperbranched polyglycerols. The

research described in these final chapters was conducted in close collaboration with Dr. H. Frey and Dr. S.-E Stiriba from the University of Freiburg in Germany.

Synthesis and properties of *para*-substituted NCN-palladium and -platinum complexes

The two main synthetic strategies available for the synthesis of *para*-functionalized NCN complexes are described in Chapter 2 (Scheme 1). The common method of choice in organometallic synthesis involves ligand functionalization prior to metallation. Since the covalent M–C bond is often the most reactive part of an organometallic metal complex, the metal is preferentially introduced in the last step of its total synthesis. The second method makes use of the high stability of the Pt–C or Pd–C bond, which is a direct result of the rigid, terdentate binding of the NCN-ligand, allowing various ligand modifications on the organometallic complex itself. A variety of *para*-substituted NCN-pincer palladium(II) and platinum(II) complexes [MX(NCN-Z)] (M = Pd(II), Pt(II); X = Cl, Br, I; NCN-Z = [2,6-$(CH_2NMe_2)_2C_6H_2$-4-Z]$^-$; Z = NO_2, COOH, SO_3H, $PO(OEt)_2$, PO(OH)(OEt), $PO(OH)_2$, CH_2OH, SMe, NH_2) were synthesized using both strategies. The influence of the substituents on the electronic properties of the metal center was probed by ^{195}Pt-NMR and DFT-calculations showing linear correlations of both the ^{195}Pt-chemical shift and the calculated Mulliken populations, with the σ_p Hammett substituent constants. The *para*-substituent exhibits a dominant influence on both the solubility, and on the solid-state properties of the pincer complexes. NCN-pincer complexes substituted with protic functional groups (CH_2OH, COOH) dimerize in the solid state by intermolecular hydrogen bonding interactions. The *para*-nitro substituted NCN-palladium complexes form, in contrast to their platinum analogues, closely packed dimers in the solid state as a result of intermolecular electron donor-acceptor interactions between the palladium atoms and the nitro-groups. Crystallographic studies on *para*-nitro functionalized complexes are described in Chapter 3.

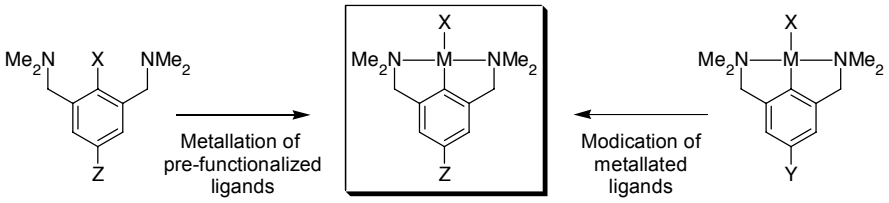

Scheme 1

NCN-palladium complexes with several anchoring points

Chapters 4 and 5 deal with the synthesis and catalytic applications of NCN-palladium complexes functionalized with both a site to modify their catalytic behavior, and an additional anchoring point for immobilization on carbosilane dendrimers. The construction of a highly flexible molecular tweezer (Chart 2) based on a *para*-hydroxyl NCN-palladium complex, a

pyren-1-oxy unit, and a xylylene based linker is described in Chapter 4. This tweezer fragment was immobilized on a G2-carbosilane dendrimer, affording a single species containing 36 tweezer units at the periphery, exemplifying the potential of NCN-pincer complexes as organometallic building blocks in the construction of intricate materials. Studies of the flexibility and conformation of the tweezer, by variable-temperature NMR, time-resolved fluorescence spectroscopy, and MM2 conformational searches, show that the NCN-palladium and the pyrenoxy fragments unit are in close proximity due to cation-π interactions. While the pyrenoxy units show affinity for picric acid (trinitrophenol) by π-π stacking interactions (association constants in the order of 10^1-10^2 M^{-1}), this affinity for aromatic molecules is hardly reflected in the performance of the NCN-palladium complex in catalysis. The initial rate of the catalyzed aldol reaction between aromatic aldehydes and methyl isocyanoacetate is enhanced only by a factor of two in the presence of the pyrenoxy unit.

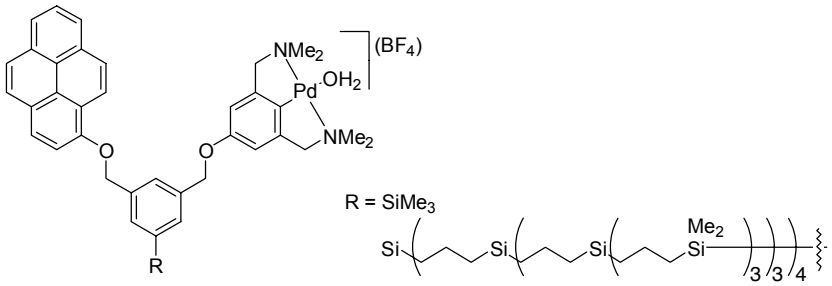

Chart 2

Chapter 5 describes the synthesis of NCN-palladium complexes with both an anchoring site for immobilization, as well as an additional reactive site for further functionalization (Chart 3). The complexes contain a trimethylsilyl group as mimic for a dendritic carbosilane support. After introduction of the trimethylsilyl-group all modifications, including metallation, can be performed nearly quantitatively. This is a necessary prerequisite for dendrimer synthesis. The functional groups (Z) placed on a distal position from the palladium site do not significantly alter the catalytic rates and product selectivity of the complexes in aldol reactions. However, since modifications on the ligand can be performed after metallation of the ligand, they offer potent starting materials for further functionalization.

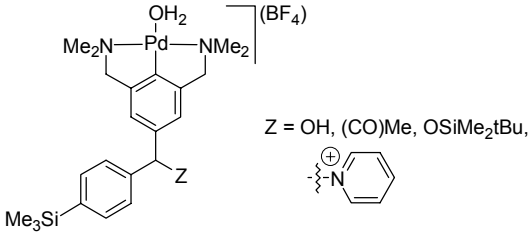

Chart 3

Hyperbranched polyglycerols as covalent and non-covalent support systems

Immobilization of (catalytically active) transition-metal complexes on macromolecular support systems offers advantages with respect to recovery of expensive or toxic ligands and catalysts. Although dendrimers have been studied in great detail for supporting homogeneous catalysts, hyperbranched polymers offer synthetically more easily accessible support systems. Hyperbranched polyglycerols with narrow polydispersities are obtained by the controlled ring-opening multi-branching (ROMB) polymerization of glycidol. Partial esterification of the hydroxyl groups affords amphiphilic nanocapsules with an inverse micelle-type architecture. Chapter 6 describes the use of these nanocapsules for the non-covalent immobilization of hydrophilic NCN-platinum sulfonates (Scheme 2). Platinum loading is achieved by liquid-liquid extractions from an aqueous NCN-platinum sulfonate solution into a dichloromethane solution containing the nanocapsules. UV/Vis- and NMR-spectroscopy, as well as elemental analysis, unequivocally show encapsulation of the NCN-platinum complexes, and the dependence of loading capacity on the nanocapsule size. The resulting materials, used as model catalysts, show rate enhancements in the double Michael addition between methyl vinyl ketone and ethyl cyanoacetate.

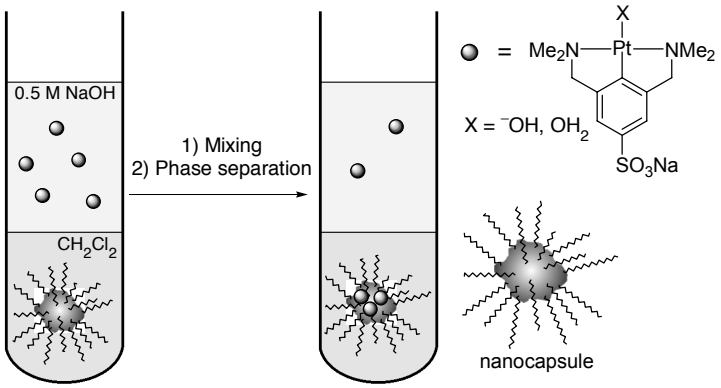

Scheme 2

Alternatively, carboxylic acid functionalized NCN-platinum complexes were covalently attached to a hyperbranched polyglycerol backbone (Chart 4). Chapter 7 describes the activation of the polyglycerol by complete tosylation of the available hydroxyl groups, followed by their partial substitution with the potassium carboxylate of the NCN-platinum complex. The presence of the heavy platinum and iodine atoms in the covalently modified hyperbranched materials renders them directly visible by transmission electron microscopy (TEM), without staining procedures. TEM micrographs showed disk-shaped structures with a small size distribution (15-20 nm) and characteristic core-shell ring structures. The thickness of the corona observed in TEM can be correlated with the degree of substitution of NCN-platinum moieties.

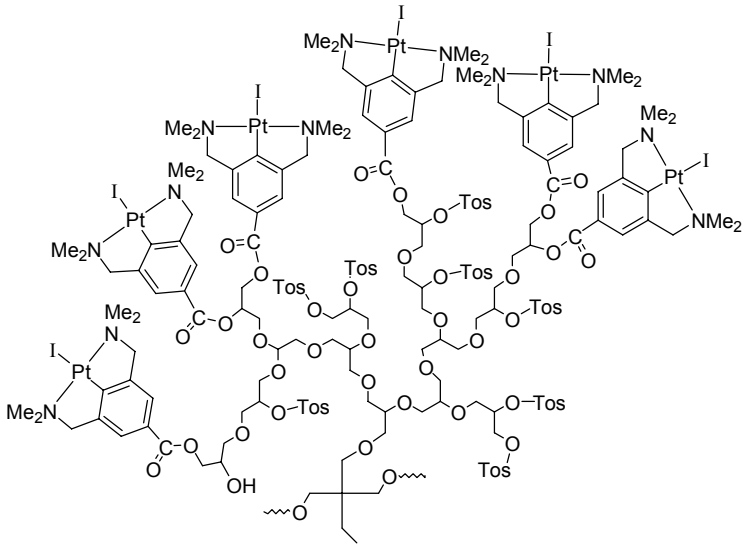

Chart 4

Chapter 8 describes both the non-covalent (see chapter 6) and the covalent (see chapter 7) immobilization of NCN-platinum complexes on chiral hyperbranched polyglycerols. These chiral materials are obtained by ROMB polymerization of either pure *(S)*- or *(R)*-glycidol, followed either by partial esterification to obtain chiral nanocapsules, or by tosylation and substitution with NCN-platinum moieties to afford chiral covalently modified polyglycerols. Circular dichroism (CD) spectroscopy showed the chiral information enclosed in the macromolecular materials. Model studies of the catalytic efficiency of the immobilized NCN-platinum complexes showed that the chiral support does not lead to chiral induction in the asymmetric Michael addition between methyl vinyl ketone and ethyl *(R/S)*-α-cyanopropionate.

General conclusions

The results described in this thesis show that NCN-pincer palladium and platinum complexes are versatile building blocks for the construction of new organometallic materials with applications in diverse fields such as catalysis, crystal engineering, and (macro)molecular visualization. The pathways presented for the synthesis of the new *para*-functionalized NCN-pincer complexes are of crucial importance for generating a suitable anchoring point for further functionalizations without affecting the M–C bond. Important aspects concerning their synthesis include: *i)* the exceptional stability of the NCN-complexes, allowing ligand modifications after the metallation step, and *ii)* the availability of various metallation procedures for selective introduction of the palladium or platinum center in the NCN-ligand. Both features offer a high degree of flexibility in the synthesis of the *para*-functionalized complexes, making functionalization with virtually any (organic) group feasible. Noteworthy

are the linear Hammett correlations found for the *para*-substituted NCN-platinum complexes. Extension of these correlations to NCN-pincer complexes of other metals, and eventually to PCP- or SCS-pincer complexes, allows subtle tuning of the electron density on their metal centers, and consequently theoretical predictions of their catalytic and/or optical properties.

The application of NCN-pincer building blocks in the examples shown in this thesis illustrate the above-mentioned features, *i.e.* selective metallation of the ligand at various stages of the syntheses and modifications on the ligand after the metallation step. The methodology employed in the preparation of the pincer complexes can be used as a starting point for the construction of new organometallic materials based on the pincer ligand. These materials can be designed to exhibit bio- or solvent-compatibility and/or specific aggregation behavior. Finally, (non)-covalent assembly of catalytically active NCN-pincer complexes with other functional moieties, *e.g.* (co)catalysts or receptor sites, offers the opportunity to construct bifunctional or supramolecular catalysts.

Samenvatting

Het gebruik van organometaal- en coördinatiecomplexen als bouwstenen voor nieuwe materialen met specifieke katalytische, redox, optische of sensor toepassingen is een snel groeiende discipline in de chemie. De functionalisatie van liganden speelt hierin een centrale rol en vindt veelal vóór of, hoewel minder gebruikelijk, ná de metalleringsstap plaats. Ligandfunctionalisering maakt naast de verankering van overgangsmetaalcomplexen aan macromoleculaire of anorganische dragers, tevens regulering van de oplosbaarheid van het complex of de fijnafstemming van elektronische eigenschappen van het metaalcentrum mogelijk. Verder kunnen deze bouwstenen worden toegepast voor de constructie van (supra)moleculaire architecturen in de vaste stof (crystal engineering) en in oplossing. Het NCN-tangligand vormt een veelzijdige bouwsteen voor deze toepassingen (NCN = 2,6-bis[(dimethylamino)methyl]phenyl anion). De palladium- en platinatangcomplexen (Figuur 1) zijn stabiel onder aërobe condities en toepasbaar als katalysator of sensor. De *para*-functionalisering van deze complexen biedt een verankeringspunt voor verdere modificatie zonder dat de structurele integriteit van het metaalcentrum wordt aangetast.

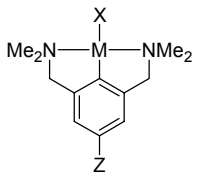

M = Pd(II), Pt(II)
X = tegenion en/of coördinerend ligand
Z = functionele groep

Figuur 1

Dit proefschrift beschrijft naast de synthese en eigenschappen van *para*-gefunctionaliseerde NCN-tangcomplexen van palladium(II) en platina(II), het gebruik van deze complexen als bouwstenen voor de constructie van nieuwe, functionele organometallische materialen. In hoofdstuk 1 wordt een kort overzicht van het gebruik van overgangsmetaalcomplexen als functionele bouwsteen gegeven. In hoofdstukken 2 en 3 worden vervolgens de synthese van verscheidene *para*-gefunctionaliseerde NCN-tangcomplexen, alsmede de invloed van de geïntroduceerde substituenten op een aantal fysisch-chemische eigenschappen van de complexen gepresenteerd. De *para*-functionalisering van NCN-palladiumcomplexen met meerdere verankeringspunten staat beschreven in de hoofdstukken 4 en 5. Naast immobilisatie van de verkregen complexen aan carbosilaandendrimeren en modellen hiervoor, kunnen additionele functionele groepen worden geïntroduceerd. De invloed van deze functionele groepen op de katalytische eigenschappen van de resulterende complexen is eveneens beschreven. Hoofdstukken 6, 7 en 8 behandelen tenslotte de covalente en niet-

covalente verankering van NCN-platinacomplexen aan polymere dragermaterialen gebaseerd op hypervertakte polyglycerolen. Het in deze laatste hoofdstukken beschreven onderzoek werd uitgevoerd in samenwerking met Dr. H. Frey en Dr. S.-E. Stiriba van de Universiteit van Freiburg.

Synthese en eigenschappen ven *para*-gesubstitueerde NCN-tangcomplexen

Er zijn in essentie twee strategieën denkbaar voor de synthese van *para*-gefunctionaliseerde NCN-tangcomplexen; beide staan beschreven in hoofdstuk 2 (Schema 1). Bij de meest gebruikelijke methode wordt het ligand vóór de metalleringsstap gefunctionaliseerd. Aangezien de covalente M–C binding vaak het meest reactieve deel van een organometaalcomplex is, wordt het metaal bij voorkeur in de laatste stap van de synthese ingevoerd. De tweede methode maakt gebruik van de grote stabiliteit van de Pt–C en Pd–C bindingen; een direct gevolg van de rigide, terdentaat binding van het NCN-ligand aan het metaal. Hierdoor kunnen een aantal modificaties aan het ligand in het organometaalcomplex zelf worden uitgevoerd. Een verscheidenheid aan *para*-gefunctionaliseerde NCN-tangcomplexen [MX(NCN-Z)] (M = Pd(II), Pt(II); X = Cl, Br, I; NCN-Z = [2,6-$(CH_2NMe_2)_2C_6H_2$-4-Z]$^-$; Z = NO_2, COOH, SO_3H, $PO(OEt)_2$, PO(OH)(OEt), $PO(OH)_2$, CH_2OH, SMe, NH_2) werd gesynthetiseerd met gebruik van beide strategieën. De invloed van de substituenten op de elektronische eigenschappen van het metaalcentrum werd gekwantificeerd met ^{195}Pt-NMR en DFT-berekeningen. Hieruit konden lineaire correlaties voor zowel de ^{195}Pt-chemische verschuiving als de berekende Mulliken-populaties met de σ_p Hammett-substituentconstanten worden opgesteld. De *para*-substituent oefent een dominante invloed uit op zowel de oplosbaarheids- als de vastestof-eigenschappen van de resulterende tangcomplexen. NCN-Metaalcomplexen met protische functionele groepen (COOH, CH_2OH) dimeriseren in de kristallijne toestand door vorming van intermoleculaire waterstofbruggen. De *para*-nitrogefunctionaliseerde NCN-palladiumcomplexen vormen als gevolg van elektron-donor-acceptor interacties tussen het palladiumatoom en de nitrosubstituent dicht opeengepakte dimeren in de kristallijne toestand, dit in tegenstelling tot de overeenkomstige platinaverbindingen. Deze kristallografische studies zijn beschreven in hoofdstuk 3.

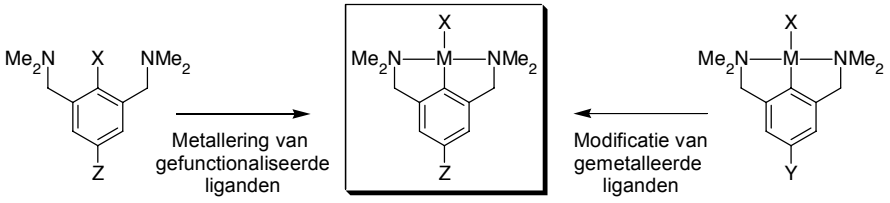

Schema 1

NCN-palladiumcomplexen met meerdere verankeringspunten

Hoofdstukken 4 en 5 behandelen de synthese en katalytische toepassingen van NCN-palladiumcomplexen, die zijn gefunctionaliseerd met groepen voor modificatie van de katalytische eigenschappen en waarbij tevens een verankeringspunt voor immobilisatie aan carbosilaandendrimeren is aangebracht. De opbouw van een zeer flexibele, moleculaire *tweezer* (Figuur 2), samengesteld uit een *para*-hydroxy NCN-palladiumcomplex, een pyren-1-oxy groep en een xylyleen verbindingsgroep, staat beschreven in hoofdstuk 4. Deze *tweezer* werd verankerd aan een G2-carbosilaan dendrimeer, waarbij een macromolecuul met 36 van deze eenheden werd verkregen. Dit benadrukt de potentie van NCN-tangcomplexen als organometaal bouwstenen voor de constructie van complexe structuren. Zowel de flexibiliteit als de conformaties van de moleculaire *tweezer* werden bestudeerd met NMR, tijdopgeloste fluorescentiespectroscopie en MM2 conformationele analyse. Hieruit bleek dat de NCN-palladiumeenheid en de pyrenoxygroep zich in elkaars nabijheid bevinden als gevolg van kation-π interacties. De pyrenoxygroep vertoont affiniteit voor picrinezuur (trinitrofenol) als gevolg van attractieve 'π-π stacking' interacties (associatieconstanten in de orde van 10^1-10^2 M^{-1}). Deze affiniteit blijkt nauwelijks van invloed te zijn op de katalytische activiteit van moleculaire *tweezers* in de aldolreactie tussen methyl isocyanoacetaat en verschillende aromatische aldehydes. De aanwezigheid van de pyrenoxygroep leidt in een aantal gevallen tot een tweevoudige verhoging van de initiële reactiesnelheid.

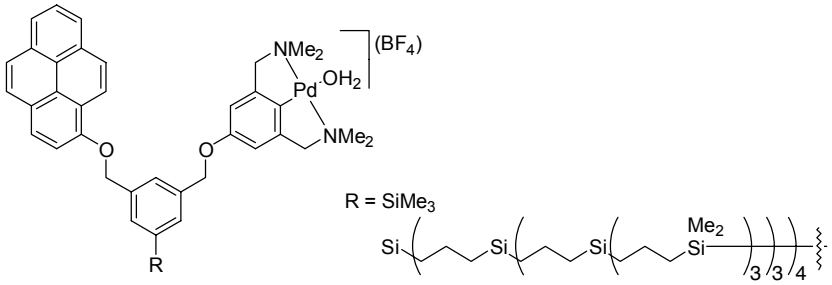

Figuur 2

In hoofdstuk 5 worden NCN-palladiumcomplexen beschreven die gefunctionaliseerd zijn met zowel een verankeringspunt voor immobilisatie alsmede een reactieve groep voor verdere modificatie (Figuur 3). De complexen bevatten een trimethylsilylgroep als model voor een dendritische carbosilaandrager. Na invoering van deze trimethylsilylgroep kunnen alle vervolgreacties, inclusief de metallering, met nagenoeg kwantitatieve opbrengsten worden uitgevoerd. Dit is een noodzakelijke voorwaarde voor synthese van dendrimeren. De functionele groep Z, die op enige afstand van het katalytisch centrum is geplaatst, beïnvloedt de katalytische activiteit en selectiviteit van de complexen nauwelijks. De in Figuur 3

weergegeven substituenten bieden echter wel een startpunt voor verdere functionalisering, aangezien modificaties mogelijk zijn na metallering van het ligand.

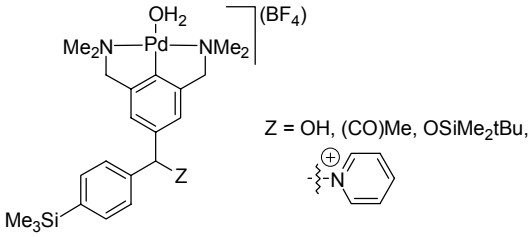

Figuur 3

Hypervertakte polyglycerolen als covalente en niet-covalente dragers

Verankering van (katalytisch actieve) overgangsmetaalcomplexen aan macromoleculaire dragers biedt als voordeel dat het terugwinnen van de vaak dure of toxische katalysatoren en liganden wordt vergemakkelijkt. Hoewel dendrimeren veelvuldig zijn bestudeerd als dragermaterialen voor homogene katalysatoren, bieden hypervertakte polymeren, synthetisch gezien, een meer toegankelijk alternatief. Hypervertakte polyglycerolen met smalle polydispersiteiten worden verkregen door gecontroleerde 'ring opening multibranching' (ROMB) polymerisatie van glycidol. Gedeeltelijke verestering van de aanwezige hydroxygroepen met vetzuren levert amfifiele nanocapsules met een geïnverteerde micel-gelijkende structuur. Hoofdstuk 6 beschrijft het gebruik van deze nanocapsules voor de niet-covalente verankering van hydrofiele NCN-platinasulfonaten. De capsules worden beladen door vloeistof-vloeistof extracties van een waterige oplossing van NCN-platinasulfonaten in een dichloormethaanoplossing van de nanocapsule (Schema 2).

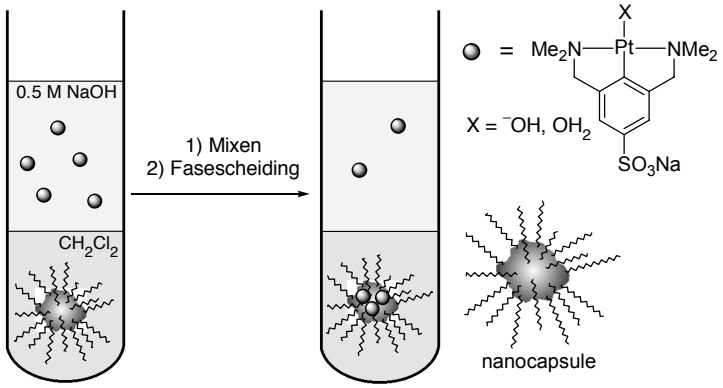

Schema 2

Uit UV/Vis- en NMR-spectroscopie, alsmede uit elementanalyse blijkt ontegenzeggelijk de opname van de complexen in de capsules en tevens de afhankelijkheid van de ladingscapaciteit en de grootte van de nanocapsule. De resulterende beladen materialen

werden toegepast als modelkatalysatoren in de dubbele Michael additie van methylvinyl keton met ethylcyanoacetaat.

Verder werden COOH-gefunctionaliseerde NCN-platinacomplexen covalent verankerd aan een drager van hypervertakt polyglycerol (Figuur 4). Hoofdstuk 7 beschrijft de activering van het polyglycerol door tosylering van de alcoholgroepen, gevolgd door de gedeeltelijke substitutie van tosylgroepen door NCN-platina-eenheden. De aanwezigheid van de zware platina- en joodatomen maakt dat de verkregen materialen direct zichtbaar zijn in elektronenmicroscopie (TEM) zonder gebruik te maken van contraststoffen. TEM-Foto's van de gefunctionaliseerde polyglycerolen laten schijfvormige structuren met een kleine spreiding in grootte (15-20 nm) en een karakteristieke kern-schil structuur zien. De dikte van de donkere, buitenste laag van deze structuur kon worden gecorreleerd met de substitutiegraad aan NCN-platina-eenheden.

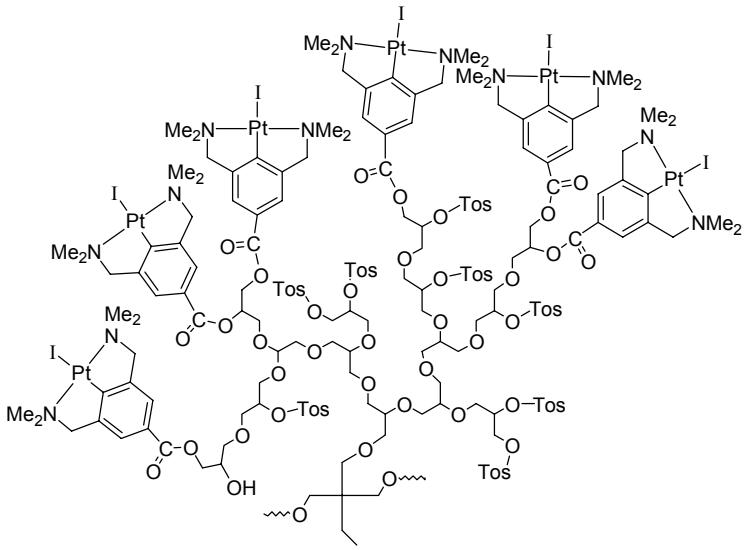

Figuur 4

Hoofdstuk 8 beschrijft tenslotte de niet-covalente (zie ook hoofdstuk 6) en covalente (zie ook hoofdstuk 7) verankering van NCN-platinacomplexen aan chirale, hypervertakte polyglycerolen. Deze chirale materialen worden verkregen door ROMB polymerisatie van puur *(S)*- of *(R)*-glycidol, gevolgd door óf gedeeltelijke verestering om chirale nanocapsules te verkrijgen óf door tosylering en substitutie met NCN-platinacomplexen om covalent gebonden gemodificeerde chirale polyglycerolen te synthetiseren. De chiraliteit van de verkregen macromoleculaire materialen werd zichtbaar gemaakt door middel van circulair dichroisme (CD) spectroscopie. Uit modelstudies naar de katalytische eigenschappen van de verankerde NCN-platinacomplexen blijkt dat het gebruik van de chirale dragermaterialen

helaas niet leidde tot chirale inductie in de asymmetrische Michael additie tussen methylvinyl keton en *(R/S)*-ethyl-α-cyanopropionaat.

Algemene conclusies

De in dit proefschrift beschreven resultaten laten zien dat NCN-tang palladium- en platinacomplexen veelzijdige bouwstenen vormen voor de constructie van nieuwe organometaalmaterialen met toepassingen in diverse disciplines, zoals katalyse, 'crystal engineering' en (macro)moleculaire visualisatie. De synthetische routes die worden gebruikt voor de synthese van de nieuwe *para*-gefunctionaliseerde NCN-tangcomplexen zijn van cruciaal belang voor het invoeren van een geschikt verankeringspunt met behoud van het metaalcentrum. Belangrijke aspecten van deze syntheses zijn: *i)* de uitzonderlijke stabiliteit van de NCN-complexen die ligandmodificatie mogelijk maakt na de metalleringsstap en *ii)* de verscheidenheid aan metalleringsprocedures voor selectieve invoering van het palladium- of platina-centrum in het NCN-ligand. Beide aspecten bieden een grote mate aan flexibiliteit binnen de synthese van *para*-gefunctionaliseerde NCN-complexen en maken de invoering van vrijwel iedere (organische) groep mogelijk. Hiernaast zijn de gevonden lineaire Hammett-correlaties voor de *para*-gesubstitueerde NCN-metaalcomplexen interessant. Uitbreiding van deze correlaties naar NCN-complexen van andere metalen, en uiteindelijk naar PCP- of SCS-tangcomplexen, maakt fijnafstemming van de elektronische eigenschappen van het metaalcentrum mogelijk. Dit biedt vervolgens de mogelijkheid tot theoretische voorspellingen van de katalytische en/of optische eigenschappen van deze complexen.

De in dit proefschrift gepresenteerde toepassingen van de NCN-bouwstenen illustreren de hierboven genoemde aspecten met betrekking tot selectieve metallering in verschillende stadia van de totale synthese en de modificatie van gemetalleerde liganden. De methodologie die wordt toegepast in de synthese van de *para*-gefunctionaliseerde complexen kan worden gebruikt als uitgangspunt voor de opbouw van nieuwe organometaalachtige materialen die gebaseerd zijn op het tangligand. Deze materialen kunnen worden ontworpen met een specifieke bio- of oplosmiddelcompatibiliteit en/of specifiek aggregatiegedrag. Tenslotte kan de (niet)-covalente assemblage van katalytisch actieve NCN-tangcomplexen met andere functionele eenheden, zoals (co)katalysatoren of moleculaire herkenningsgroepen, leiden tot bifunctionele of supramoleculaire katalysatoren.

Dankwoord

Het is gelukt! Mijn boekje, scriptie, werkstuk, proefschrift of hoe het dan ook werd genoemd is af. Na vijf jaar kan ik, ondanks de soms grote tegenslagen, terugkijken op een geweldige tijd, zowel binnen als buiten de sectie organische synthese. Ik ben dan ook erg dankbaar voor de steun, getoonde interesse en gezelligheid die ik de afgelopen jaren van familie, vrienden en collega's heb mogen ontvangen. Zonder hen was het niet mogelijk geweest om deze klus te klaren.

Allereerst wil ik mijn ouders Cors en Henny bedanken. Door jullie onvoorwaardelijke steun en liefde heb ik alle vrijheid gehad om mezelf te ontwikkelen en vormen tot wie ik ben. Ik heb veel van jullie geleerd, en kan altijd terecht voor een luisterend oor. Ik mag van geluk spreken met zulke ouders.

Vervolgens wil ik mijn promotor Prof. Dr. Gerard van Koten bedanken. Beste Gerard, ik ben je dankbaar voor de inspiratie die je me gaf tijdens mijn onderzoek in jouw groep. De combinatie van je nimmer aflatende ideeën en de vrijheid die ik kreeg in de invulling van mijn project heb ik als zeer leerzaam ervaren en hebben voor een belangrijk deel bijgedragen aan mijn wetenschappelijke ontwikkeling. Je luisterde naar en respecteerde mijn argumenten zodat er altijd ruimte was voor discussie. Hiernaast wist je mij tijdens de onvermijdelijke tegenslagen in het onderzoek altijd weer te motiveren, zodat ik er weer tegenaan kon.

Ik ben ook veel dan verschuldigd aan mijn copromotor Dr. Bert Klein Gebbink. Beste Bert, in de laatste jaren van mijn promotieonderzoek ben je voor mij onmisbaar geweest. Hierbij denk ik aan je tips en enthousiasme voor de behaalde resultaten, maar ook aan onze discussies en de nauwkeurige manier waarop je mijn manuscripten corrigeerde. Ook wil ik Dr. Johann Jastrzebski bedanken voor de dagelijkse begeleiding tijdens de beginperiode van mijn onderzoek.

De overige leden van de vaste staf, Dr. Jaap Boersma, Dr. Gerard van Klink, Dr. Berth-Jan Deelman, wil ik bedanken voor de goede en plezierige samenwerking, discussies, correcties en het plezier aan de koffietafel. Met name Margo, maar ook Esther en Hester, wil ik bedanken voor alle hulp met (promotie)papieren, publicaties, congressen (zelfs Lunteren) en andere klusjes die ik niet alleen af kon.

I would like to thank Prof. Dr. Holger Frey and Dr. Salah-Eddine Stiriba from (at that time) the University of Freiburg for the successful collaboration, which resulted in chapters 6-8 of this thesis. Dear Holger, thanks for your hospitality to have me in your group, and our discussions concerning the results of the work. Dear Salah, I admire your enthusiasm and dedication to chemistry and enjoyed working with you during my stay in Freiburg and your stay in Utrecht.

Prof. Dr. Jan Verhoeven en John van Ramesdonk van de Universiteit van Amsterdam wil ik graag bedanken voor de mogelijkheid tot het doen van (tijdopgeloste) fluorescentiemetingen en de hulp bij de interpretatie hiervan. Wim Klopper wil ik bedanken voor zijn hulp bij het opzetten en interpreteren van de DFT berekeningen. Hoewel de resultaten niet in dit proefschrift beschreven staan wil ik

Moniek Tromp en Prof. Dr. Diek Koningsberger graag bedanken voor de succesvolle samenwerking met de AXAFS metingen.
Hiernaast wil ik graag de leden van de CW-STW gebruikerscommissie, Dr. Pim Mul, Dr. Frits van Buren, Prof. Dr. Hans de Vries, Prof. Dr. Piet van Leeuwen, Dr. Joost Reek en Rieko van Heerbeek, bedanken voor hun aanwezigheid en suggesties tijdens de halfjaarlijkse bijeenkomsten.
Een deel van het in dit proefschrift beschreven werk is uitgevoerd in samenwerking met een aantal studenten: Jeroen de Pater, Don van Zwieten, Robin Spelbrink, Michiel Grutters, Daan Moerkerk en Vajk Deáky. Hoewel niet al jullie werk in het boekje terecht is gekomen ben ik jullie zeer dankbaar voor al het prachtige werk.
Voor het oplossen van de kristalstructuren in dit proefschrift wil ik graag bedanken Dr. Martin Lutz, Prof. Dr. Ton Spek, Dr. Dianne Ellis en Dr. Alison Mills. Voor allerhande grafische hulp ben ik dank verschuldigd aan Jan de Boesterd, Ingrid van Rooijen en Alois Lurvink van de AV-dienst.
Voor allerhande tips, hulp, gebruik van apparatuur en het delen van de koffietafel wil ik de leden van de buursectie Fysisch Organische Chemie enorm bedanken.
Alle AIO's, postdocs, studenten en andere medewerkers die tijdens mijn promotieonderzoek aan de Sectie Organische Synthese hebben gewerkt wil ik graag bedanken voor alle nuttige en nutteloze discussies, steun, samenwerking, de sfeer op de labzaal en aan de koffietafel, de labstaps, Lunteren-sessies, feesten, borrels en andere gebeurtenissen voor, na en tijdens werktijd. Bedankt allemaal, in willekeurige volgorde: Elwin de Wolf, Silvia Gosiewska, Marcella Gagliardo, Marion Bruin, Marianne Stol, Serenella Medici, Martin Albrecht, Jim Brandts, Henk Hagen, Marieke Spee, Arjan Kleij, Pablo Steenwinkel, Rob Abbenhuis, Paulo Dani, Rob Kreiter, Rob van de Coevering, Jeroen de Pater, Gabriela Guillena, Gema Rodríguez, Henk Klein, Peter Wijkens, Catelijne Amijs, Nilesh Mehendale, Kees Kruithof, Bart Suijkerbuijk, Pieter Bruijnincx, Joke Scholten, Irene Eijgendaal, Claudia Kronenburg, Alexey Chuchurjukin, Philippe en Laurence Merle, Scott Williams, Diego Ramon, Patrick O'Leary, Guido Batema, Kristel Flinzner, Judith Firet, en alle anderen die ik hier vergeten ben te noemen. Een speciaal woord van dank wil ik richten aan Michel Meijer, Harm Dijkstra, Sander Thoonen, Joep van den Broeke en Anne Arink. Michel, Harm, Joep en Sander, als vaste bewoners van de tweede zuidzaal ofwel de RISC-zone (Really Important Science and Chemistry of was het nu Retarded Incompetent Sad Couch-patatoes?) tijdens het grootste deel van mijn onderzoek en (bijna) kamergenoten hebben we de afgelopen jaren veel plezier beleefd met de chemie, Mac- en andere ergernissen en van alles buiten de chemie. Michel, bedankt voor de tips, hulp en lol bij het praktische werk en voor die keer dat je het hebt aangedurfd mijn labbank schoon te maken. Harm, bedankt voor het beschikbaar stellen van de wereldvoorraad van je 'dodecapincer' voor de TEM studies in hoofdstuk 7. Helaas zullen we het over muziek wel nooit volledig eens worden. Sander, bedankt voor alle klusjes die je voor me hebt opgeknapt als ik thuis zat te werken, al heb ik dat voldoende gecompenseerd als jouw telefoonbeantwoorder. Anne, ik heb veel plezier beleeft aan onze koper-platina samenwerking, de voorbereidingen op het bezoek van Sinterklaas en andere momenten.

Ik ben dan ook blij dat je mij tijdens mijn promotie als paranimf wil assisteren. Gema, Gabriela, Harm en Bart wil ik in het bijzonder danken voor de goede samenwerking op het gebied van de *para*-pincers.
Naast mijn ouders wil ik ook mijn familie, Jeroen, Mariska, Liza, Vincent en Elke Slagt, Chris, Astrid en Aike van Beekum en Oma Heijser, bedanken voor alle interesse, steun, plezier tijdens vakanties, etentjes en andere (familie)gebeurtenissen in de afgelopen jaren. Helaas voor Liza zitten er in dit boekje geen noetes.
Bijna als laatste, maar zeker niet de minste, wil ik mijn vrienden bedanken voor de noodzakelijke ontspanning buiten het laboratorium. Andor en Roos Buisman, Gerrie en Alies Elfrink, Marko en Marije Roenhorst, Jeroen ten Voorde, Michel Tijsterman, Michel Frederiks en Liesbeth Volmer, bedankt voor alles! Samen met de heren van Yukka, Arjan Brentjes, Jasper Slaghuis en (weer) Jeroen Slagt, heb ik ook veel plezier beleeft in de oefenruimte, op het podium, maar ook daarbuiten. Arjan wil ik nog bedanken voor het ontwerp van de omslag, ik vind het erg geslaagd.
Lieve Randi, de laatste zinnen van dit proefschrift heb ik bewaard voor jou. Je hebt heel wat moeten doorstaan met de enorme stapels papieren/zooi in de kamer en mijn geklaag wanneer het niet helemaal ging zoals ik wilde. Ik ben je dankbaar voor al je liefde tijdens de mooie en soms ook minder mooie momenten. Samen zijn we vier handen op één buik!

29 september 2002

Martijn

Curriculum Vitae

De schrijver van dit proefschrift, Martijn Quico Slagt, werd geboren op 8 maart 1973 te Zevenaar. In juni 1992 behaalde hij het Atheneum diploma aan het Liemers College te Zevenaar. In augustus van datzelfde jaar werd begonnen met de studie Scheikunde aan de Universiteit Utrecht. In augustus 1993 werd het propedeutisch examen afgelegd. Het doctoraal examen, met de keuzeonderdelen Fysisch Organische Chemie (Prof. Dr. L.W. Jenneskens) en NMR-spectroscopie (Prof. Dr. R. Boelens) en als hoofdvak Metaal-Gestuurde Organische Synthese (Prof. Dr. G. van Koten) werd cum laude afgelegd op 25 augustus 1997. In de periode februari tot april 1997 verrichtte hij een onderzoeksproject Organometaalchemie aan de Universiteit van Sassari in Italië (Prof. Dr. S. Gladiali). Vanaf november 1997 tot maart 2002 verrichte de schrijver het in dit proefschrift beschreven onderzoek als Onderzoeker in Opleiding (OIO) in de Sectie Organische Synthese (Prof. Dr. G. van Koten) van het Debije Instituut aan de Universiteit Utrecht. In maart 2001 werd een werkbezoek gebracht aan de groep van Prof. Dr. H. Frey (Universiteit Freiburg, Duitsland) voor een gezamenlijk onderzoeksprojekt. Het onderzoek werd financieel ondersteund door het gebied Chemische Wetenschappen (CW) van de Nederlandse Organisatie voor Wetenschappelijk Onderzoek (NWO) en Technologiestichting STW.

List of Publications

Self-Assembly of para-Nitro NCN-Pincer Palladium Complexes into Dimers through Electron Donor-Acceptor Interactions
Martijn Q. Slagt, Harm P. Dijkstra, Aidan McDonald, Robertus J. M. Klein Gebbink, Martin Lutz, Dianne D. Ellis, Allison M. Mills, Anthony L. Spek, Gerard van Koten *Organometallics*, accepted.

Para-Functionalized NCN-pincer Palladium(II) Complexes: Synthesis, Catalysis and DFT-calculations
Harm P. Dijkstra, Martijn Q. Slagt, Aidan McDonald, Cornelis A. Kruithof, Robert Kreiter, Allison M. Mills, Martin Lutz, Anthony L. Spek, Wim Klopper, Gerard P. M. van Klink, Gerard van Koten *Eur. J. Inorg. Chem.*, accepted.

Synthetic Strategies towards New para-Functionalised NCN-Pincer Palladium(II) and Platinum(II) Complexes
Martijn Q. Slagt; Robertus J. M. Klein Gebbink; Martin Lutz; Anthony L. Spek; Gerard van Koten *J. Chem. Soc., Dalton Trans.* **2002**, 2591-2592.

Encapsulation of Hydrophilic Pincer-Platinum(II) Complexes in Amphiphilic Hyperbranched Polyglycerol Nanocapsules
Martijn Q. Slagt; Salah-Eddine Stiriba; Robertus J. M. Klein Gebbink; Holger Kautz; Holger Frey; Gerard van Koten *Macromolecules* **2002**, *35*, 5734-5737.

Platinum-pincer introduction using active ester chemistry
Bart M. J. M. Suijkerbuijk; Martijn Q. Slagt; Robertus J. M. Klein Gebbink; Martin Lutz; Anthony L. Spek; Gerard van Koten *Tetrahedron Lett.* **2002**, *43*, 6565-6568.

Selective Liquid-Phase Semihydrogenation of Functionalized Acetylenes and Propargylic Alcohols with Silica-Supported Bimetallic Palladium-Copper Catalysts
Marieke P. R. Spee; Jaap Boersma; Michel D. Meijer; Martijn Q. Slagt; Gerard van Koten; John W. Geus *J. Org. Chem.* **2001**, *66*, 1647-1656.

Ace[c,d]fluoranthene
Martin Sarobe; Judith D. Snoeijer; Leo W. Jenneskens; Martijn Q. Slagt; Jan W. Zwikker *Tetrahedron Lett.* **1995**, *36*, 8489-8492.